A NEW APPROACH FOR MERGING ZONE-FLOW INJECTION ANALYSIS

A Thesis

Submitted to the Council of the College of Science
University of Babylon
In Partial Fulfillment of the Requirements for the Degree of
Doctor of Philosophy in Chemistry

By

Dakhil Nassir Taha AL-Zerkany

December, 2002 A.D. **Shawal, 1423H**

Certification

We certify that this thesis is prepared under our supervision at the Department of Chemistry, College of Science, University of Babylon, as a partial requirement for the degree of Doctor of Philosophy in Chemistry and this work has never been published anywhere.

Signature:

Name : Dr. Falah H. Hussein

Title : Professor.

Address : University of Babylon , College of the Science , Department of Chemistry .

Date : /12/2002

Signature

Name: Dr. Issam M.A. Shakir

Title : Professor.

Address : University of Baghdad , College of the Science , Department of Chemistry .

Date : /12/2002

In the view of the available recommendation , 1 forward this thesis for debate by the Examining Committee.

Signature:

Name : Dr. Ali , A. Mahdi

Title : Assistant Professor.

Address : Head of Chemistry Department, College of the Science, University of Babylon

Date : / 12/2002

Examination Committee

We, are the examining committee, certify that we have read this thesis and examined the student **Dakil Nassir Taha** in its content, and that in our opinion it is adequate with **"Excellent"** standing as a thesis for the degree of Doctor of Philosophy in Chemistry. Date 12/12/2002.

Signature:
Name:
Tittle:
Address:
Date:
(Chairman)

Signature:
Name:
Tittle:
Address:
Date:
(Member)

Signature:
Name:
Tittle:
Address:
Date:
(Member)

Signature:
Name:
Tittle:
Address:
Date:
(Member)

Signature:
Name:
Tittle:
Address:
Date:
(Member)

Signature:
Name: Dr. Falah H. Hussein
Tittle: Professor.
Address: University of Babylon, College of the Science, Department of Chemistry.
Date:
(Supervisor)

Signature:
Name: Dr. Issam M.A. Shakir
Title : Professor.
Address: University of Baghdad, College of the Science, Department of Chemistry.
Date :
(Supervisor)

Approved for the College Committee on Graduate Studies

Signature:
Name : Dr. Falah H. Hussein
Title : Professor.

Address : Ministry of Higher Education, University of Babylon , Dean of College of Science.
Date : /12/2002

نمط مستحدث للتحليل بالحقن الجرياني-رحيل وتداخل المناطق

رسالة مقدمة الى
مجلس كلية العلوم وهي جزء من متطلبات نيل درجة دكتوراه فلسفة في الكيمياء

من قبل

داخل ناصر طه

بكالوريس علوم - جامعة البصرة
ماجستير علوم – جامعة سترثكلايد-انكلترا

1423هـ 2002 م

﴿قَالُوا سُبْحَانَكَ لَا عِلْمَ لَنَا إِلَّا مَا

عَلَّمْتَنَا إِنَّكَ أَنْتَ الْعَلِيمُ الْحَكِيمُ﴾

سورة البقرة

الاية (32)

قال رسول الله ﷺ

﴿طلب العلم فريضة على كل مسلم ومسلمة﴾

صدق رسول الله

ملخص البحث

يضم البحث اربعة فصول، تضمن الفصل الاول –الاطار المنهجي للبحث- والذي يضم مشكلة البحث المتركزة في الاستفهام عن مدى استفادة فنان المسرح العراقي من اشتغال التبادلية بين المضامين التعليمية والتربوية في مسرح بريخت مع ماقدم من مسرحيات عراقية تحمل الخصوصية ذاتها.

وتتجلى اهمية البحث في تعميم المضامين التربوية والتعليمية التي يتم استنباطها من المسرح البريختي في المؤسسات والكليات والمعاهد الفنية والفرق المسرحية التي تهتم بالتجربة المسرحية العالمية بغية تطوير التجربة العملية والنظرية للمسرح العراقي وكذلك الافادة من التجربتين في الدراسات المتخصصة.

اما اهداف البحث فتمثلت في الكشف عن المضامين التعليمية والتربوية واستنباط التعريف الخاص بها في مسرح بريخت كذلك اجراء المقارنة لكشف اوجه العلاقة بين التجربة البريختية وتجربة الفنان العراقي اما حدوده فقد اقتصرت على النصوص المسرحية البريختية ونظيراتها المعرقة من قبل الكتاب المسرحيين العراقيين والتي قدمت من قبل الفرقة القومية للتمثيل وفرقة المسرح الفني الحديث في العراق للفترة من 1970-1985 متوخين دقة الاختيار اذ ان هذه العينات تنسجم مع متطلبات البحث. وأختتم الفصل بتعريف المصطلحات الاساسية.

اما الفصل الثاني: الاطار النظري والدراسات السابقة، فتضمن اربعة مباحث، عني الاول منها بدراسة المرجعيات المسرحية لدى بريخت بدأ المسرح الياباني (النو) ومروراً بالمسرح الثيني والاليزابيثي والاغريقي والسوفيتي مسلطاً الضوء على مواءمة بريخت لكثير من التجديدات والتجارب والاساليب التي تنتمي الى المسارح السابقة وبدراسة تقابلية.

فيما عني المبحث الثاني بالمرجعيات الفكرية والفلسفية في مسرح بريخت، مستعرضاً فيه تأثره واستفادته من الكتاب والمنظرين الذين سبقوه امثال، برنادشو بسكاتور، كايزر، فالنتين، ودكنر، بوخنر، ايرش انجل، وتأثره فكرياً بالمادية الديالكتيكية والمادية الجادلية وكيف وضف ابعادهما باساليب فنية ومسرحية غيرت من اتجاه اهداف المسرح في القرن العشرين.

وتناول الباحث المرحلة التعبيرية كمرحلة اولى من حياة بريخت المسرحية وما قدمه مكن اعمال في هذه المرحلة مضمناً محاور المبحث الامثلة المسرحية وابرز السمات الفلسفية والفكرية التي خلصَّ اليها بريخت واستوعبها ممن سبقوه في الشكل والمضمون ولكنه بقي محافظاً على اسلوبه ورؤيته وشخصيته مما جعلَّ المسرح الملحمي يظل مرتبطاً باسم بريخت.

اما المبحث الثالث فقد تضمن المرحلة الثانية من مراحل بريخت المسرحية وهي المرحلة التعليمية في مسرح بريخت، فيتم تسليط الضوء على التعليمية بالمسرح تاريخياً ومن ثم انواع

التعليمية، والتعليمية عند بريخت كدروس وحلقات دراسية مع تضمين ذلك امثلة من المسرحيات التعليمية البريختية شارحاً ابعادها ومضامينها.

والمبحث الرابع والاخير تضمن دراسة خصائص المسرح الملحمي البريختي، مستعرضاً فيه ومن خلال محاوره، وظيفة المسرح والتمثيل والاخراج والاسلوبية والتقريب والجمهوري وبنية النص الملحمي والجمهور، موضحاً ابرز خصائص النظرية الملحمية مقارنةً بالمسرح القديم (الارسطي)، ورغم ان بعض مفردات هذا المبحث تبدو غريبة على نسيج الرسالة ولكننا اثرنا وجودها لتكتمل صورة المسرح الملحمي لدى الدراسيين آخذين في نظر الاعتبار الاختصار الشديد للامور التي تتعلق بالاسلوبية ولمفردات العرض المسرحي.

ثم اختتم الفصل الثاني بما اسفر عنه الاطار النظري، وتم الاشارة الى الدراسات السابقة، فهي خمسة، الاولى دراسة الدكتور جميل نصيف التكريتي الموسومة (الجذور الاجتماعية للمسرح الملحمي عند بريخت) والثانية اطروحة الدكتوراه الموسومة ( ) للباحث عوني كرومي، والثالثة اطروحة الدكتوراه الموسومة (الملحمية في النص المسرحي العربي) للباحث فؤاد علي حارز، والرابعة رسالة الماجستير الموسومة (كيف تم منهج بريخت من قبل المؤلف والمخرج في المسرح العراقي) للباحث سلام مهدي الاعرجي، والخامسة رسالة الماجستير الموسومة ( ) للباحث رياض موسى سكران.

اما الفصل الثالث، فقد تضمن اجراءات البحث وهي: مجتمع البحث، وعيناته وادواته وطريقته، وتم اختيار عدد من النصوص المسرحية البريختية والتي تم تعريفها بقصد معرفة توظيف المضامين التعليمية والتربوية ومن خلال الدراسة المقارنة.

اما الفصل الرابع، فقد احتوى على نتائج البحث التي توصل اليها الباحث وعرض للاستنتاجات كما احتوى الفصل على مجموعة من التوصيات والمقترحات وثبتت المصادر والمراجع وملخص باللغة الانكليزية.

Abstract

This work falls into three parts the first one covers the basic presentation of flow injection analysis as a way of conducting analysis. It includes basic definitions, comparison with other more or less related techniques, and chromatography or classic way of analysis (beaker chemistry). It also includes the main modes of operation. The second part describes all the chemicals used and their preparation as well as the steps leading to 2×6 - port injection valve with variable loops size for conducting merging zone techniques. It also deals with the flow cell design arrived at as a real practice adopted for the work in this project.

The third part developed to the application conducted throughout this work in determining hydronium ion as a leading spectrophotometric based on an ON-line approach. The determination of Hydrochloric acid linear ranges (for extend) from 8×10^{-5}– 3.5×10^{-4} M with theoretical limit of detection (L.O.D) of 2.9×10^{-8} g/40µl and practical of 4.8×10^{-8} g/40µl, sulphuric acid (range 2×10^{-5} – 1.5×10^{-4}M) with theoretical L.O.D of 6.27×10^{-8} g/40µl and practical of 9.24×10^{-8} g/40µl, phosphoric acid (range 10^{-4}– 3.5×10^{-4}M) with theoretical L.O.D of 7.84×10^{-8} g/40µl and practical of 7.87×10^{-8} g/40µl , nitric acid (range 7×10^{-5} – 3.5×10^{-4}M) with theoretical L.O.D of 6.44×10^{-8} g/40µl and practical of 5.04×10^{-8} g/40µl, perchloric acid (range 10^{-4}–3.5×10^{-4}M) with theoretical L.O.D of 8.03×10^{-8} g/40µl and practical of 13.11×10^{-8} g/40µl, formic acid (range 1.5×10^{-4}–4.5×10^{-4}M) with theoretical L.O.D of 3.68×10^{-8} g/40µl practical of 3.8×10^{-8} g/40µl, acetic acid (range 6×10^{-5} – 3.5×10^{-4}M) with theoretical L.O.D of 3.84×10^{-8} g/40µl and practical of 5.93×10^{-8} g/40µl, citric acid (range 5×10^{-5}-2×10^{-5}M) with theoretical L.O.D 16.8×10^{-8} g/40µl and practical of 90.06×10^{-8} g/40µl, triflouoroacetic acid (range

1.5×10^{-4}–4.5×10^{-4}M) with theoretical L.O.D 19.5×10^{-8} g/40µl and practical of 25.87×10^{-8} g/40µl and buffer range (3×10^{-5} - 7×10^{-5}M) with theoretical L.O.D of 4.4 $\times10^{-8}$ g/40µl and practical of 6.2×10^{-8} g/40µl comparison of theoretically calculated value from acid concentration obtained from practical measure agrees well with pH-meter reading. Also the pH-meter cannot read microliter sample volume. Hydrogen peroxide was determined through the relased Iodine, linear analytical range extended from 1×10^{-6} to 3×10^{-3} mol.l^{-1} using 40µl. which corresponded to 4.08×10^{-4}µg to 1.22 µg with a detection limit of 1.36×10^{-10} g /40µl which is regarded as a very good linearity (four order of magnitude). Iodate and iodide ion were also determined at 2×10^{-6}- 40×10^{-6} mol.l^{-1} which corresponded to 13.99×10^{-3} µg to 27.98×10^{-2}µg. with a detection limit of 1.4×10^{-8} g. IO^{-}_{3} per sample at 3σ and from 8×10^{-4} -4×10^{-3} Mol.l^{-1} which corresponded to 40.6×10-1 µg to 20.60 µg with a detection limit of 5×10^{-7}g, I^{-} per sample at 3σ consequently. Nitrate and Nitrite ion were determined at 0.4×10^{-5} - 8×10^{-5} mol.l^{-1} which corresponded to 4.96×10^{-3}µg to 0.049 µg/ injected sample. Nitrate ion was determined via reduction to nitrite ion then the mixture of both was also determined.

المستخلص

يتضمن هذا العمل ثلاثة اجزاء، شمل الجزء الاول عرض المفاهيم الاساسية لتحليل الحقن الجرياني كطريقة متبعة في التحليل. وقد تناول التعاريف الاساسية، المقارنة مع تقنيات التحليل الكلاسيكية ذات العلاقة كما تضمن انماط العمل الرئيسية. وشمل الجزء الثاني المواد الكيميائية وطرق تحضيرها. وتضمن بشكل مختصر المراحل المتبعة لعمل الصمام ذو وصلتي الانموذج كاسلوب لتقنية المناطق المتداخلة المعمول به ضمن هذا المشروع. كما تناول تصميم خلية جريان عابر مناسبة للعمل.

يتضمن الجزء الثالث تطبيقات هذا العمل في تقدير ايون الهيدرونيوم بطريقة المطيافية الضوئية المعتمدة على اسلوب الخط الواحد في تقدير حامض الهيروكلوريك في مدى (8×10^{-5} – 3.5×10^{-4} مولاري) وبحد كشف نظري (2.9×10^{-8} غم/40 مايكروليتر) وحد كشف عملي (4.8×10^{-8} غم/ 40مايكرولتر). حامض الكبريتيك مدى (2×10^{-5} –1.5×10^{-4} مولاري) وبحد كشف نظري (6.27×10^{-8} غم/40 مايكروليتر) وحد كشف عملي (9.24×10^{-8} غم/ 40مايكرولتر). حامض الفسفوريك ضمن مدى (10^{-4} – 3.5×10^{-4} مولاري) وبحد كشف نظري (7.84×10^{-8} غم/40 مايكروليتر) وحد كشف عملي (7.87×10^{-8} غم/ 40مايكرولتر). حامض النتريك بمدى (7×10^{-5} – 3.5×10^{-4} مولاري) وحد كشف نظري (6.44×10^{-8} غم/40 مايكروليتر) وحد كشف عملي (5.04×10^{-8} غم/ 40مايكرولتر). حامض البيركلوريك ضمن مدى (10^{-4} – 3.5×10^{-4} مولاري) وحد كشف نظري (8.03×10^{-8} غم/40 مايكروليتر) وحد كشف عملي (13.11×10^{-8} غم/ 40مايكرولتر). وحامض الفورميك بمدى (1.5×10^{-4} – 4.5×10^{-4} مولاري) وبحد كشف نظري (3.68×10^{-8} غم/40 مايكروليتر) وحد كشف عملي (3.81×10^{-8} غم/ 40مايكرولتر). وحامض الخليك ضمن مدى (6×10^{-5} – 3.5×10^{-4} مولاري) وبحد كشف نظري (3.84×10^{-8} غم/40 مايكروليتر) وحد كشف عملي (5.93×10^{-8} غم/ 40مايكرولتر). و حامض الستريك ضمن مدى (5×10^{-5} – 2×10^{-5} مولاري) وبحد كشف نظري (16.8×10^{-8} غم/40 مايكروليتر) وحد كشف عملي (90.06×10^{-8} غم/ 40مايكرولتر). وحامض ثلاثي فلور حامض الخليك مدى (1.5×10^{-4} – 4.5×10^{-4} مولاري) وبحد كشف نظري (19.5×10^{-8} غم/40 مايكروليتر) وحد كشف عملي (25.87×10^{-8} غم/ 40مايكرولتر).

ومحلول منظم بمدى (3×10^{-5} - 7×10^{-5} مولاري). وكانت النتائج المحسوبة مقارنة مع قراءات مقياس الدالة الحامضية متقاربة جداً. علماً انه مقياس الدالة الحامضية لايستطيع قراءة مايكروليترات من النموذج ومن التطبيقات الاخرى.. تقدير بيروكسيد الهيدروجين عن طريق قياس اليود المتحرر وبمدى (10^{-6} -3×10^{-3} مولاري) باستعمال 40 مايكرولتر. والذي يساوي لـ (4.0×10^{-4} – 1.22 مايكروغرام) وبحد كشف (1.36×10^{-10} غرام/40 مايكرولتر) وهو يعبر عن خطية جيدة جداً. كذلك تقدير الايوداید والايوديت ضمن مدى (2×10^{-6} – 40×10^{-6} مولاري) والذي يساوي (13.992×10^{-3} – 27.984 مايكروغرام) وبحد كشف مقداره (1.4×10^{-8} غرام. ايوديت) لكل نموذج عند (3σ) وبمدى (8×10^{-4} – 4×10^{-3} مولاري) والذي يساوي (40.6×10^{-1} – 20.6 مايكروغرام) وبحد كشف مقداره (5×10^{-7} غرام. ايوداید) لكل نموذج عند (3σ).

وقد تم تقدير ايوني النترات والنتريت وبمدى (0.4×10^{-5} – 8×10^{-5} مولاري) والذي يساوي (4.96×10^{-3} – 0.049 مايكروغرام) لكل نموذج. وقد تم تقدير النترات عند طريق اختزالها الى النتريت. وكذلك تم تقدير النترات والنتريت في مزيج لهما.

Acknowledgement

I would like first to thank **Prof. Dr**. **Falah H. Hussein** and **Prof. Dr. Issam M.A. Shakir** for their able guidance and continuous encouragement and support during the various stages of this project.

Thanks are due to the University of Babylon, College of Science and Department of Chemistry for providing the necessary facilities during this study.

Thanks also so for Miss **Duha Kahled Gazalaa** for typing this thesis.

Δακη

ιλ

1.1 General Introduction

Flow-injection analysis (FIA) is defined as an automated or semiautomated analytical process cosisting of a sequential insertion of a discrete sample solution into an unsegmented continuously flowing liquid stream with subsequent detection of the analyte. It is a relatively new analytical process(1), which shows a considerable potential for high-speed precise. Flow-injection analysis is based on the injection of a liquid sample into a moving nonsegmented continuos carries stream of a suitable liquid. The injection sample forms a zone, which is then transported toward a detector that continuously records the absorbance(2). (FIA is based on the technology of flow (FIA), the quick chemistry offers high sample throughput couppled with simple and rapid method changeover to maximize productivity in determining ionic species in a diversity of sample matrices from sub-ppb to percent concentrations). The simplicity and ruggedness of FIA and combined with the outstanding accuracy, precision, and minimum detection limits. Automated flow injection systems have been applied to on-line process analysis in industrial and environmental situations with a great deal of success. Flow injection analysis is also ideally suited to monitoring solution phase chemiluminescence reactions due to the capability to mix-sample and reagent in close proximity to a detector.

The whole process of sample/standard injection, transport, reagent addition, reaction and detection can be accomplished very rapidly (seconds to loss of seconds), using minimum amounts of sample and reagents, with excellent reproducibility (e.g., coefficient of variation, cv, generally <2%).

1.2 Flow Injection Analyzer

The samplest flow-injection analyzer is shown in Fig(1-1). It consists of a pump, is used to propel the carrier stream through a thin tube, which an injection part by means of which a well-defined volume of a sample solution (S) is injected into the carrier stream in a very reproducible manner, as well as a reaction coil in which the sample zone disperses and react with the components of the carrier stream forming a species sensed by a flow-through detector where the signal is presented an a reorder. A typical recorder output has the form of a peak Fig(1-1b), and the height (H) of which is related to the concentration of the analyte. The time span between the sample injection (S) and the peak maximum, which yields the analytical readout, is the residense time (T) during which the chemical reaction takes place usually within less than 30 seconds. The injected volume is between 1 and 200 μl, which in turn usually requires no more than half a milliliter of reagent per analysis. This makes FIA an automated microchemical technique, capable of a sampling rate of at least 100 measurements per hour, with minimum reagent consumption[(3)]. Two types of automated continuous flow methods are encountered: segmented flow method, in which the analytical stream is divided into discrete segments by periodic injection of bubbles of air, and non-segmented flow procedure in which the analytical-stream is unbroken. The latter is generally termed as flow-injection analysis[(4)].

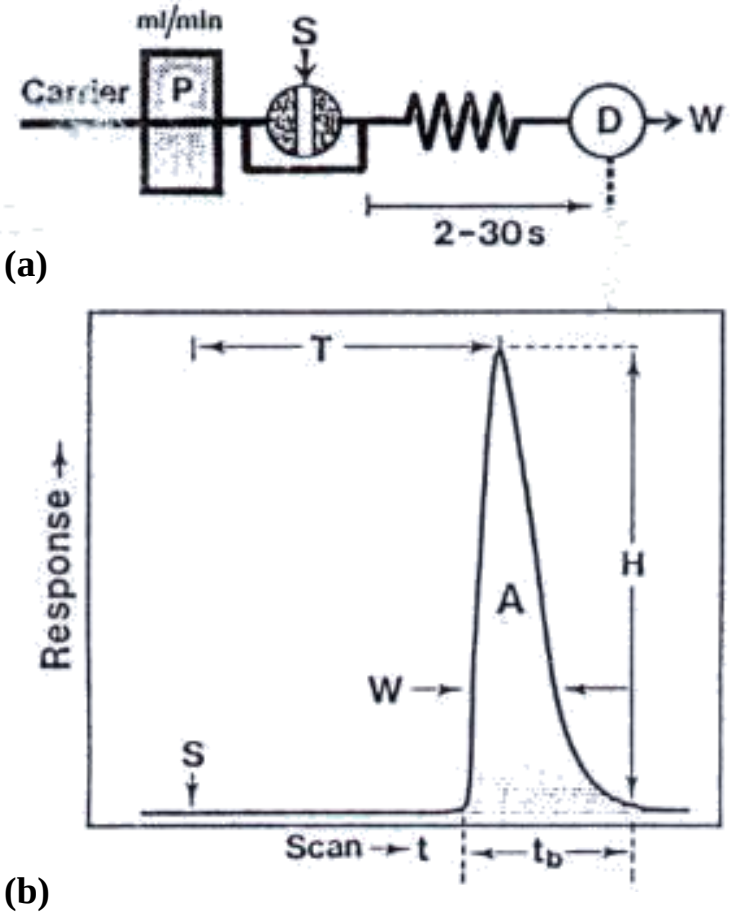

Fig. (1-1): a- Single-line FIA manifold , b-Recorder output

The conventional continuous flow analyzer shown in Fig. (1-2-a) is based on the use of air-segmented stream[5]. The purpose of segmentation is to preserve the identity of the individual samples. In such an analyzer, the samples are successive introductions from their individual containers into a tube and then forward through a pump farther into a system. The following stream is regularly segmented by air-bubbles delivered by another pump tube. The reagent is added to all individual segments, which then pass through a reaction coil, where the chemical reaction takes place. The air segmentation has to be removed in a debubber (d);

otherwise, the flow through detector would yield a disturbed signal unsuitable for direct recording of the resulting signal as shown in Fig. (1-2-b).

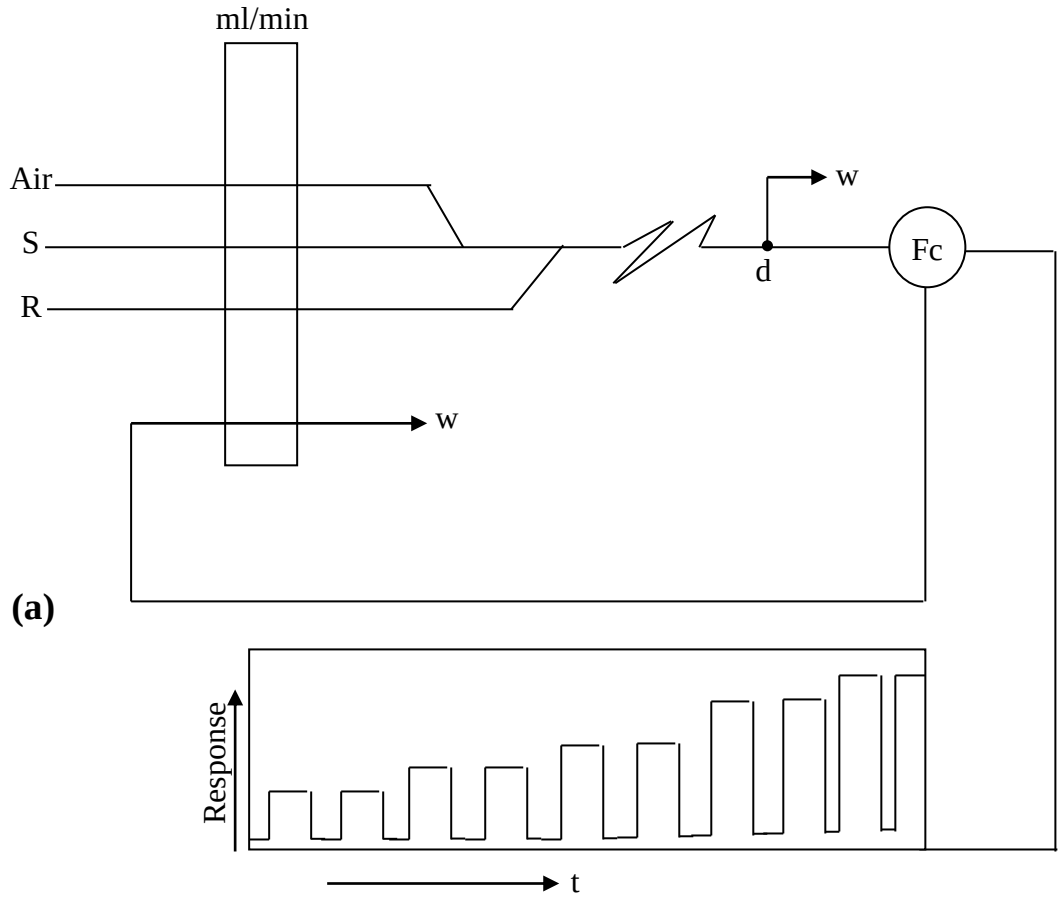

Fig. (1-2) a) Air-sementation Continuos Flow System

b) The Analysis of Fine Samples With Increasing Analyte Amount.

In the air segmented stream, each segment of fluid can be viewed as an individual container, separated from neighboring ones by an air bubble on each side, in which the liquid is homogeneously mixed as a result of circular movement caused by friction with the tube walls[6-8]. Each segment carrying a fraction of a long aspirated sample zone contributes to the gradual build up of the signal recorded by a spectrophotometric flow-through cell. The beneficial effect of air segmentation in preventing

carryover has been so obvious that the necessity of introducing air bubbles is never really doubted, although the drawbacks of their presence in the flowing stream are well known:

a) Because of the compressibility of air, the stream tends to pulsate rather than flow regularly.

b) Stream, have to be debubbled before they enter the flow cell.

c) The size of the air bubbles has to be controlled for faster sampling rates.

d) The pressure drop and flow velocities vary in the presence of air for different tubing materials[9].

e) Air bubbles in plastic tubes act as electrical insulators supporting a buildup of static electricity which disturbs potentlometric sensors[10].

f) The efficiency of dialysis, gas diffusion across in membrance and solvent extraction is lowered as a result of a decrease in the effective transfer surfaces.

g) The movement of the carrier stream cannot be exactly controlled or instantly stopped. The main features of FIA are the absence of air segmentation and the method of injecting the sample into the flowing stream, as a result of which the method merely offers some kind of technical improvement, such as: a higher sampling rate and very rapid availability of the analytical readout. Yet the most important aspect of the FIA is the concept of controlled dispersion of the sample zone, which is entirely new in analytical chemistry and an understanding of which allows the design of a FIA system exactly suited to automate a given analytical procedure[11].

1-2-1 Comparison between Beaker Chemistry and Continuous flow-injection

The rapid development of continuous flow-injection analysis and the expansion on its use are due to the number of advantages over manual operations. The aim is to replace the glassware such as beaker, pipettes, burettes, flasks,…etc by tubes, pump and valves. The FIA methods are more rapid than manual methods, within a minimal contact between the operator and toxic reagents. It can operate reproducible over long periods and the precision of analysis has been shown to be consistently good because it reduces human error[12]. In addition, it is a closed system where oxidation and contamination of samples and reagents by atmospheric air is prevented[13].

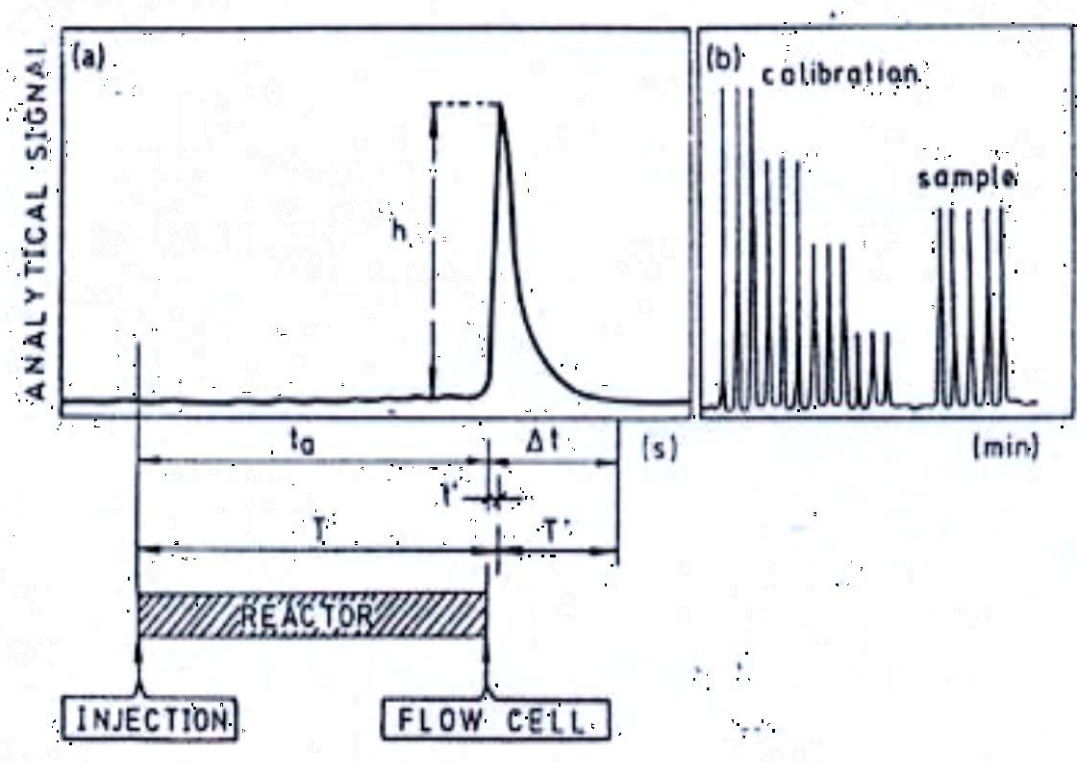

Fig. (1-3) a) FIA curve recorded at high chart-speed showing the important parameters.

b) FIA curve registered at low speed, the typical situation, injection of four standards in triplicate and an unknown sample in quintuplicate.

1-2-2 Flow-injection Analysis Signals

A schematic diagram of two FIA recording signals, which will variously be called FIA curves, or record, is shown in Fig. (1-3) where there are plots of the analytical signal (absorbance, fluorescence, intensity and potential) as a function of time.

The essential features are as follows:

i) Peak height h, which is related to the concentration of the component determined in the injected sample and the peak area could also be used.

ii) Residence time T, which is defined as the span elapsed from the injection until the maximum signal is attained. It should not be confused with the travel time, t_a, which is the period elapsed from injection to the start of the signal (1-2 % increase above base line). However, the difference between the two parameters, $t'=T-t_a$, is usually very small.

iii) Return time T′, which is the period between the appearance of the maximum signal and the return to the baseline.

iv) Baseline to baseline, Δt, defined as the interval between the start of the signal and its return to the baseline. This parameter is a measure of the dispersion or dilution of the analyte so

$$T + T' = ta + \Delta t$$

$$\Delta t = t' + T'$$

The record shown in Fig. (1-3-a) corresponds to that of a well-established FIA method, and was registered at a lower chart speed than that shown in Fig. (1-3-b) which shows the signals corresponding to four standards injected in triplicate-the usual practice- and those of a sample injected in quintuplicate.

1-2-3 Comparison between two Chief Continuous Analysis; Segmented (SFA) and unsegmented (FIA)

A detailed summary with specific data is presented in table (1-1). It should be stressed that FIA offers higher sample throughput, uses smaller a mounts of reagent, provides a larger number analytical data and opens new possibilities.

Table (1-1) Comparison between SFA and FIA

Parameter	SFA	FIA	Refe.
Sample introduction	Aspiration	in	14
Sample volume	0.2-2 ml	10-100 μl	15
Response time	2-30 min	3-60 sec.	16
Bore tubing	2 mm	0.5-0.7 mm	17
Detection	At equilibrium (homogeneity)	With controlled (dispersion)	18
Sample throughput	≤ 80 sample/hr	≤ 300 samples/hr	19
Precision	1-2 %	1-2%	20
Reagent consumption	High	Low	21
Wash-out cycle	Essential	Not required	22
Continuous kinetic analysis	Not feasible	Stopped-flow	23
Titrations	Not possible	Possible	24
Data produced	Peak height	Peak height Peak area	

		Peak width Peak to peak distance	

1-2-4 Selectivity in Continuous Flow Analysis

When all experimental parameters such as sample volume, residence, dispersion, temperature, time of exposure of sample and interferent to reagent can be rigidly controlled and reproducibility maintained with these conditions met, it makes sence to express the selectivity of a method for B of concentration of C_B, by a numerical value. As any interfering species A of concentration C_A, toward an interfering species always appear as positive or negative, this interference can be expressed quantitatively as the selectivity coefficient K_{AB}[25].

$$C'_A = C_A + K_{AB} C_B \qquad \ldots(1\text{-}1)$$

where C'_A is the total concentration of A measured, and K_{AB} is the selectivity coefficient of B in determination of A. The dispersion coefficient of the species are

$$D_A = \frac{C^\circ_A}{C_A}, \quad D_B = \frac{C^\circ_B}{C_B} \qquad \ldots(1\text{-}2)$$

If the height h of analytical signal obtained and the height of the detection response are linearly related to the concentration of A and B, the actual height of the signal will be given by:

$$H = KC'A \qquad \ldots(1\text{-}3)$$

where K is the proportionality constant between signal height and concentration. If no interferent is present, then:

$C^\circ_B = C_B = 0$ the height of signal could be obtained as follows:

$$h_1 = K_{CA} = K\frac{C^{\circ}_A}{C_A}, \quad D_B = \frac{C^{\circ}_B}{C_B} \qquad \ldots(1\text{-}4)$$

whereas if B contributes to the signal yield by A, the signal height is

$$h_2 = K(C_A + KABCB) = K\left[\frac{C^{\circ}_A}{D_A} + K_{AB} = \frac{C^{\circ}_B}{D_B}\right] \qquad \ldots(1\text{-}5)$$

If all measurements were made at a point where both dispersion coefficients have the came value $D_A = D_B$, then:

$$D = K\frac{C^{\circ}_A}{h_1} = \frac{K}{h_2}\left[C^{\circ}_A + K_{AB}C^{\circ}_B\right] \qquad \ldots(1\text{-}6)$$

Hence

$$K_{AB} = K\frac{C^{\circ}_A}{C^{\circ}_B} = \left(\frac{h_2}{h_1} - 1\right) \qquad \ldots(1\text{-}7)$$

This expression allows the selectivity coefficient to be calculated from the initial analyte, the interfernt concentration, the signal obtained in the presence and the absence of the interferent. The K_{AB} values could be positive or negative, depending on the sign of the interference. Solving Eq. ( ) for h_2 gives

$$h_2 = \frac{h_1 K_{AB}}{C^{\circ}_A} C^{\circ}_B + h_1 \qquad \ldots(1\text{-}8)$$

The plot of h2 against C°_B for series of experiments gives straight lines with slopes of h_1K_{AB}/ C°_B and intercept h_1. The slope gives the selectivity coefficient ($\pm K_{AB}$).

Three ways could be used to overcome the interferences[25]:

i) Injection using a dual valve into separate channels with synchronous merging.

ii) Injection using a dual valve into separate channels with an asynchronous merging.

iii) Injection, using two valve series into a single channels with an asynchronous merging[26].

The first method is applied with the aid of manifold illustrated in Fig.(1-4).

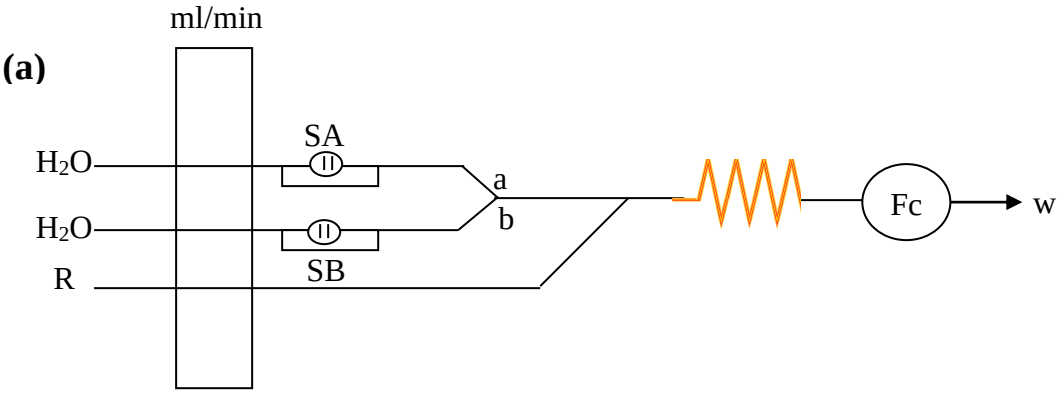

Fig. (1-4) Synchronous merging of samples . S^A and S^B injected simultaneously into two separate carrier stream (water).

a) Manifold with identical length of a and b.

b) Test of sychroization, where identical sample volumes of S^A and S^B are injected.

The synchronous merging is achieved by pumping to injected zones equal volumes of A and B through equally long lines a=b in which the pumping rates are identical. As shown in Fig. (1-4), a single peak was recorded and it increased as the concentration did. When an exact sychronization of the two injected zones is achieved, the dispersion of both species in the merged zone is identical along the whole merged gradient, and it is practical to measure peak maximum height and to calculate the K_{AB} value. The second method deals with the injection into separate lines with a synchronous merging[27]. The signal must be measured at t_m so that $D_A=D_B$. For brevity, only the manifold used to implement that method with a dual injection value will be discussed. Its basic design is shown in Fig. (1-5)

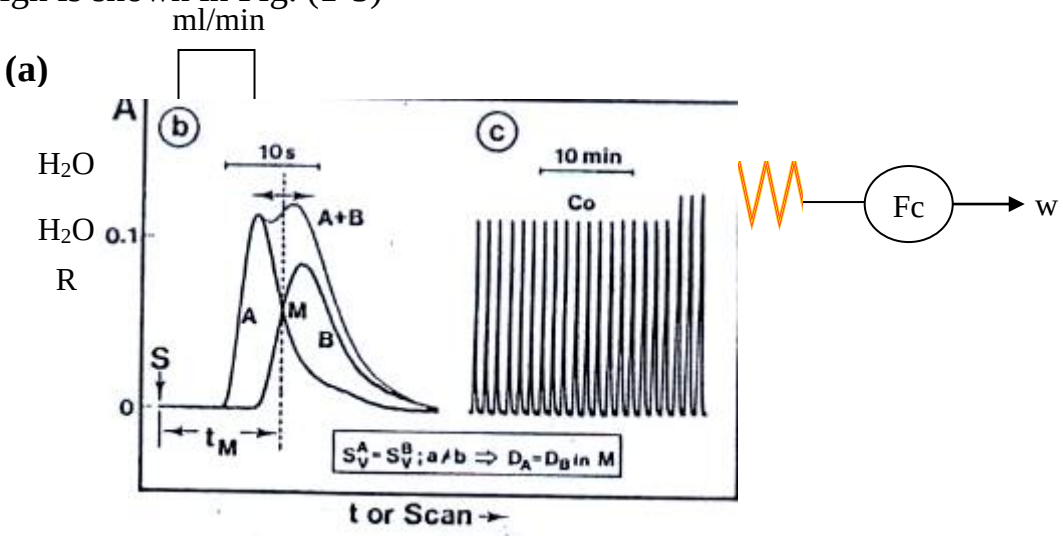

Fig. (1-5) Synchronous merging of samples . S^A and S^B injected simultaneously into two separate carrier stream .

a) Manifold with (a ≠b. b) The signals obtained by injection samples of identical volume .

The dual injection valve injects two equal volumes into anaqueous carriers which circulate along lines with different lengths where a≠b between the valve and merging point. The resulting mixtures pass through the reaction coil, which leads them to the photometer. Fig. (1-5)

shows the FIA record of the behaviour of each species, S^A and S^B when injected separately and together S^A+S^B. At the point where both peaks obtained by separate injection intercept each other, $D_A=D_B$, therefore this point indicates the measurement time t_m. The point M indicates the dispersion for S^A and S^B are identical. Fig. (1-6) shows the merging zones for S^A and S^B separately and together.

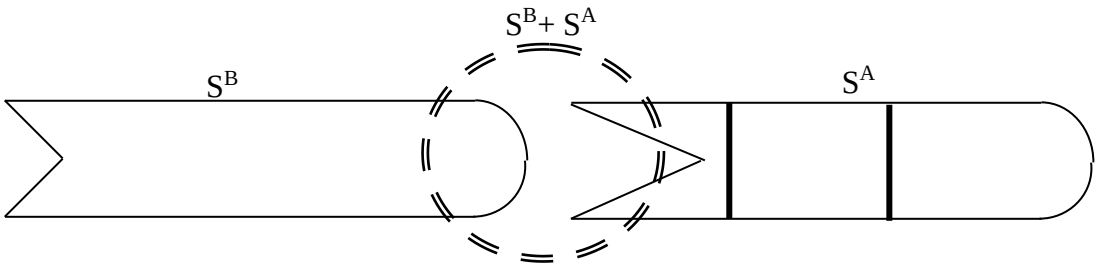

Fig. (1-6) The merging zones of S^A and S^B

The practical advantage of the separated solutions methods is that only a few solutions; essentially only a single solution of A and a few solution of B. Moreover, this method has a serious draw back; it is essential that the flow rates in both channels shown be maintained absolutely constant through all the experiments. The injected zones must merge stoictly reproducible at all times, for both synchronous and asynchronous merging. The precision is critically dependent on maintaining not only the two pumping rates, but also their absolute values, which is significantly more difficult[25]. The third method deals with the injection into a single live with asynchronous merging as shown in Fig. (1-7).

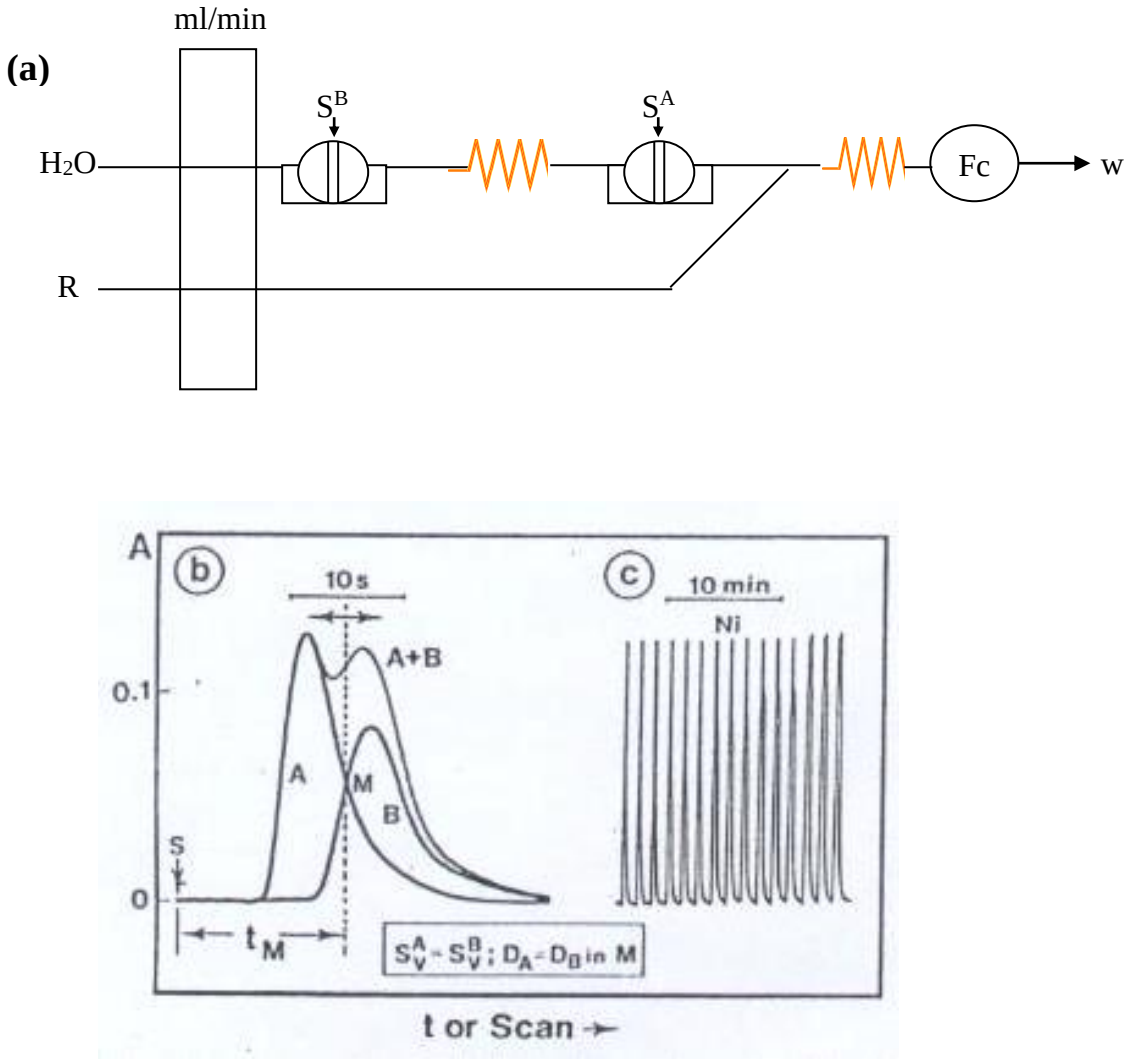

Fig. (1-7) Asynchronous Merging of Identical Volumes of Samples S^A and S^B.

1-2-5 Selectivity in Flow-injection Analysis

As a rule, FIA methods are less sensitive then their manual and segmented flow Analysis (SFA) counterparts for two reasons:

1- As the reaction time is rather short, equilibrium is not attained.

2- The physical dispersion or dilution of the sample in the carrier results in a signal of lower intensity than that corresponding to the undiluted plug. Valcarcel and Castro[12] attempted to improve the sensitivity by adjusting either reaction time or the dispersion leads to opposing effects, since the use of a lower flow-rate, to increase the reaction yields, results in an increased dispersion. Both the chemical and FIA variables of each flow-injection manifold should be optimized in order to attain the maximum sensitivity level.

The sensitivity can be improved by introducing suitable modifications to the FIA manifolds, i.e., a merging (where the reagent converges with a pure solvent stream into which the sample plug is injected) is used to achieve a greater extent mixing of reagent sample and plug. In addition, the sensitivity will be increased by increasing the injected sample volume when using this type of configuration instead of injecting samples directly into the reagent stream. Moreover, to improve the sensitivity by using continuous separation system incorporated into FIA, assemblies can achieved by using a microcoloum pack with cheating exchange resin to concentrate heavy-metal ions in sea-water samples[12].

The two zones A and B are injected by means of a double valve into a single carrier line, and the two injection zones are separated by a suitable length of delay coil. Sample A reaches the detector before sample B. As sample B has to travel through a longer path than A, the injection of identical concentration in the two valves will result in peaks of different heights. Once M and t_m have been determined, they can readily be rechecked by injecting a fixed concentration of alternately by each value: if M is unchanged, the peak height measurement for each injection should be identical. It is interesting to know that the three methods provide K_{AB} values that are consistent with one another.

1-2-6 Flow-injection and Chromatography

In this section a simplified comparison is presented to show the great similarity of this technique with high performance liquid chromatography[28].

Continuous flow analysis

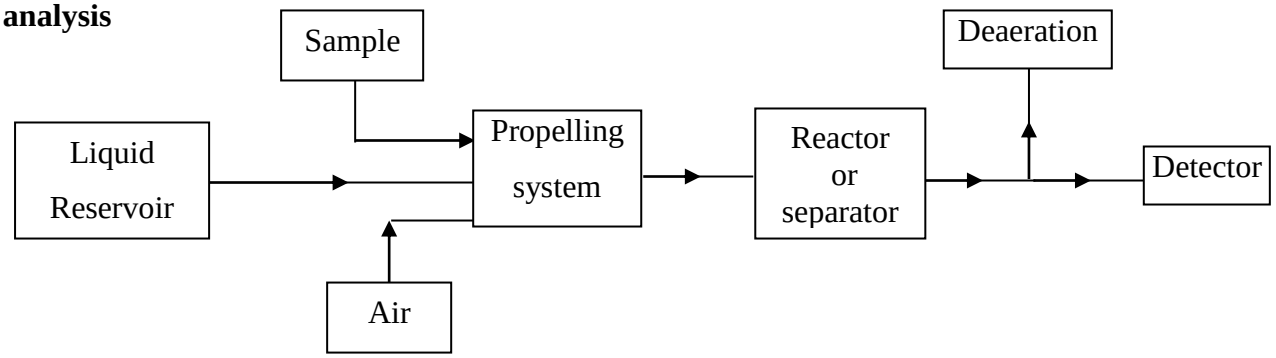

Flow-injection analysis

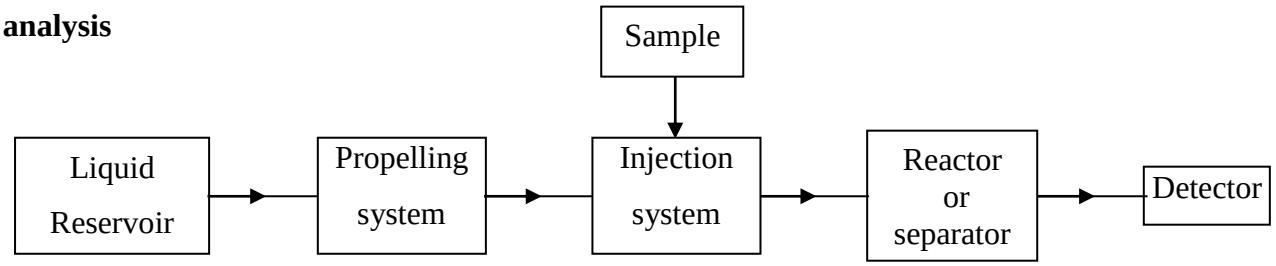

Liquid chromatography

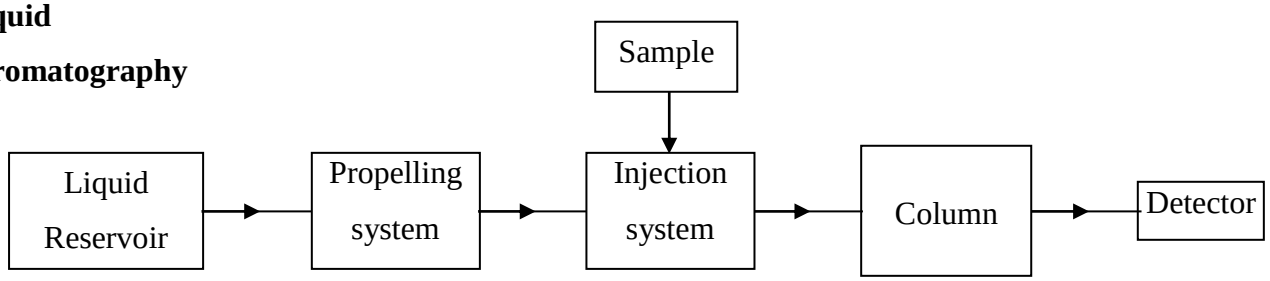

Fig. (1-8): Schematic Block diagram representation of FIA, SEF and (Liquid chromatography)

According to Vandereslice *et. al.,*[28-29] the following similarities should be emphasized, miniaturization capability, injection, unsegmented flow, small sample volume, signal profile and the fact that lack the characteristic lag phase of SFA. Table (1-2) shows common characteristic of HPLC and FIA.

Table (1-2) list the common differential features FIA and HPLC (high performance liquid chromatography)

Common characteristics		**Differential characteristic**	
		HPLC	**FIA**
Unsegmented flow	Interface	Always	Accasionally
Sample introduction injection	Column	Essential	Possible
Sample volume: small	Pressure	High	Low
Flow-rate: variable	Data produced	Peak height/area	Peak heigh/area width, peak to peak distance
Tubing diameter: small	Cost	High	Low
Lag phase: negligible	Versatility main	Limited	Great
	analytical purpose	Several components in a single sample	A single component in many sample

The substantial difference between FIA HPLC, is that HPLC operates at pressure more than 70 atm whereas a FIA system could be

operates at about 0.5 atm by using a simple peristaltic pump. That is because in HPLC the liquid has to be forced through a tightly packed column material, whereas in FIA the sample zone passes through short length of narrow tube. Basically, however, FIA and HPLC are two quit different techniques, because their principles and purpose are different[30-32].

1-2-7 Dispersion

Dispersion is defined as the ratio of the concentration before and after the dispersion process has taken place in those elements of fluid, which correspond to the maximum on the dispersion curve, Fig. (1-9), by denoting C: as the original concentration of the injected sample solution and C^{max} as the concentration in the element of fluid corresponding to the peak maximum[30].

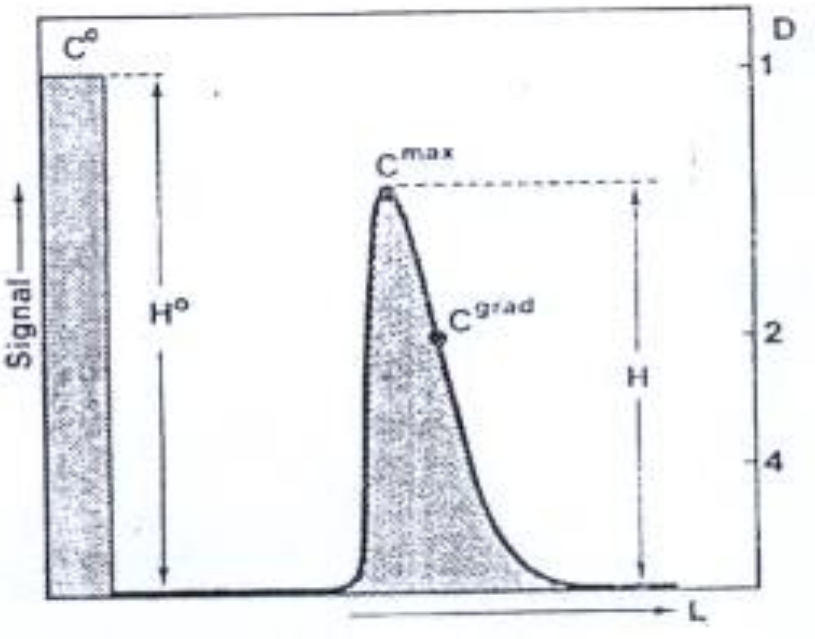

Fig. (1-9) Dispersion D in the FIA system

The controlled dispersion of the sample zone which occurs during its passage through the system towards the detector results in a response curve as shown in Fig. 10. Fig. (1-10) shows a peak shape characteristic of the flow injection system. Naturally, the sample zone bradens as it moves downstream and changes from the original asymmetrical shape to a more symmetrical and eventually Gaussian form[28].

Fig. (1-10) Typical peak forms and corresponding concentration profile observed: (A) at the point of injection; (B) shortly after injection; and (C) after passage through an open narrow tube.

Generally, dispersion can be classified into three brad categories; limited, medium and large, which can be employed in the following ways.

If the original composition of the sample solution is to be measured, e.g., pH or conductivity, limited dispersion pf the sample zone is required. Inorder to ensure that the readout as obtained at the centre of the sample zone is not effected by any mixing with the surrounding carrier stream. Also when the flow injection system is to serre merely as a means of reproducible introduction of the samples into a detector, the conditions of limited dispersion are most suitable[33]. However, in medium dispersion the centre of the sample zone must be mixed effectively with the carrier stream and often with several reagents in sequence and if the interfacial concentration profiles between the sample plug and the carrier stream or to be employed, a large dispersion of the sample zone is required. Fig. (1-11) shows the types of dispersion together with the corresponding vessel geometries.

D 1 to 3

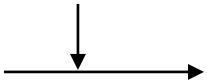

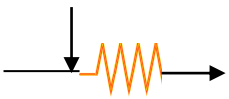

D 3 to 10

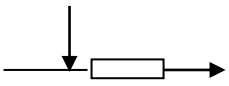

D ≥ 10

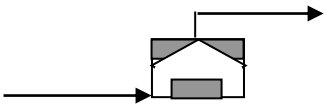

Fig. (1-11) Types of dispersion (D), together with the corresponding vessel geometries.

1-2-7-1 Factors affacting dispersion

The overall dispersion within an FIA system is the sum of the dispersions originating in three main parts of system[34]:

$$D = D_{injection} + D_{transport} + D_{dectector} \quad ...(1\text{-}10)$$

Where $D_{injection}$ is the dispersion due to the sample volume and to the geometric aspects of the system, $D_{transport}$ is the most significant contribution to the overall dispersion which includes the contribution of the reactor geometry and the flow rate, and $D_{decteror}$ donetes the contribution of the flow cell geometry (shape and dimensions) to the dilution. All three terms include contributions from factors such as deal volumes connectors, which can be very important in some instances.

Sample volume

Fig. (1-12) shows the FIA signals obtained with an elementary FIA system which increasing volume ($v_1<v_2<v_3<v_4$) of a dye have been introduced, and recorded by starting from the same position on the chart so as to obtain a series superimposed curves. Ruzicka *et. al.*,[35] concluded that travel time does not depend on the injected volume however the residence time and baseline-to-baseline are both increases with the injected volume. The dispersion coefficient decreases with mcreasing

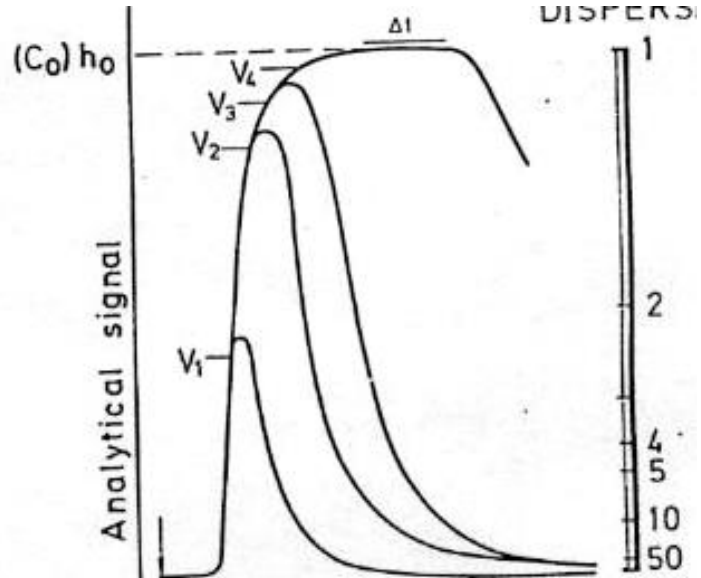

Fig. (1-12) Influence the injected sample volume on dispersion coefficient

(i) Hydrodynamic factors

Vanderslice's expressions indicate the relation between the flow rate, q and baseline-to-line times

$$t_a = \frac{K}{q^{0.125}} \qquad \ldots(1\text{-}11)$$

and K constant which = $\frac{109R^2D^{0.025}.L^{1.025}}{f}$

K′: constant =

$$\frac{35.4R^2D^{0.025}.fl^{0.64}}{D^{0.36}}$$

$$\Delta t = \frac{K'}{q^{0.64}} \qquad \ldots(1\text{-}12)$$

where t_a is travel time , Δt is baseline-to-line time and q is the flow-rate. Fig. (1-13) shows that the dispersion, t_a, Δt, should decrease with the increasing flow-rate[35].

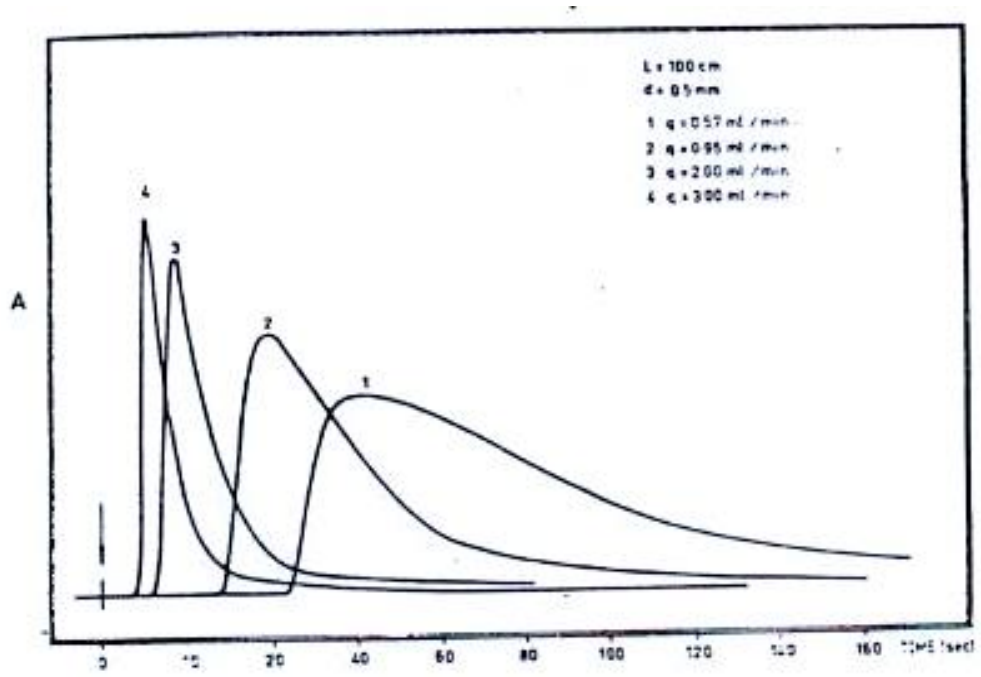

Fig. (1-13) Influence of flow-rate an the dispersion, time and peak width.

(ii) Geometric factors

Geometric factors deals with the influence of the reactor shape and its dimensions on the dispersion[36]. There are two shapes of reactor:

(a) straight tubes

Fig. (1-14) shows that t_a Δt increase with the reactor length according to Vanderslice's predictions

$Ta = KL1.025$

and

$$\Delta t = K'L^{0.64} \quad \ldots(1\text{-}14)$$

where L is the reactor length.

The dispersion coefficient increases with the increasing reactor length, which is consistent with Ruzicka's expression.

$$D = KL^{1/2} \quad \ldots(1\text{-}15)$$

Where D is the dispersion coefficient

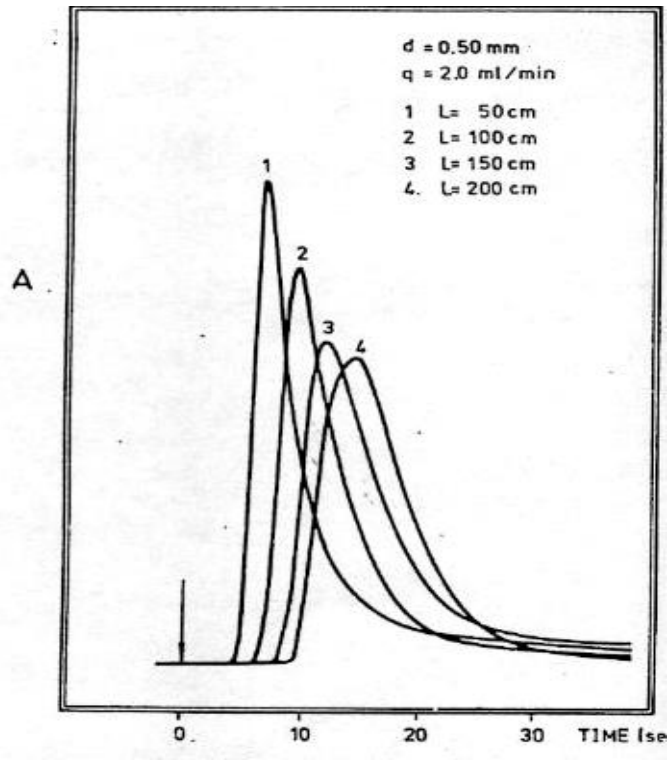

Fig. (1-14) influence of reactor length on the signal obtained which shers brocedeing increased (50-200 cm) as the length (b) coils

Fig. (1-15) shows the signals obtained with a conventional FIA system for a reactor of constant length L=125 cm in the form of straight tubing(1), a coil with diameter 26mm (2), and a coil with diameter 4mm(3). From this curve the smaller diameter, the smaller the

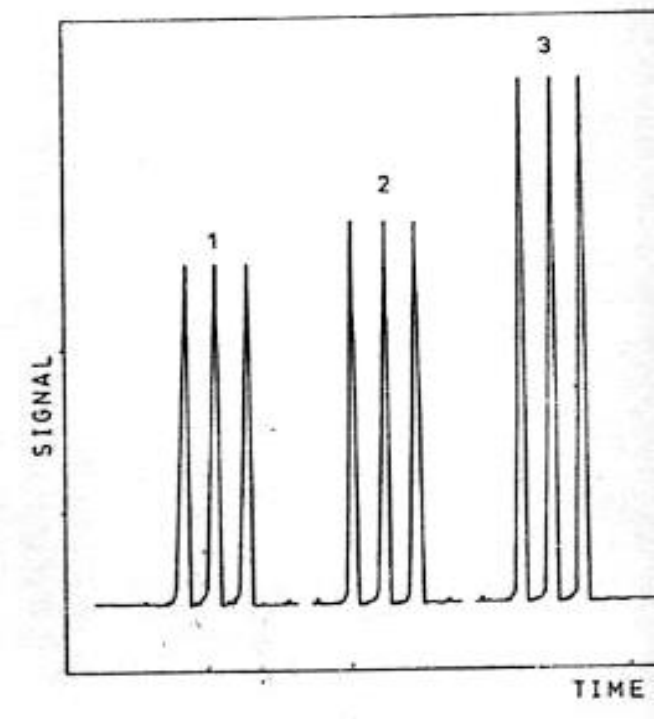

dispersion[37].

Fig. (1-15) influence of coil diameter an the dispersion

1-2-8 The stimulus response technique

The flow injection analysis response curve is a result of two processes, the physical process of dispersion of the sample zone within the carrier stream and the chemical process of formation of a chemical species. The physical process of material dispersion is due to the hydrodynamic processes which take place in the flow through system and is therefore conveniently investigated by stimulus response technique[38]. This technique is based on introduction of tracer into flowing stream and on measurement of the dispersion of the tracer as caused by the transport process throughout the system. If the tracer is injected as a zone (stimulus), then the observed response reflects the dispersion in the system through the increase of the width of the tracer zone as increased by the combined contribution from convection and diffusion. These two steps occur simultaneously. If the response curve has a Gaussian shape, then its first statistical moment, the mean of the tracer curve corresponds to the maximum peak, when expressed by units of time. The first moment allows estimation of the average time available for chemical conversion, since it constitutes the mean residence time that the tracer material in average has spent in the reactor. The second statistical moment is proportional to the peak width, and for the Gaussian peak, it is the second power of the half peak width measured at 0.61 peak height[30] as shown in Fig. (1-16).

The increase of the second moment caused by transport through the reactor is due to the dispersion. The relation between dispersion and

residence time is an important parameter for optimization of all types of flow systems as shown in Fig. (1-17).

It is application varies depending on the purpose. These are two reasons: first is that the mixing in FIA is nonhomogeneous and directional (since it yields a concentration gradient in both axial and radial direction), and as a result of this stratification the ensuing chemical reactions take place gradually, while the reagent penetrates the sample gradient during the movement of the dispersing zone through the channel. Therefore, the FIA response curve is not only a result of the processes that occur at the detector location, but also of all the processes that gradually take place upstream in the FIA system at variable reagent concentration. The FIA readout is selected at peak maximum according to Seberga's model[38] as shown in Fig. (1-18) and Fig. (1-19) the movement of the liquids in the tubes could described by the convective-diffusion equation.

$$D_m\left(\frac{\partial^2 c}{\partial x^2}+\frac{\partial^2 c}{\partial r^2}+\frac{1}{r}\frac{\partial c}{\partial t}\right)=\frac{\partial c}{\partial t}+2F(1-\frac{r^2}{R^2})\frac{\partial c}{\partial x} \qquad \ldots(1\text{-}16)$$

where D_m is the molecular diffusion coefficient, c is the concentration, x is the distance along the tube, r is the radial distance from the tube axis, R is the tube radius, t is the time and F is the average flow velocity. The reduced velocity is described by the peclet]Number

$$Pe = R(2F)/D_m \qquad \ldots(1\text{-}17)$$

the reduced distance x

$$x = D_m\, x / R^2(2F) \qquad \ldots(1\text{-}18)$$

The reduced time T

$$T= D_m\, t /R^2 \qquad \ldots(1\text{-}19)$$

Were selected to approximate the range of FIA conditions, that is, Pe>1000

$0.004 < x < 1.0$

$0.002 < T < 0.8$

When the contribution of diffusion to radial transfer in negligible, a sharp rise at the peak leading edge and exponential decay at its tail, characteristic of convective dispersion due to a poisseuille profile are observed. For long residence times (T=0.4) a nearly Gaussian peak is observed, while for shorter residence times a peculiar double-humped peak is observed. Ruzicka and Hansen[38] are another equation for baseline to baseline value.

$$\Delta t_b = 56.7\, R^{0.293}\, L^{0.107}\, Q^{1.057} \qquad \ldots(1\text{-}20)$$

and for dispersion coefficient D at any time t:

$$D = C_o / C_{max} = 2.342\, L^{0.106}\, Q^{0.206}\, R^{0.496} \qquad \ldots(1\text{-}21)$$

The second reason is that flow injection analysis encompasses a much wider range of solution, that is sample dilution, preconcentration, reaction rate measurement and multicomponent detection.

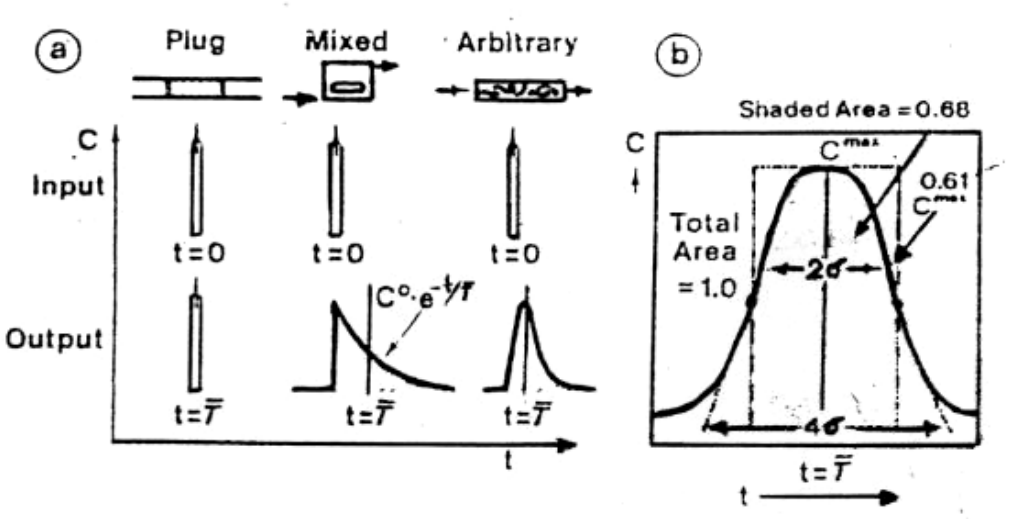

Fig. (1-16) a- Curves for plug, mixed and arbitrary flow

b- For arbitrary flow, a Gaussion-shaped curve is eventually achieved

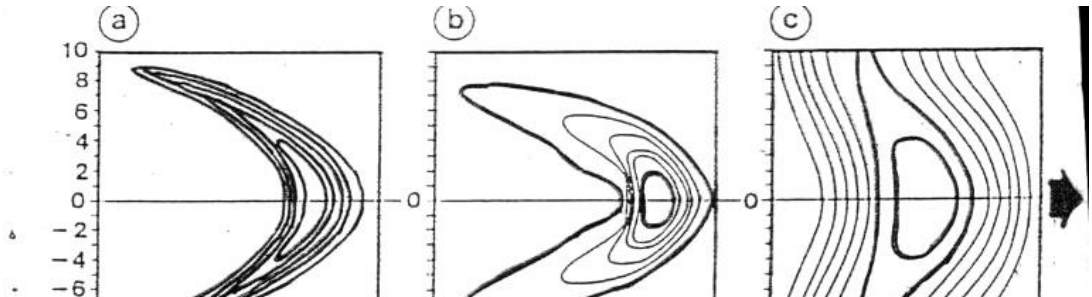

Fig. (1-17) Dispersion of a sample plug in a straight tubular channel.

Fig. (1-17) Dispersion of a sample plug in a straight tubular channel.

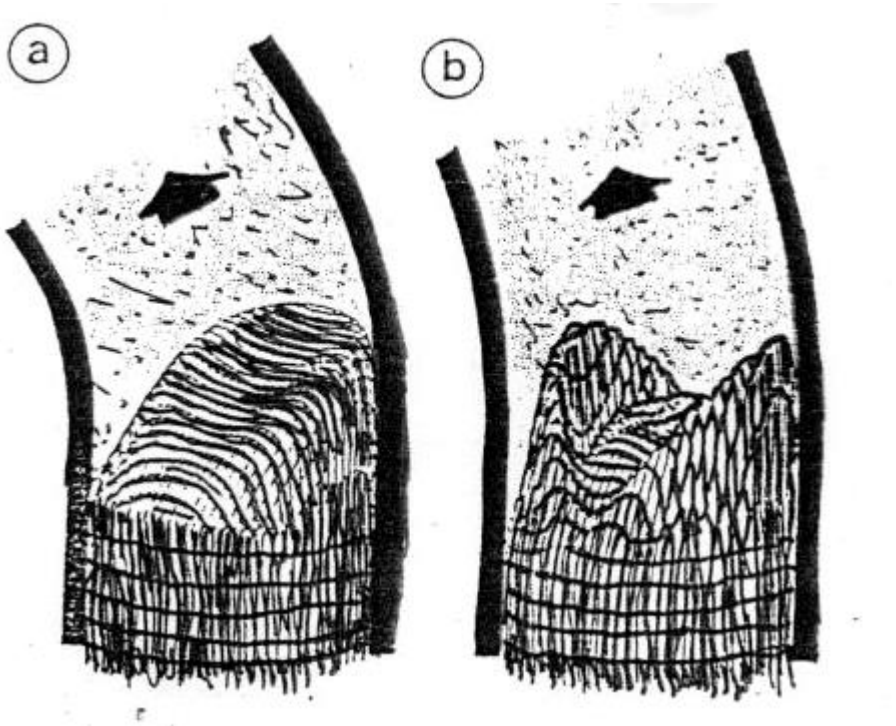

Fig (1-18) Dispersion in coiled tubes. a) Equivelocity profiles in axial direction. b- Equivelocity profiles in radial direction

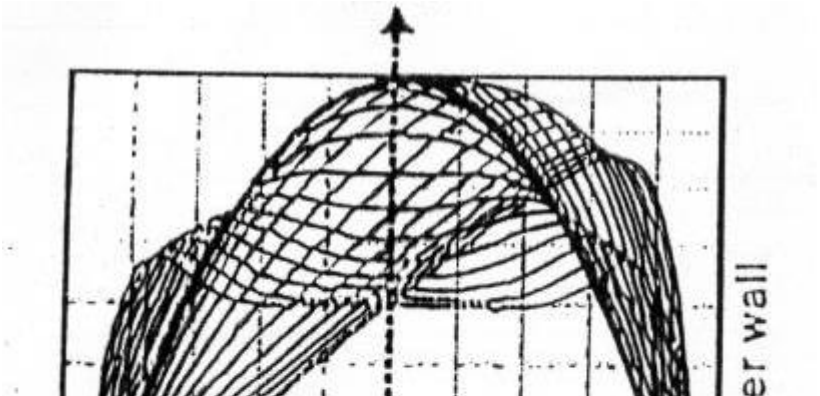

Fig (1-19) Axial velocity profiles in a coil tube.

1-2-9 Operation modes of manifold

Diff voracious mode of operation could be conducted in FIA system mainly single line and multiple line system in the following section a brief clisscussion is presented

(i) Single-line manifolds Fig. (1-20) shows the simplest FIA system which consists of one tube through which the carrier stream moves towards the flow through detector. Depending on injected volume sample(s) tube length (L) and flow geometry. In this system, limited, medium, and large dispersion can be achieved[39,40].

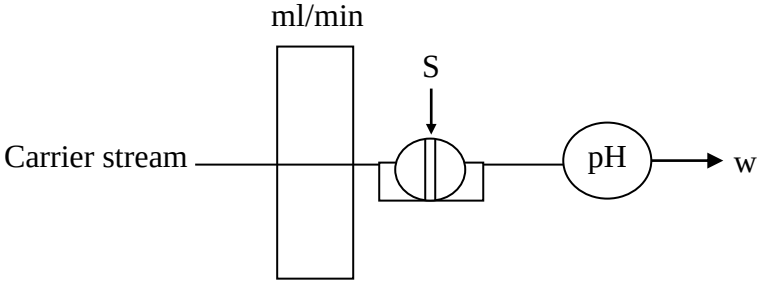

Fig. (1-20) single-line manifolds

(ii) multiple lines sequential use of only two reagents is a simple matter because a manifold designed for this purpose involves only one confluence point at which a second reagent is added to the sample zone when carried by the stream of the first reagent[41] as shows in Fig. (1-21).

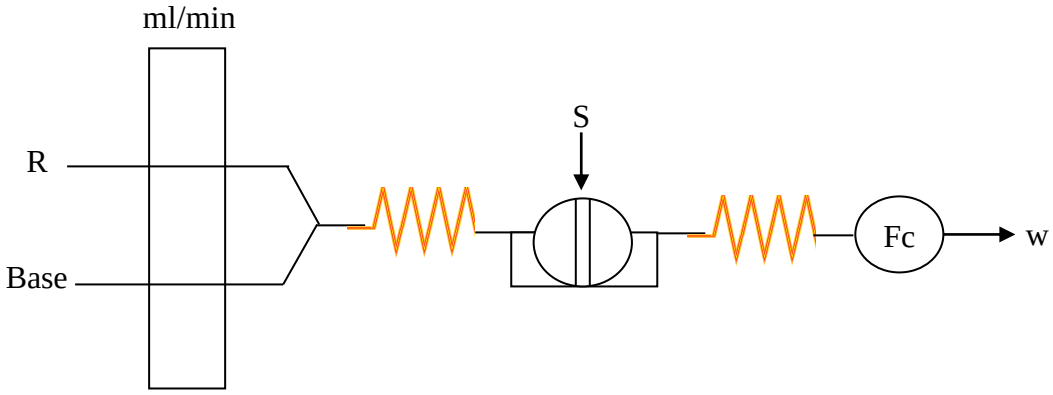

Fig. (1-21) Two-lines manifolds

And, Fig. (1-22) shows the manifolds of three lines where the reagent are added sequentially and then the reaction product was occurs[42,43].

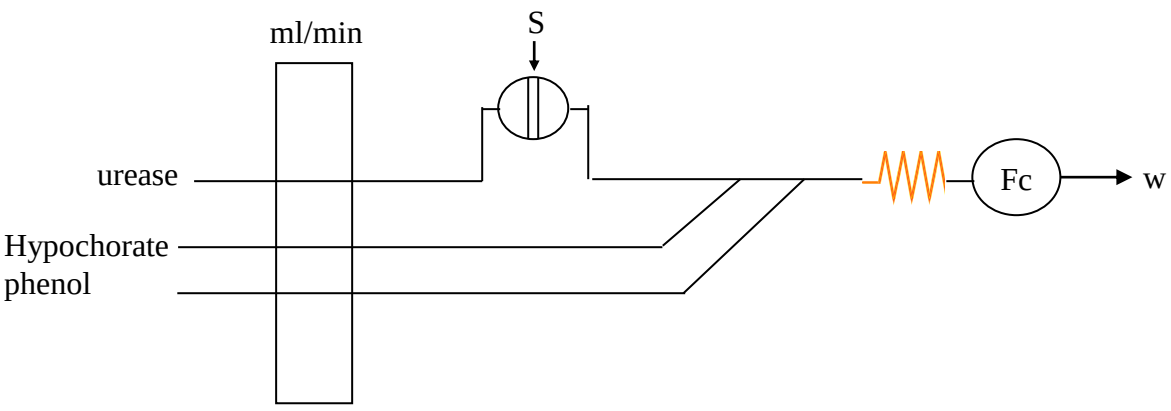

Fig. (1-22) Three-lines manifolds

1-2-10 The merging zones

The relatively high reagent consumption is the main disadvantage of all continuous flow systems, which, in contrast to batch analyzer , use the reagent continuously even when there is no sample present in the apparatus notably during the startup and shutdown procedures.

This problem is not as great in FIA, where the volume of the sample path is seldom larger than a few hundred microliters and therefore easy to fill and wash in a very short period using small amounts of reagent or wash solutions. If however, an expensive reagent or enzyme is used, it is wasteful to pump solutions continuously, because the reagent also occupies those section of the sample path where the sample zone is not present simultaneously[44]. The merging zones principle avoids this uneconomic approach by injecting the sample and introducing the reagent solution in such a way that the sample zone meets the selected section of the reagent stream in a controlled manner. The rest of the FIA system is filled with wash solution or only pure water. This can be achieved in two different ways, by the merging zones systems which are based on intermittent pumping[45] as shown in Fig. (1-23.a), where two pumps are operated is such a way that when pump 1 is the position, pump II is in the position, and vice versa. Thus the sample zone is first transported from

the injection port by mean of pump I, then when a chosen distance from the merging point is reached pump II is started, which continues to bring the carrier stream forward while the reagent is being added Fig. (1-24). After the sample zone has passed the merging point, point I is reactivated

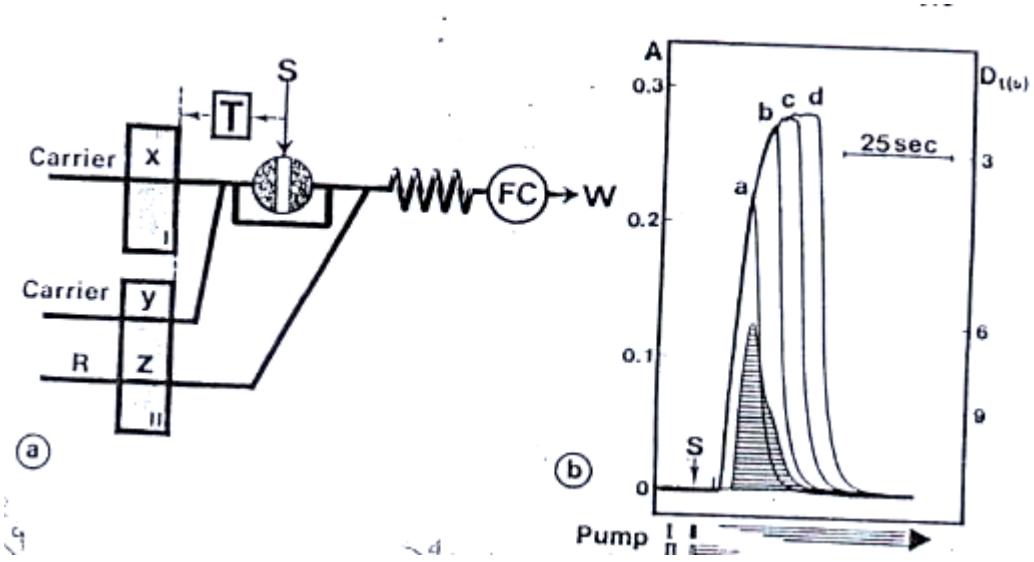

Fig. (1-23) a) FIA manifold for merging zones system based on intermittent pumping.

b) Recorder trace obtained with the system in (a).

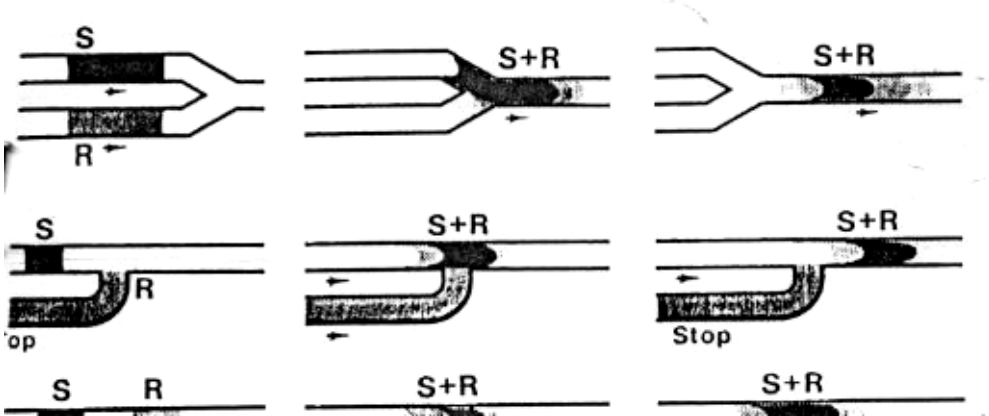

Fig. (1-24) The principle of zone merging a) intermitlent pumping b) zone penetration c)showing, from left to right, the sample(s) zone and reagent (R) zone separately, during the initial contact, and then merged further downstream.

while pump II is stopped again. This approach allows the length of the reagent zone to be regulated simply by choosing different go and stop periods by means of the timer (T), and makes it possible to create different concentration gradients on the interface between the sample zone, reagent solution and carrier stream Fig. (1-23.b). Variations on theme are numerous. Thus, by choosing different lengths of reagent zone, and by letting it overlap in different ways over the sample zone, an individual blank for the reagent alone and for the sample zone alone, as well as the peak height resulting from the chemical reaction between the components of the sample and reagent solution[46]. And by the suggestion of the use of a multiinjection value for the FIA merging zone approach[47], the purpose of using a value, such as that shown in Fig. (1-25) and Fig. (1-26) , is to inject sample and reagent zones into two separate carrier stream pumped at balanced flow rates so that they meet in a controlled manner. As distilled water (or diluted buffer-detergent mixture) might be used as carrier in both stream. The reagent volume consumed per determination may be 30μl or less[43]. The carrier streams might be pumped continuously-for single- point measurement or intermittently, for stopped flow measurements. The advantages of the merging zones are,

that it alleviated the reagent blank problem[48], cheap, rapid, and flexible analytical facilities that could be used even in small laboratories[49,50,51].

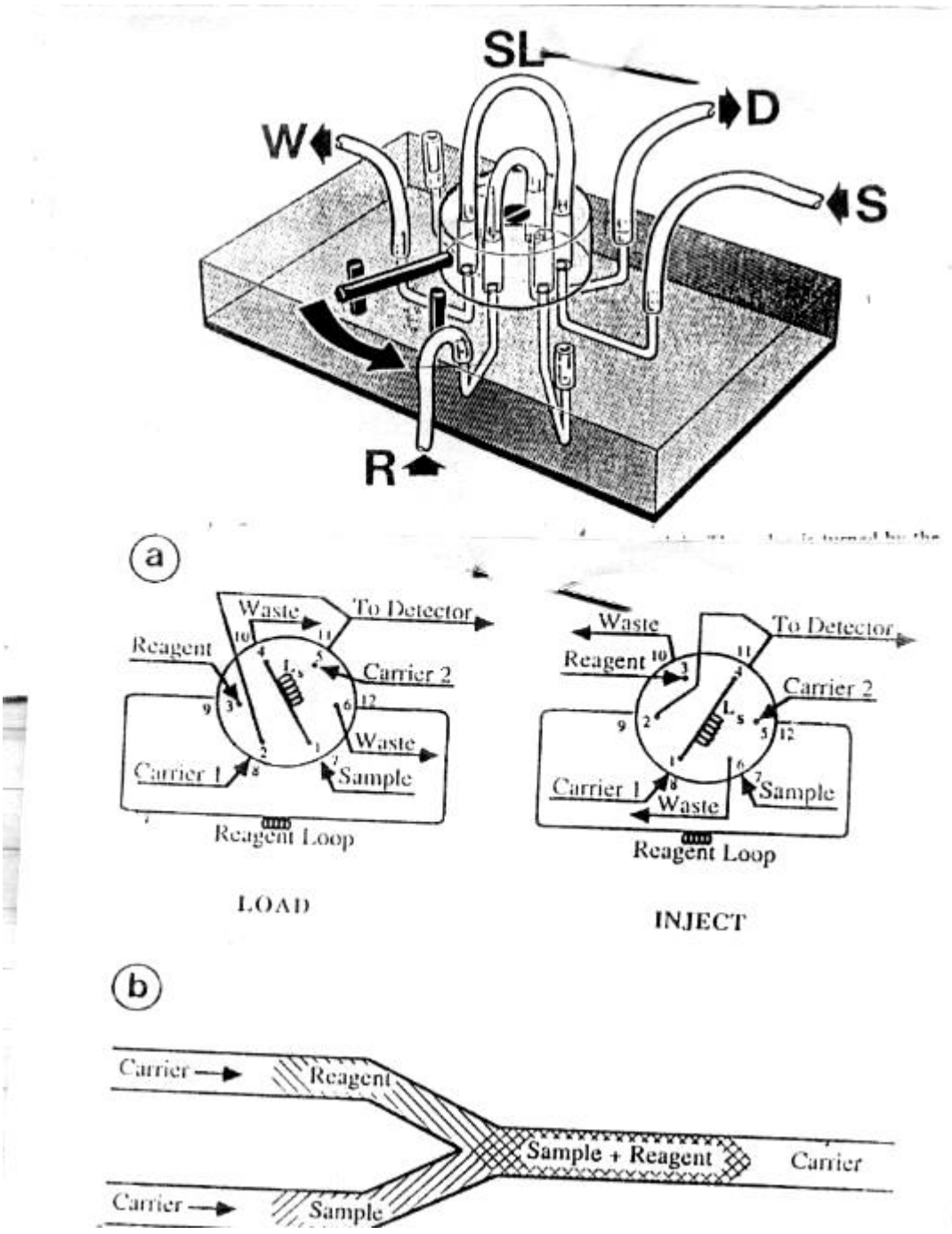

Fig. (1-25)

Fig. (1-26).

1-3 Hydronium ion “Oxonium ion”

The acid name comes from the Latin “acidus” which means “Sour” and refers to the sharp order and sour taste of many acids. Vinger, for example, tastes sour because it is a dilute solution of acetic acid in water. Lemon juice testes sour because it contains citric acid. Milk turns Sour when it spoils because of the formation of Lactic acid, and the unpleasant, sour odor of rotten meat or butter can be attributed to compounds, such as butyric acid, that is formed when fat spoils. Vegetable dyes, such as litmus, have been used for more than 300 years to distinguish between acids and bases(52). Acids were already known in antiquity of their sour taste and for their power to solubilize metals. The Latin word for sour is “acidus”. In the early middle ages, the Arabs used intric acid to separate silver from gold by selective dissolution, the use of vegetable dyes as acid –base- indicators goes back at least to Robert Boyle (1627-1691). However, the nature of acids was still obscure. In the eightieth century it was believed that photgiston, from the Greek work for flame, φλοζ (pronounced ‘phlox’), was the acidic principle,. Lavoisier observed that burining elements such as carbon, nitrogen and sulfure in oxygen gave compounds that, when dissolved in water, produced acids(52). He therefore associated acidity with oxygen, which he named the generator of acid (from οζνσ), pronounced “oxus”. Greek for acid . It was only after Davy showed in (1811) that hydrochloric acid conteins no oxygen, and Von Liebig introduced the concept of mobile, replaceable hydrogen (1838) that acidity can to be associated with the presence of hydrogen rather than oxygen.

Arrhenius introduced the idea of electrolytic dissociation in 1884. The replaceable hydrogen then became a hydrogen ion which could dissociate from an acid as in

$$HA \rightleftharpoons H^+ + A^- \qquad \ldots(1\text{-}22)$$

The Arrhenius definition is quit appropriate for aqueous solutions, because water itself can dissociate into H^+ (or, written in its hydrated from as H^+_3O) and OH^-. The alternative definition, given by Bronsted (1923), which emphasizes the complementary nature of acids in aqueous solutions. It considers as an acid any substance that can donate s proton. This definition is independent of the nature of the solvent, and applies even in the absence of any solvent, as in the vapour phase reaction of HCl with NH_3 to yield NHuCl. At the same time, Lewis (1923) suggested a further generalization, by considering as acid any substance that can accept an electron pair(52). In water, this definition is equivalent to those Arrhenius and Bronsted, since H^+ lacks electrons, while OH^- has a pair of electrons it can share. The Lewis definition has been proved very useful in non-aqueous chemistry. Such as in molten salts(52). There is no such theory as an H^+ ion in aqueous solution. The H^+ ion is produced where an acid ionizes is attached to at least one water molecule to form an H^+_3O ion. There is a reason to believe that the H^+H produced in this reaction actually shared by at least by four H_2O molecules, to form an $H(H_2O)^+_4$ or $H_9O^+_4$ ion as shows in Fig. (1-27).

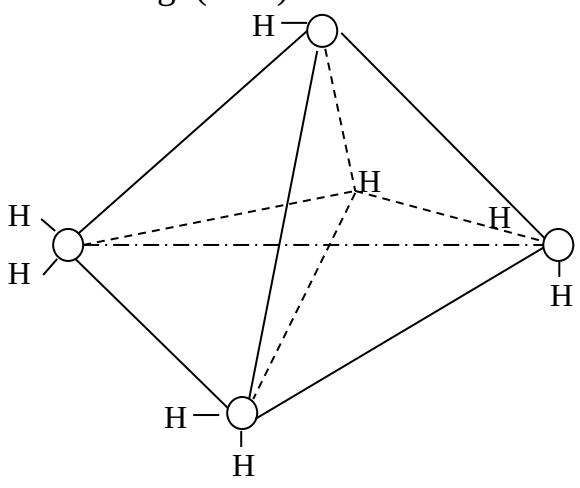

Fig. (1-27) shows the structure of $H_9O^+_4$ ion

Different method even a restricted numbers of paper that were found that mainly deals with weak acid determination especially ascorbic acid, citric acid, oxalic acid because of their vital importance medically and industricaly. The lecterature conducted for last thirty years shows that no available spectrophotometric method for acid determination is quoted unless very rare. Table (1-3) shows the miscellaneous methods used for the determination of some acids. It seems that the glass electrode occupy the whole area of acid determination.

Table (1-3) miscellaneous methods for determination acids

Acid	Method	Wave length nm	Range of	Refe.
Citric acid	Ttitrimetric citrate with potentiometric end point detection	-	10^{-2}-10^{-6}M	53 , 54
Mixture acids (HCl, H_2SO_4, HNO_3, Formic acetic, Malonic acid)	Titration of buffer mixture with strong acid	-	0.025-0.025M	55
Ascorbic acid	Potentiometric of LAA+1/2/o2 →deyhyrascorbic acid+H2O	-	-	56
Phosphoric, succinic, Maleic, oxalic, Tartaric Acetic and propionic acid	Partial-least sequares		1.8-7.2M	57-62
Ascorbic acid	Oxidimetric with potassium hexacyyano ferrate (III) in acid medium		20-200μgml^{-1}	64
Citric acid in milk	Spectrophotometric of pyridine, acetic anhydride and citrate	428	0-300μgml^{-1}	64
Ascorbic acid in citrus fruits	Spectrometric reduction of iron (III).	562	5 μg/25 ml 10μg/ 25 ml	65
Ascorbic acid in soft	Spectrophotometric titratin with	293	-	66

drink, fruit juices	2,6 dichlorp indophenol			
Ascorbic acid in vegetable and fruit	Spectrophotometric molybdenum blue complex	760	2-23μgml^{-1}	64-68
Vitamin C	Spectrophotometric reaction with ferricinium cation	440	-	69
Asorbic acid in tabletes	Gas chromatography. Converted ascorbic acid to its derivative (trimethysilgl)	-	50-400μg	70
Ascorbic acid	Photobleaching of methylene blue	655	0.004-0.5M	71

1-3-1 Flow-injection methods

A single-point titrimetric system based on the flow injection principle was used to determine acids. The sample introduced into a water stream then reacts with basic buffer solution in a merging stream and the peak height is recorded potentiometrically with a glass electrode in a flow through cell. The relative standard deviation is less that 1%[72]. Foggand Summan[73] studied that a scorbic acid can be determined by flow-injection analysis at a sessile mercury drop electrode without the need to deoxygenate the samples. This methods is found to be accurate for concentration higher than 60μg ml^{-1} and coefficients of variation were less than 1%. Ascorbic acid was determined in range of 0.1-40 μg ml^{-1} by flow injection analysis based on the generated iodine as triiodide ion or the triiodidel starch complex which giving a steady spectrophotemetric signal as 350 or 580 nm respectively[74]. The method is applied to the determination of ascorbic acid in a fruit juice, jam and prepared vitamin[75-76]. Flow-injection analysis method involves spectrophotometric determination of carboxylic in drugs based on the formation of 2-nitrophenyhydrazide derivatives mediated by water-soluble carbodiemide[77]. A number of drug preparations were also analysed with a coefficient of variation of less than 1%.

Flow-injection method for determination of oxonium ion in strongly ionisable inorganic acids such as sulphuric, hydrochloric, perchloric, nitric, and phosphoric acids. In addition, halogeno-substitued acetic acids such as chloroacetic, trichloro acetic and trifluoro acetic acids can be determined. Formic acid can be detected at the 0.1M level but acetic acid could not be detected up to 0.2M[80]. The method is based on the generation of bromine from

$Bro^-_3 - Br - H_3^+O$ reaction.

The bromine is then reacted with H_2O_2 to liberate oxygen for the oxidation of Luminol. A Flow-injection method for determination of ascorbic acid by measurement of the chemiluminescence from direct oxidation with permanganate in an acidic medium[81]. The method is applied to fruit drinks and nutritional supplements. Cui. *Et. al.,* studied that was found to inhibit chemiluminescence of the luminol-H2O2 reaction catalyzed by Cu^{2+}. Within detection limit of 9×10^{-9} M and the variation coefficient is 2.5% The method has been successfully applied to the determination of tannic acid in real Chinese gall and hop pellets samples. A Flow- injection system for the fluorescence determination of low level of ascorbic acid was proposed Ensafi and Rezaci[83] used a method which is based on the rapid oxidation of ascorbic acid by thallium(1). The fluorescence signal at 419 nm is proportional to the amount of ascorbic acid. The usefulness of the method was tested in the determination of ascorbic acid in Fruit juices and vitamin C tablets.

Spectrophotometric with flow injection analysis was used to determine a mixture of weak acids by using multiivariate calibration. This method was based on spectrophotometric data which is generated by following the colour change of a combination of acid-base indicators caused by an alkaline gradient. This gradient is generated by introducing a NaOH solution into a flow injection analysis titration system. Partial

least squares modeling is used to reduce and treat the titration data. This model predicts individual acid concentration of acid presented in the mixture of weak acid. This method was used to detect citric and tartaric acids in the 1×10^{-3}-4×10^{-3} M range, acetic and benzoic acids in the 1×10^{-3}-4×10^{-3} M and hydrochloric and acetic acid in the 1.25×10 - 5×10^{-3} M range[84-85]. Mixtures of succinic and oxalic acid were determined by titration. In flow injection analysis with potentionetric flow cell with a stainless steel electrode[86]. Partial least sequares regression as multivariate calibration tool was applied for data treatment with a relative error of 4.3% for succinic acid and 5.5% for oxalic acid. This method can be applicated in pharmaceutical or food samples. A flow injection analysis system with potentiometric detection has been developed for the determination of citric acid in commercial fruit juces using copper-selective tubular electrode[87]. It consists of the complexation of citrate ion with copper(II) ion. Citric acid was determined by indirect flow injection atomic absorption spectrometric, the method is based on the continuous precipitation and filtration flow system for the separation of citric acid by precipitation with lead and indirect flame atomic absorption spectrometry is proposed[88].The precipitate is formed by injecting the lead solution into a carrier containing the sample and is subsequently retained on a filter. This method has been applied to the determination of citric acid in fruit juices, carbonated soft drinks and sweets. New approach for the determination of ascorbic acid via on-line automatic through the consumption of the relased bromine with detection limit of 7.045mg[89]. Ascrobic acid can be determined in pharmaceutial preparation and from natural juice obtained from naturally occuring citrons fruits using flow injection analysis according to this reaction

$$B\bar{r} - Br\overline{O}_3 - H_3^+O$$

via consumption of relased bromine[90].

1-4 Nitrate and Nitrite ions

Nitrate may be quantitatively reduced to nitrite and nitrite quantitatively oxidized to nitrate. Nitrate and nitrite play on important role in the nitrogen cycle. Both are present in food and water, and then they are two, of the most frequently required determination in environmental investigations. Nitrate is necessary for plant growth and is important in soil as relating to fertilization. Oxides of nitrogen absorbed from the air are determined as nitrate. There are industrial materials containing desired or contaminating amounts. Nitrate ion is acting as a depolarizer and reduced to nitrate ion[91-93].

Several spectrophotometric methods used for the determination of nitrate and nitrite ions as shows in table (1-4).

Table (1-4) Spectrophotometric methods for determination of nitrate and nitrite

Ion determine	Method	Wave length nm	Range	Reference
Nitrate and Nitrite	Method based on the reaction between nitrite, sulphanilamide and naphthylethylene diamine	543 mμ	40-50μg NO_3 0-10μg NO_2	94
Nitrate and Nitrite	Forming aZo dye	400-600	0.05-0.5M	95
Nitrate	Using the reaction of nitrite with α-naphthylamine	527.5		96
Nitrate in water	Using of different cadimum column to reduce nitrate to nitrite	543	0.02-0.2M	97
Nitrate	Base on the reaction of nitrate with 4,5 dihydroxycounmarin	410	0.2-7.5ppm	98
Nitrate vegetable	Using 2-sec-Butylphenol	418	0.13-2.5M	99

Nitrate and Nitrite	Modified of Gries Iiosvoy reaction		0.025-0.356 Mg $.g^{-1}$ NO_2^- 0.212-8.559 Mg $.g^{-1}$ NO_3^-	100

1-4-1 Flow injection methods for determination of nitrate and nitrite ions

Nitrate and nitrite can be determined by Flow-injection method which consists of the reduction of nitrate with copperzed cadimium with the nitrite thus produced, diazoisation of sulpanilamide, the product being coupled with N-1-naphthylethlenediaimine to from a highly coloured azo dye, which measured at 520nm. Automated procedure for determination of ammonium and nitrate in soil extracts were described, distillation of the extract with magnesium oxide with subsequent determination of ammonia by automated indophenol method used for ammonium. For ammonium plus nitrate, the nitrate is reduced with titanium(III) sulphate during distillation with magnesium oxide. The method has wider application is, for example, analysis of fertilisers and water samples[(102)]. Flow injection principle is used with the noval design of a flow cell, in which the ion-selective and reference electrode are incorporated. The method was used for the determination of nitrate in soil extracts with standard deviation of only 0.8% and the detection limit was approximately 10^{-5} M nitrate[(103)], automated method for determination of nitrate and nitrite by flow injection analysis was used nitrate[(104)] is reduced to nitrate with copperized cadmium coloumn. Nitrite is diazotized and coupled with N-(1-naphthyl) ethylene diammonium dichloride. In this method the merginh zones approach is used to minimize reagent consumption. Tow peak are obtained, one of them corresponds to nitrite and the other nitrite plus nitrate. The precision is

more than 0.5% for nitrite in the range 0.1-0.5 mgL^{-1} and 1.5% for nitrate in the range 1.0-5.0 mgL^{-1} . Flow injection principle is used in the photometric determination of nitrite and nitrate with sulfanilamide an N-(1 naphthyl) ethylenediamine as reagents. On-line copper-coated cadmium reductor reduces nitrate to nitrite. The detection limit as a 0.05μM for nitrite and 0.1 μM for nitrate at a total sample volume of 200μl[105-106]. Nitrite can be determined by its reaction with cerium(IV) using inverse spectrophotometric detection in flow injection analysis[107]. The system was applied to the determination of nitrite in culture media. Spectrophotometric determination of aromatic primary amines and nitrate by flow injection analysis are used, which based on the injection of aromatic primary amines into dilute hydrochloric acid carrier which merges sequentially with 4-N methylaminophenol and dichromate. The purple-red color formed by oxidative coupling of amines with 4-N-methylaminophenol is measured at 530 nm. In contrast to the manual procedure, the flow-injection procedure avoided errors arising from the instability of the coupling intermediate, oxidation of the amine, and too great an excess of the oxidant[108].

Nitrite can be determined in water by flow-injection with chemiluminescence[109]. In this method nitrogen monoxide, which exists in equilibrium with HNO_2, is separated from the aqueous flowing eluate by entraiment in Ar carrier gas and is detected with high specificity in the gas stream by the chemiluminesence associated with its reaction with ozone. The sequence of reactions involves in the chemiluminesence determination of nitrite ions.

$$NO_2^- + H^+ \qquad NONO \rightarrow NO \qquad \ldots(1\text{-}23)$$

$$NO + O_3 \rightarrow NO_2 \rightarrow NO_2 + hv \qquad \ldots(1\text{-}24)$$

Nitrate was determined by spectrophotometric with electrochemical reductor using flow-injection analysis[110]. This method is based on a column electrode paked with co-electrodeposited Cu-Cd glassy carbon grains which has been shown to be excellent for the reduction of nitrate to nitrite and its application to the flow injection analysis of nitrate in sample of natural water has been used. The detection limit was 7×10^{-7}M.

To minimize the sample size, reagent consumption and waste, a micro-Flow-injection analysis was investigated and applied to the simultaneous determination of nitrate and nitrite ion in water sample[111]. Nitrate was reduced to nitrite by cadmium copperized. Detection was carried out at 538 nm with a height-emitting diode used as an azo dye. The detection limits of nitrate and nitrite were about 10^{-7} M. Amoter flow injection method was used to determine of nitrate and nitrite in human saliva[112]. It is based on the reaction of nitrite with iodide in acidic medium, the triiodide formed being amperometrically monitored at +0.2V with platinum microelectrode. The method was used in the study of the conversion of nitrate to nitrite in the oral cavity by bacteria. Amperonometric detection with microelectrodes in flow injection analysis was used to determine of nitrite in saliva[113,114]. This method was based on the reaction of nitrite with iodide in acidic medium and the triiodide was formed. This limit of detection of the method was 0.2 $\mu mol^{-1}l$. Simultaneous spectrophotometric determination of nitrite and nitrite in food stuffs and water by flow injection analysis[115]. In this method cadmium is used to reduce nitrate to nitrite. Nitrite is diazotised in the FIA system with N-(1-napthyl) ethylenediammonium dichloride to form the highly colpured aZo-dye, which is measured at 540nm. The detection limit is $0.085\mu^{-1}$ for a sample injection of 400 μl at relative standard deviation was 1.56%, and 0.77% for both nitrate and nitrite, respectively.

A Flow injection system with spectrophotometric detection is proposed for determination of low levels of nitrite based on its catlytic effect on the oxidation of gallocyanine such as bromate in acidic media[116]. The calibration graph was linear for 0.02-0.2 μg/ml of nitrite. A sequential injection analysis system for the simultaneous determination of nitrite and nitrate in waste waters has been developed. The nitrate determination is based on the Griess-Liosvay reaction. Nitrate is previously reduced to nitrite in a copperized cadmium column and analyzed as nitrite. The absorbance is measured at 540nm. The standard deviation better than 2% for nitrite and 0.7% for nitrite[117-118]. Nitric oxide (NO) is an important intracellular and extracellular signal substance[119]. Nitrite is one product of the oxidative metabolism of NO. So a flow injection method is based on the Griess reaction. The purpose of this method is to determine nitrite to provide a means of estimating the endogenous formation of NO or NO_2^-.

The reversed phase flow injection spectrophotometric determination of trace nitrite nitrogen in water has been studied[120]. N-(1-Naphthyl)ethylene diamine dihydrochloride solution was injected into the mixed flow of the water sample sulfanilamide solution. Red dye formed by the reaction and spectrophotometrically monitored at λ_{max} 540nm. The detection limit is 0.0012 mg/l. A thin film of mixed-valent cupt Cl_6 is deposited on a glassy carbon electrode by continuous cyclic scanning in a solution containing 3×10^{-3} M $CuCl_2$, 3×10^{-3} M K_2PtCl_6 and MKCl. In the potential range is from 700 to 800 mv[121]. The cyclic voltammetry is used to study the electrocheical behaviors of nitrite on $CuPtCl_6$/GC modified electrode and electrode displays a good activity toward the oxidation of nitrite.

The linear relationship between flow injection peak currents and concentration of nitrite is at range of 1×10^{-7} - 2×10^{-3} M with detection limit of 5×10^{-8} M. Non-equilibrium flow injection spectrophotometry used for determination of nitrite. This method was based on the reaction of nitrite with basic fuchin in an acid medium. The linear range for nitrite is 0.0-0.5 mg/l. The method was applied to direct determination of nitrite in collapase lake water, fishpond water, power plant wastewater and well water with satisfactory results[122]. An automatic direct spectrophotometric method for the simultaneous determination of nitrite and nitrate by flow-injection analysis has been developed[123]. The method is based on the reaction of nitrite and nitrate with the spectrophotometric reagent N-phenylanthranilic acid(I) in sulfuric acid medium pH (0.4-0..6) to form the same color product while the absorbance is measured at 410 nm. One half of the sample flow is treated with sulfanilic acid, which reacts with the nitrite and thus makes it subsequent reaction with I. So that the nitrite portion can be calculated by difference. This method has the advantage of direct determination of nitrite and nitrate without reducing nitrate as in other reported methods. The detection limit is 2.5 ng/ml for nitrite and 12 ng/ml for nitrate. The concentration of nitrate in biological fluids has been determined using nitrate reduotase (NR) in a flow system. A merging zone method was applied, in which a zone of NR and that of nitrate in separated stream has been merged, and allow to react. The decrease in NADPH caused by the reaction between NR and nitrate is measured at 340nm. The detection limit was 0.2 μM. Flow injection method was applied to determine the amount of nitrate in serum, plasma, and uria using samples that had not been deproteinized. The concentration of nitrate within each sample was calculated from differences in the peak areas obtained in the absence or presence of nitrate reductase[124].

ODS coloumn dynamically coated with cetylpridinium chloride, eluting with acitrate method solution after deproteinisation of the serum using ultrafilter-paper and measuring the absorbance at 210 nm. The proposed method was also applied to the determination of the four anions in human saliva an urine[131]. The detection limit was 0.005μgml^{-1} for nitrite and 0.008 μgml^{-1} for nitrate. The oxidation of nitrate at boron-doped diamand (BDD) electrode was investigated by use of anodic voltammetry. The voltametric curves exhibit well-defined anodic ppeak, with response that is superior to that obtained with glassy carbon electrodes. It is shown that BDD is a very promising electrode material for the detector of nitrogen oxides (NO, NO_2) in gases[132].

The color fading reaction on potassium bromate with victonia green stand G by the catalysis of nitrite in hydrochloric acid medium was studied using flow injection analysis[125]. The linear range for the determination of nitrite is 0-0.3 mg/l and 0.3-2.0 mg/l. It was used to determine trace nitrite in the collapse lake water, fishpond water, power plant wastewater and well water.

Miscellaneous method used for the determination of nitrate and nitrite as shown in table (1-5).

Table (1-5) Miscellaneous methods

Ion determine	**Method**	**Wave length nm**	**Range**	**Refere .**
Nitrate in water	Automatic kinetic method based on frming of aZo dye	540	0.025-2 ppm	126
Nitrate	Molecular emission cavity method	500	10-400 ppm	127
Nitrite in sauage	Amperometric method base on the anodic oxidation of nitrate at a molybdenum oxide layer		5-1000 μM	128

Nitrate in river water	Capillary electrophoresis method with indirect μv detection, separation and determination of Cl^-, NO_3^- and $SO_4^=$			129
يهفقهفث	Ion chromatography with photometric measurment of iodine		0-1.5×10^{-3}M	130
Nitrateind nitrite in human serum, lake water, river, sewage works water and snow samples	Ion chromatography method	210	Nitrite 0.03-10 μg ml^{-1} Nitrate 0.05-5 μg ml^{-1}	131
Nitrite	Voltametric method based on oxidation of nitrate at boron-doped diamand electrode		0.002-1 Mm	132
Nitrate in water	Ion selective electrode method		1-10 Mg l^{-1}	133

1-5 Hydrogen peroxide

Hydrogen peroxide is an exidant used widely in industry, laboratories and in domestic purpose. It is unstable and easily decomposable due to the uncommon oxidation state of oxygen in H_2O_2 molecule which is (-1). It is important in some polymers study when self decomposition may be relase H_2O_2. It has been proposed that natural humane materials in waters might photochemically reduce oxygen to give

the superoxide O^{-}_{2} and that subsequent disproportionation of this free radical could lead to the formation of H_2O_2[134]. Fig.(26) shows the H_2O_2 molecule is not planar. Each atom has two unshard electron could as well as in the O-H bonds repel each other. The twisted structure called skew-chain structure accommodates these intermolecular repulsions best[135].

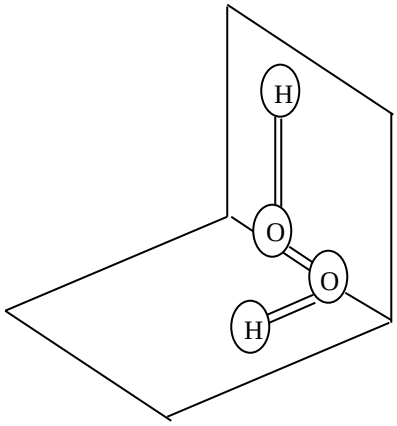

Fig. (1-26) Hydrogen peroxide structure

Miscellaneous method used for the determination of hydrogen peroxide as shown in table (1-6)

Table (1-6) miscellaneous methods

H_2O_2	**Method**	**Wave length nm**	**Range**	**Refere.**
H_2O_2 in atomspheric precipitation	Fluorometric method based on the reaction of H_2O_2 with horseradish peroxides and p-hydroxyphenyl acetic acid		$10\text{-}8\text{-}105\times10^{-4}$M	136
H_2O_2 in water	Lodometric method based on the oxidize of iodide by hydrogen peroxide at pH=4, the iodine formed was reacted with the phenylarsine			137

	oxide			
H_2O_2 in water	Spectrophotometric method using sodium salts	540	$(7\text{-}40)\times10^{-4}$M	138
H_2O_2 in water	A chemiluminescent method based on oxidation of lumin of in alkaline medium in presence of Cu(II) as catalyst		10^{-8}-10^{-5}M	139

1-5-1 Flow-injection methods for determination of hydrogen peroxide

A flow-injection system based on the p-hydroxy phenyl-acetate peroxide-peroxides reaction allows the simultaneous determination of hydrogen peroxide and CH_3HO_2 in water samples in range of 0.3-2 μg l^{-1} and the detection of 0.1 μg l^{-1}[140]. An amperometric method with flow-injection was used to determine hydrogen peroxide in a range of 10^{-4} to 10^{-1} M. This method is based on the production of dihydroxyacetone from glycerol by immobilized bacteria. The H_2O_2 was oxidized at 1.2 V.VS SCE at a glassy carbon flow-through electrode after dilution in a flow injection analysis system[141]. Chehemiluminscence from the reaction of bis(2,4,5, trichloro-6-carbopentoxy phenyl) oxalate with hydrogen peroxide in the presence of triethyl amine in –butanol-water has been investigated as a means of determining hydrogen peroxide with range of 2×10^{-8}-10^{-3}M[142]. Hydrogen peroxide can be determined by flow-injection chemiluminscence method by using reagent containing 100μM huminal and 3μM microperoxidase at pH=4, the range of this method was 3×10^{-9}M – 10^{-5}M[143]. Also H_2O_2 was determined in aqueous samples by flow injection techinque using solid state peroxyalate chemiluminscence, Bis(2,4,6-trichloro phenoyl) oxalate in solid from is packed into a bed

reactor, which eliminates mixing problems, perylene is added as a sensitizer to a water/acetonitrile carrier stream into which the samples (200-600 Vl) are injected, the calibration graph is linear up to 10^{-5}M with detection of limit 0.2μgl^{-1}[144].

Fluorometric Flow-injection procedure with a single reagent solution containing p-hydroxypenyl acetic acid peroxidase and ammonia were used to determine hydrogen peroxide in the range of 10^{-8}-10^{-4}M with detection limit of 10^{-8}M[145]. Hydrogen peroxide was determined in flowing stream by immobilized luminol chemiluminscence reagent in flow-injection system with a low detection limit of 100 pmol and the linear working range is (40-600)μM[146]. 1,1′-oxalyldimidozol as chemiluminscence reagent was used to determine the low hydrogen peroxide concentration by flow injection analysis, the estimated detection limit for H_2O_2 in water was 10^{-8}M with the linear range of 1.5-6μM[147]. Flow-injection technique is used to determine nanomolar concentration of H_2O_2, the concentration of H_2O_2 was determined as the coloured of condensation product of N-ethyl-N-(sulfopropyl) aniline and H-aminoantipyrene with detection limit os 12 nM[148]. It has been found that a flow injection system with an immobilized enzyme reaction coloumn could be utilized for the determination of hydrogen peroxide in some water samples. The coloumn was packed with chitosan beads immobilizing horseradisn peroxide, the detection limit was 3ng. dm^{-3} and the relative standard deviation at 1 mg dm^{-3} of H_2O_2 was 1.5%(149). The sensitivity of a flow-injection analysis system for measuring hydrogen peroxide could be remarkably imporoved using immunooaffinity-layered horseradisin peroxidase[150]. Flow injection analysis method for automated determination of hydrogen peroxide in the presence of even stronger oxidants is presented based on the immediate formation of a colored adduct between hydrogen peroxide and dinuclear IronIII

complex. A reagent stream with the complex and carrier stream into which the sample is injected are combined in a low dead volume mixing tee. The absorbance was measured at 570nM[151].

All the methods above were suffered from interferences compare with the method used in this work also the detection limit was better.

1-6 Iodide and iodate ion

Iodide and iodate ions are very important in food, water, plant, and pharmaceutical product. The Ioody needs iodide ion each day to prevent goiter, adistiguring enlargement of the thyroid gland. Iodine exists in a number of oxidation states commonly used in a analytical chemistry being iodide and troiidode. Strong oxidising agents reacts quantitatively with the easily oxidised iodide ion. Iodination reaction have been extensively to determine numerous organic compounds that either iodinated or oxidised by iodine[135]. The misellaneous method which used the determination of iodide and iodate ions are shown in table (1-7).

Table (1-7): miscellaneous methods

Ion determine	Method	Detection limit	Range	Refere.
Iodide	Fluorimetric method used cerium(IV)	-	0.6-2.5 μg/100ml	152
Iodide	Fluorimetric method used 2,7-di(acetoxymercuri)fluorescein	-	0.87-9.81 ng/25ml	153
Iodide in sea water	Neutron activation analysis	6×10^{-3}	-	154
Iodide in table salts and	Spectrophotometric based on the reaction of palladium with 3-(2	-	0.6-127μgl^{-1}	156

pharmaceutit al products	thiazolylazo)2,6-diaminotoluene			
Iodide in sea water	Ion chromatography with μV detection	0.2 μgl^{-1}	-	157
Iodate in salt	Amperometric method based on the detection at a molybdenum oxide modified electrode	6×10^{-6}M	10×10^{-6}-10×10^{-7}M	158
Iodide in environment al equeous samples	Inductivety couplet plasma atomic emission spectrometry	0.04$\mu g.ml^{-1}$	-	159
Iodide in natural water sample	Spectrophotommetric determination by solvent extraction with methylen blue	1.5×10^{-6}M	7.5×10^{-8}-3×10^{-6}M	160
Iodide	Chemiluminescence based on the oxidatation of ascorbic acid with copper(II)	5.8×10^{-8}M	4.6×10^{-5}-4.2×10^{-3}M	161

1-6-1 Flow-injection methods

Iodide can be determined by amperometric Flow-through wire electrode flow-injection analysis with detection limit of 10^{-5} M[162]. Chromium (IV) as strongly reagent was used in Flow-injection analysis to determine iodate ion, with spectropotometric detection, based on the absorption of chromium (III)-ENTA at 600nm. The detection limit was 8.3×10^{-5}M, and the range of concentration was 1.66×10^{-4}-1.66×10^{-3}M[163]. The iodide ion was determined in detection limit of 5×10^{-10}M by using vibrating wire electrode for ampermetric in flow injection system[164]. Automatic method was used to determine the free iodide ion in drinking

water. This method was based on the catalytic effect of iodide on the destruction of the thiocyanate ion by the nitrite ion, the detection limit of this method was 0.4μg.l^{-1} with linear working range 0.4-5 μg.l^{-1} [165]. Liquid core optical fiber total reflection call as a colorimetric detection for flow injection analysis was used to determine iodide ion. 0.1 μg.l^{-1} can be detected based on the iodine absorption at 540nm[166]. Flow-injection with spectrophotometric system was used to determine iodide ion. The iodide ion oxidise by bromine water to iodate, most of the excess of bromine is reduced by formic acid, and the iodate is reacted with more iodide to from triiodide, which is determined spectrophotomtrically at 351 nmm, with detection limit and range were 3-9×10^{-7}M, (0.7-3.9) ×10^{-5}M respectively[167]. Stop-flow method was used to detect iodide ion, based on the reaction between cerium(IV) and arsenic(III) which catalysed by iodide ion. This method can be used to determined iodide ion in pharmaceutial pro-paration, table salt and Cow's mulk. The decrease in absorbance during the reaction was monitored at 365 nm, with detection limit of 0.7 ng ml^{-1}[168]. Iodometric method was used to determine iodate ion by using flow injection amperometry, range of (0-1.5)×10^{-4}M and the iodate ion was detected in this method as iodine[169]. Also a flow injection analysis method was used to determine a microchemical amount of iodate and iodide in sea water. This system involves spectrophotometric detection. This method was based on the catalytic effect of either iodate and iodide on the indicator reaction of Iron(III), thiocyanate and nitrite with range of 0.75-150μgl^{-1}[170].

CHAPTER ONE

1- Introduction

1-1 General Introduction

Flow-injection analysis (FIA) is defined as an automated or semiautomated analytical process consisting of a sequential insertion of a discrete sample solution into an unsegmented continuously flowing liquid stream with subsequent detection of the analyte. It is a relatively new analytical process[(1)], which shows a considerable potential for high-speed precise. Flow-injection analysis is based on the injection of a liquid sample into a moving nonsegmented continuos carries stream of a suitable liquid. The injectied sample forms a zone, which is then transported toward a detector that continuously records the absorbance[(2)]. FIA is based on the technology of flow (FIA), the quick chemistry offers high sample throughput couppled with simple and rapid method changeover to maximize productivity in determining ionic species in a diversity of sample matrices from sub-ppb to percent concentrations. The simplicity and ruggedness of FIA are combined with the outstanding accuracy, precision, and minimum detection limits. Automated flow injection systems have been applied to on-line process analysis in industrial and environmental situations with a great deal of success. Flow injection analysis is also ideally suited to monitoring solution phase chemiluminescence reactions due to the capability to mix-sample and reagent in close proximity to a detector.

The whole process of sample/standard injection, transport, reagent addition, reaction and detection can be accomplished very rapidly (seconds to 10’s of seconds), using minimum amounts of sample and reagents, with excellent reproducibility (e.g., coefficient of variation, cv, generally <2%).

1-2 Flow Injection Analyzer

The simplest flow-injection analyzer is shown in Fig(1-1a). It consists of a pump, is used to propel the carrier stream through a thin tube, which is an injection part by means of which a well-defined volume of a sample solution (S) is injected into the carrier stream in a very reproducible manner, as well as a reaction coil in which the sample zone disperses and reacts with the components of the carrier stream forming a species sensed by a flow-through detector where the signal is presented on a reorderer. A typical recorder output has the form of a peak Fig(1-1b), and the height (H) of which is related to the concentration of the analyte. The time span between the sample injection (S) and the peak maximum, which yields the analytical readout, is the residense time (T) during which the chemical reaction takes place usually within less than 30 seconds. The injected volume is between 1 and 200 μl, which in turn usually requires no more than half a milliliter of reagent per analysis. This makes FIA an automated microchemical technique, capable of a sampling rate of at least 100 measurements per hour, with minimum reagent consumption[3]. Two types of automated continuous flow methods are encountered: segmented flow method, in which the analytical stream is divided into discrete segments by periodic injection of bubbles of air, and non-segmented flow procedure in which the analytical-stream is unbroken. The latter is generally termed as flow-injection analysis[4].

The conventional continuous flow analyzer shown in Fig. (1-2-a) is based on the use of air-segmented stream[5]. The purpose of segmentation is to preserve the identity of the individual samples. In such an analyzer, the samples are successive introductions from their individual containers into a tube and then forward through a pump farther into a system. The following stream is regularly segmented by air-bubbles delivered by

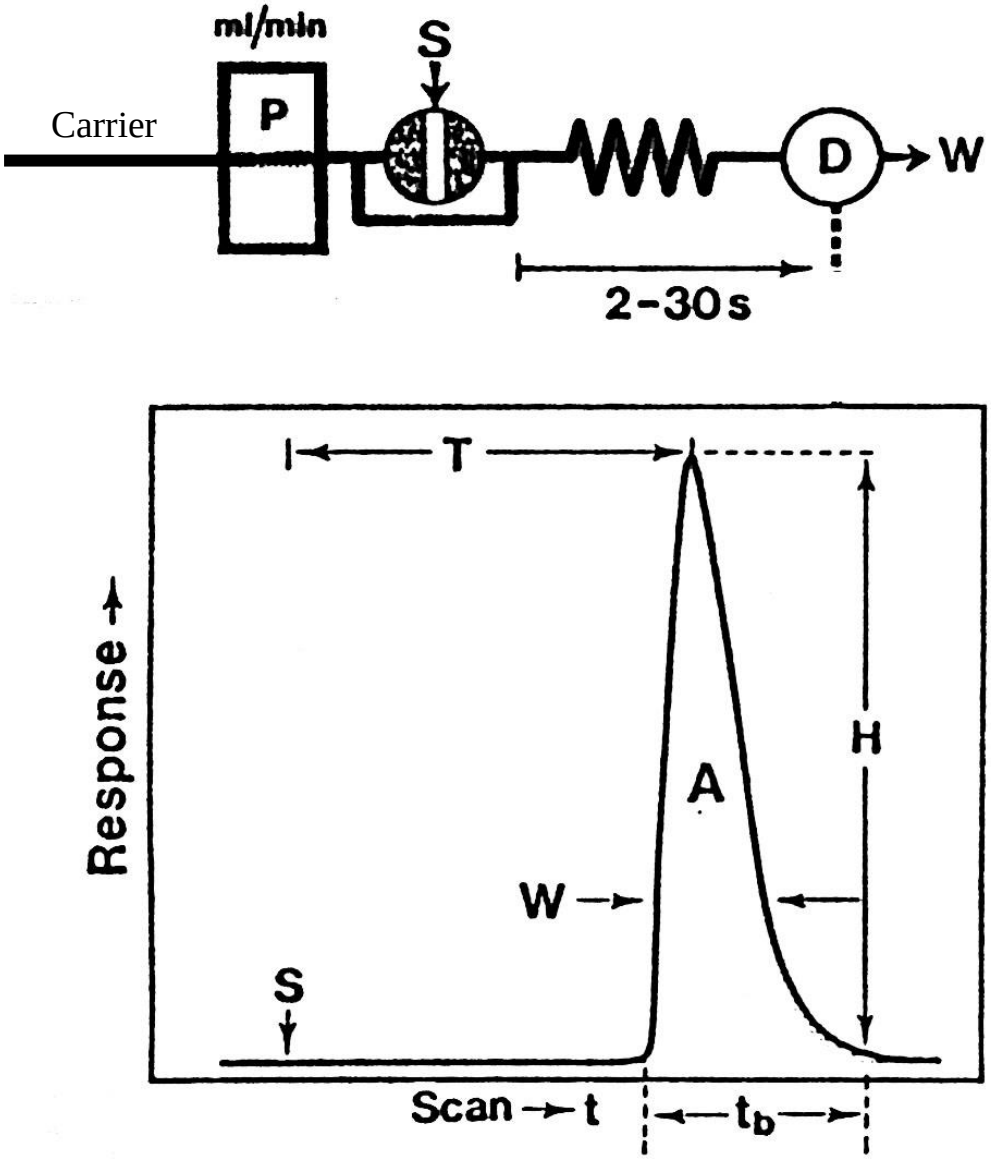

Fig. (1-1): a- Single-line FIA manifold ,

b-Recorder output

another pump tube. The reagent is added to all individual segments, which then pass through a reaction coil, where the chemical reaction takes place. The air segmentation has to be removed in a debubber (d); otherwise, the flow through detector would yield a disturbed signal unsuitable for direct recording of the resulting signal as shown in Fig. (1-2-b).

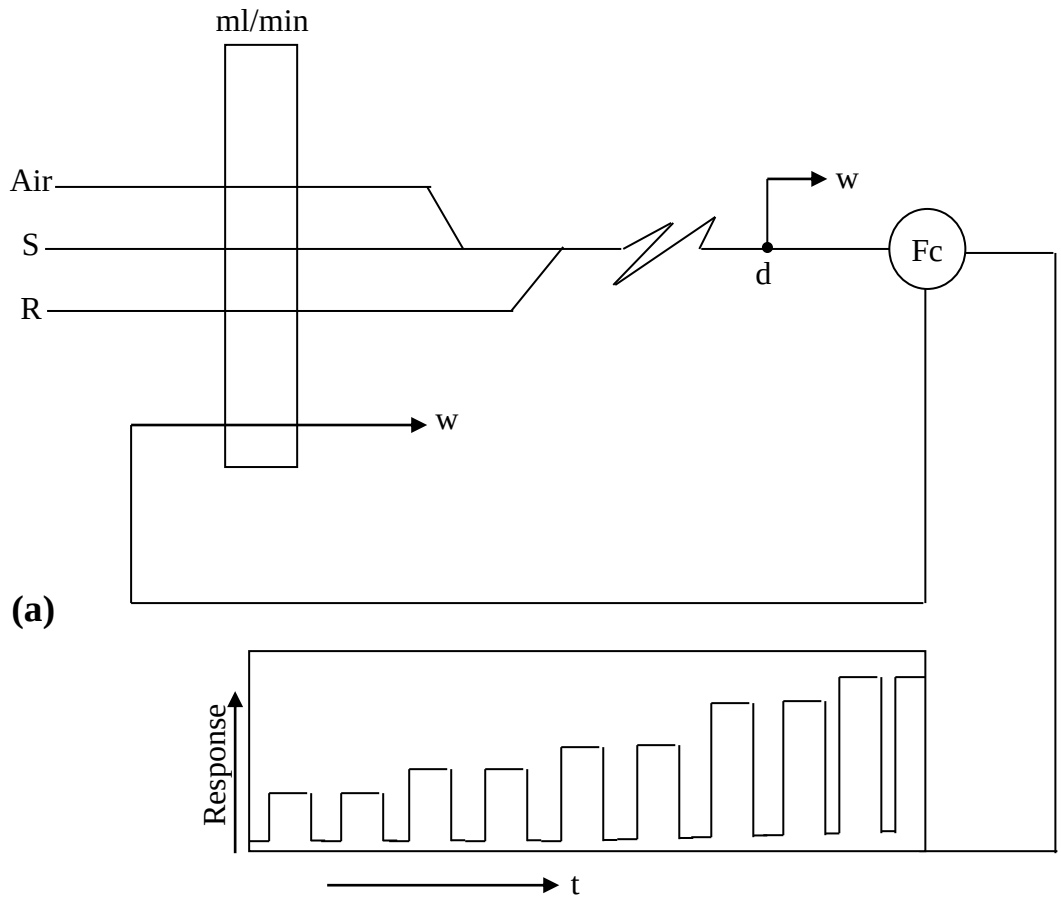

Fig. (1-2) a- Air-segmentation Continuos Flow System

b- The Analysis of Five Samples with Increasing Analyte Concentration.

In the air segmented stream, each segment of fluid can be viewed as an individual container, separated from neighbouring ones by an air bubble on each side, in which the liquid is homogeneously mixed as a

result of circular movement caused by friction with the tube walls[6-8]. Each segment carrying a fraction of a long aspirated sample zone contributes to the gradual buildup of the signal recorded by a spectrophotometric flow-through cell. The beneficial effect of air segmentation in preventing carryover has been so obvious that the necessity of introducing air bubbles is never really doubted, although the drawbacks of their presence in the flowing stream are well known:

a) Because of the compressibility of air, the stream tends to pulsate rather than flow regularly.

b) Stream, have to be debubbled before they enter the flow cell.

c) The size of the air bubbles has to be controlled for faster sampling rates.

d) The pressure drop and flow velocities vary in the presence of air for different tubing materials[9].

e) Air bubbles in plastic tubes act as electrical insulators supporting a buildup of static electricity which disturbs potentiometric sensors[10].

f) The efficiency of dialysis, gas diffusion across in membrance and solvent extraction is lowered as a result of a decrease in the effective transfer surfaces.

g) The movement of the carrier stream cannot be exactly controlled or instantly stopped. The main features of FIA are the absence of air segmentation and the method of injecting the sample into the flowing stream, as a result of which the method merely offers some kind of technical improvement, such as: a higher sampling rate and very rapid availability of the analytical readout. Yet the most important aspect of the FIA method is the concept of controlled dispersion of the sample zone, which is entirely new in analytical chemistry and an understanding of which allows the design of a FIA system exactly suited to automate a given analytical procedure[11].

1-2-1 Comparison between Beaker Chemistry and Continuous Flow-injection

The rapid development of continuous flow-injection analysis and the expansion on its use are due to the number of advantages over manual operations. The aim is to replace the glassware such as beaker, pipettes, burettes, flasks,…etc by tubes, pump and valves. The FIA methods are more rapid than manual methods, within minimal contact between the operator and toxic reagents. It can operate reproducible over long periods and the precision of analysis has been shown to be consistently good because it reduces human error[12]. In addition, it is a closed system oxidation and contamination of samples and reagents by atmospheric air is prevented[13].

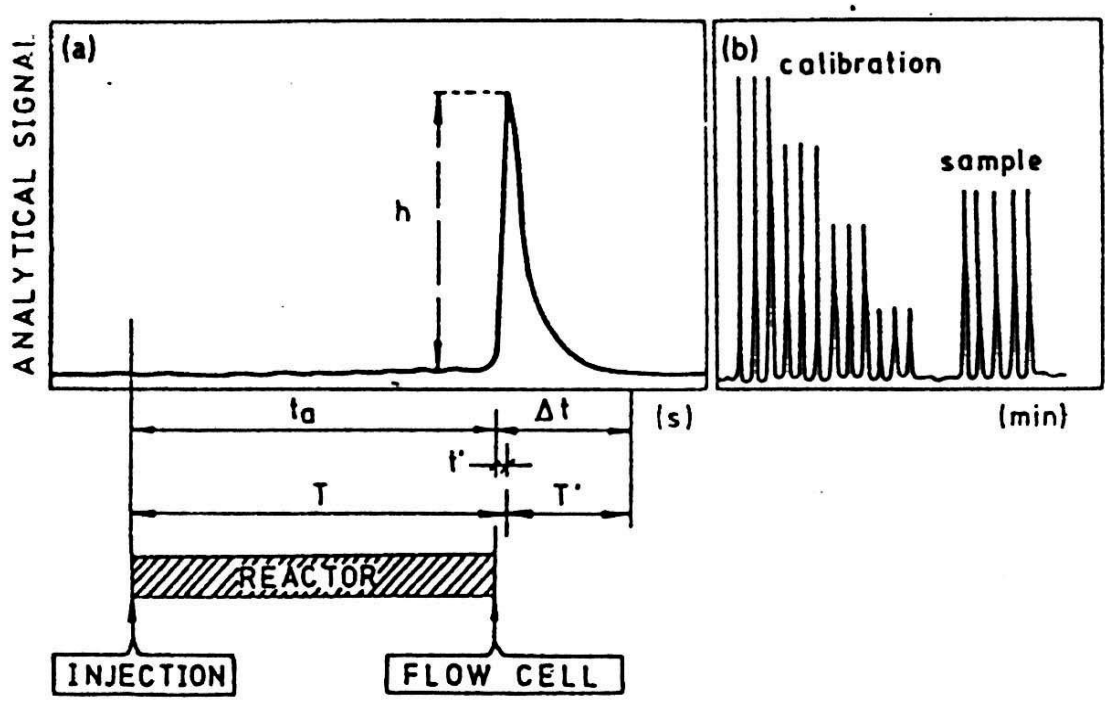

Fig. (1-3) a- FIA curve recorded at high chart-speed showing the important parameters.

b- FIA curve registered at low speed, the typical situation, injection of four standards in triplicate and an unknown sample in quintuplicate.

1-2-2 Flow-injection analysis signals

A schematic diagram of two FIA recording signals, which will variously be called FIA curves, or record, is shown in Fig. (1-3) where there are plots of the analytical signal (absorbance, fluorescence, intensity and potential) as a function of time.

The essential features are as follows:

i) Peak height h, which is related to the concentration of the component determined in the injected sample and the peak area could also be used.

ii) Residence time T, which is defined as the span elapsed from the injection until the maximum signal is attained. It should not be confused with the travel time, t_a, which is the period elapsed from injection to the start of the signal (1-2 % increase above base line). However, the difference between the two parameters, $t' = T - t_a$, is usually very small.

iii) Return time T′, which is the period between the appearance of the maximum signal and the return to the baseline.

iv) Baseline to baseline, Δt, defined as the interval between the start of the signal and its return to the baseline. This parameter is a measure of the dispersion or dilution of the analyte so

$$T + T' = ta + \Delta t$$

$$\Delta t = t' + T'$$

The record shown in Fig. (1-3-a) corresponds to that of a well-established FIA method and was registered at a lower chart speed than

that shown in Fig. (1-3-b) which shows the signals corresponding to four standards injected in triplicate-the usual practice- and those of a sample injected in quintuplicate.

1-2-3 Comparison between Two Chief Continuous Analysis; Segmented (SFA) and Unsegmented (FIA)

A detailed summary with specific data is presented in table (1-1). It should be stressed that FIA offers higher sample throughput, uses smaller a mounts of reagent, provides a larger number analytical data, and opens new possibilities.

Table (1-1) Comparison between SFA and FIA

Parameter	SFA	FIA	Refe.
Sample introduction	Aspiration	injection	14
Sample volume	0.2-2 ml	10-100 μl	15
Response time	2-30 min	3-60 sec.	16
Bore tubing	2 mm	0.5-0.7 mm	17
Detection	At equilibrium (homogeneity)	With controlled (dispersion)	18
Sample throughput	≤ 80 sample/hr	≤ 300 samples/hr	19
Precision	1-2 %	1-2%	20
Reagent consumption	High	Low	21
Wash-out cycle	Essential	Not required	22
Continuous kinetic analysis	Not feasible	Stopped-flow	23
Titrations	Not possible	Possible	24
Data produced	Peak height	Peak height Peak area Peak width Peak to peak distance	

1-2-4 Selectivity in Continuous Flow Analysis

When all experimental parameters such as sample volume, residence, dispersion, temperature, time of exposure of sample and interferent to reagent can be rigidly controlled and reproducibility maintained with these conditions met, it makes sence to express the selectivity of a method for B of concentration C_B, by a numerical value. As any interfering species A of concentration C_A, toward an interfering species always appear as positive or negative, this interference can be expressed quantitatively as the selectivity coefficient K_{AB}[25].

$$C'_A = C_A + K_{AB} C_B \qquad \ldots(1\text{-}1)$$

where C'_A is the total concentration of A measured, and K_{AB} is the selectivity coefficient of B in determination of A. The dispersion coefficient of the species are

$$D_A = \frac{C^\circ_A}{C_A}, \quad D_B = \frac{C^\circ_B}{C_B} \qquad \ldots(1\text{-}2)$$

If the height h of analytical signal obtained and the height of the detection response are linearly related to the concentration of A and B, the actual height of the signal will be given by:

$$h = KC'_A \qquad \ldots(1\text{-}3)$$

where K is the proportionality constant between signal height and concentration. If no interferent is present, then:

$C^\circ_B = C_B = 0$ the height of signal could be obtained as follows:

$$h_1 = K_{CA} = K\frac{C^\circ_A}{D_A} \qquad \ldots(1\text{-}4)$$

whereas if B contributes to the signal yield by A, the signal height is

$$h_2 = K(C_A + K_{AB}C_B) = K\left[\frac{C^\circ_A}{D_A} + K_{AB} \times \frac{C^\circ_B}{D_B}\right] \quad \ldots(1\text{-}5)$$

If all measurements were made at a point where both dispersion coefficients have the came value $D_A = D_B$, then:

$$D = K\frac{C^\circ_A}{h_1} = \frac{K}{h_2}\left[C^\circ_A + K_{AB}C^\circ_B\right] \quad \ldots(1\text{-}6)$$

Hence

$$K_{AB} = K\frac{C^\circ_A}{C^\circ_B} = \left(\frac{h_2}{h_1} - 1\right) \quad \ldots(1\text{-}7)$$

This expression allows the selectivity coefficient to be calculated from the initial analyte, the interfernt concentration, and the signal obtained in the presence and the absence of the interferent. The K_{AB} values could be positive or negative, depending on the sign of the interference. Solving Eq. (1-6) for h_2 gives

$$h_2 = \frac{h_1 K_{AB}}{C^\circ_A} C^\circ_B + h_1 \quad \ldots(1\text{-}8)$$

The plot of h2 against C°_B for series of experiments gives straight lines with slopes of h_1K_{AB}/ C°_A and intercept h_1. The slope gives the selectivity coefficient ($\pm K_{AB}$).

Three ways could be used to overcome the interferences[25]:

i) Injection, using a dual valve into separate channels with synchronous merging.

ii) Injection, using a dual valve into separate channels with an asynchronous merging.

iii) Injection, using two valve series into a single channels with an asynchronous merging[26].

The first method is applied with the aid of manifold illustrated in Fig.(1-4).

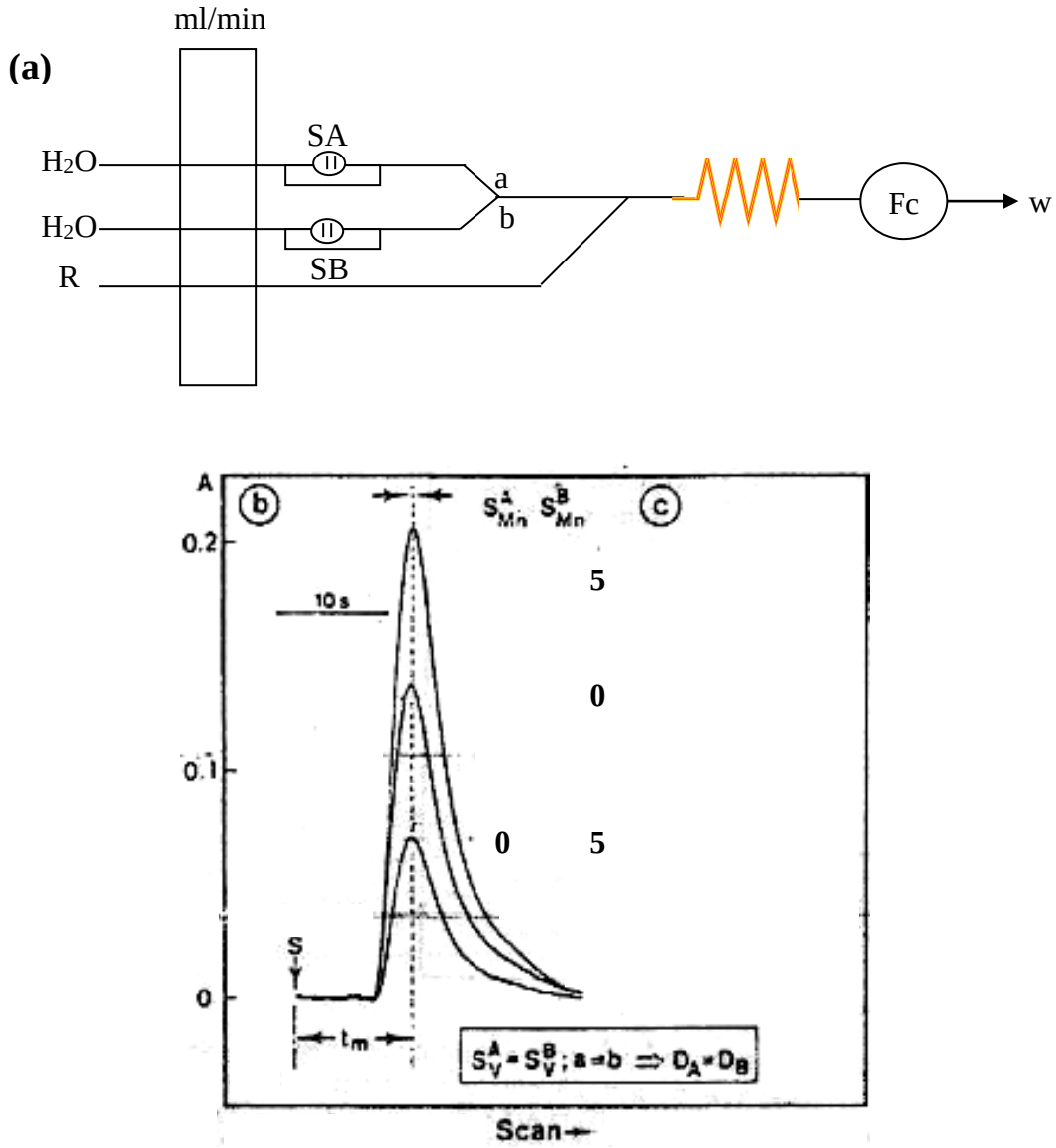

Fig. (1-4) Synchronous merging of samples . S^A and S^B injected simultaneously into two separate carrier stream (water).

a-Manifold with identical length of a and b.

b-Test of synchroization, where identical sample volumes of S^A and S^B are injected.

The synchronous merging is achieved by pumping to injected zones equal volumes of A and B through equally long lines a=b in which the pumping rates are identical. As shown in Fig. (1-4) a single peak was recorded and it increased as the concentration did. When an exact sychronization of the two injected zones is achieved, the dispersion of both species in the merged zone is identical along the whole merged

gradient, and it is most practical to measure peak maximum heights and to calculate the K_{AB} value. The second method deals with the injection into separate lines with asynchronous merging[27]. The signals must be measured at t_m so that $D_A=D_B$. For brevity, only the manifold used to implement that method with a dual injection valve will be discussed. Its basic design is shown in Fig. (1-5)

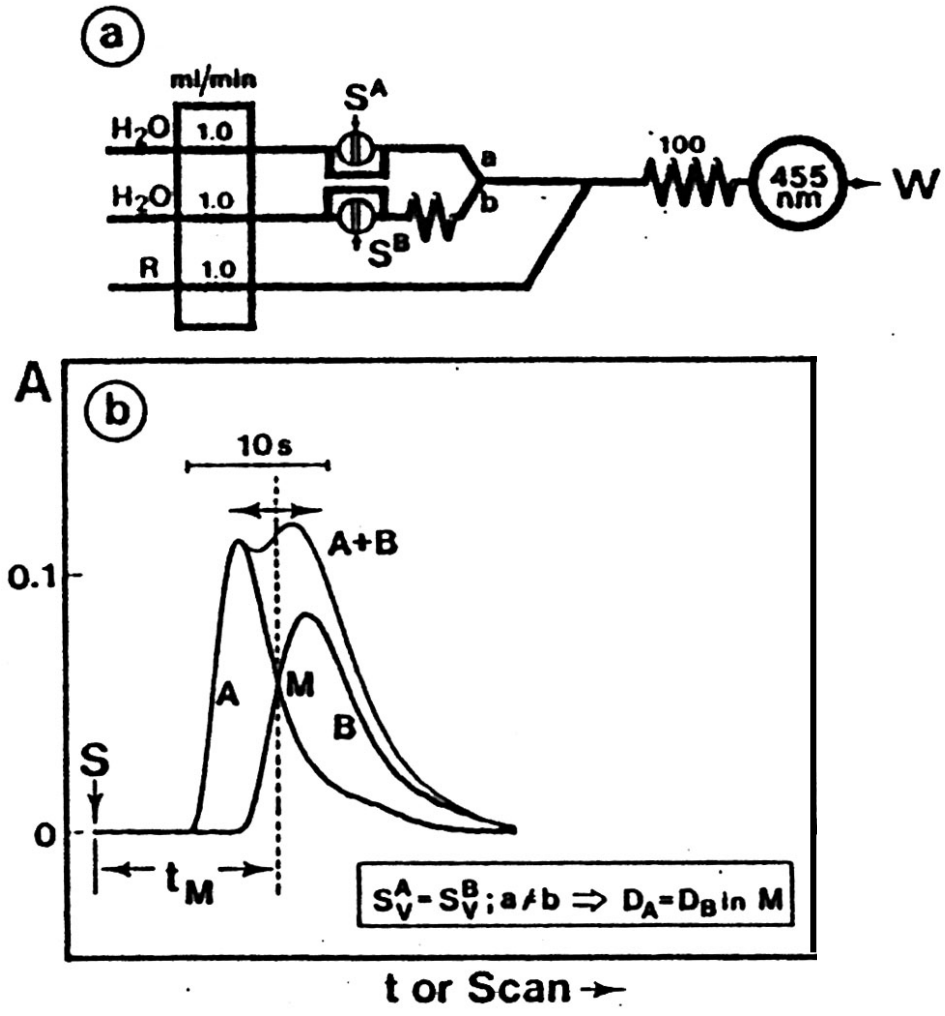

Fig. (1-5) Asynchronous merging of samples . S^A and S^B injected simultaneously into two separate carrier stream .

a- Manifold with a ≠b.

b- The signals obtained by injection samples of identical volume .

The dual injection valve injects two equal volumes into anaqueous carriers which circulate along lines with different lengths where a≠b between the valve and merging point. The resulting mixtures pass through the reaction coil, which leads them to the photometer. Fig. (1-5) shows the FIA record of the behaviour of each species, S^A and S^B when injected separately and together S^A+S^B. At the point where both peaks obtained by separate injection intercept each other, D_A=D_B, therefore this point indicates the measurement time t_m. The point M indicates the dispersion for S^A and S^B are identical. Fig. (1-6) shows the merging zones for S^A and S^B separately and together.

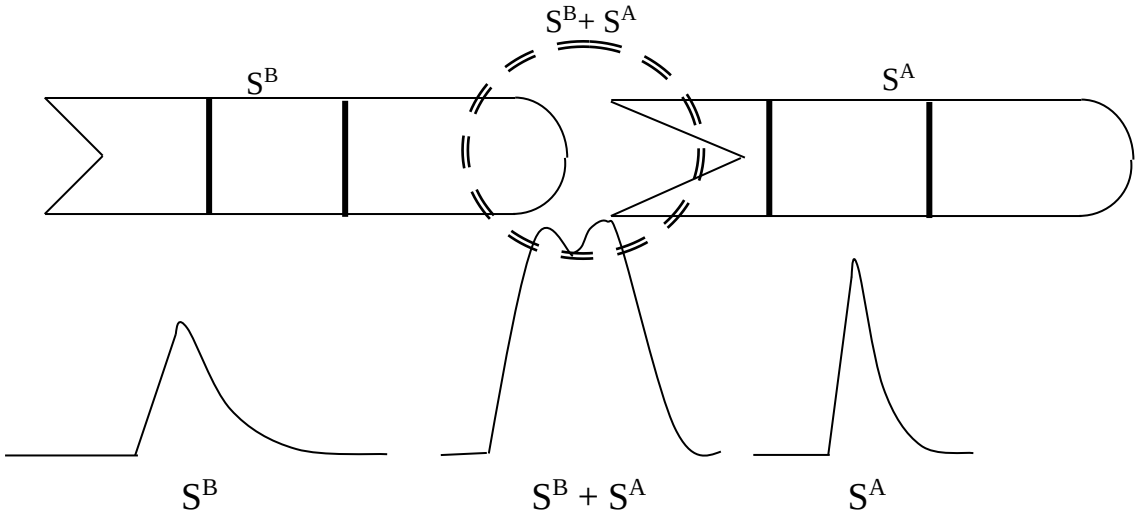

Fig. (1-6) The merging zones of S^A and S^B

The practical advantage of the separated solutions methods is that only a few solutions; essentially only a single solution of A and a few solution of B. Moreover, this method has a serious drawback; it is essential that the flow rates in both channels should be maintained absolutely constant through all the experiments. The injected zones must merge strictly reproducible at all times, for both synchronous and

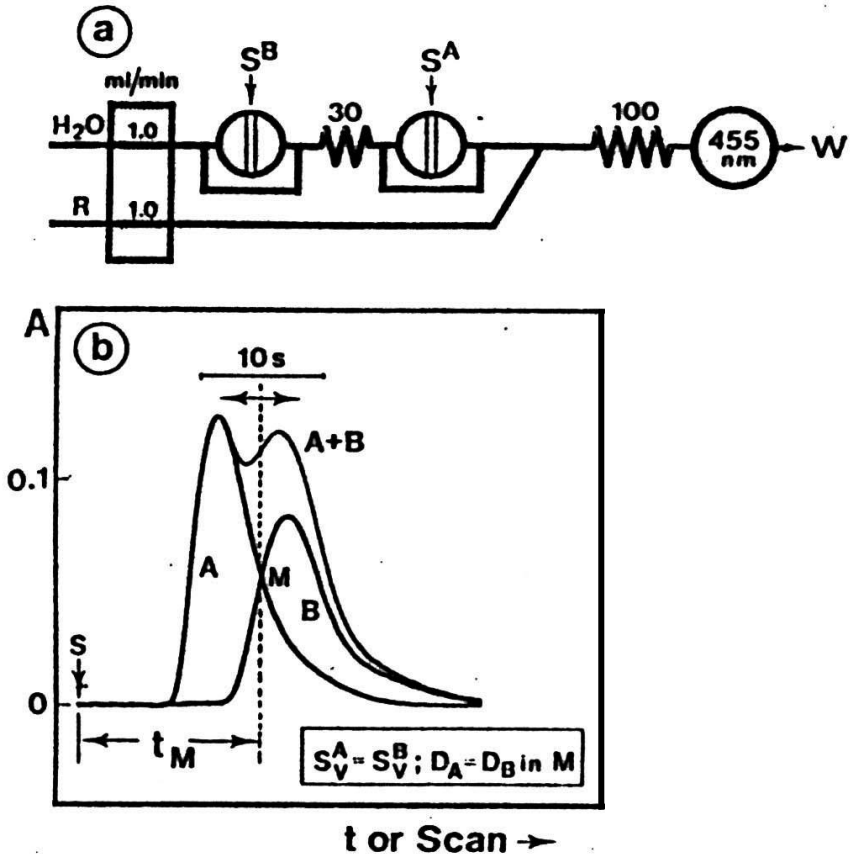

asynchronous merging. The precision is critically dependent on maintaining not only the two pumping rates, but also their absolute values, which is significantly more difficult[25]. The third method deals with the injection into a single live with asynchronous merging as shown in Fig. (1-7).

Fig. (1-7) Asynchronous merging of identical volumes of samples S^A and S^B.

1-2-5 Selectivity in Flow-injection Analysis

As a rule, FIA methods are less sensitive than their manual and segmented flow Analysis (SFA) counterparts for two reasons:

1- As the reaction time is rather short, equilibrium is not attained.

2- The physical dispersion or dilution of the sample in the carrier results in a signal of lower intensity than that corresponding to the undiluted plug. Valcarcel and Castro[12] attempted to improve the sensitivity by adjusting either reaction time or the dispersion leads to opposing effects, since the use of a lower flow-rate, to increase the reaction yields, results in an increased dispersion. Both the chemical and FIA variables of each flow-injection manifold should be optimized in order to attain the maximum sensitivity level.

The sensitivity can be improved by introducing suitable modifications to the FIA manifolds, i.e., a merging (where the reagent converges with a pure solvent stream into which the sample plug is injected) is used to achieve a greater extent mixing of reagent sample and plug. In addition, the sensitivity will be increased by increasing the injected sample volume when using this type of configuration instead of injecting samples directly into the reagent stream. Moreover, to improve the sensitivity by using continuous separation system incorporated into FIA assemblies can

achieved by using a microcoloum pack with chelating exchange resin to concentrate heavy-metal ions in sea-water samples[12].

The two zones A and B are injected by means of a double valve into a single carrier line, and the two injection zones are separated by a suitable length of delay coil. Sample A reaches to the detector before sample B. As sample B has to travel through a longer path than A, the injection of identical concentration in the two valves will result in peaks of different heights. Once M and t_m have been determined, they can readily be rechecked by injecting a fixed concentration of alternately by each value: if M is unchanged, the peak height measurement for each injection should be identical. It is interesting to know that the three methods provide K_{AB} values that are consistent with one another.

1-2-6 Flow-injection and Chromatography

In this section a simplified comparison is presented to show the great similarity of this technique with high performance liquid

Continuous flow analysis (CFA)

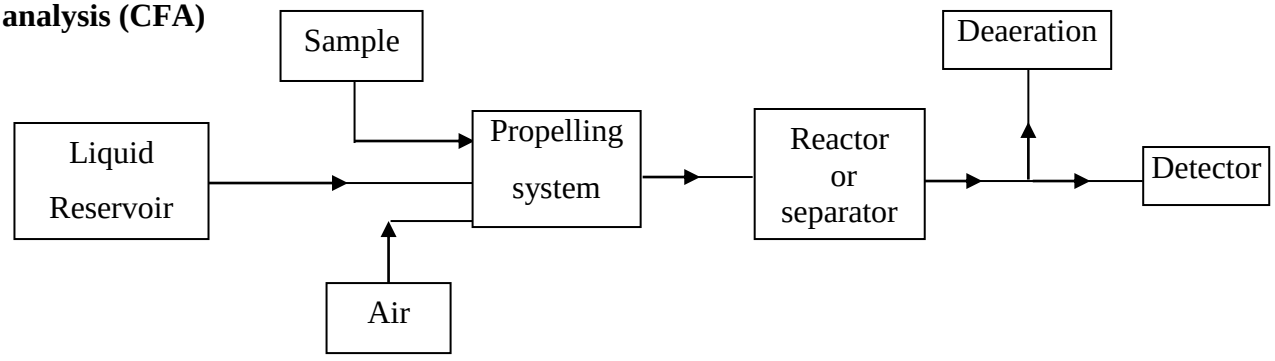

Flow-injection analysis (FIA)

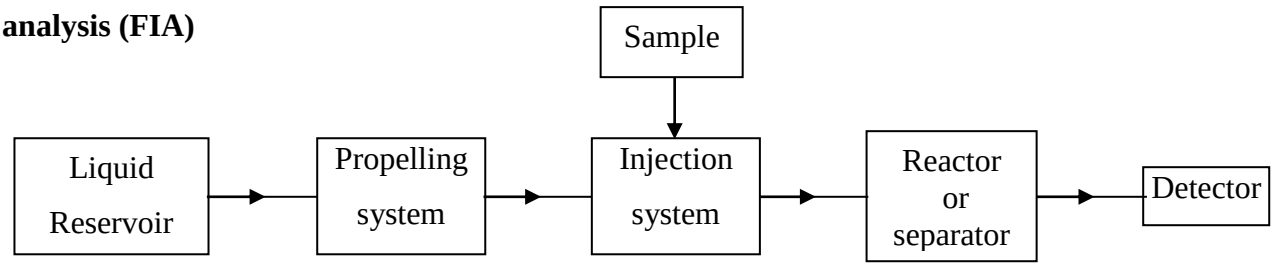

Liquid chromatography(LC)

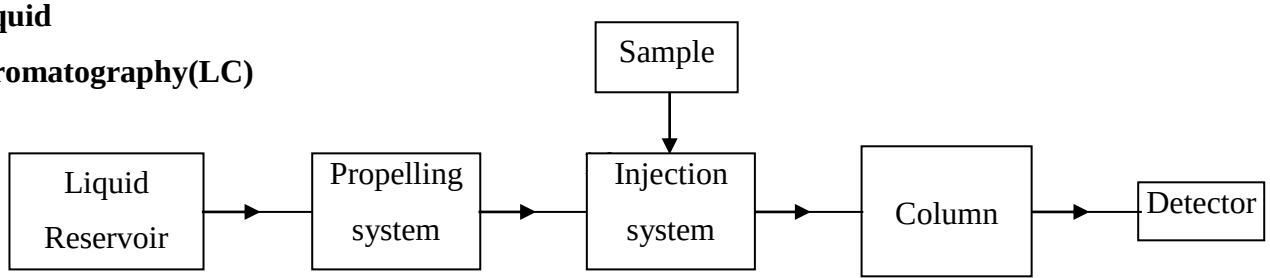

chromatography[28].

Fig. (1-8): Schematic Block diagram representation of CFA, FIA and LC (Liquid chromatography)

The (Fig.1-8) shows the great apparent similarity between FIA and chromatography. In fact, as a whole, FIA resembles chromatography more than classical segmented continuous flow methods do.

According to Vandereslice *et. al.*,[28-29] the following similarities should be emphasized: miniaturization capability, injection, unsegmented flow, small sample volume, signal profile and the lack of the characteristic lag phase of SFA. Table (1-2) shows common characteristic of HPLC and FIA.

Table (1-2) list the common differential features FIA and HPLC (high performance liquid chromatography)

Common characteristics		**Differential characteristic**	
		HPLC	**FIA**
Unsegmented flow	Interface	Always	Occasionally
Sample introduction: injection	Column	Essential	Possible
Sample volume: small	Pressure	High	Low
Flow-rate: variable	Data produced	Peak height/area	Peak heigh/area width, peak to peak distance
Tubing diameter: small	Cost	High	Low
Lag phase: negligible	Versatility main	Limited	Great
	analytical purpose	Several components in a single sample	A single component in many samples

The substantial difference between FIA HPLC is that HPLC operates at pressure more than 70 atm whereas a FIA system could operate at about 0.5 atm by using a simple peristaltic pump because, in HPLC, the liquid has to be forced through a tightly packed column material, whereas in FIA the sample zone passes through short length of narrow tube. Basically, however, FIA and HPLC are two quite different techniques, because their principles and purposes are different[30-32].

1-2-7 Dispersion

Dispersion is defined as the ratio of the concentration before and after the dispersion process has taken place in those elements of fluid, which correspond to the maximum on the dispersion curve, Fig. (1-9), by denoting C: as the original concentration of the injected sample solution and C^{max} as the concentration in the element of fluid corresponding to the peak maximum[30].

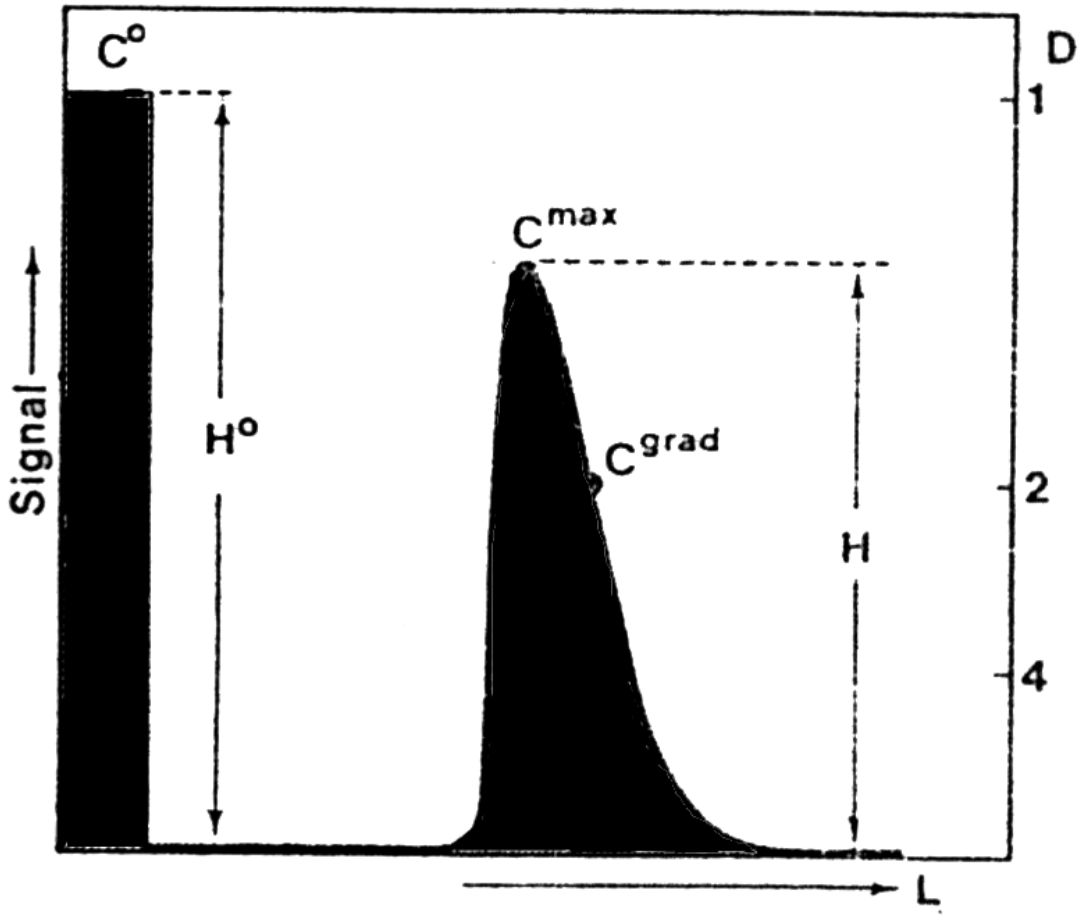

Fig. (1-9) Dispersion D in the FIA system

The controlled dispersion of the sample zone which occurs during its passage through the system towards the detector results in a response curve as shown in. Fig. (1-10) which shows a peak shape, characteristic of the flow injection system. Naturally, the sample zone broadens as it moves downstream and changes from the original asymmetrical shape to a more symmetrical and eventually Gaussian form[28].

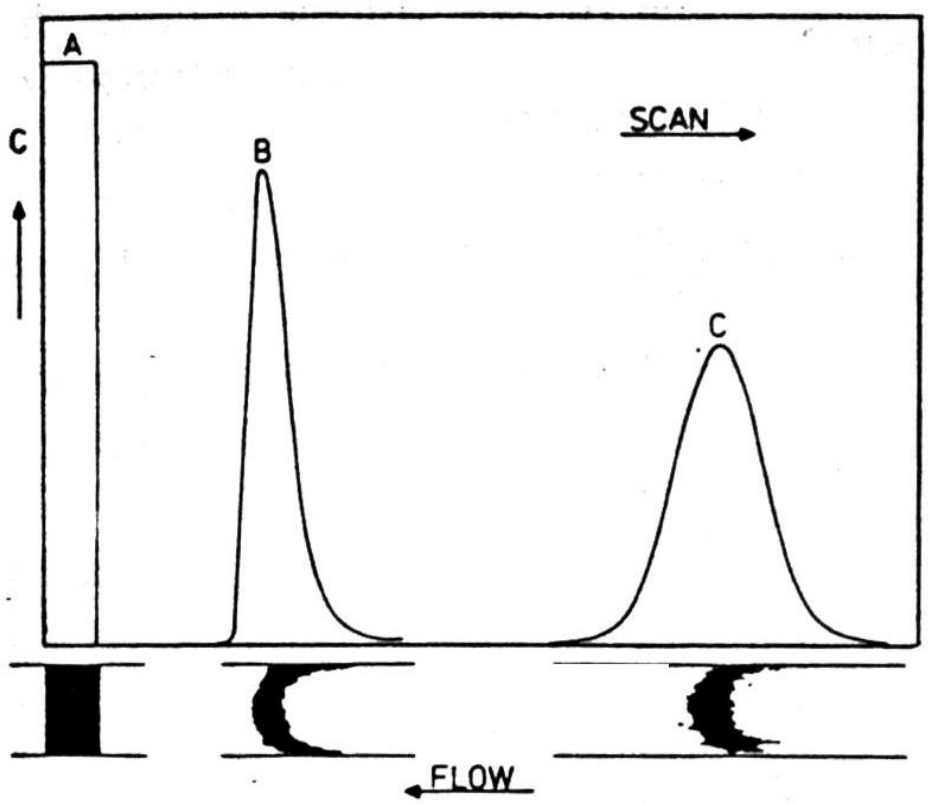

Fig. (1-10) Typical peak forms and corresponding concentration profile observed: (A) at the point of injection; (B) shortly after injection; and (C) after passage through an open narrow tube.

Generally, dispersion can be classified into three brad categories; limited, medium and large, which can be employed in the following ways.

If the original composition of the sample solution is to be measured, e.g., pH or conductivity. A limited dispersion of the sample zone is required. Inorder to ensure that the readout as obtained at the centre of the sample zone is not effected by any mixing with the surrounding carrier stream. Also when the flow injection system is to serre merely as a means

of reproducible introduction of the samples into a detector, the conditions of limited dispersion are most suitable[33]. However, in medium dispersion the centre of the sample zone must be mixed effectively with the carrier stream and often with several reagents in sequence and if the interfacial concentration profiles between the sample plug and the carrier stream or to be employed, a large dispersion of the sample zone is required. Fig. (1-11) shows the types of dispersion together with the corresponding vessel geometries.

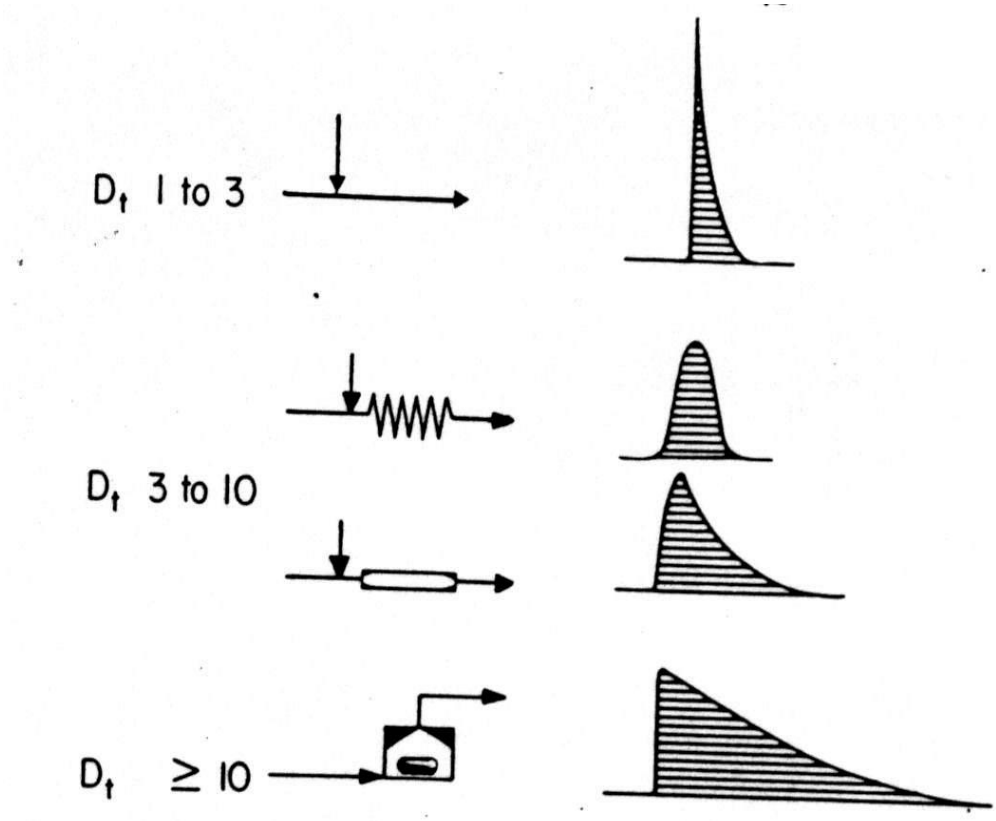

Fig. (1-11) Types of dispersion (D), together with the corresponding vessel geometries.

1-2-7-1 Factors affecting dispersion

The overall dispersion within an FIA system is the sum of the dispersions originating in three main parts of system[34]:

$$D = D_{injection} + D_{transport} + D_{dectector} \quad ...(1\text{-}10)$$

Where $D_{injection}$ is the dispersion due to the sample volume and to the geometric aspects of the system, $D_{transport}$ is the most significant contribution to the overall dispersion which includes the contribution of the reactor geometry and the flow rate, and $D_{decteror}$ donetes the contribution of the flow cell geometry (shape and dimensions) to the dilution. All three terms include contributions from factors such as deal volumes connectors, which can be very important in some instances.

(i)Sample volume

Fig. (1-12) shows the FIA signals obtained with an elementary FIA system which increasing volume ($v_1<v_2<v_3<v_4$) of a dye have been introduced, and recorded by starting from the same position on the chart so as to obtain a series superimposed curves. Ruzicka *et. al.*,[35] concluded that travel time does not depend on the injected volume however the residence time and baseline-to-baseline are both increases with the injected volume. The dispersion coefficient decreases with increasing the injected volume.

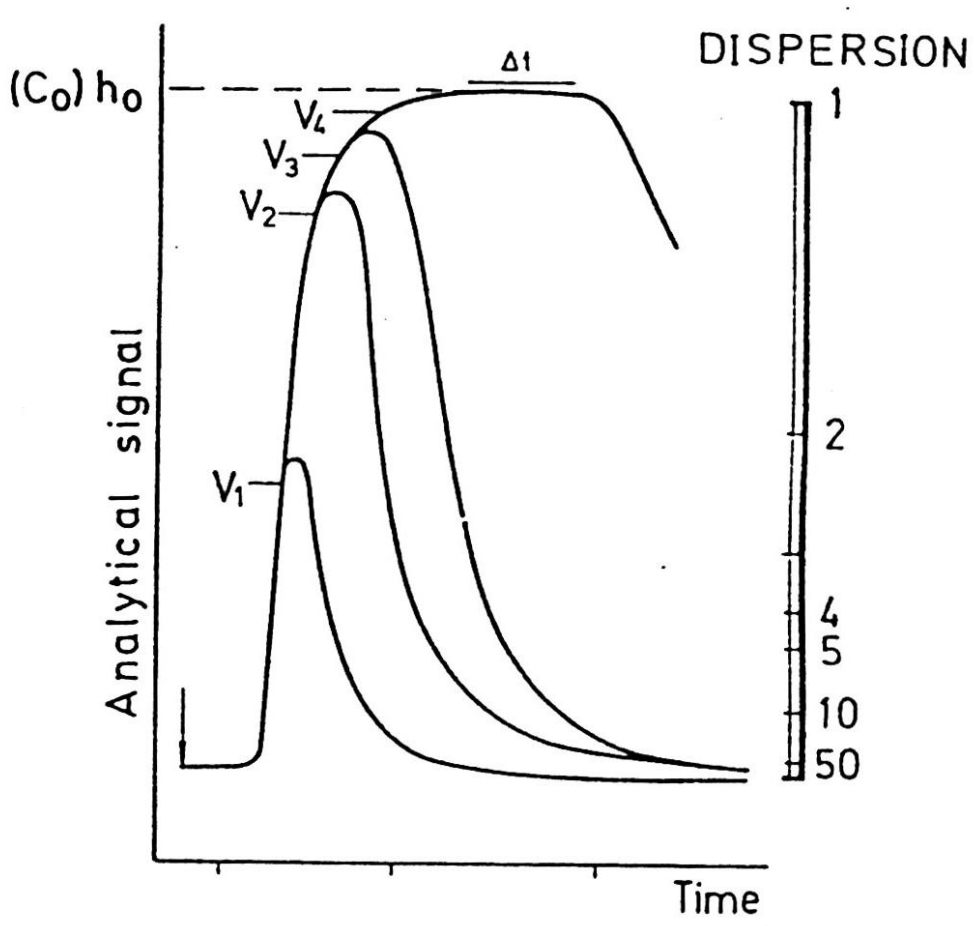

Fig. (1-12) Influence the injected sample volume on dispersion coefficient

(ii) Hydrodynamic factors

Vanderslice's expressions indicate the relation between the flow rate, q and baseline-to-line times

$$t_a = \frac{K}{q^{0.125}} \qquad \ldots(1\text{-}11)$$

and K constant which = $\frac{109R^2D^{0.025}.L^{1.025}}{f}$

K′: constant =

$$\frac{35.4R^2 fl^{0.64}}{D^{0.36}}$$

and

$$\Delta t = \frac{K'}{q^{0.64}} \qquad \ldots(1\text{-}12)$$

where t_a is travel time , Δt is baseline-to-line time and q is the flow-rate. Fig. (1-13) shows that the dispersion, t_a, Δt, should decrease with the increasing flow-rate[35].

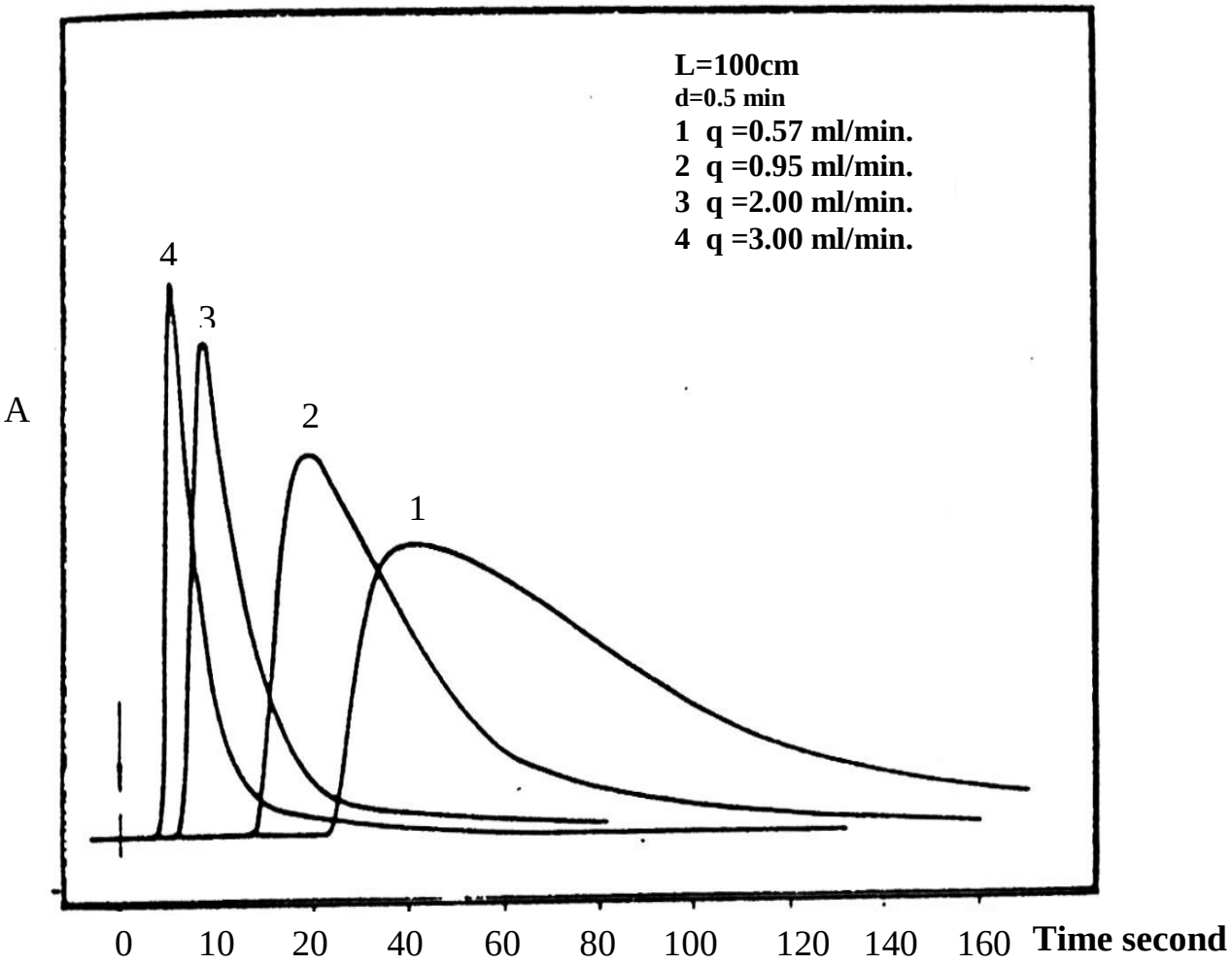

Fig. (1-13) Influence of flow-rate on the dispersion, time and peak width.

(iii) Geometric factors

Geometric factors deals with the influence of the reactor shape and its dimensions on the dispersion[36]. There are two shapes of reactor:

(a) straight tubes

Fig. (1-14) shows that t_a and Δt increase with the reactor length according to Vanderslice's predictions

$ta = KL^{1.025}$

and

$$\Delta t = K'L^{0.64} \quad \ldots(1\text{-}14)$$

where L is the reactor length.

The dispersion coefficient increases with the increasing reactor length, which is consistent with Ruzicka's expression.

$$D = KL^{1/2} \quad \ldots(1\text{-}15)$$

Where D is the dispersion coefficient

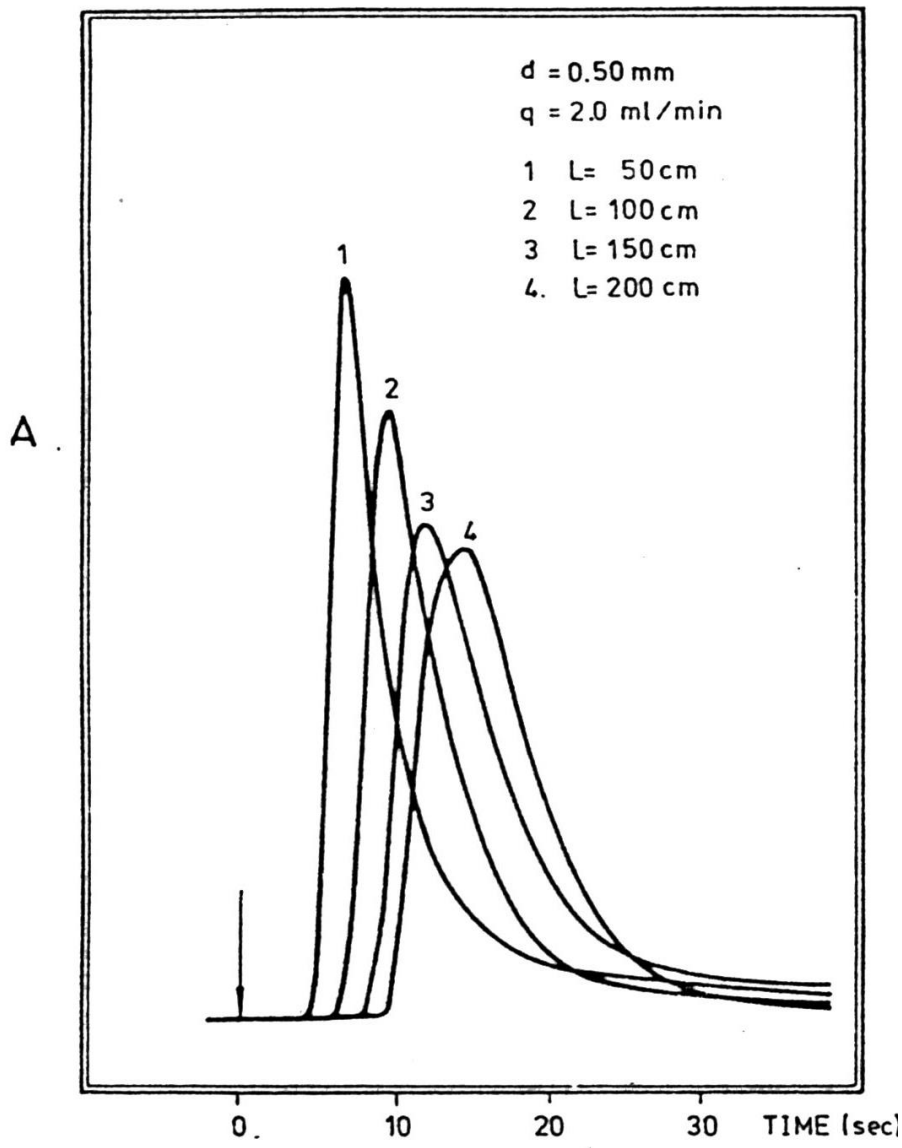

Fig. (1-14) influence of reactor length on the signal obtained which shows brocedeing increased (50-200 cm) as the length.

(b) coils

Fig. (1-15) shows the signals obtained with a conventional FIA system for a reactor of constant length L=125 cm in the form of straight tubing(1), a coil with diameter 26mm (2), and a coil with diameter 4mm(3). From this curve the smaller diameter, the smaller the dispersion[37].

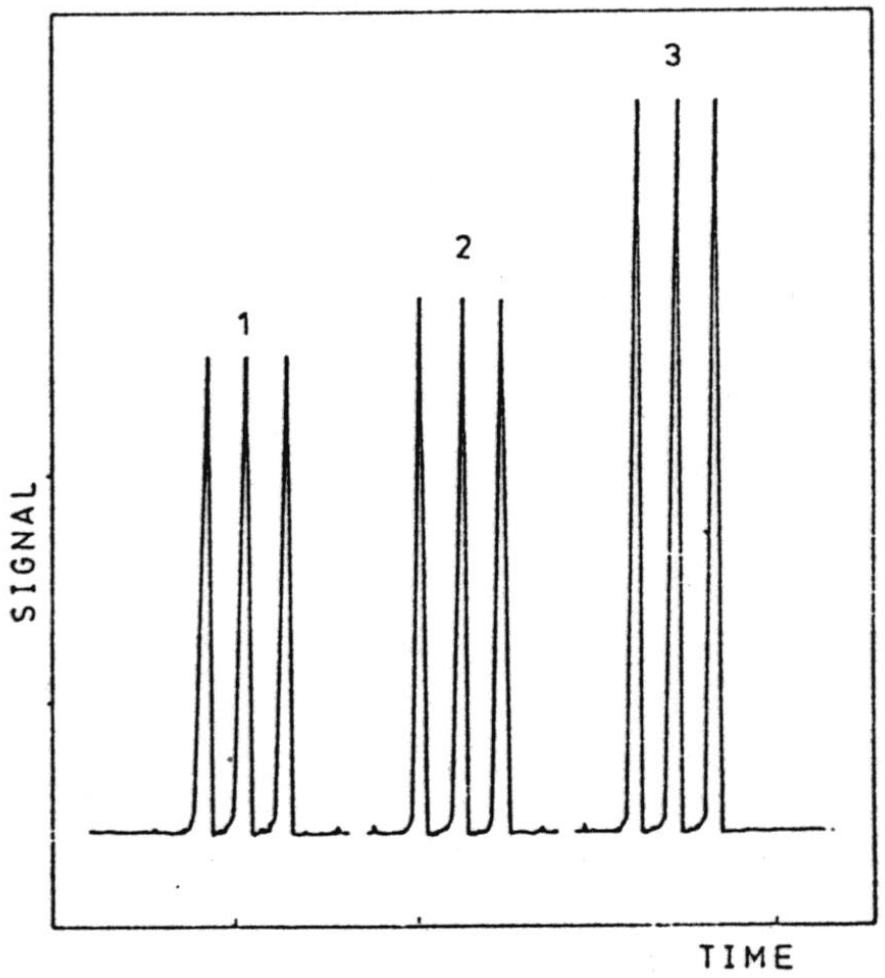

Fig. (1-15) influence of coil diameter an the dispersion

1-2-8 The stimulus response technique

The flow injection analysis response curve is a result of two processes, the physical process of dispersion of the sample zone within the carrier stream and the chemical process of formation of a chemical species. The physical process of material dispersion is due to the hydrodynamic processes which take place in the flow through system and is therefore conveniently investigated by stimulus response technique[38]. This technique is based on introduction of a tracer into flowing stream and on measurement of the dispersion of the tracer as caused by the transport process throughout the system. If the tracer is injected as a zone (stimulus), then the observed response reflects the dispersion in the system through the increase of the width of the tracer zone as increased by the combined contribution from convection and diffusion. These two steps occur simultaneously. If the response curve has a Gaussian shape, then its first statistical moment, the mean of the tracer curve corresponds to the maximum peak, when expressed by units of time. The first moment allows estimation of the average time available for chemical conversion, since it constitutes the mean residence time that the tracer material in average has spent in the reactor. The second statistical moment is proportional to the peak width, and for the Gaussian peak, it is the second power of the half peak width measured at 0.61 peak height[30] as shown in Fig. (1-16).

The increase of the second moment caused by transport through the reactor is due to the dispersion. The relation between dispersion and residence time is an important parameter for optimization of all types of flow systems as shown in Fig. (1-17).

It is application varies depending on the purpose. These are two reasons: first is that the mixing in FIA is nonhomogeneous and directional (since it yields a concentration gradient in both axial and

radial direction), and as a result of this stratification the ensuing chemical reactions take place gradually, while the reagent penetrates the sample gradient during the movement of the dispersing zone through the channel. Therefore, the FIA response curve is not only a result of the processes that occur at the detector location, but also of all the processes that gradually take place upstream in the FIA system at variable reagent concentration. The FIA readout is selected at peak maximum according to Qebergas model[38] as shown in Fig. (1-18) and Fig. (1-19) the movement of the liquids in the tubes could described by the convective-diffusion equation.

$$D_m\left(\frac{\partial^2 c}{\partial x^2}+\frac{\partial^2 c}{\partial r^2}+\frac{1}{r}\frac{\partial c}{\partial t}\right)=\frac{\partial c}{\partial t}+2F(1-\frac{r^2}{R^2})\frac{\partial c}{\partial x} \qquad \ldots(1\text{-}16)$$

where D_m is the molecular diffusion coefficient, c is the concentration, x is the distance along the tube, r is the radial distance from the tube axis, R is the tube radius, t is the time and F is the average flow velocity. The reduced velocity is described by the peclet]Number

$$Pe = R(2F)/D_m \qquad \ldots(1\text{-}17)$$

the reduced distance x

$$x = D_m\, x / R^2(2F) \qquad \ldots(1\text{-}18)$$

The reduced time *T*

$$T = D_m\, t /R^2 \qquad \ldots(1\text{-}19)$$

Were selected to approximate the range of FIA conditions, that is, Pe>1000

$0.004 < x < 1.0$

$0.002 < T < 0.8$

When the contribution of diffusion to radial transfer is negligible, a sharp rise at the peak leading edge and exponential decay at its tail, characteristic of convective dispersion due to a poisseuille profile are observed. For long residence times (T=0.4) a nearly Gaussian peak is

observed, while for shorter residence times a peculiar double-humped peak is observed. Ruzicka and Hansen[38] are another equation for baseline to baseline value.

$$\Delta t_b = 56.7\ R^{0.293}\ L^{0.107}\ Q^{1.057} \qquad \ldots(1\text{-}20)$$

and for dispersion coefficient D at any time t:

$$D = C_o / C_{max} = 2.342\ L^{0.106}\ Q^{0.206}\ R^{0.496} \qquad \ldots(1\text{-}21)$$

The second reason is that flow injection analysis encompasses a much wider range of solution, that is sample dilution, preconcentration, reaction rate measurement and multicomponent detection.

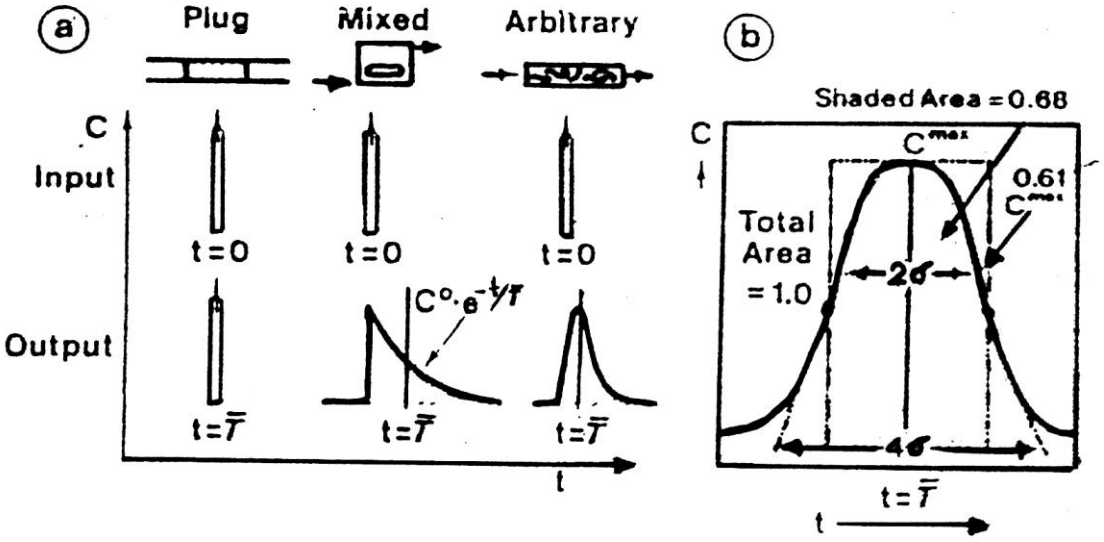

Fig. (1-16) a- Curves for plug, mixed and arbitrary flow

b- For arbitrary flow, a Gaussion-shaped curve is eventually achieved

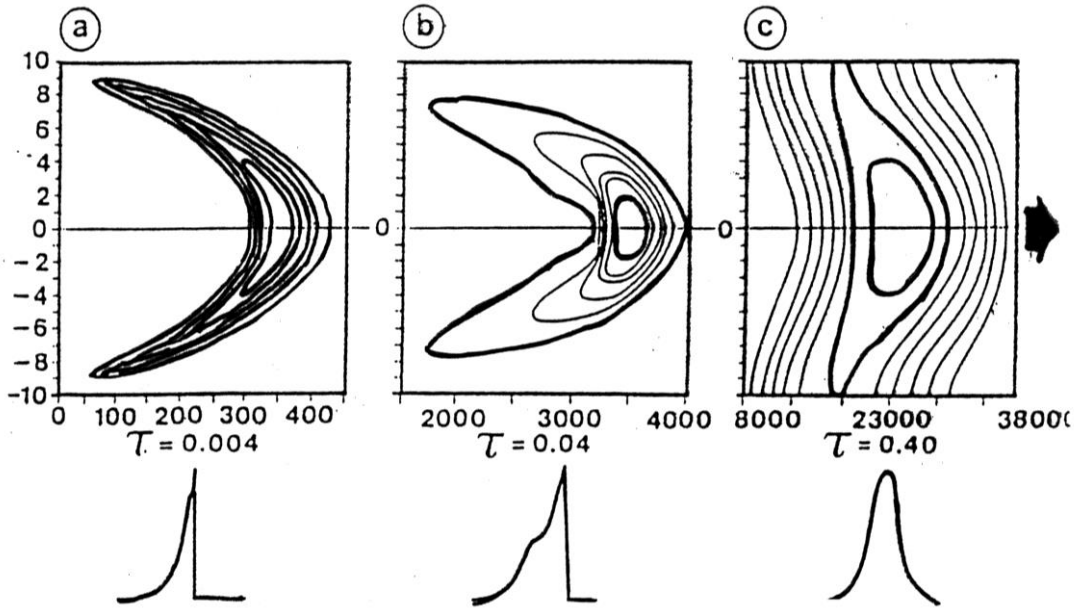

Fig. (1-17) Dispersion of a sample plug in a straight tubular channel.

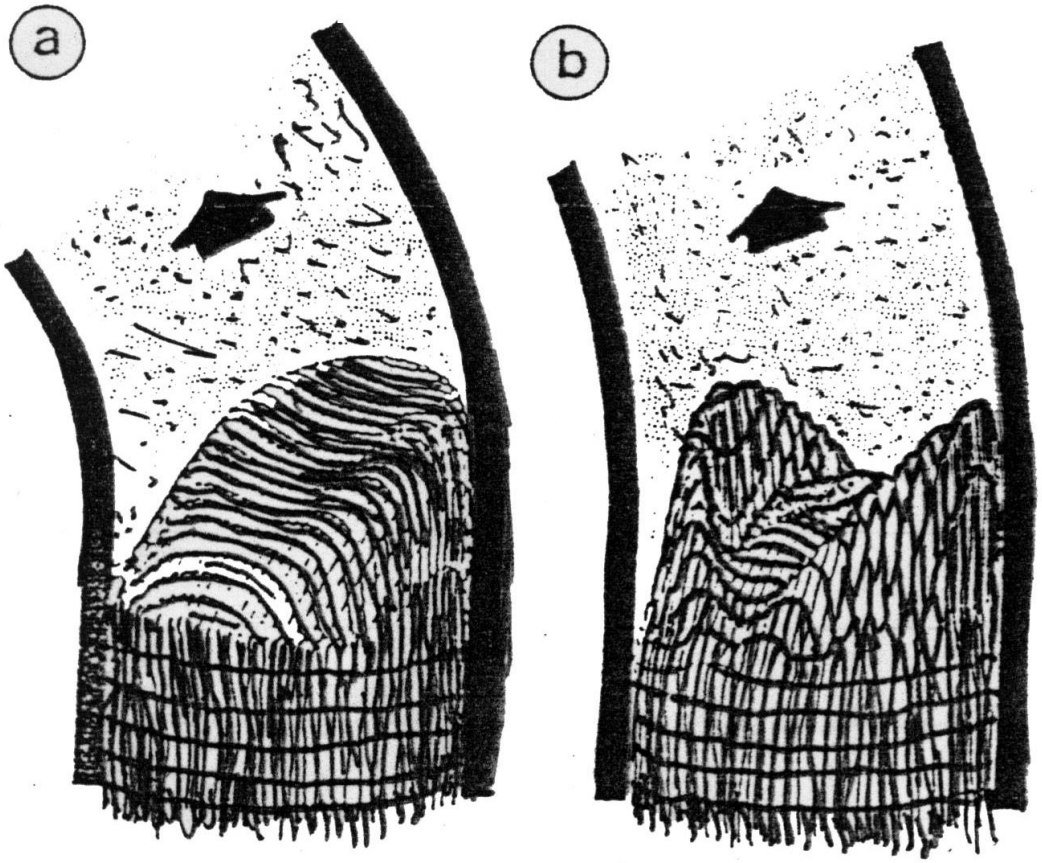

Fig (1-18) Dispersion in coiled tubes. a) Equivelocity profiles in axial direction. b- Equivelocity profiles in radial direction

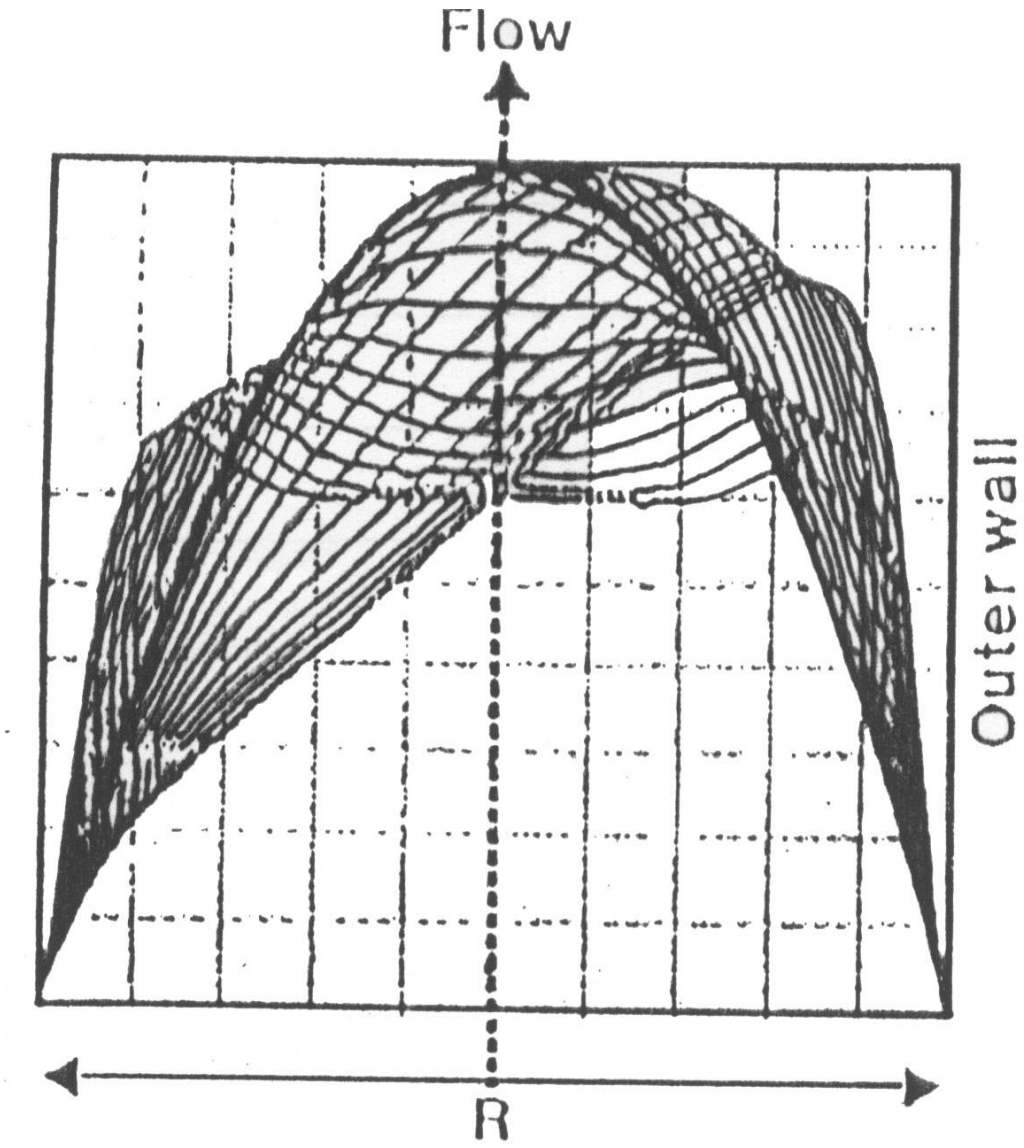

Fig (1-19) Axial velocity profiles in a coil tube.

1-2-9 Operation modes of manifold

Various mode of operation could be conducted in FIA system mainly single line and multiple line system in the following section a brief clisscussion is presented

(i) Single-line

manifolds Fig. (1-20) shows the simplest FIA system which consists of one tube through which the carrier stream moves towards the flow

through detector. Depending on injected volume sample(s) tube length (L) and flow geometry. In this system, limited, medium, and large dispersion can be achieved[39,40].

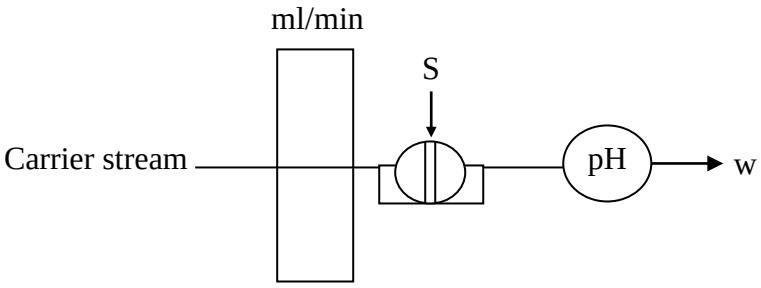

Fig. (1-20) single-line manifolds

(ii) Multiple lines

Sequential use of only two reagents is a simple matter because a manifold designed for this purpose involves only one confluence point at which a second reagent is added to the sample zone when carried past by the stream of the first reagent[41] as shows in Fig. (1-21).

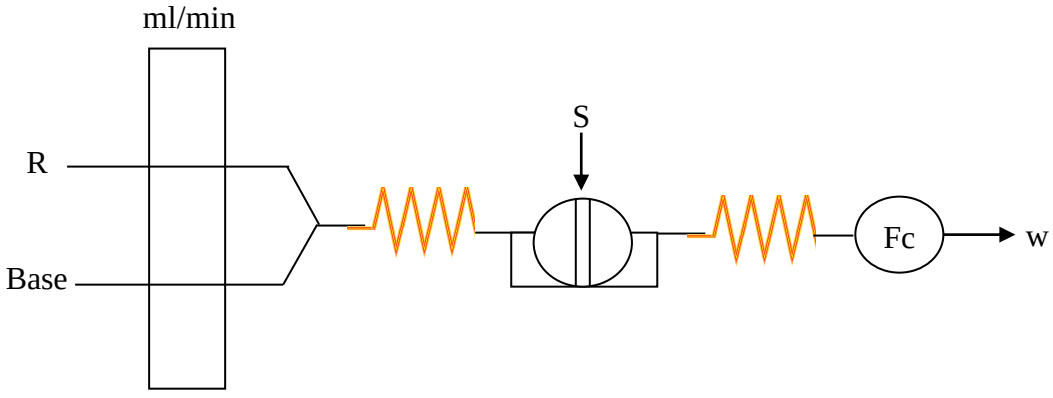

Fig. (1-21) Two-lines manifolds

And, Fig. (1-22) shows the manifolds of three lines where the reagent are added sequentially and then the reaction product was occurs[42,43].

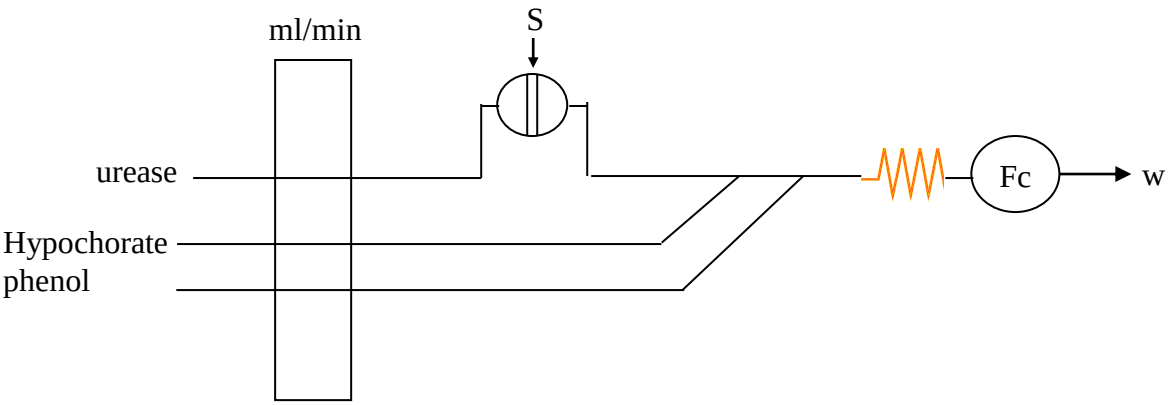

Fig. (1-22) Three-lines manifolds

1-2-10 The merging zones

The relatively high reagent consumption is the main disadvantage of all continuous flow systems, which, in contrast to batch analyzer , use the reagent continuously even when there is no sample present in the apparatus notably during the startup and shutdown procedures.

This problem is not as great in FIA, where the volume of the sample path is seldom larger than a few hundred microliters and therefore easy to fill and wash in a very short period using small amounts of reagent or wash solutions. If however, an expensive reagent or enzyme is used, it is wasteful to pump solutions continuously, because the reagent also occupies those section of the sample path where the sample zone is not present simultaneously[44]. The merging zones principle avoids this uneconomic approach by injecting the sample and introducing the reagent solution in such a way that the sample zone meets the selected section of the reagent stream in a controlled manner. The rest of the FIA system is filled with wash solution or only pure water. This can be achieved in two

different ways, by the merging zones systems which are based on intermittent pumping[45] as shown in Fig. (1-23.a), where two pumps are operated is such a way that when pump 1 is in the position, pump II is in the stop position, and vice versa. Thus the sample zone is first transported from the injection port by mean of pump I, then when a chosen distance from the merging point is reached pump II is started, which continues to bring the carrier stream forward while the reagent is being added Fig. (1-24). After the sample zone has passed the merging point, point I is reactivated

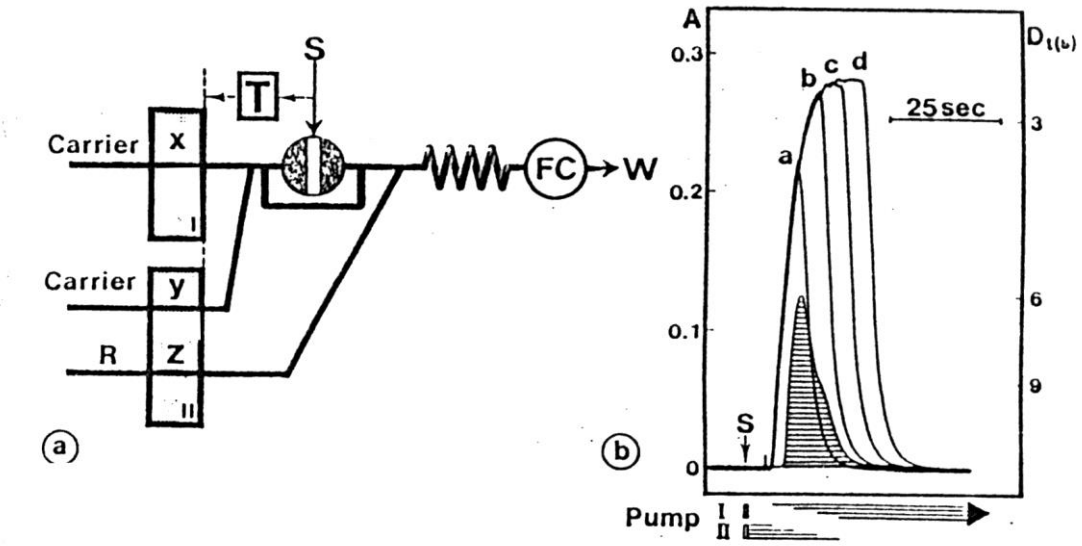

Fig. (1-23) a) FIA manifold for merging zones system based on intermittent pumping.

b) Recorder trace obtained with the system in (a).

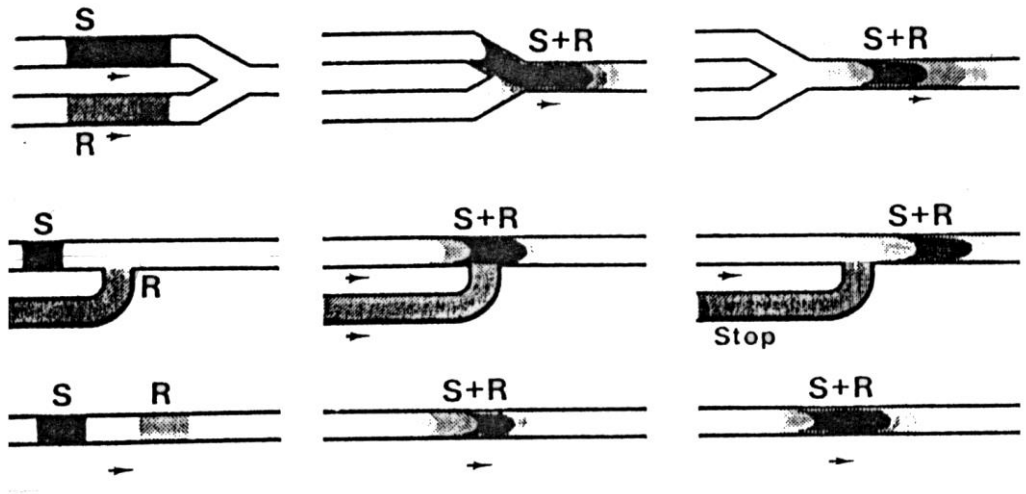

Fig. (1-24) The principle of zone merging a) intermitlent pumping b) zone penetration, c)showing, from left to right, the sample(s) zone and reagent (R) zone separately, during the initial contact, and then merged further downstream.

while pump II is stopped again. This approach allows the length of the reagent zone to be regulated simply by choosing different go and stop periods by means of the timer (T), and makes it possible to create different concentration gradients on the interface between the sample zone, reagent solution and carrier stream Fig. (1-23.b). Variations on this theme are numerous. Thus, by choosing different lengths of reagent zone, and by letting it overlap in different ways over the sample zone, an individual blank for the reagent alone and for the sample zone alone, as well as the peak height resulting from the chemical reaction between the components of the sample and reagent solution[(46)]. And by the suggestion of the use of a multiinjection value for the FIA merging zone approach[(47)], the purpose of using a value, such as that shown in Fig. (1-25) and Fig. (1-26) , is to inject sample and reagent zones into two separate carrier

stream pumped at balanced flow rates so that they meet in a controlled manner. As distilled water (or diluted buffer-detergent mixture) might be used as carrier in both stream. The reagent volume consumed per determination may be 30µl or less[43]. The carrier streams might be pumped continuously-for single- point measurement or intermittently, for stopped flow measurements. The advantages of the merging zones are, that it alleviated the reagent blank problem[48], cheap, rapid, and flexible analytical facilities that could be used even in small laboratories[49,50,51].

(b) coils

Fig. (1-15) shows the signals obtained with a conventional FIA system for a reactor of constant length L=125 cm in the form of straight tubing(1), a coil with diameter 26mm (2), and a coil with diameter 4mm(3). From this curve, the smaller diameter is, the smaller the dispersion[37].

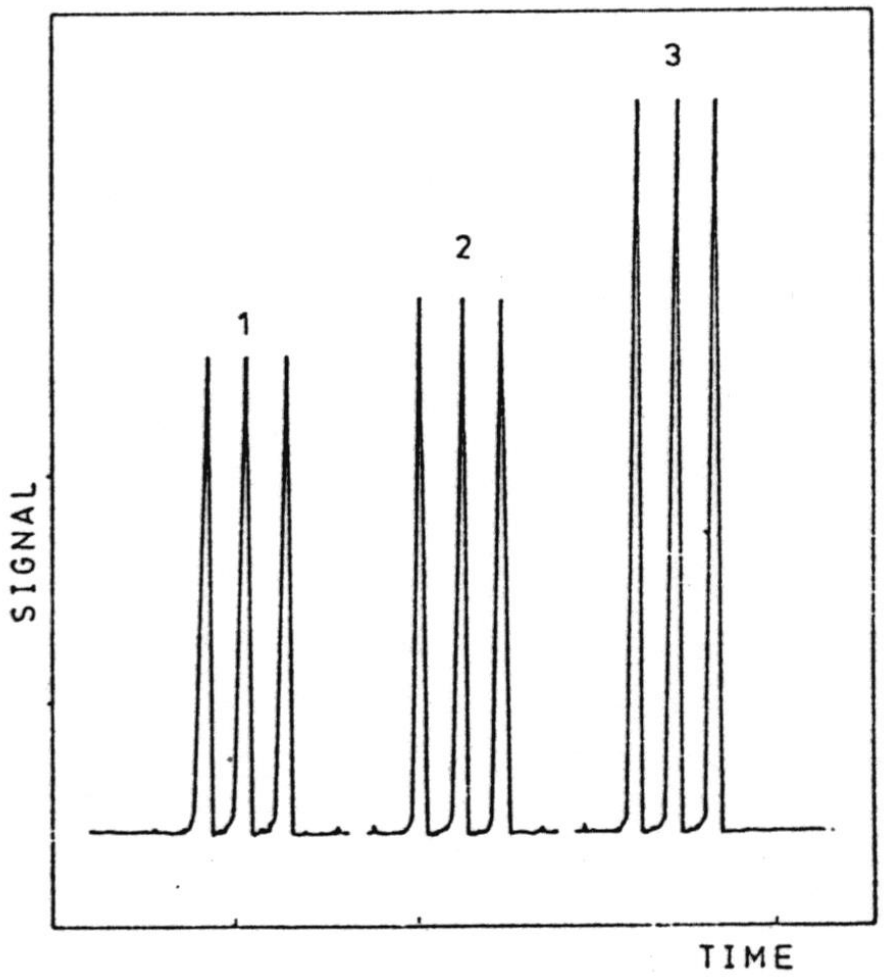

Fig. (1-15) influence of Coil Diameter an the Dispersion

1-2-8 The Stimulus Response Technique

The flow injection analysis response curve is a result of two processes: the physical process of dispersion of the sample zone within the carrier stream, and the chemical process of formation of a chemical species. The physical process of material dispersion is due to the hydrodynamic processes which take place in the flow through system and is therefore conveniently investigated by stimulus response technique[38]. This technique is based on the introduction of a tracer into flowing stream and on measurement of the dispersion of the tracer as caused by the transport process throughout the system. If the tracer is injected as a zone (stimulus), the observed response reflects the dispersion in the system through the increase of the width of the tracer zone as increased by the combined contribution from convection and diffusion. These two steps occur simultaneously. If the response curve has a Gaussian shape, its first statistical moment, the mean of the tracer curve, corresponds to the maximum peak, when expressed by units of time. The first moment allows estimation of the average time available for chemical conversion, since it constitutes the mean residence time that the tracer material in average has spent in the reactor. The second statistical moment is proportional to the peak width, and for the Gaussian peak, it is the second power of the half peak width measured at 0.61 peak height[30] as shown in Fig. (1-16).

The increase of the second moment caused by transport through the reactor is due to the dispersion. The relation between the dispersion and residence time is an important parameter for the optimization of all types of flow systems as shown in Fig. (1-17). Iis application varies depending on the purpose. There are two reasons, first the mixing in FIA is nonhomogeneous and directional (since it yields a concentration gradient in both axial and radial direction), and as a result of this stratification the

ensuing chemical reactions take place gradually, while the reagent penetrates the sample gradient during the movement of the dispersing zone through the channel. Therefore, the FIA response curve is not only a result of the processes that occur at the detector location, but also of all the processes that gradually take place upstream in the FIA system at variable reagent concentrations. The FIA readout is selected at peak maximum according to Qebergas model[38] as shown in Fig. (1-18) and (1-19). The movement of the liquids in the tubes could described by the convective-diffusion equation.

$$D_m\left(\frac{\partial^2 c}{\partial x^2}+\frac{\partial^2 c}{\partial r^2}+\frac{1}{r}\frac{\partial c}{\partial t}\right)=\frac{\partial c}{\partial t}+2F(1-\frac{r^2}{R^2})\frac{\partial c}{\partial x} \qquad \ldots(1\text{-}16)$$

where D_m is the molecular diffusion coefficient, c the concentration, x the distance along the tube, r the radial distance from the tube axis, R the tube radius, t the time and F the average flow velocity. The reduced velocity is described by the peclet]Number $Pe = R(2F)/D_m$

…(1-17)

the reduced distance x

$$x = D_m x / R^2(2F) \qquad \ldots(1\text{-}18)$$

The reduced time *T*

$$T = D_m t /R^2 \qquad \ldots(1\text{-}19)$$

Were selected to approximate the range of FIA conditions, that is, Pe>1000

$0.004 < x < 1.0$

$0.002 < T < 0.8$

When the contribution of diffusion to radial transfer is negligible, a sharp rise at the peak leading edge and exponential decay at its tail, and characteristic of convective dispersion due to a poisseuille profile are observed. For long residence times (T=0.4) a nearly Gaussian peak is observed, while for shorter residence times a peculiar double-humped

peak is observed. Ruzicka and Hansen[38] are another equation for baseline to baseline value:

$$\Delta t_b = 56.7\ R^{0.293}\ L^{0.107}\ Q^{1.057} \qquad \ldots(1\text{-}20)$$

and for dispersion coefficient D at any time t:

$$D = C_o / C_{max} = 2.342\ L^{0.106}\ Q^{0.206}\ R^{0.496} \qquad \ldots(1\text{-}21)$$

The second reason is that flow injection analysis encompasses a much wider range of solution, i.e., sample dilution, preconcentration, reaction rate measurement, and multicomponent detection.

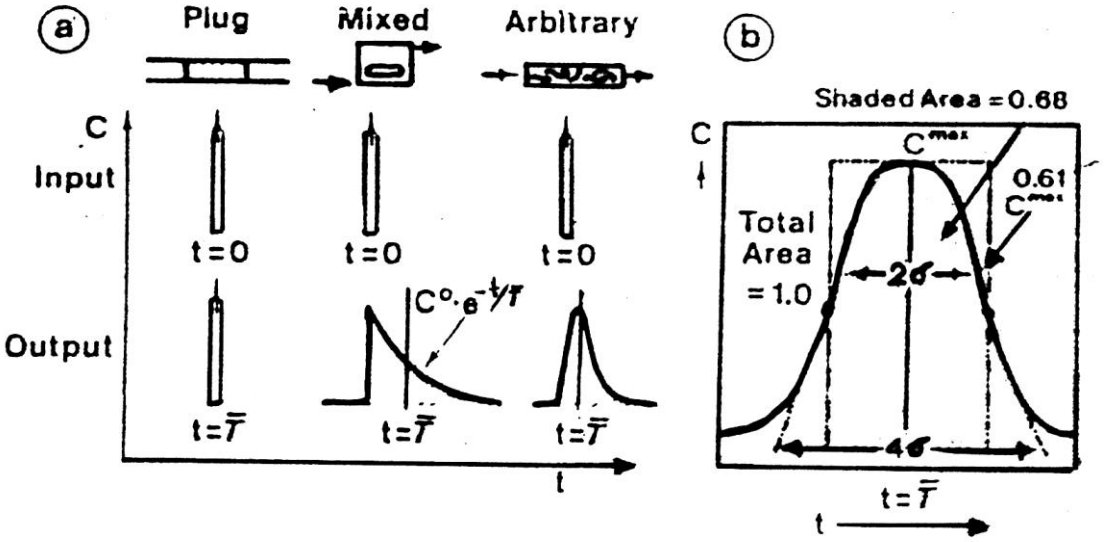

Fig. (1-16) a- Curves for plug, mixed and arbitrary flow

b- For arbitrary flow, a Gaussion-shaped curve is eventually achieved

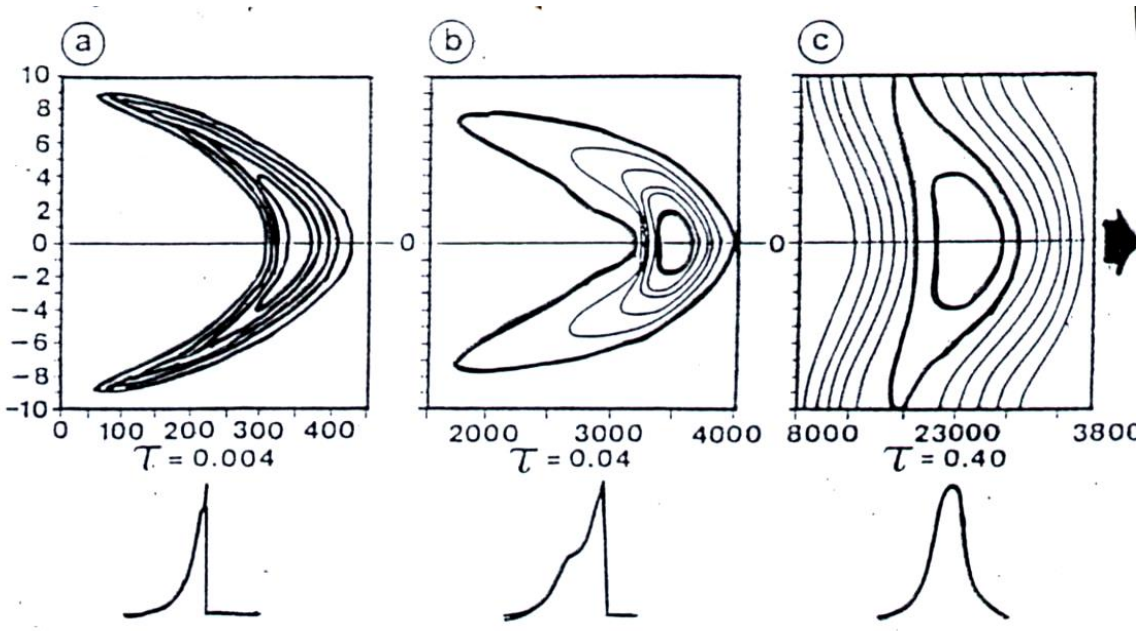

Fig. (1-17) Dispersion of a Sample Plug in a Straight Tubular Channel.

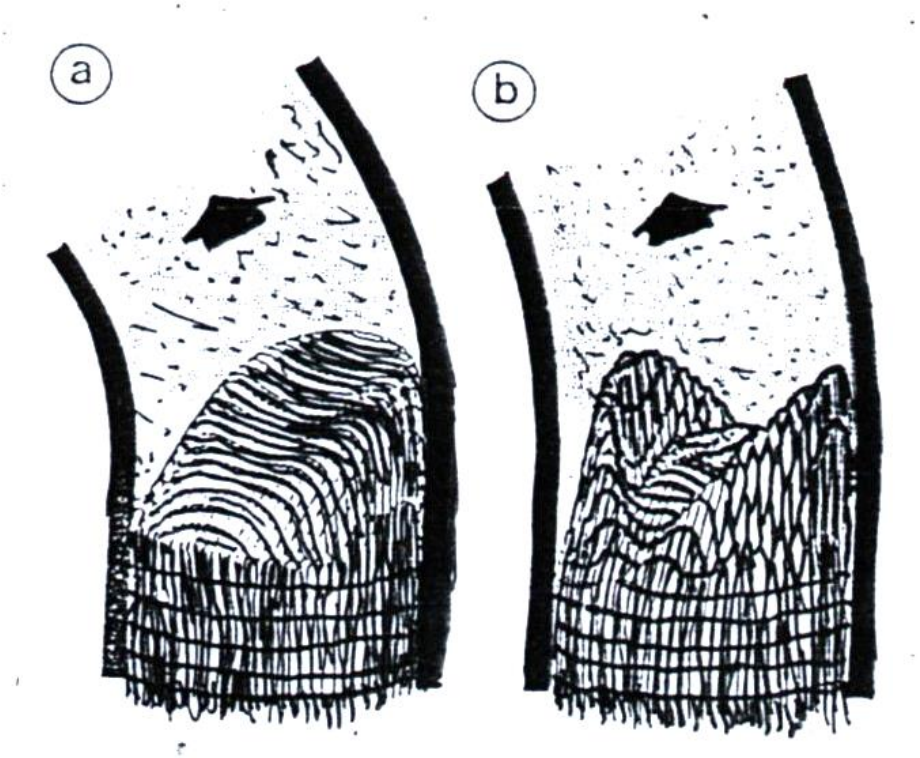

Fig (1-18) Dispersion in coiled tubes. a) Equivelocity profiles in axial direction. b- Equivelocity profiles in radial direction

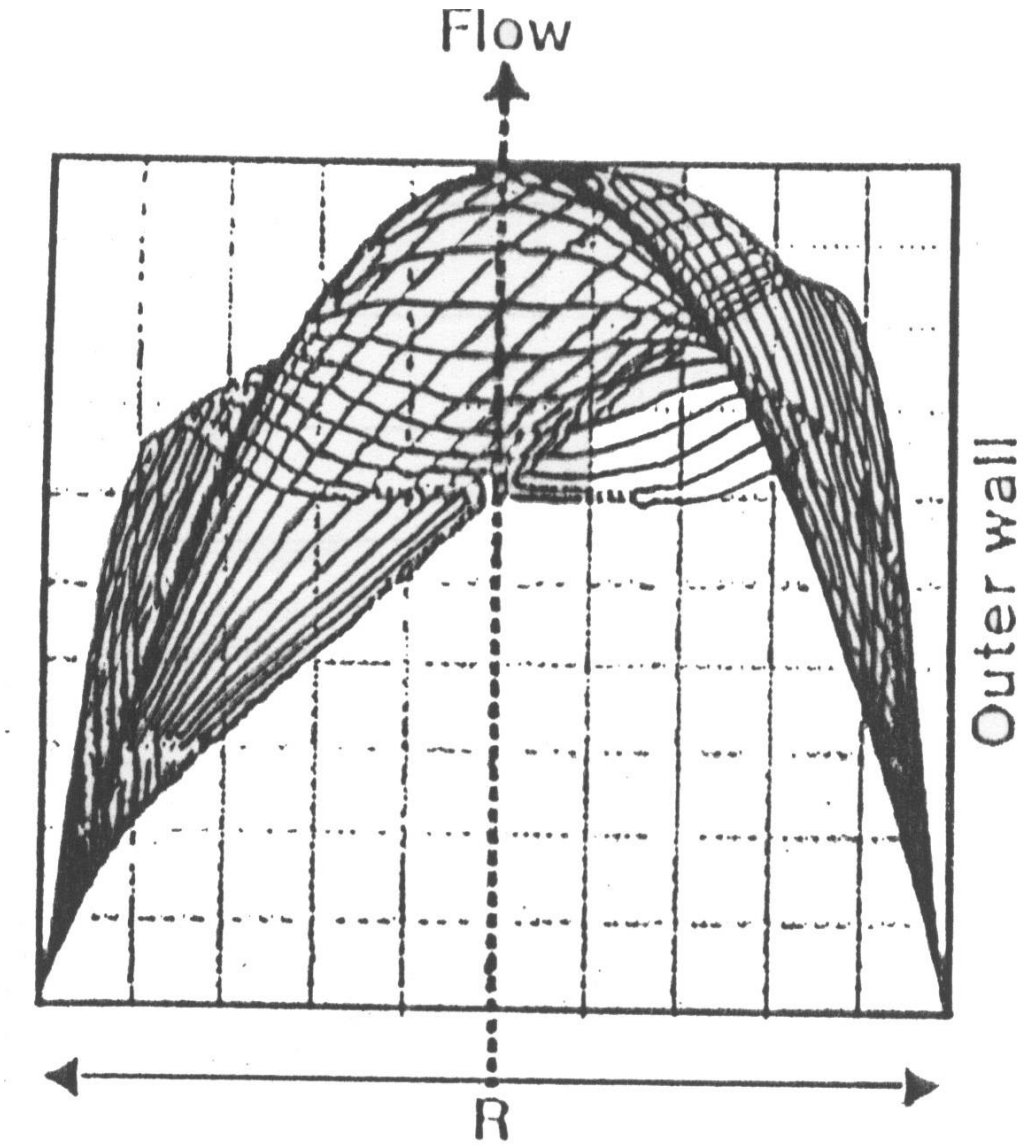

Fig (1-19) Axial velocity profiles in a coil tube.

1-2-9 Operation Modes of Manifold

Various mode of operation could be conducted in FIA system mainly single line and multiple line system in the following section a brief clisscussion is presented

(i) Single-line manifolds Fig. (1-20) shows the simplest FIA system which consists of one tube through which the carrier stream moves towards the flow through detector depending on injected volume

sample(s) tube length (L) and flow geometry. In this system, limited, medium, and large dispersion can be achieved[39,40].

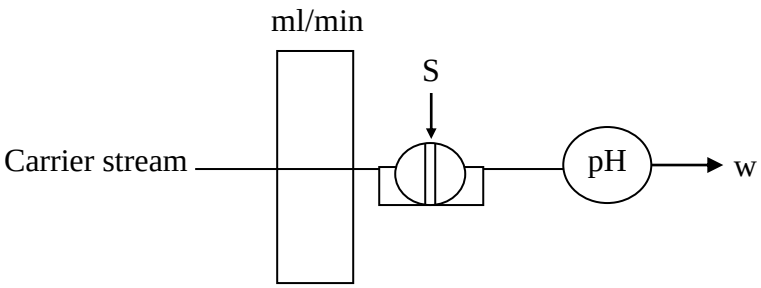

Fig. (1-20) single-line manifolds

(ii) Multiple Lines

The sequential use of only two reagents is a simple matter, because a manifold designed for this purpose involves only one confluence point at which a second reagent is added to the sample zone when carried past by the stream of the first reagent[41] as shown in Fig. (1-21).

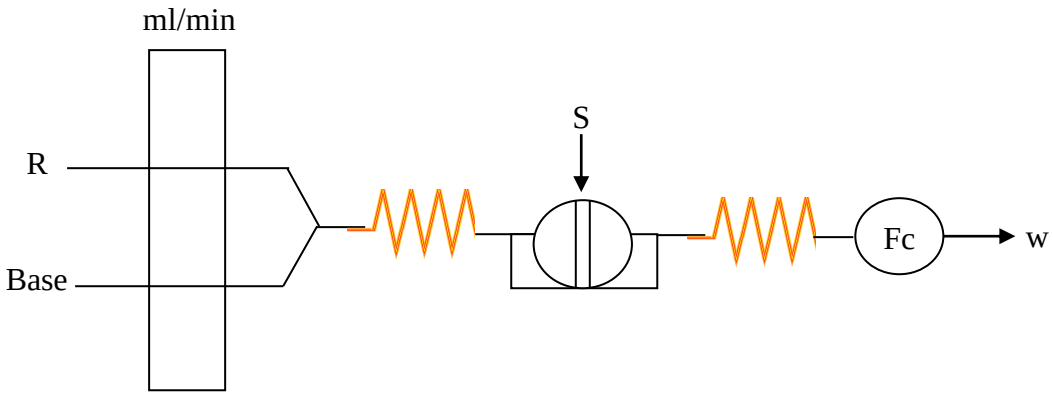

Fig. (1-21) Two-lines manifolds

Fig. (1-22) shows the manifolds of three lines where the reagent are added sequentially and then the reaction product occurs[42,43]:

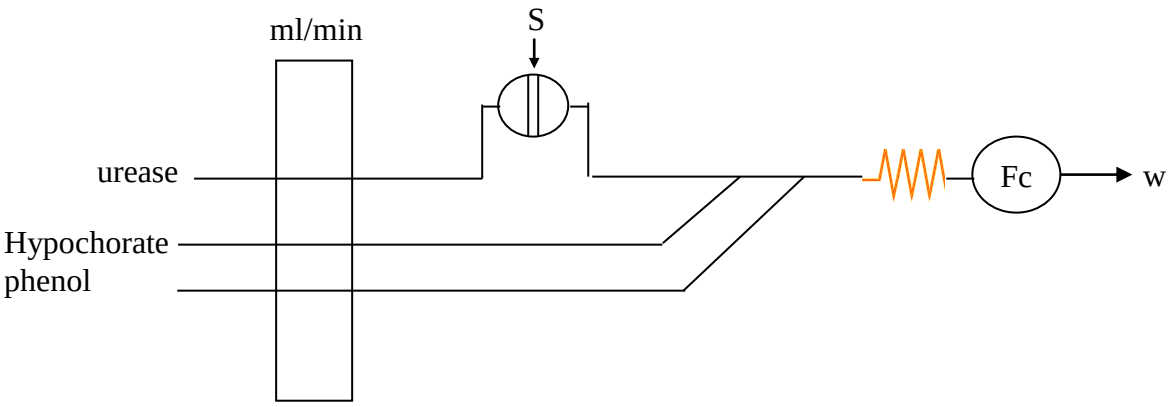

Fig. (1-22) Three-lines manifolds

1-2-10 The Merging Zones

The relatively high reagent consumption is the main disadvantage of all continuous flow systems, which, in contrast to batch analyzer , use the reagent continuously even when there is no sample present in the apparatus notably during the startup and shutdown procedures.

This problem is not as great in FIA, where the volume of the sample path is seldom larger than a few hundred microliters and, therefore, easy to fill and wash in a very short period, using small amounts of reagent or wash solutions. If, however, an expensive reagent or enzyme is used, it is wasteful to pump solutions continuously, because the reagent also occupies those sections of the sample path where the sample zone is not present simultaneously[44]. The merging zones principle avoids this uneconomic approach by injecting the sample and introducing the reagent solution in such a way that the sample zone meets the selected section of the reagent stream in a controlled manner. The rest of the FIA system is filled with wash solution or only pure water. This can be achieved in two different ways: the merging zones systems which are based on

intermittent pumping[45] as shown in Fig. (1-23.a), where two pumps are operated, is such a way that when pump 1 is in the position, pump II is in the stop position, and vice versa. Thus the sample zone is first transported from the injection port by mean of pump I, then when a chosen distance from the merging point is reached, pump II is started, which continues to bring the carrier stream forward while the reagent is being added Fig. (1-24). After the sample zone has passed, the merging point, point I is reactivated

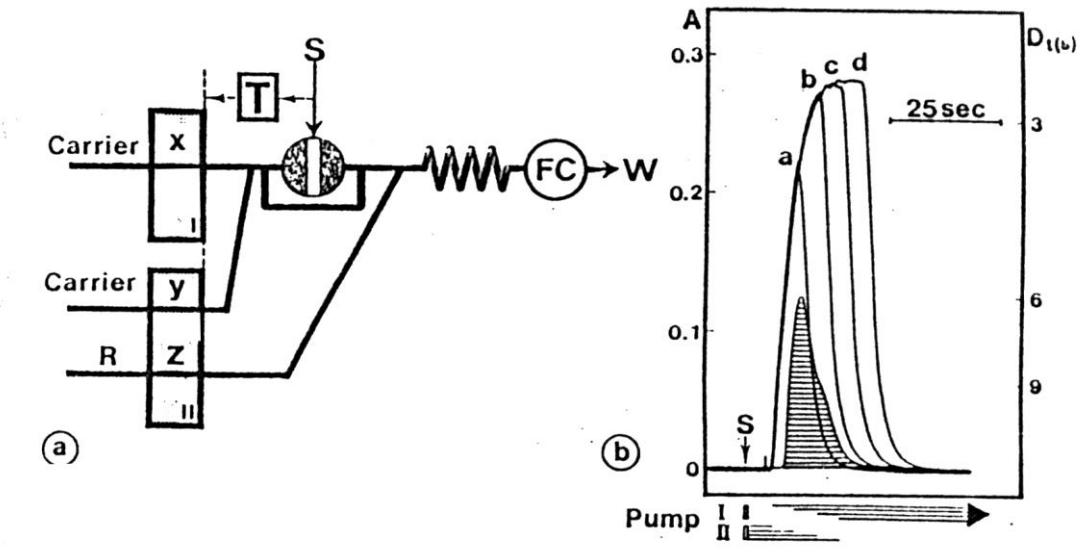

Fig. (1-23) a) FIA manifold for merging zones system based on intermittent pumping.

b) Recorder trace obtained with the system in (a).

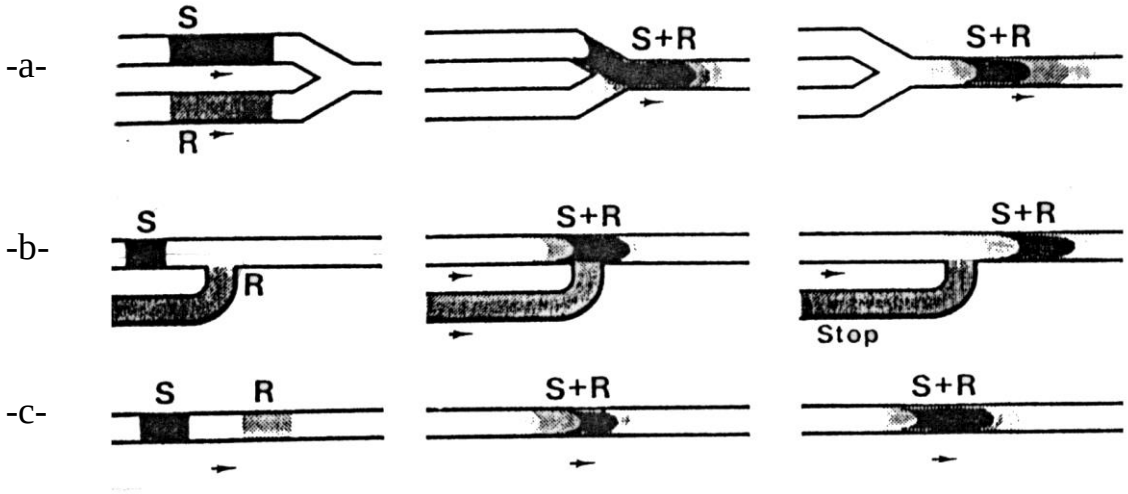

Fig. (1-24) The principle of zone merging a) intermittent pumping b) zone penetration, c)showing, from left to right, the sample(s) zone and reagent (R) zone separately, during the initial contact, and then merged further downstream.

while pump II is stopped again. This approach allows the length of the reagent zone to be regulated simply by choosing different go-and-stop periods by means of the timer (T), and makes it possible to create different concentration gradients on the interface between the sample zone, reagent solution and carrier stream Fig. (1-23.b). Variations on this theme are numerous. Thus, by choosing different lengths of reagent zone, and by letting it overlap in different ways over the sample zone, an individual blank for the reagent alone and for the sample zone alone, as well as the peak height resulting from the chemical reaction between the components of the sample and reagent solution[46] and by the suggestion of the use of a multiinjection valve for the FIA merging zone approach[47], the purpose of using a valve, such as that shown in Figs.(1-25) and (1-26) is to inject sample and reagent zones into two separate carrier stream

pumped at balanced flow rates so that they meet in a controlled manner. As distilled water (or diluted buffer-detergent mixture) might be used as carrier in both streams the reagent volume consumed per determination may be 30μl or less[43]. The carrier streams might be pumped continuously for single- point measurement or intermittently for stopped flow measurements. The advantages of the merging zones are, that alleviated the reagent blank problem[48], cheap, rapid, and flexible analytical facilities that could be used even in small laboratories[49,50,51].

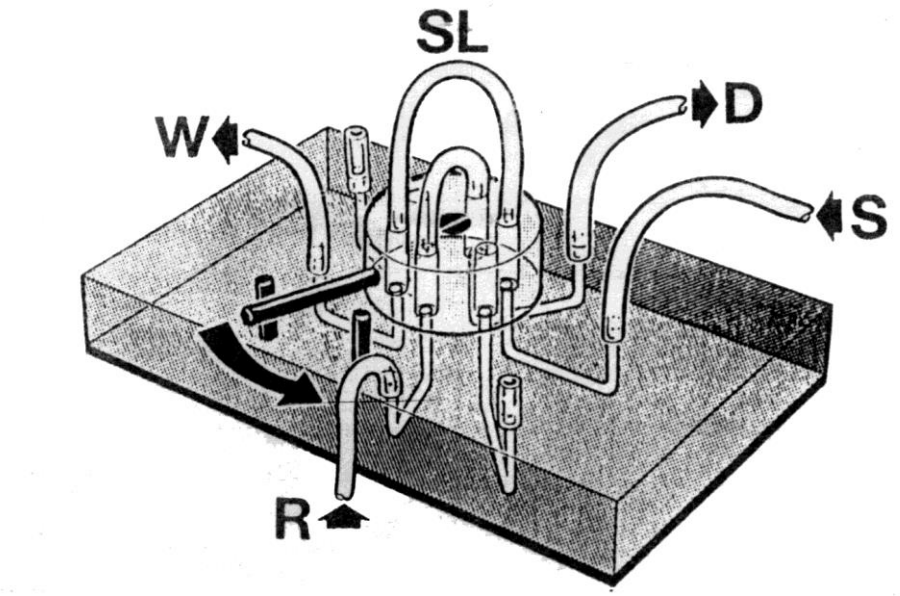

Fig. (1-25) : Six-port Valve Integrated into a FIA

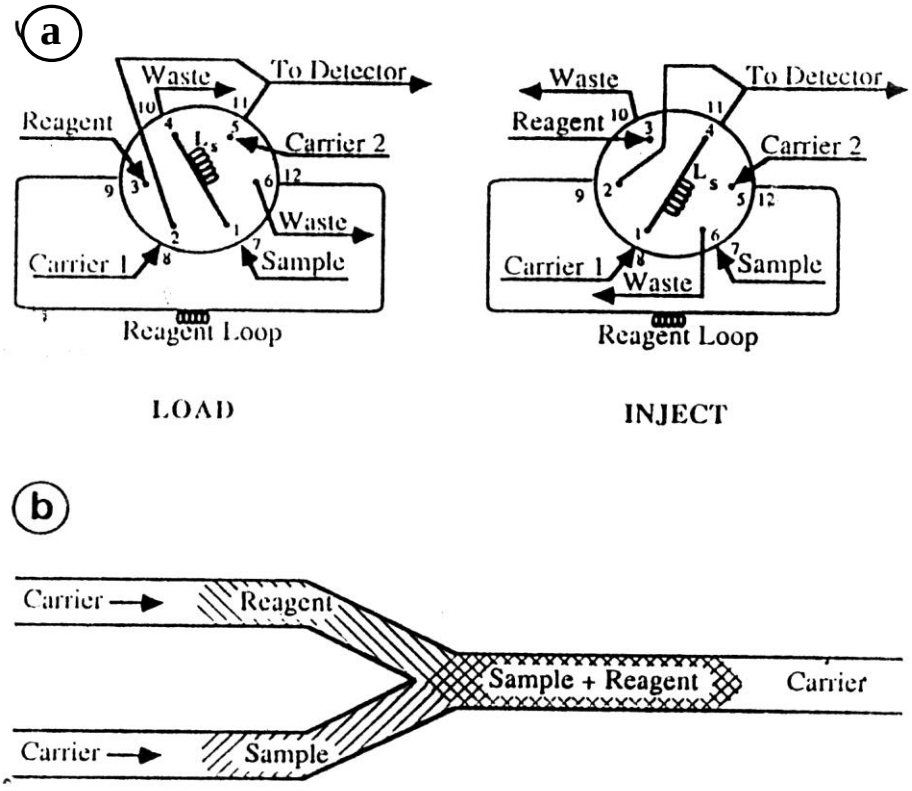

Fig. (1-26) : (a)Six-port Valve Configuration for Metering of Separate Volumes of Sample (Ls) and Reagent. (b) The Merging might either be Effected Synchronously (as shown here) or Asynchronously. Integrated into a FIA

1-3 Hydronium Ion “Oxonium Ion”

The acid name comes from the Latin “acidus” which means “sour” and refers to the sharp odour and sour taste of many acids. Vinger, for example, tastes sour because it is a dilute solution of acetic acid in water. Lemon juice testes sour because it contains citric acid. Milk turns sour when it spoils because of the formation of Lactic acid, and the unpleasant, sour odor of rotten meat or butter can be attributed to compounds, such as butyric acid, that is formed when fat spoils. Vegetable dyes, such as litmus, have been used for more than three hundred years to distinguish between acids and bases(52). Acids were already known in antiquity of their sour taste and for their power to solubilize metals. [The Latin word for sour is “acidus”]. In the early middle ages, the Arabs used nitric acid to separate silver from gold by selective dissolution, the use of vegetable dyes as acid –base- indicators goes back at least to Robert Boyle (1627-1691). However, the nature of acids was still obscure. In the eighteenth century it was believed that phlotgiston, from the Greek word for flame, φλοζ (pronounced ‘phlox’), was the acidic principle,. Lavoisier observed that burining elements such as carbon, nitrogen and sulfure in oxygen gave compounds that, when dissolved in water, produced acids(52). He therefore associated acidity with oxygen, which he named the generator of acid (from οζνσ), pronounced “oxus” Greek for acid . It was only after Davy had showin in (1811) that hydrochloric acid conteins no oxygen, and Von Liebig introduced the concept of mobile, replaceable hydrogen (1838) that acidity can be associated with the presence of hydrogen rather than oxygen.

Arrhenius introduced the idea of electrolytic dissociation in 1884. The replaceable hydrogen then became a hydrogen ion which could dissociate from an acid as in

$$HA \rightleftharpoons H^+ + A^- \qquad \ldots(1\text{-}22)$$

The Arrhenius definition is quite appropriate for aqueous solutions, because water itself can dissociate into H^+ (or, written in its hydrated from as H^+_3O) and OH^-. The alternative definition given by Bronsted (1923) emphasizes the complementary nature of acids in aqueous solutions. It consider an acid any substance that can donate s proton. This definition is independent of the nature of the solvent, and applies even in the absence of any solvent, as in the vapour phase reaction of HCl with NH_3 to yield NH_4Cl. At the same time, Lewis (1923) suggested a further generalization by considering an acid any substance that can accept an electron pair(52). In water, this definition is equivalent to those of Arrhenius and Bronsted, since H^+ lacks electrons, whereas OH^- has a pair of electrons it can share. The Lewis definition has been proved very useful in non-aqueous chemistry, such as in molten salts(52). There is no such theory as an H^+ ion in aqueous solution. The H^+ ion is produced where an acid ionizes is attached to at least one water molecule to form an H^+_3O ion. There is a reason to believe that the H^+ produced in this reaction is actually shared at least by four H_2O molecules, to form an $H(H_2O)^+_4$ or $H_9O^+_4$ ion as shown in Fig. (1-27).

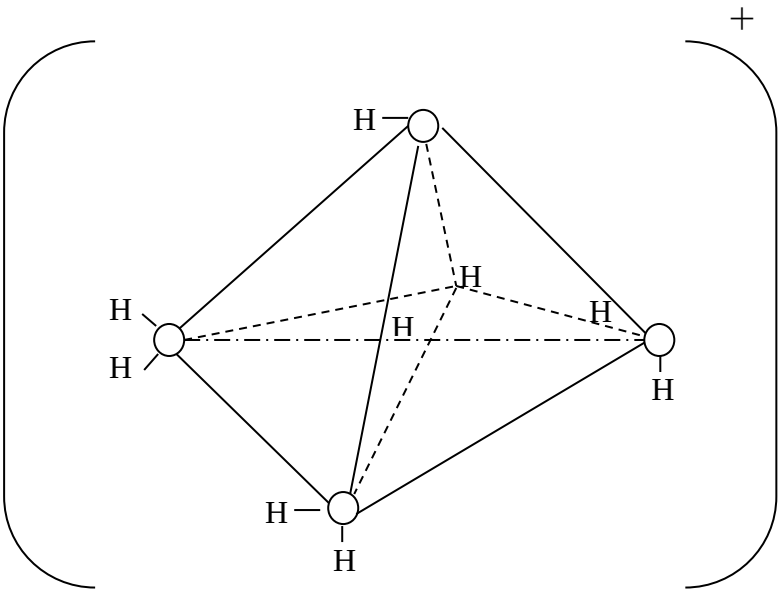

Fig. (1-27) Shows the Structure of $H_9O^+_4$ Ion

Different method in a restricted numbers of paper [that were] found that mainly deals with weak acid determination especially ascorbic acid, citric acid, oxalic acid because of their vital importance medically and industricaly. The literatures conducted for the last thirty years shows that no available spectrophotometric method for acid determination is quoted [unless very rare]. Table (1-3) shows the miscellaneous methods used for the determination of some acids. It seems that the glass electrode occupies the whole area of acid determination.

Table (1-3) miscellaneous methods for determination acids

Acid	Method	Wave length nm	Range of	Refe.
Citric acid	Ttitrimetric citrate with potentiometric end point detection	-	10^{-2}-10^{-6}M	53 , 54
Mixture acids (HCl, H_2SO_4, HNO_3, Formic acetic, Malonic) acid	Titration of buffer mixture with strong acid	-	0.025-0.25M	55
Ascorbic acid	Potentiometric of LAA+1/2/O2 →dehydroascorbic acid+H2O	-	-	56
Phosphoric, succinic, Maleic, oxalic, Tartaric Acetic and propionic acid	Partial-least sequares		1.8-7.2M	57-62
Ascorbic acid	Oxidimetric with potassium hexacyyano ferrate (III) in acid medium		20-200μgml^{-1}	63
Citric acid in milk	Spectrophotometric of pyridine, acetic anhydride and citrate	428	0-300μgml^{-1}	64
Ascorbic acid in citrus fruits	Spectrometric reduction of iron (III).	562	5 μg/25 ml 10μg/ 25 ml	65
Ascorbic acid in soft drink, fruit juices	Spectrophotometric titration with 2,6 dichloro phenol indophenol	293	-	66
Ascorbic acid in vegetable and fruit	Spectrophotometric molybdenum blue complex	760	2-23μgml^{-1}	67-68
Vitamin C	Spectrophotometric reaction with ferricinium cation	440	-	69
Asorbic acid in tabletes	Gas chromatography. Converted ascorbic acid to its derivative (trimethysilgl)	-	50-400μg	70
Ascorbic acid	Photobleaching of methylene blue	655	0.004-0.5M	71

1-3-1 Flow-injection Methods

A single-point titrimetric system based on the flow injection principle was used to determine acids. The sample is introduced into a water stream then reacts with basic buffer solution in a merging stream and the peak height is recorded potentiometrically with a glass electrode in a flow through cell. The relative standard deviation is less that 1%[72]. Foggand Summan[73] studied that a scorbic acid can be determined by flow-injection analysis at a sessile mercury drop electrode without the need to deoxygenate the samples. This methods is found to be accurate for concentration higher than 60μg ml^{-1} and coefficients of variation were less than 1%. Ascorbic acid was determined in range of 0.1-40 μg ml^{-1} by flow injection analysis based on the generated iodine as triiodide ion or the triiodidel starch complex which gives a steady spectrophotemetric signal as 350 or 580 nm respectively[74]. The method is applied to the determination of ascorbic acid in a fruit juice, jam and prepared vitamin C[75-76]. Flow-injection analysis method involves spectrophotometric determination of carboxylic in drugs based on the formation of 2-nitrophenyhydrazide derivatives mediated by water-soluble carbodiemide[77]. A number of drug preparations were also analysed with a coefficient of variation of less than 1%.

Flow-injection method for the determination of oxonium ion in strongly ionisable inorganic acids such as sulphuric, hydrochloric, perchloric, nitric, and phosphoric acids. In addition, halogeno-substitued acetic acids such as chloroacetic, trichloro acetic and trifluoro acetic acids can be determined. Formic acid can be detected at the 0.1M level but acetic acid couldn't be detected up to 0.2M[80]. The method is based on the generation of bromine from

$BrO^-_3 - Br^- - H_3{}^+O$ reaction.

The bromine is then reacted with H_2O_2 to liberate oxygen for the oxidation of Luminol. A Flow-injection method for the determination of ascorbic acid by the measurement of the chemiluminescence from direct oxidation with permanganate in an acidic medium[81]. The method is applied to fruit drinks and nutritional supplements. Cui. *et. al.*, studied that tannic acid was found to inhibit chemiluminescence of the luminol-H_2O_2 reaction catalyzed by Cu^{2+}. Within a detection limit of 9×10^{-9} M, the variation coefficient is 2.5% The method has been successfully applied to the determination of tannic acid in real Chinese gall and hop pellets samples. A Flow- injection system for the fluorescence determination of low level of ascorbic acid was proposed. Ensafi and Rezaci[83] used a method based on the rapid oxidation of ascorbic acid by thallium(1). The fluorescence signal at 419 nm is proportional to the amount of ascorbic acid. The usefulness of the method was tested in the determination of ascorbic acid in fruit juices and vitamin C tablets.

Spectrophotometric with flow injection analysis was used to determine a mixture of weak acids by using multiivariate calibration. This method was based on spectrophotometric data generated by following the colour change of a combination of acid-base indicators caused by an alkaline gradient. This gradient is generated by introducing a NaOH solution into a flow injection analysis titration system. Partial least squares modeling is used to reduce and treat the titration data. This model predicts individual acid concentration of acid presented in the mixture of weak acid. This method was used to detect citric, tartaric, acetic and benzoic acids in the 1×10^{-3}-4×10^{-3} M and hydrochloric and acetic acid in the 1.25×10^{-3} - 5×10^{-3} M range[84-85]. Mixtures of succinic and oxalic acid were determined by titration in flow injection analysis with potentionetric flow cell with a stainless steel electrode[86]. Partial least sequares

regression as multivariate calibration tool was applied for data treatment with a relative error of 4.3% for succinic acid and 5.5% for oxalic acid. This method can be applied in pharmaceutical or food samples. A flow injection analysis system with potentiometric detection has been developed for the determination of citric acid in commercial fruit juces using copper-selective tubular electrode[87]. It consists of the complexation of citrate ion with copper(II) ion. Citric acid was determined by indirect flow injection atomic absorption spectrometric, the method is based on the continuous precipitation and filtration flow system for the separation of citric acid by precipitation with lead and indirect flame atomic absorption spectrometry is proposed[88].The precipitate is formed by injecting the lead solution into a carrier containing the sample and is subsequently retained on a filter. This method has been applied to the determination of citric acid in fruit juices, carbonated soft drinks and sweets. New approach for the determination of ascorbic acid via on-line automatic through the consumption of the relased bromine with detection limit of 7.045mg[89]. Ascrobic acid can be determined in pharmaceutial preparation and from natural juice obtained from naturally occuring citrons fruits using flow injection analysis according to this reaction

$$B\bar{r} - Br\overline{O}_3 - H_3^+O \rightarrow 3Br_2 + 3H_2O$$

via consumption of relased bromine[90].

1-4 Nitrate and Nitrite Ions

Nitrate may be quantitatively reduced to nitrite and nitrite quantitatively oxidized to nitrate. Nitrate and nitrite play an important role in the nitrogen cycle. Both are present in food and water, and then they are two of the most frequently required determination in environmental investigations. Nitrate is necessary for plant growth and is important in soil as relating to fertilization. Oxides of nitrogen absorbed from the air are determined as nitrate. There are industrial materials containing desired or contaminating amounts. Nitrate ion is acting as a depolarizer and reduced to nitrate ion[91-93].

Several spectrophotometric methods are used for the determination of nitrate and nitrite ions are shows in table (1-4).

Table (1-4) Spectrophotometric Methods for Determination of Nitrate and Nitrite

Ion determine	Method	Wave length nm	Range	Reference
Nitrate and Nitrite	Method based on the reaction between nitrite, sulphanilamide and naphthylethylene diamine	543 mμ	4-50μg NO_3 0-10μg NO_2	94
Nitrate and Nitrite	Forming aZo dye	400-600	0.05-0.5M	95
Nitrate	Using the reaction of nitrite with α-naphthylamine	527.5		96
Nitrate in water	Using of different cadimum column to reduce nitrate to nitrite	543	0.02-0.2M	97
Nitrate	Base on the reaction of nitrate with 4,5 dihydroxycounmarin	410	0.2-7.5ppm	98
Nitrate vegetable	Using 2-sec-Butylphenol	418	0.13-2.5M	99
Nitrate and Nitrite	Modified of Griesliosvoy reaction		0.025-0.356 μg $.g^{-1}$ NO_2^- 0.212-8.559 μg $.g^{-1}$ NO_3^-	100

1-4-1 Flow Injection Methods for Determination of Nitrate and Nitrite Ions

Nitrate and nitrite can be determined by Flow-injection method which consists of the reduction of nitrate with copperized cadimium with the nitrite thus produced, diazotisation of sulpanilamide, the product being coupled with N-1-naphthylethlenediaimine to from a highly coloured azo dye, which measured at 520nm. Automated procedures for determination of ammonium and nitrate in soil extracts were described, distillation of the extract with magnesium oxide with subsequent determination of ammonia by automated indophenol method used for ammonium. For ammonium plus nitrate, the nitrate is reduced with titanium(III) sulphate during distillation with magnesium oxide. The method has wider application was, for example, analysis of fertilisers and water samples[(102)]. Flow injection principle is used with the noval design of a flow cell, in which the ion-selective and reference electrode are incorporated. The method was used for the determination of nitrate in soil extracts with standard deviation of only 0.8% and the detection limit was approximately 10^{-5} M nitrate[(103)], automated method for determination of nitrate and nitrite by flow injection analysis was used. Nitrate[(104)] is reduced to nitrate with copperized cadmium coloumn. Nitrite is diazotized and coupled with N-(1-naphthyl) ethylenediammonium dichloride. In this method, the merginhg zones approach is used to minimize reagent consumption. Two peaks are obtained: one of them corresponds to nitrite and the other to nitrite plus nitrate. The precision is more than 0.5% for nitrite in the range 0.1-0.5 mgL^{-1} and 1.5% for nitrate in the range 1.0-5.0 mgL^{-1} . Flow injection principle is used in the photometric determination of nitrite and nitrate with sulfanilamide an N-(1-naphthyl) ethylenediamine as reagents. On-line copper-coated

cadmium reductor reduces nitrate to nitrite. The detection limit is 0.05μM for nitrite and 0.1 μM for nitrate at a total sample volume of 200μl[105-106]. Nitrite can be determined by its reaction with cerium(IV) using inverse spectrophotometric detection in flow injection analysis[107]. The system was applied to the determination of nitrite in culture media. Spectrophotometric determination of aromatic primary amines and nitrate by flow injection analysis are used, are based on the injection of aromatic primary amines into dilute hydrochloric acid carrier which merges sequentially with 4-N methylaminophenol and dichromate. The purple-red colour formed by oxidative coupling of amines with 4-N-methylaminophenol is measured at 530 nm. In contrast to the manual procedure, the flow-injection procedure avoided errors arising from the instability of the coupling intermediate, oxidation of the amine, and too great an excess of the oxidant[108].

Nitrite can be determined in water by flow-injection with chemiluminescence[109]. In this method nitrogen monoxide, which exists in equilibrium with HNO_2, is separated from the aqueous flowing eluate by entraiment in Ar carrier gas and is detected with high specificity in the gas stream by the chemiluminesence associated with its reaction with ozone. The sequence of reactions involves the chemiluminesence determination of nitrite ions.

$$NO_2^- + H^+ \longleftrightarrow NONO \rightarrow NO \qquad \ldots(1\text{-}23)$$

$$NO + O_3 \rightarrow NO^*_2 \rightarrow NO_2 + hv \qquad \ldots(1\text{-}24)$$

Nitrate is determined by spectrophotometric with electrochemical reductor using flow-injection analysis[110]. This method is based on a column electrode paked with co-electrodeposited Cu-Cd glassy carbon grains which has been shown to be excellent for the reduction of nitrate to nitrite and its application to the flow injection analysis of nitrate in

sample of natural water has been used. The detection limit was 7×10^{-7}M.

To minimize the sample size, reagent consumption and waste, a micro-Flow-injection analysis was investigated and applied to the simultaneous determination of nitrate and nitrite ion in water sample[111]. Nitrate was reduced to nitrite by cadmium copperized. Detection was carried out at 538 nm with a height-emitting diode used as an azo dye. The detection limits of nitrate and nitrite were about 10^{-7} M. Amoter flow injection method was used to determine of nitrate and nitrite in human saliva[112]. It is based on the reaction of nitrite with iodide in acidic medium, the triiodide formed being amperometrically monitored at +0.2V with platinum microelectrode. The method was used in the study of the conversion of nitrate to nitrite in the oral cavity by bacteria. Amperonometric detection with microelectrodes in flow injection analysis was used to determine of nitrite in saliva[113,114]. This method was based on the reaction nitrite with iodide in acidic medium and the triiodide was formed. This limit of detection of the method was 0.2 $\mu mol^{-1}l$. Simultaneous spectrophotometric determination of nitrate and nitrite in foodstuffs and water was doneby flow injection analysis[115]. In this method cadmium is used to reduce nitrate to nitrite. Nitrite is diazotised in the FIA system with N-(1-napthyl) ethylenediammonium dichloride to form the highly coloured aZo-dye, which is measured at 540nm. The detection limit is $0.085\mu g.l^{-1}$ for a sample injection of 400 μl at relative standard deviation was 1.56%, and 0.77% for both nitrate and nitrite, respectively. A Flow injection system with spectrophotometric detection was proposed for determination of low levels of nitrite based on its catlytic effect on the oxidation of gallocyanine such as bromate in acidic media[116]. The calibration graph was linear for 0.02-0.5 μg/ml of

nitrite. A sequential injection analysis system for the simultaneous determination of nitrite and nitrate in waste waters has been developed. The nitrate determination is based on the Griess-Liosvay reaction. Nitrate is previously reduced to nitrite in a copperized cadmium column and analyzed as nitrite. The absorbance is measured at 540nm. The standard deviation better than 2% for nitrite and 0.7% for nitrate[117-118]. Nitric oxide (NO) is an important intracellular and extracellular signal substance[119]. Nitrite is one product of the oxidative metabolism of NO. So a flow injection method is based on the Griess reaction. The purpose of this method is to determine nitrite to provide a means of estimating the endogenous formation of NO or NO_2^-.

The reversed phase flow injection spectrophotometric determination of trace nitrite nitrogen in water has been studied[120]. N-(1-Naphthyl) ethylenediamine dihydrochloride solution was injected into the mixed flow of the water sample sulfanilamide solution. Red dye formed by the reaction and spectrophotometrically monitored at λ_{max} 540nm. The detection limit is 0.0012 mg/l. A thin film of mixed-valent cupt Cl_6 is deposited on a glassy carbon electrode by continuous cyclic scanning in a solution containing 3×10^{-3} M $CuCl_2$, 3×10^{-3} M K_2PtCl_6 and IMKCl. In the potential range was from 700 to 800 mv[121]. The cyclic voltammetry is used to study the electrochemical behaviors of nitrite on $CuPtCl_6$/GC modified electrode and electrode displays a good activity toward the oxidation of nitrite.

The linear relationship between flow injection peak currents and concentration of nitrite is at range of 1×10^{-7} - 2×10^{-3} M with detection limit of 5×10^{-8} M. Non-equilibrium flow injection spectrophotometry is used for thedetermination of nitrite. This method was based on the reaction of nitrite with basic fuchin in an acid medium. The linear range

for nitrite is 0.0-0.5 mg/l. The method was applied to direct determination of nitrite in collapase lake water, fishpond water, power plant wastewater and well water with satisfactory results[122]. An automatic direct spectrophotometric method for the simultaneous determination of nitrite and nitrate by flow-injection analysis has been developed[123]. The method is based on the reaction of nitrite and nitrate with the spectrophotometric reagent N-phenylanthranilic acid(I) in sulfuric acid medium pH (0.4-0..6) to form the same colour product whereas the absorbance is measured at 410 nm. One half of the sample flow is treated with sulfanilic acid, which reacts with the nitrite and thus makes it subsequent reaction with I. So that the nitrite portion can be calculated by difference. This method has the advantage of direct determination of nitrite and nitrate without reducing nitrate as in other reported methods. The detection limit is 2.5 ng/ml for nitrite and 12 ng/ml for nitrate. The concentration of nitrate in biological fluids has been determined using nitrate reduotase (NR) in a flow system. A merging zone method was applied, in which a zone of NR and that of nitrate in separated stream has been merged, and allow to react. The decrease in NADPH caused by the reaction between NR and nitrate was measured at 340nm. The detection limit was 0.2 μM. Flow injection method was applied to determine the amount of nitrate in serum, plasma, and uria using samples that had not been deproteinized. The concentration of nitrate within each sample was calculated from differences in the peak areas obtained in the absence or presence of nitrate reductase[124].

The colour fading reaction on potassium bromate with victoria green stand G by the catalysis of nitrite in hydrochloric acid medium was studied using flow injection analysis[125]. The linear range for the determination of nitrite was 0-0.3 mg/l and 0.2-0.3 mg/l. It was used to determine trace nitrite in the collapse lake water, fishpond water, power plant wastewater and well water.

Miscellaneous methods are used for the determination of nitrate and nitrite as shown in table (1-5).

Table (1-5) Miscellaneous methods for determination of nitrate and nitrite

Ion determine	Method	Wave length nm	Range	Refere.
Nitrate in water	Automatic kinetic method based on forming of aZo dye	540	0.025-2 ppm	126
Nitrate	Molecular emission cavity method	500	10-400 ppm	127
Nitrite in sauage	Amperometric method base on the anodic oxidation of nitrate at a molybdenum oxide layer		5-1000 μM	128
Nitrate in river water	Capillary electrophoresis method with indirect μv detection, separation and determination of Cl^-, NO_3^- and $SO_4^=$			129
Nitrite	Ion chromatography with photometric measurment of iodine		$0\text{-}1.5\times10^{-3}$M	130
Nitrateind nitrite in human serum, lake water, river, sewage works water and snow samples	Ion chromatography method	210	Nitrite 0.03-10 μg ml^{-1} Nitrate 0.05-5 μg ml^{-1}	131
Nitrite	Voltametric method based on oxidation of nitrate at boron-doped diamand electrode		0.002-1 mM	132
Nitrate in water	Ion selective electrode method		1-10 μg l^{-1}	133

1-5 Hydrogen Peroxide

Hydrogen peroxide is an oxidant used widely in industry, laboratories and in domestic purpose. It is unstable and easily decomposable due to the uncommon oxidation state of oxygen in H_2O_2 molecule which is (-1). It is important in some polymers studies when self-decomposition may H_2O_2. It has been proposed that natural human materials in water might photochemically reduce oxygen to give the superoxide $O^{\cdot}_2$ and that subsequent disproportionation of this free radical could lead to the formation of H_2O_2[134]. Fig.(26) shows that the H_2O_2 molecule is not planar. Each atom has two unshard electron, which could as in the O-H bonds, repel each other. The twisted structure called skew-chain structure accommodates these intermolecular repulsions best[135].

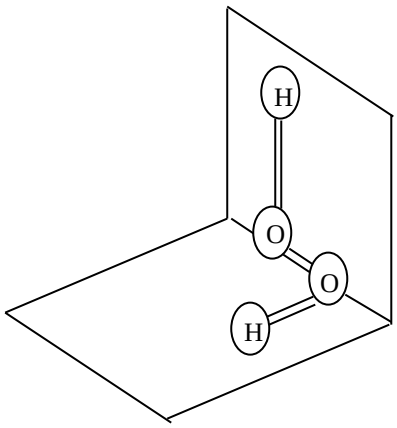

Fig. (1-28) Hydrogen Peroxide Structure

Miscellaneous methods are used for the determination of hydrogen peroxide as shown in table (1-6):

Table (1-6) Miscellaneous methods for determination of Hydrogen peroxide

H_2O_2	Method	Wave length nm	Range	Refere.
H_2O_2 in atomspheric precipitation	Fluorometric method based on the reaction of H_2O_2 with horseradish peroxides and p-hydroxyphenyl acetic acid		10^{-8}-1.5×10^{-4}M	136
H_2O_2 in water	Lodometric method based on the oxidize of iodide by hydrogen peroxide at pH=4, the iodine formed was reacted with the phenylarsine oxide			137
H_2O_2 in water	Spectrophotometric method using sodium salts	540	$(7\text{-}40)\times10^{-4}$M	138
H_2O_2 in water	A chemiluminescent method based on oxidation of luminol in alkaline medium in presence of Cu(II) as catalyst		10^{-8}-10^{-5}M	139

1-5-1 Flow-injection Methods for Determination of Hydrogen Peroxide

A flow-injection system based on the p-hydroxy phenyl-acetate peroxide-peroxides reaction allows the simultaneous determination of hydrogen peroxide and CH_3HO_2 in water samples in range of 0.3-2 μg l^{-1} and the detection of 0.1 μg $l^{-1(140)}$. An amperometric method with flow-injection was used to determine hydrogen peroxide in a range of 10^{-4} to 10^{-1} M. This method is based on the production of dihydroxyacetone from glycerol by immobilized bacteria. The H_2O_2 was oxidized at 1.2 V.VS SCE at a glassy carbon flow-through electrode after dilution in a flow

injection analysis system[141]. Chehemiluminscence from the reaction of bis(2,4,5, trichloro-6-carbopentoxy phenyl) oxalate with hydrogen peroxide in the presence of triethyl amine in –butanol-water have been investigated as a means of determining hydrogen peroxide with range of 2×10^{-8}-10^{-3}M[142]. Hydrogen peroxide can be determined by flow-injection chemiluminscence method by using reagent containing 100μM huminol and 3μM microperoxidase at pH=4. The range of this method was 3×10^{-9}M – 10^{-5}M[143]. Also H_2O_2 was determined in aqueous samples by flow injection techinque using solid state peroxyalate chemiluminscence, Bis(2,4,6-trichloro phenoyl) oxalate in solid from is packed into a bed reactor, which eliminates mixing problems, perylene is added as a sensitizer to a water/acetonitrile carrier stream into which the samples (200-600μl) are injected, the calibration graph is linear up to 10^{-5}M with detection of limit 0.2μgl^{-1}[144].

Fluorometric Flow-injection procedure with a single reagent solution containing p-hydroxypenyl acetic acid peroxidase and ammonia was used to determine hydrogen peroxide in the range of 10^{-8}-10^{-4}M with detection limit of 10^{-8}M[145]. Hydrogen peroxide was determined in flowing stream by immobilized luminol chemiluminscence reagent in flow-injection system with a low detection limit of 100 pmol and the linear working range was (40-600)μM[146]. 1,1′-oxalyldimidozol as chemiluminscence reagent was used to determine the low hydrogen peroxide concentration by flow injection analysis, the estimated detection limit for H_2O_2 in water was 10^{-8}M with the linear range of 1.5-6μM[147]. Flow-injection technique is used to determine nanomolar concentration of H_2O_2, the concentration of H_2O_2 was determined as the coloured of condensation product of N-ethyl-N-(sulfopropyl) aniline and 4-aminoantipyrene with detection limit of 12 nM[148]. It has been found that a flow injection system with an

immobilized enzyme reaction coloumn could be utilized for the determination of hydrogen peroxide in some water samples. The coloumn was packed with chitosan beads immobilizing horseradisn peroxide, the detection limit was 3ng. dm^{-3} and the relative standard deviation at 1 mg dm^{-3} of H_2O_2 was 1.5%[149]. The sensitivity of a flow-injection analysis system for measuring hydrogen peroxide could be remarkably imporoved using immunoaffinity-layered horseradisin peroxidase[150]. Flow injection analysis method for automated determination of hydrogen peroxide in the presence of even stronger oxidants is presented, based on the immediate formation of a colored adduct between hydrogen peroxide and dinuclear IronIII complex. A reagent stream with the complex and carrier stream into which the sample is injected are combined in a low dead volume mixing tee. The absorbance was measured at 570nM[151].

All the methods above suffered from interferences compare with the method used in this work also the detection limit was better.

1-6 Iodide and Iodate Ion

Iodide and iodate ions are very important in food, water, plant, and pharmaceutical products. The body needs iodide ion each day to prevent goiter, a disfiguring enlargement of the thyroid gland. Iodine exists in a number of oxidation states commonly used in a analytical chemistry being iodide and troiidode. Strong oxidising agents reacts quantitatively with the easily oxidised iodide ion. Iodination reactions have been extensively to determine numerous organic compounds that either iodinated or oxidised by iodine[135]. The misellaneous method which used the determination of iodide and iodate ions are shown in table (1-7).

Table (1-7): Miscellaneous methods for determination of Iodide and Iodate

Ion determine	Method	Detection limit	Range	Refere.
Iodide	Fluorimetric method used cerium(IV)	-	0.6-2.5 μg/100ml	152
Iodide	Fluorimetric method used 2,7-di(acetoxymercuri)fluorescein	-	0.87-9.81 ng/25ml	153
Iodide in sea water	Neutron activation analysis	6×10^{-3}M	-	154
Iodide in table salts and pharmaceutital products	Spectrophotometric based on the reaction of palladium with 3-(2 thiazolylazo)2,6-diaminotoluene	-	0.6-127μgl^{-1}	155
Iodide in aqueous solution	Ion selective electrode methode using piezeelectric detector	0.6-127 μgl^{-1}		156
Iodide in sea water	Ion chromatography with μV detection	0.2 μgl^{-1}	-	157
Iodate in salt	Amperometric method based on the detection at a molybdenum oxide modified electrode	6×10^{-6}M	10×10^{-6}-10×10^{-7}M	158
Iodide in environmental equeous samples	Inductivety coupled plasma atomic emission spectrometry	0.04$\mu g.ml^{-1}$	-	159
Iodide in natural water sample	Spectrophotommetric determination by solvent extraction with methylen blue	1.5×10^{-6}M	7.5×10^{-8}-3×10^{-6}M	160
Iodide	Chemiluminescence based on the oxidatation of ascorbic acid with copper(II)	5.8×10^{-8}M	4.6×10^{-5}-4.2×10^{-3}M	161

1-6-1 Flow-injection Methods

Iodide can be determined by amperometric Flow-through wire electrode flow-injection analysis with a detection limit of 10^{-5} M[162]. Chromium (IV) as strongly reagent was used in Flow-injection analysis to determine iodate ion, with a spectropotometric detection, based on the absorption of chromium (III)-EDTA at 600nm. The detection limit was 8.3×10^{-5}M, and the range of concentration was 1.66×10^{-4}-1.66×10^{-3}M[163]. The iodide ion was determined within detection limit of 5×10^{-10}M by using vibrating wire electrode for ampermetric in flow injection system[164]. Automatic method was used to determine the free iodide ion in drinking water. This method was based on the catalytic effect of iodide on the destruction of the thiocyanate ion by the nitrite ion, the detection limit of this method was 0.4μg.l^{-1} with linear working range 0.4-5 μg.l^{-1} [165]. Liquid core optical fiber total reflection call as a colorimetric detection for flow injection analysis was used to determine iodide ion. 0.1 μg.l^{-1} can be detected based on the iodine absorption at 540nm[166]. Flow-injection with spectrophotometric system was used to determine iodide ion. The iodide ion oxidise by bromine water to iodate, most of the excess of bromine is reduced by formic acid, and the iodate is reacted with more iodide to form triiodide, which is determined spectrophotomtrically at 351 nmm, with detection limit and range were 3.9×10^{-7}M, $(0.7\text{-}3.9)\times10^{-5}$M respectively[167]. Stop-flow method was used to detect iodide ion, based on the reaction between cerium(IV) and arsenic(III) which catalysed by iodide ion. This method can be used to determined iodide ion in pharmaceutial preparation, table salt and Cow's milk. The decrease in absorbance during the reaction was monitored at 365 nm, with detection limit of 0.7 ng ml^{-1}[168]. Iodometric method was used to determine iodate ion by using flow injection amperometry, range of (0-

1.5)×10^{-4}M and the iodate ion was detected in this method as iodine[169]. Also a flow injection analysis method was used to determine a microchemical amount of iodate and iodide in sea water. This system involves spectrophotometric detection. This method was based on the catalytic fading effect of either iodate and iodide on the indicator reaction of Iron(III), thiocyanate and nitrite with range of 0.75-150μgl^{-1}[170].

Aim of the Project

Due to the continuos demand of flow injection analysis and because of the lock of both experience and flow injection tools which requires micro tools for micro analysis, and because it is a leading techniques, and most of the paper concerning this technique is almost restricted to foreign countries. It require micro flow through cell for almost pocket size spectrophotometer, with a necessary. Sample introduction device and chemical propellant. Main target of this project is to facillitate the check of a few home made tools at a level that is capable of performing continuos on-line analyse. An easy, fast, sensitive economic, reliable method even for a well known reactions. The $IO^-_3 – I^-$ - H^+_3O reaction system was used for establishing the test of a new home made two six-port injection valve in one unit the challenge the legend forgein six port injection valve. To our knowledge no person or company or a research institute was capable of dring so, also the flow through cell that fit usual commercial spectrophotometric is the researcher target. New mode of merging zero reaction technique using all homemade unit application of the use of this units matched to commercial spectrophotemetric for acids hydrogen peroxide, nitrate , nitrite, iodide, iodate determination were tried.

(b) coils

Fig. (1-15) shows the signals obtained with a conventional FIA system for a reactor of constant length L=125 cm in the form of straight tubing(1), a coil with diameter 26mm (2), and a coil with diameter 4mm(3). From this curve, the smaller diameter is, the smaller the dispersion[37].

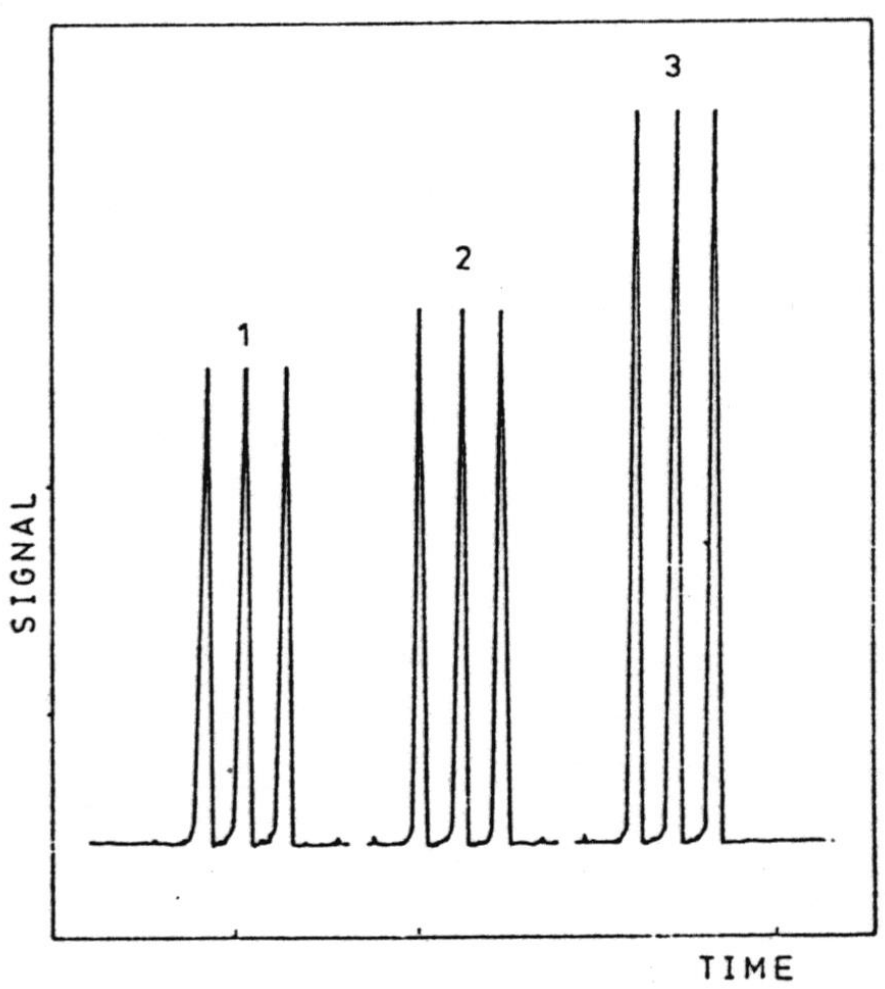

Fig. (1-15) influence of Coil Diameter an the Dispersion

1-2-8 The Stimulus Response Technique

The flow injection analysis response curve is a result of two processes: the physical process of dispersion of the sample zone within the carrier stream, and the chemical process of formation of a chemical species. The physical process of material dispersion is due to the hydrodynamic processes which take place in the flow through system and is therefore conveniently investigated by stimulus response technique[38]. This technique is based on the introduction of a tracer into flowing stream and on measurement of the dispersion of the tracer as caused by the transport process throughout the system. If the tracer is injected as a zone (stimulus), the observed response reflects the dispersion in the system through the increase of the width of the tracer zone as increased by the combined contribution from convection and diffusion. These two steps occur simultaneously. If the response curve has a Gaussian shape, its first statistical moment, the mean of the tracer curve, corresponds to the maximum peak, when expressed by units of time. The first moment allows estimation of the average time available for chemical conversion, since it constitutes the mean residence time that the tracer material in average has spent in the reactor. The second statistical moment is proportional to the peak width, and for the Gaussian peak, it is the second power of the half peak width measured at 0.61 peak height[30] as shown in Fig. (1-16).

The increase of the second moment caused by transport through the reactor is due to the dispersion. The relation between the dispersion and residence time is an important parameter for the optimization of all types of flow systems as shown in Fig. (1-17). Iis application varies depending on the purpose. There are two reasons, first the mixing in FIA is nonhomogeneous and directional (since it yields a concentration gradient in both axial and radial direction), and as a result of this stratification the

ensuing chemical reactions take place gradually, while the reagent penetrates the sample gradient during the movement of the dispersing zone through the channel. Therefore, the FIA response curve is not only a result of the processes that occur at the detector location, but also of all the processes that gradually take place upstream in the FIA system at variable reagent concentrations. The FIA readout is selected at peak maximum according to Qebergas model[38] as shown in Fig. (1-18) and (1-19). The movement of the liquids in the tubes could described by the convective-diffusion equation.

$$D_m\left(\frac{\partial^2 c}{\partial x^2}+\frac{\partial^2 c}{\partial r^2}+\frac{1}{r}\frac{\partial c}{\partial t}\right)=\frac{\partial c}{\partial t}+2F(1-\frac{r^2}{R^2})\frac{\partial c}{\partial x} \qquad \ldots(1\text{-}16)$$

where D_m is the molecular diffusion coefficient, c the concentration, x the distance along the tube, r the radial distance from the tube axis, R the tube radius, t the time and F the average flow velocity. The reduced velocity is described by the peclet]Number $Pe = R(2F)/D_m$

…(1-17)

the reduced distance x

$$x = D_m x / R^2(2F) \qquad \ldots(1\text{-}18)$$

The reduced time *T*

$$T = D_m t /R^2 \qquad \ldots(1\text{-}19)$$

Were selected to approximate the range of FIA conditions, that is, Pe>1000

$0.004 < x < 1.0$

$0.002 < T < 0.8$

When the contribution of diffusion to radial transfer is negligible, a sharp rise at the peak leading edge and exponential decay at its tail, and characteristic of convective dispersion due to a poisseuille profile are observed. For long residence times (T=0.4) a nearly Gaussian peak is observed, while for shorter residence times a peculiar double-humped

peak is observed. Ruzicka and Hansen[38] are another equation for baseline to baseline value:

$$\Delta t_b = 56.7\ R^{0.293}\ L^{0.107}\ Q^{1.057} \quad \ldots(1\text{-}20)$$

and for dispersion coefficient D at any time t:

$$D = C_o / C_{max} = 2.342\ L^{0.106}\ Q^{0.206}\ R^{0.496} \quad \ldots(1\text{-}21)$$

The second reason is that flow injection analysis encompasses a much wider range of solution, i.e., sample dilution, preconcentration, reaction rate measurement, and multicomponent detection.

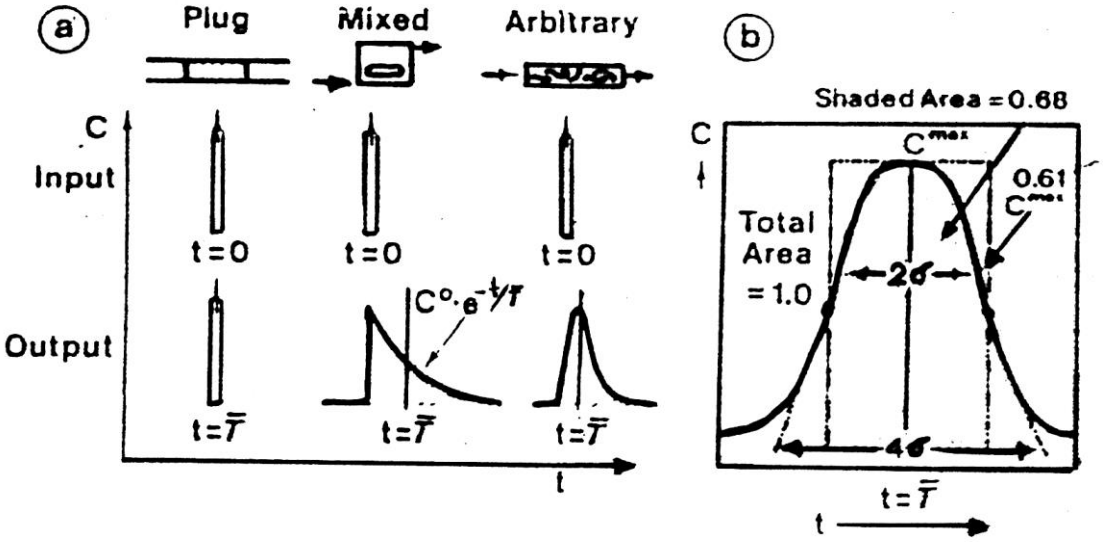

Fig. (1-16) a- Curves for plug, mixed and arbitrary flow

b- For arbitrary flow, a Gaussion-shaped curve is eventually achieved

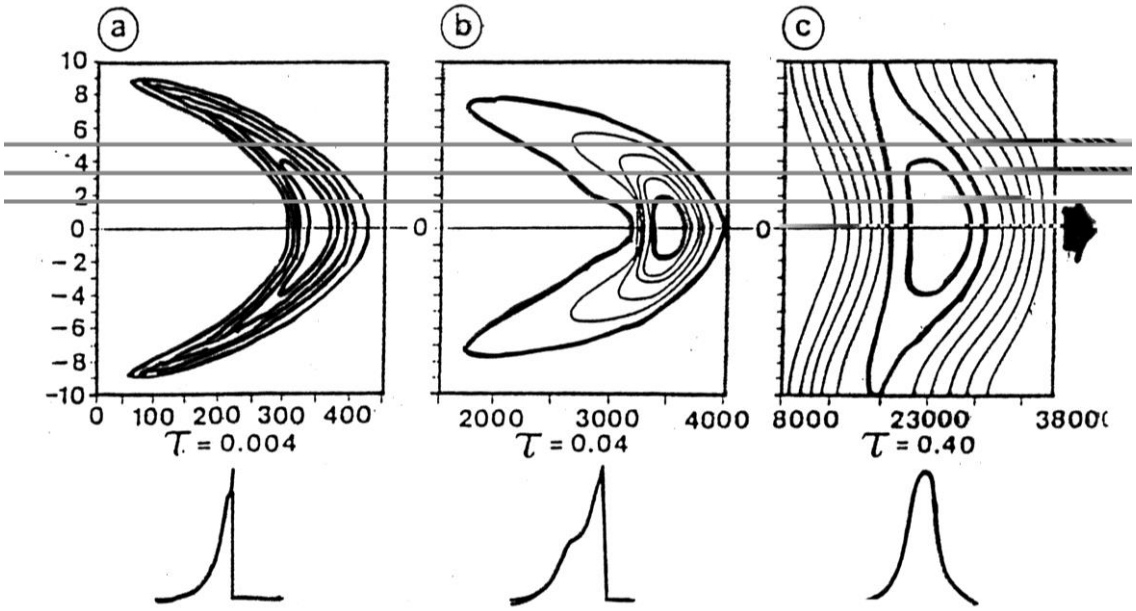

Fig. (1-17) Dispersion of a Sample Plug in a Straight Tubular Channel.

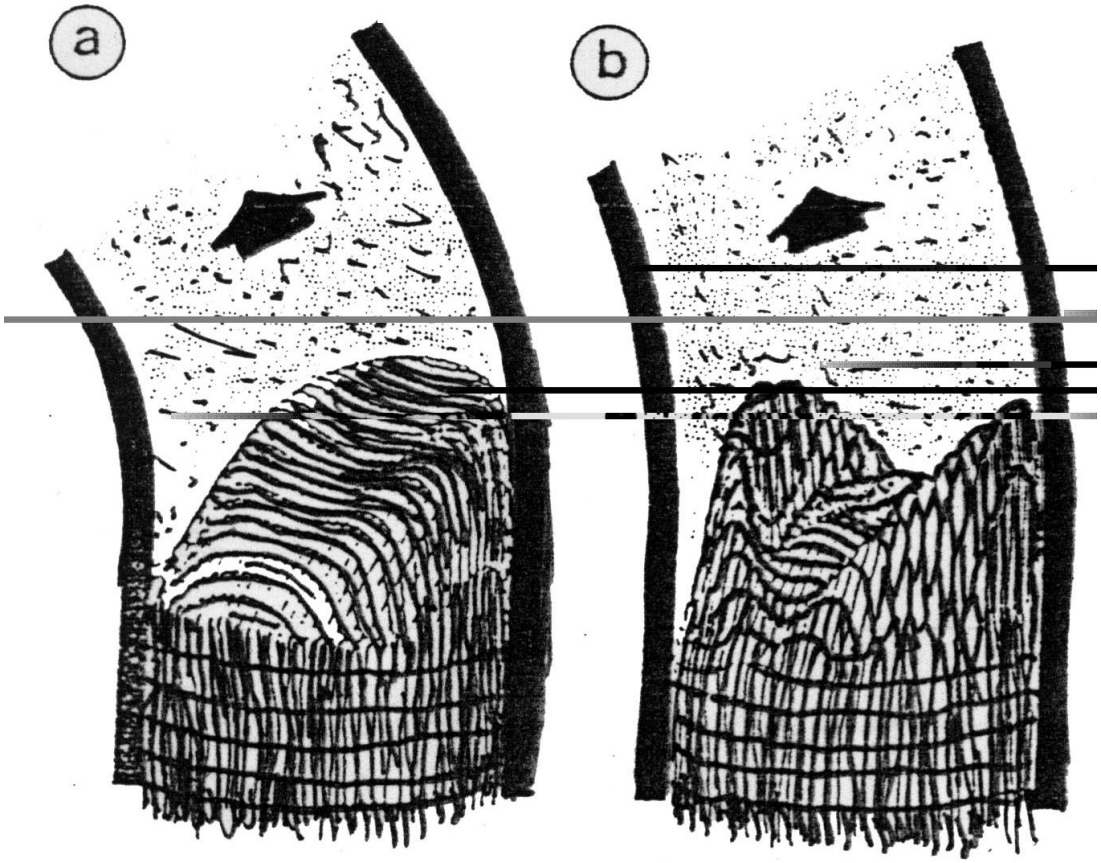

Fig (1-18) Dispersion in coiled tubes. a) Equivelocity profiles in axial direction. b- Equivelocity profiles in radial direction

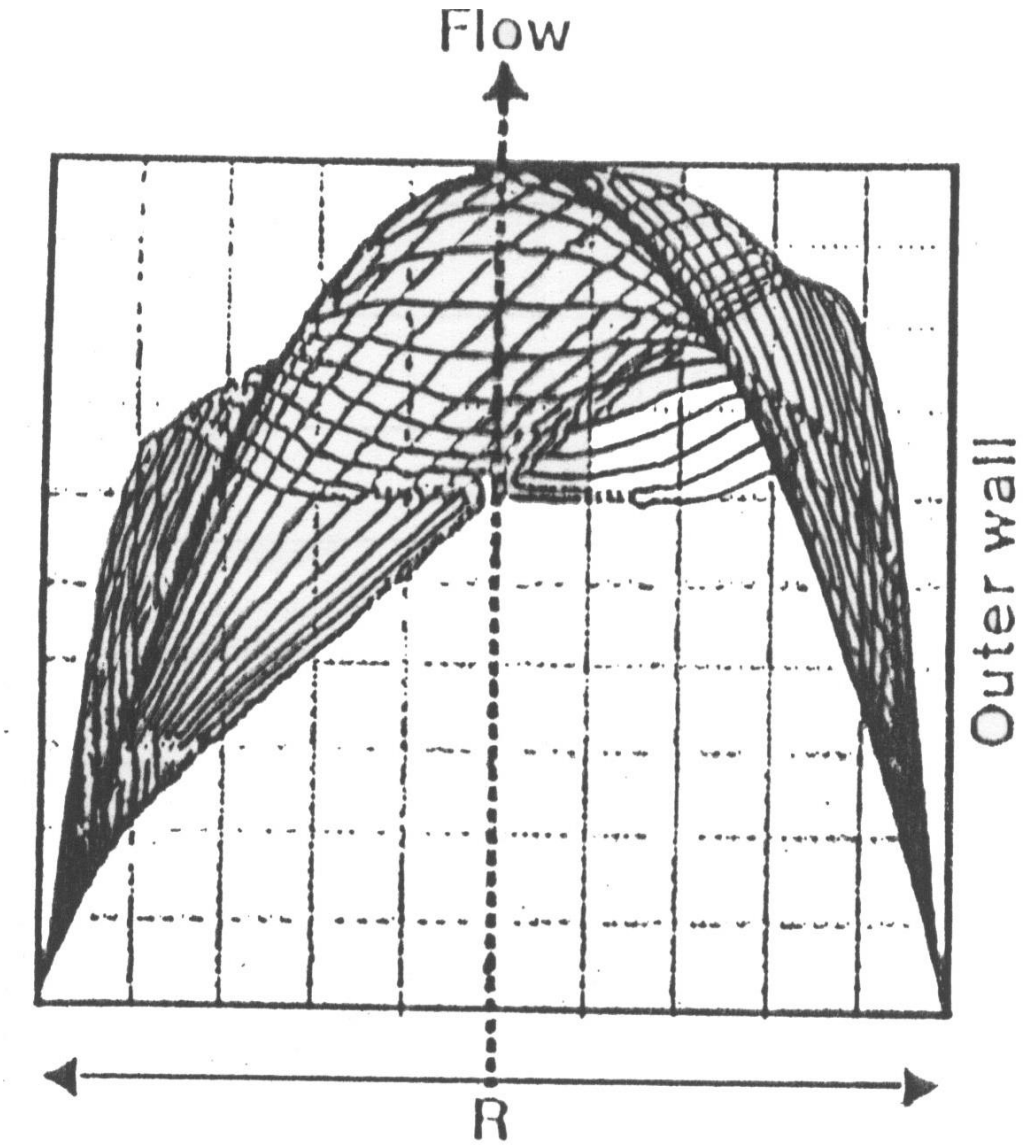

Fig (1-19) Axial velocity profiles in a coil tube.

1-2-9 Operation Modes of Manifold

Various mode of operation could be conducted in FIA system mainly single line and multiple line system in the following section a brief clisscussion is presented

(i) Single-line manifolds Fig. (1-20) shows the simplest FIA system which consists of one tube through which the carrier stream moves towards the flow through detector depending on injected volume

sample(s) tube length (L) and flow geometry. In this system, limited, medium, and large dispersion can be achieved[39,40].

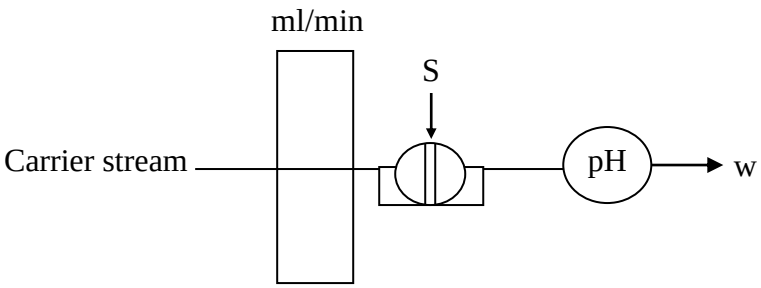

Fig. (1-20) single-line manifolds

(ii) Multiple Lines

The sequential use of only two reagents is a simple matter, because a manifold designed for this purpose involves only one confluence point at which a second reagent is added to the sample zone when carried past by the stream of the first reagent[41] as shown in Fig. (1-21).

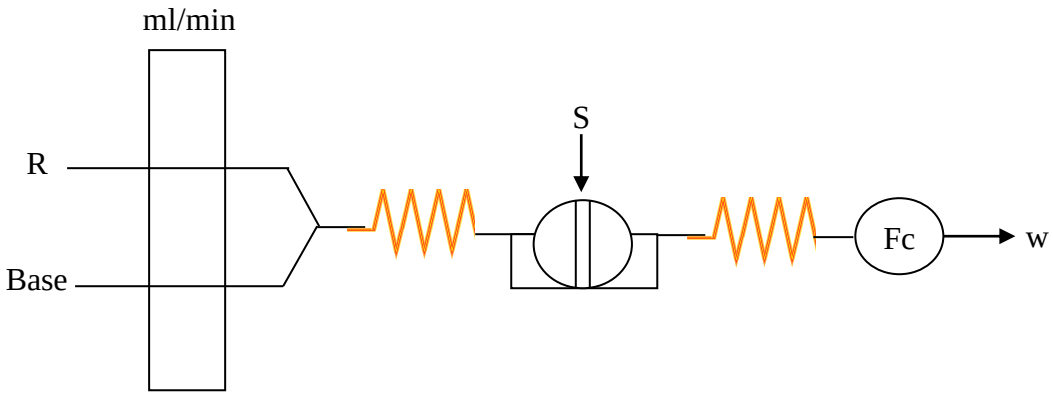

Fig. (1-21) Two-lines manifolds

Fig. (1-22) shows the manifolds of three lines where the reagent are added sequentially and then the reaction product occurs[42,43]:

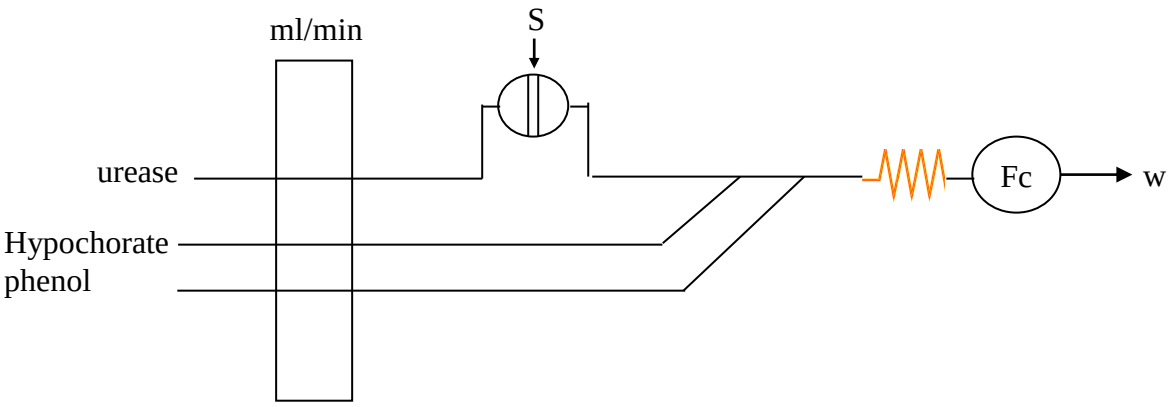

Fig. (1-22) Three-lines manifolds

1-2-10 The merging zones

The relatively high reagent consumption is the main disadvantage of all continuous flow systems, which, in contrast to batch analyzer , use the reagent continuously even when there is no sample present in the apparatus notably during the startup and shutdown procedures.

This problem is not as great in FIA, where the volume of the sample path is seldom larger than a few hundred microliters and, therefore, easy to fill and wash in a very short period, using small amounts of reagent or wash solutions. If, however, an expensive reagent or enzyme is used, it is wasteful to pump solutions continuously, because the reagent also occupies those sections of the sample path where the sample zone is not present simultaneously[44]. The merging zones principle avoids this uneconomic approach by injecting the sample and introducing the reagent solution in such a way that the sample zone meets the selected section of the reagent stream in a controlled manner. The rest of the FIA system is filled with wash solution or only pure water. This can be achieved in two different ways: the merging zones systems which are based on

intermittent pumping[45] as shown in Fig. (1-23.a), where two pumps are operated, is such a way that when pump 1 is in the position, pump II is in the stop position, and vice versa. Thus the sample zone is first transported from the injection port by mean of pump I, then when a chosen distance from the merging point is reached, pump II is started, which continues to bring the carrier stream forward while the reagent is being added Fig. (1-24). After the sample zone has passed, the merging point, point I is reactivated

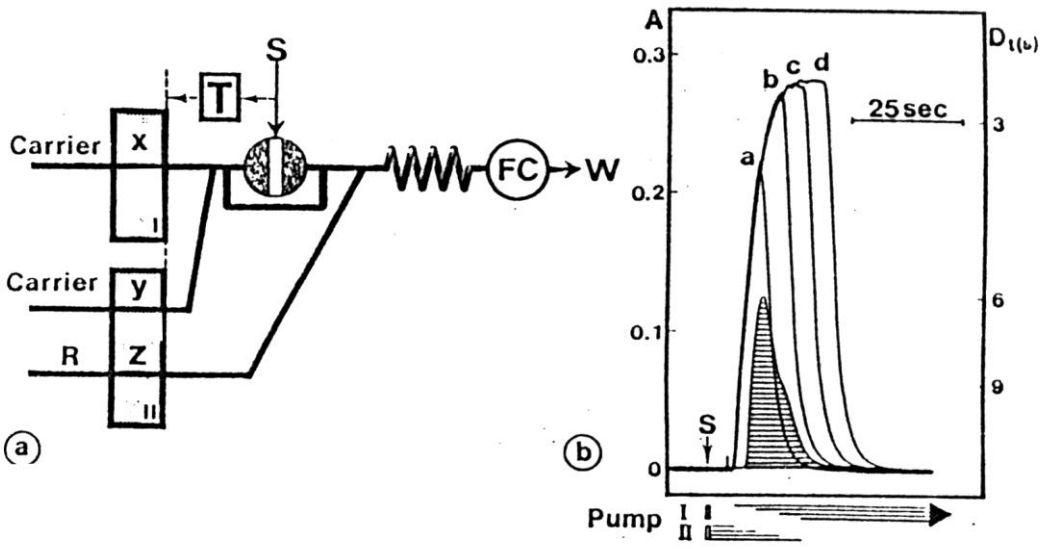

Fig. (1-23) a) FIA manifold for merging zones system based on intermittent pumping.

b) Recorder trace obtained with the system in (a).

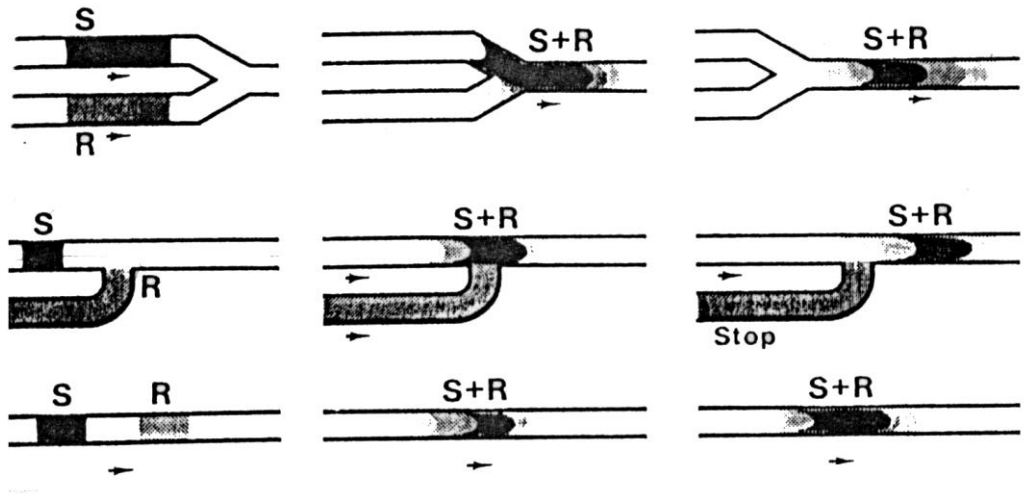

Fig. (1-24) The principle of zone merging a) intermittent pumping b) zone penetration, c)showing, from left to right, the sample(s) zone and reagent (R) zone separately, during the initial contact, and then merged further downstream.

while pump II is stopped again. This approach allows the length of the reagent zone to be regulated simply by choosing different go-and-stop periods by means of the timer (T), and makes it possible to create different concentration gradients on the interface between the sample zone, reagent solution and carrier stream Fig. (1-23.b). Variations on this theme are numerous. Thus, by choosing different lengths of reagent zone, and by letting it overlap in different ways over the sample zone, an individual blank for the reagent alone and for the sample zone alone, as well as the peak height resulting from the chemical reaction between the components of the sample and reagent solution[46] and by the suggestion of the use of a multiinjection valve for the FIA merging zone approach[47], the purpose of using a value, such as that shown in Figs. (1-25) and (1-26) is to inject sample and reagent zones into two separate carrier stream

pumped at balanced flow rates so that they meet in a controlled manner. As distilled water (or diluted buffer-detergent mixture) might be used as carrier in both streams the reagent volume consumed per determination may be 30μl or less[43]. The carrier streams might be pumped continuously-for single- point measurement or intermittently for stopped flow measurements. The advantages of the merging zones are, that alleviated the reagent blank problem[48], cheap, rapid, and flexible analytical facilities that could be used even in small laboratories[49,50,51].

CHAPTER TWO

2- Experimental

2-1 Chemicals

All chemicals were used as supplied without further purification

No.	Chemicals	Purity %	Supplied company
1	Nitric Acid	70	BDH
2	Sulphuric Acid	98	BDH
3	Hydrochloric Acid	35	BDH
4	Acetic Acid	99.5	BDH
5	Formic Acid	99	BDH
6	Citric Acid	99.5	BDH
7	Hydrogen Peroxide	30	BDH
8	Sodium Nitrate	98	BDH
9	Sodium Nitrite	96	BDH
10	Copper Sulfate	99	BDH
11	Potassium Iodate	99.5	BDH
12	Copper Nitrate	95	BDH
13	Manganese	97	BDH
14	Tin Chloride	97	BDH
15	Znic Chloride	98	BDH
16	Ferous Ammonium Alum	95	BDH
17	Silver Nitrate	99.8	BDH
18	Potassium Chromate	99.5	BDH
19	Potassium Dichromate	99.5	BDH
20	Sodium Carbonate	99.5	BDH
21	Sodium Sulphate	99.5	BDH
22	Perchloric Acid	70	Merck
23	Phosphoric Acid	85	Merck

24	Potassium Iodide	99.5	Merck
25	Cadmium Nitrate	99.5	Merck
26	Ammonium Chloride	99.5	Merch
27	Sodium Phosphate	99	Merck
28	Potassium Nitrate	99	Fluka
29	Magnesium Chloride	99	Fluka
30	Cadmium	99.9	Fluka
31	Ferric Nitrate	98	Fluka
32	Lead Nitrate	95	Hopkin and Williams
33	Potassium Bromide	100	M & B
34	Chromium Nitrate	95	Riedel deheanag

2-2 Preparation of Solution

2-2-1 Stock Solutions

Reagent stock solutions were made up in advance as follows:

- Nitric acid, 1M. Dilute 128 ml of 70% HNO_3 (sp.gr, 1.42) with distilled water in a 2L calibrated flask.
- Sulphuric acid, 1M. Dilute 108.68 ml of 98% H_2SO_4 (sp. gr, 1.8) with distilled water in a 2L calibrated flas.
- Hydrochloric acid, 1M. Dilute 176.05 ml of 35% HCl (sp. gr, 1.18) with distilled water in a 2L calibrated flask.
- Perchloric acid, 1M. Dilute 173 ml of 70% $HClO_4$ (sp. gr, 1.66) with distilled water in a 2L calibrated flask.
- Phosphoric acid, 1M. Dilute 136.5 ml of 85% H_3PO_4 (sp. gr, 1.69) with distilled water in a 2L calibrated flask.
- Acetic acid, 1M. Dilute 115 ml of 99.5% CH_3COOH (sp. gr, 1.05) with distilled water in a 2L calibrated flask.

- Formic acid, 1M. Dilute 76.3 ml of 99% HCOOH(sp. gr, 1.22) with distilled water in a 2L calibrated flask.
- Trifluoro acetic acid, 1M. Dilute 19.14 ml of 99 % CF_3COOH(sp. gr, 1.49) with distilled water in a 2L calibrated flask.
- Potassium iodide (0.1M) was prepared by dissolving 16.6g in distilled water and complete to 1L.
- Hydrogen peroxide, 30% used to prepare of H_2O_2 stock solution and standards after standardization with Std $KMNO_4$ Solution.
- Sodium nitrate (0.1M) was prepared by dissolving 4.25g of an oven dried sodium nitrate (for 1.5h at 100°C) in distilled water and diluting to 500ml. The solution was treated with few drops of Chloroform and kept in a refrigerator.
- Sodium nitrite (0.1M) was prepared by dissolving 3.45g (dried for 1.5h at 110°C) Sodium nitrite in distilled water and made up to 500ml. It was standardized against a 0.02M premanganate solution, treated with few drops of Chloroform and stored in a refrigerator.
- Copper sulfate, 1% W/V.
- Potassium iodate (0.1M) was prepared by dissolving 10.695g in distilled water and completed to 500ml.

2-2-2- Interferences Solutions

All the solutions were prepared at the concentration of 1000ppm by dissolving an appropriate amount of each substance in distilled water and completed to 250ml volumetric flask.

2-2-2-1 The cation solution

Substance	Chemical formula	Interference ion	Weight (g)
Cadimium Nitrate	$Cd(NO_3)_2.4H_2O$	Cd^{2+}	0.68603
Copper Nitrate	$Cu(NO_3)_2.3H_2O$	Cu^{2+}	0.95058
Manganese Nitrate	$Mn(NO_3)_2.4H_2O$	Mn^{2+}	1.14224
Tin Chloride	$SnCl_2.2H_2O$	Sn^{2+}	0.31337
Chromium Nitrate	$Cr(NO_3)_2.9H_2O$	Cr^{3+}	1.92394
Lead Nitrate	$pb(NO_3)_2$	Pb^{2+}	0.39963
Znic Chloride	$ZnCl_2$	Zn^{2+}	0.52112
Magnesium Chloride	$MgCl_2.6H_2O$	Mg^{2+}	2.09080
Ferrus Ammonium Alum	$(NH_4)_2SO_4.FeSO_4.6H_2O$	Fe^{2+}	1.75540
Ammonium Chloride	NH_4Cl	NH^+_4	0.74290
Potassium Nitrate	KNO_3	K^+	0.64645
Sodium Nitrate	Na_2NO_3	Na^+	0.57602
Silver Nitrate	$AgNO_3$	Ag^+	0.39370
Ferric Nitrate	$Fe(NO_3)_3.9H_2O$	Fe^{2+}	1.80851

2-2-2-2 Anion Solution

Substance	Chemical formula	Inteferebnce ion	Weight (g)
Potassium Chromate Nitrate	K_2CrO_4	CrO^{2-}_4	0.20928
Potassium Nitrate	KNO_3	NO^{-}_3	0.40767
Potassium Dichromate	$K_2Cr_2O_7$	$Cr_2O^{2-}_7$	0.32547
Potassium Bromide	KBr	Br^{-}	0.37229
Znic Chloride	$ZnCl_2$	Cl^{-}	0.52112
Sodium Carbonate	Na_2CO_3	CO^{2-}_3	0.44162
Sodium Sulphate	Na_2SO_4	SO^{2-}_4	0.36987
Sodium Phosphate	Na_3PO_4	PO^{3-}_4	0.43175

2-3 Apparatus

No.	Instrument or Equipment	Company
1	Tubing Pump Model 395 A	U.S.A
2	Spectronic 21 (Uv-Vis)	Milton Roy U.S.A
3	Pm 8222 Dual-pen Recorder	Philips Holland
4	6-Ways Injection Valve (Merging Zone Version)	Home made
5	Reaction Coil Made From Glass I.D=1.5mm O.D=6 Mm, Length 2m	Home made
6	Flow Injection Cell (1 Cm)	Home made
7	Cadmium Reductor Column 22 Cm Length Of 0.8 Cm Bore Tubing (Glass)	Home made
8	Tubes A- Sample loop, Made from Teflon (1 Mm I.D) B- Glasses (2 Mm I.D) C- Nipples	
9	Ph M62 Standard pH Meter	Orion-U.S.A

2-4 Design of a new manifold System

Building of a new developed unit includes three important parts which are the valve, the cell, and the coil.

2-4-1 The valve

Three designs of the valve are constructed which are five –3way. Seven 3-way and six 3-ways plastic valves.

2-4-1-1 Five 3-ways valve

This design with one loop moves at 90° degree at three directions. The liquid passes in the five 3-way valves as illustrated in Fig. (2-1). The

design includes two parts: the first one shows the loading of the sample loop, and the second part does the introduction of sample into reaction manifolds through injection position as shown in Fig. (2-2). This design gave results but the repeatability was not accepted and was obsolete due to irreproducible results.

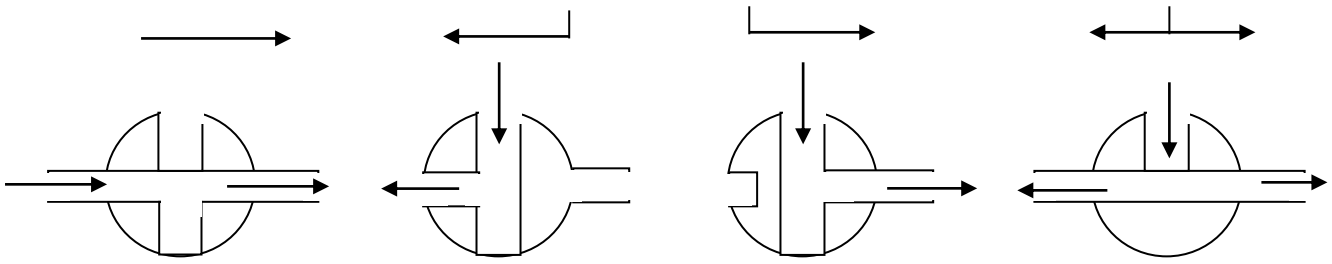

Fig. (2-1): Selection of Liquid Travel

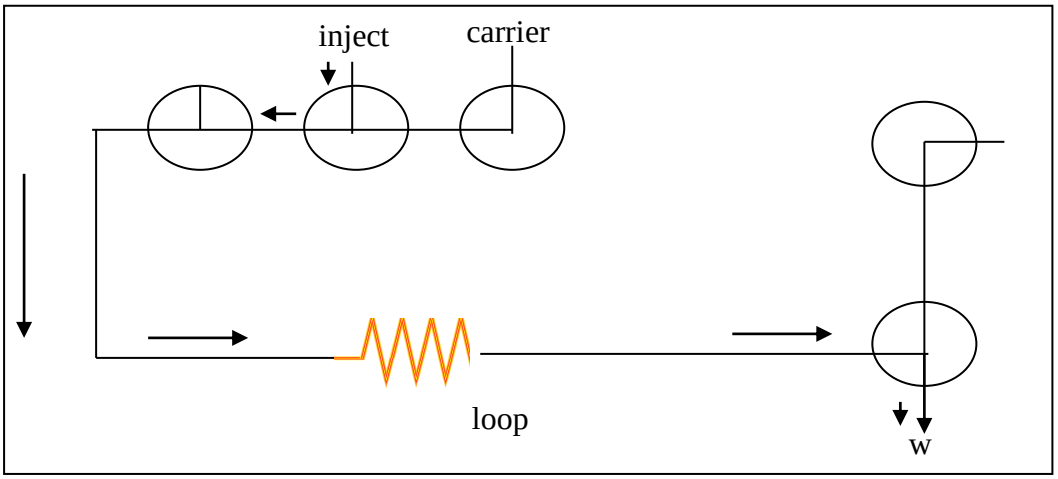

(a)

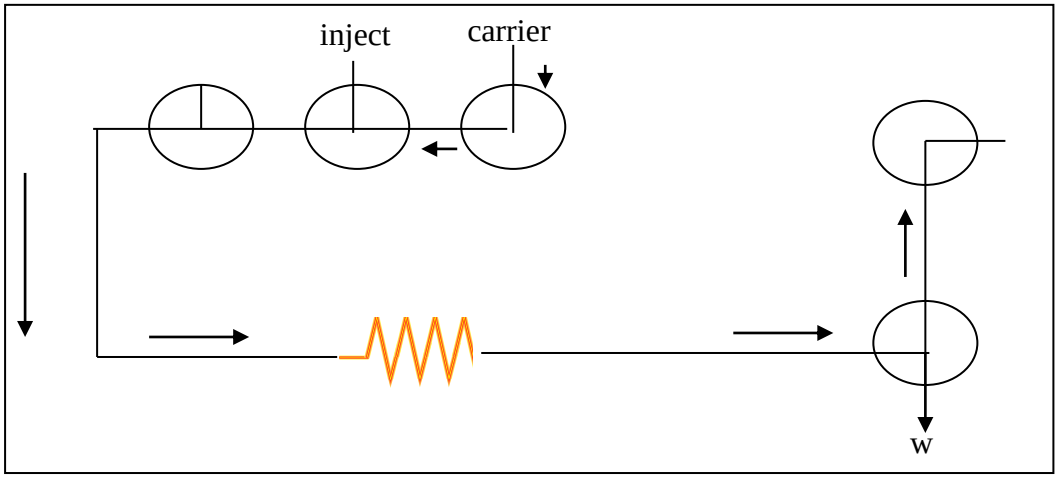

(b)

Fig. (2-2) a- Loading of the sample loop, b- Introduction of sample into reaction manifold.

A modified version with the added knowledge first experience was used to try a second attempt to have a new setting leading to a better sample introducing design.

2-4-1-2 The Seven 3-way Valves

This design contains seven 3-way valves, which move at 90 degree with three directions and two loops. Good results were obtained from this design but the repeatability was not accepted. Fig. (2-3) shows this design.

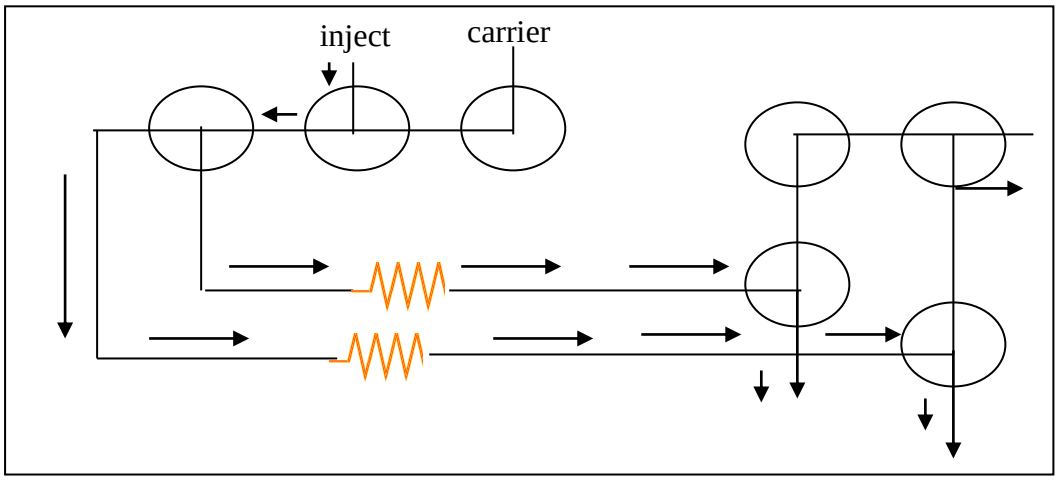

(a)

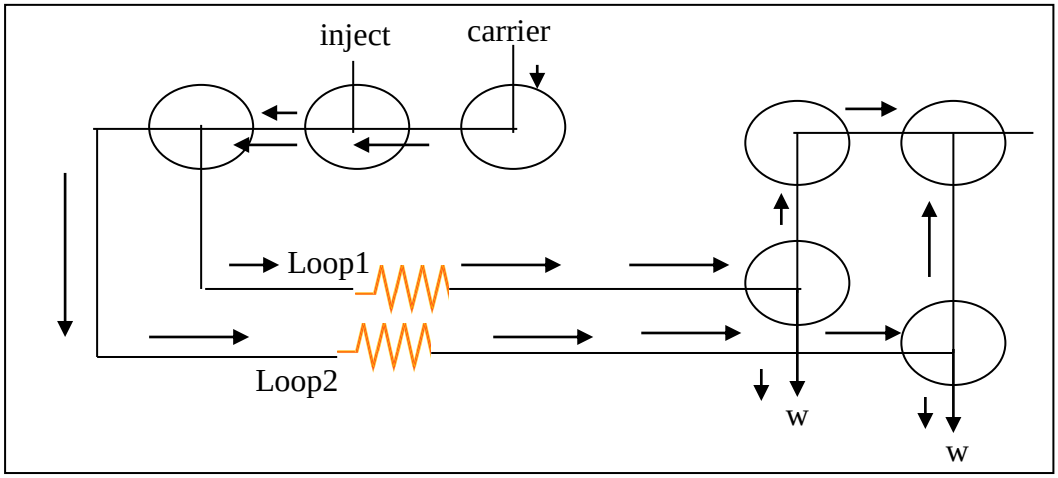

(b)

Fig. (2-3) a- Show the loading of the Sample Loops. b- Introduction of Sample into Reaction Manifold.

2-4-1-3 Six 3-way Plastic Valves

This design containes six 3-ways plastic valves, which move at 90 degree with three direction and two loops as shown in Fig. (2-4). This type of valves gave good repeatability and were used as a part in the newely developed unit.

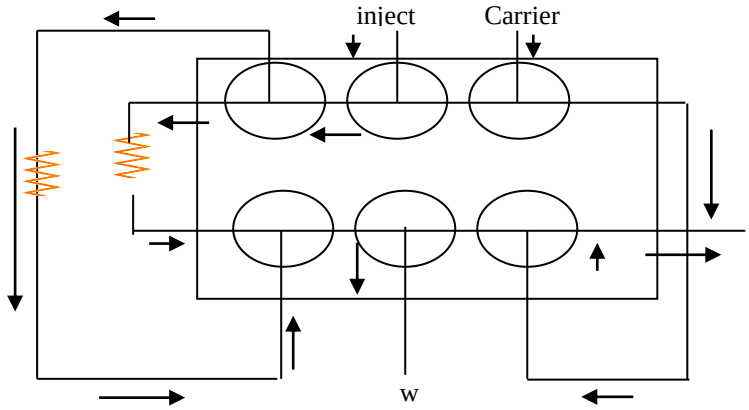

(a)

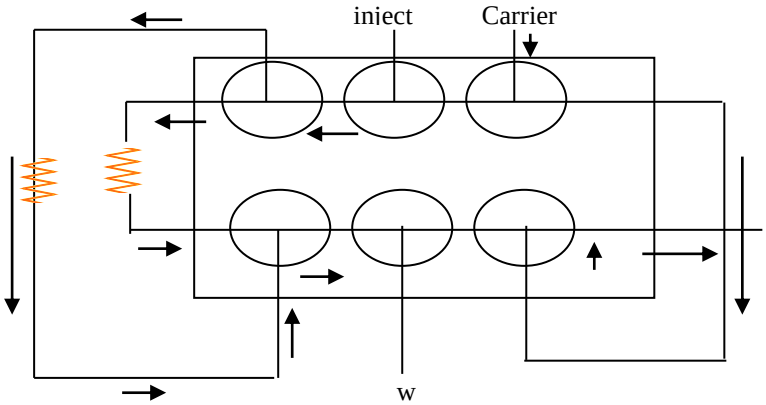

(b)

Fig. (2-4) a- Loading of Sample loops. b- Show the Introduction of Sample into Reaction Manifold.

2-4-2 Flow-through Cell

The flow-through cell was one of the important part in the newely developed unit, which the light paned and the absorbance operation happened to give response. Fig. (2-5A) shows the original cell which is not available; Therefore, a new cell was designed from the available materials. The construction of the cell underwent periodic and different stages. The first stage was shown in Fig. (2-5B) during the research, and was digged from in-side consist two tubes: one of them is for the intery of liquid and the second for letting it out. The contact with the area of the passing of light made of quartiz that was gathered from broken quartiz cells. This cell was connected in the developed unit that gave results, but the repeatability was not acceptable because of the difficulties of controlling the air inside the cell. Fig. (2-5 C,D) shows the second and the third stages which change through it the position of the tube that the liquid goes out.

The two stages gave results, but the repeatability was not acceptable. Fig. (2-5 E) represent, another form of a cell which was made, was design will the ends of the two tubes (in and out liquid) akin to the figure “eight” in Arabic to avoid the air bubbles, but it did not give acceptable results because the existence of air bubble causes pressure on the liquid and finally unstability of reading. The new stage (fifth) was designed in waking curved surface; the lower end represents the entery liquid and the upper end the going out of the liquid. Here the air bubbles were removed that enters and exit quickly, this cell gives acceptable results but less sense because the dilution, as shown in Fig. (2-5 F).

Fig. (2-5 G) shows the sixth stage which was designed and it gathered all the features required. The final and the most fit design was the one with an inclined out-left surface which ensured that any trapped air bubble with never been the path of the light source of the

spectrophotometer and also ensure an enclosed volume above liquid level that incase of relase oxygen or any gaseous by product with not affect the measurements. This cell gave acceptable repeatability through the work conducted in this project and was used as the most suitable are used can be replaced by available materials.

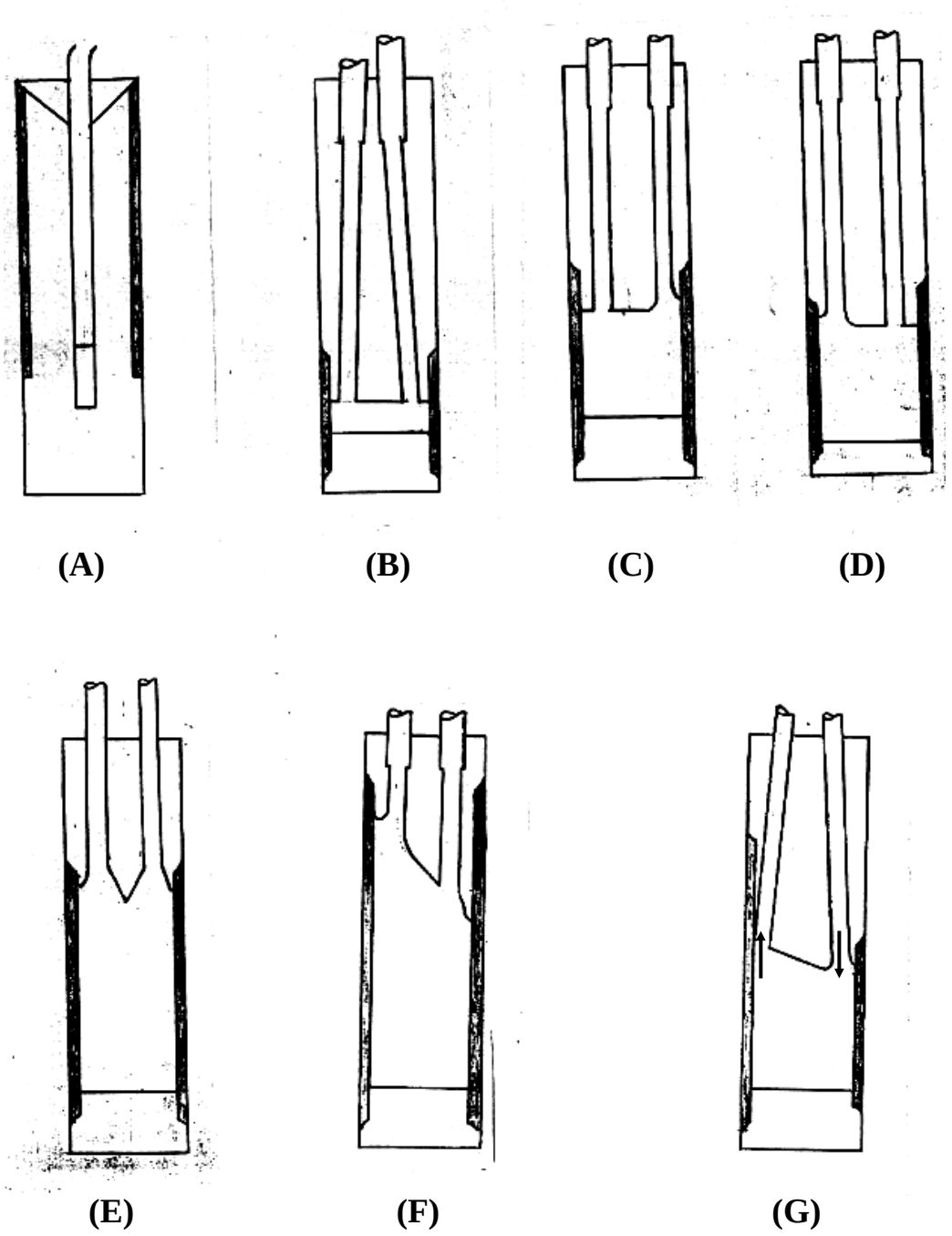

Fig. (2-5) cells design

2-4-3 The Reaction Coil

The reaction coil represent the mixing, at a pre selected reaction time (depending on flow rate, length of the tube, the diameter and kind of material the coil in made of). The coil receives a turbulent flow of mixed reactant component which homegenizes through travel inside the coil. Various lengths were used as seen in Fig. (2-6) which shows that 2m is most optimum value.

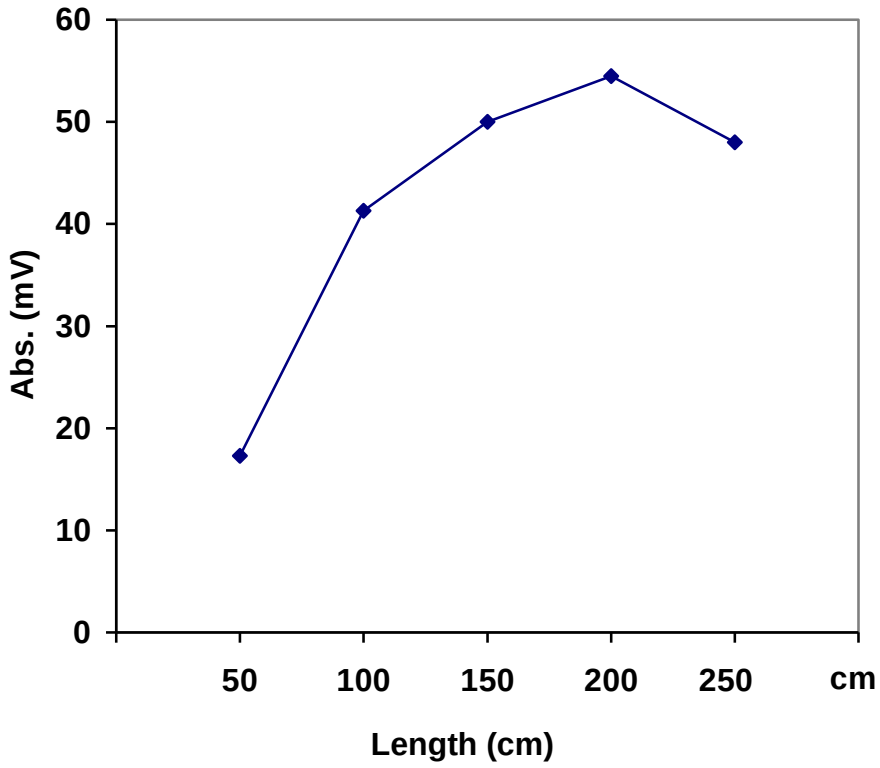

Fig. (2-6) Optimization of delay reaction coil length

2-5 General Properties

2-5-1 The Measure of λ_{max}

Insitu prepared iodine solution made by reacting 10^{-3} M of each KI, KIO_3 and H_2SO_4, and then from in. Thus form more or less measurable iodine formed. It can be seen that ≅350 nm at dilute solution in the optimum maximum wavelength while at little higher concentration (i.e. prepared solution) 363 nm is the highest λ_{max} obtained. Measurements were done at 350 nm which agree quite well with reported λ_{max} at the literature.

2-5-2 The study of dispersion

Through two experiments, the study of dispersion was done. The first experimental , the usage of the unit as in Fig. (2-7). The iodine solution which was formed from the system (I^--IO^-_3-H_3^+O) was pumped instead of the distilled water (carrier solution) and measurement of the iodine obsorbance was at wavelength of 350 nm. It was noticed that the increase in the absorbance at continuous form until reaching a constant absorbance, which represented non-exist was of the effect of dispersion by convection or diffusion. This state represent C_o=976 mv as shown in Fig. (2-7).

In the second experiment, the carrier solution was the distilled water. The iodine solution was injected at the same consternation which was used in the first experiment, then the absorbance was measured and the results were less than that in the first experiment. This state represents C=960 mV. The reason for this difference was the convection or diffusion which cause the spread of the iodine on the surfaces of the tubes by mixing the sample with the carrier solution

$C_o - C = 976 - 960 = 16$ mV

The dispersion is expressed as a ratio between the response without dispersion to the response occurred as shown in the dark areas in Fig. (2-7)

The dispersion is measured

$$D = \frac{C_o}{C} = \frac{976}{960} = 1.016$$

From the value above we conclude that the dispersion is a limit state in this newely are developes. The dispersion depends on the length of the distance between the injection value and the flow through cell, the average flow and the injected volume of the sample or the length of its way.

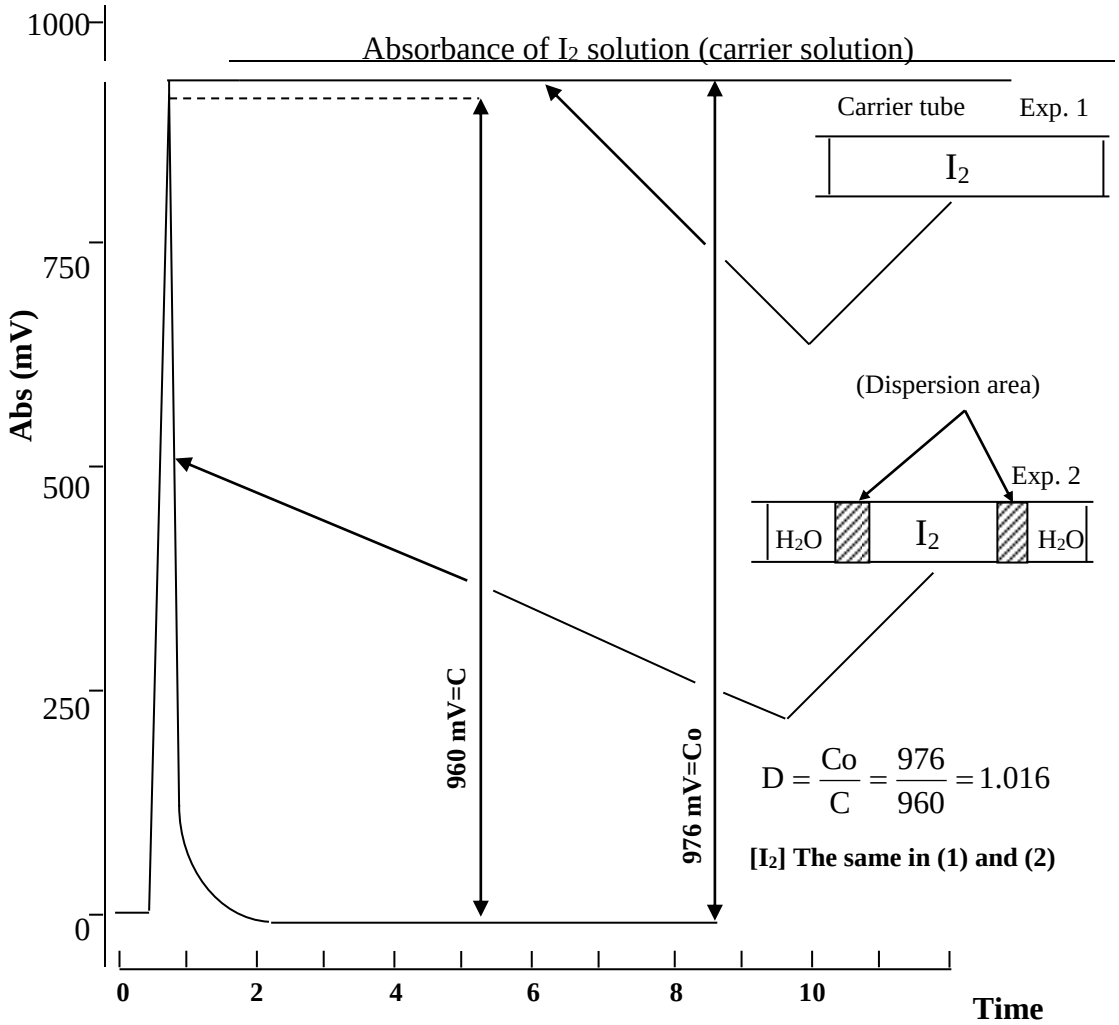

Fig. (2-7) The Dispersion

2-5-3 Reproducibility

For the study of the reproducibility of the newely developed unit shown in Fig. (2-8), a concentration of 2.5×10^{-4} M of HCl was taken, under the usage of all the optimum conditions (the chemical changes, KI(6×10^{-2}M), KIO3 (4×10^{-4}M), and physical changes, volume of injected sample (40µl), flow rate 2.3ml.min^{-1}. It was obtained of a high reproducibility with standard deviation equal to zero by a short analysis time as shown in Fig. (2-8) and table (2-1).

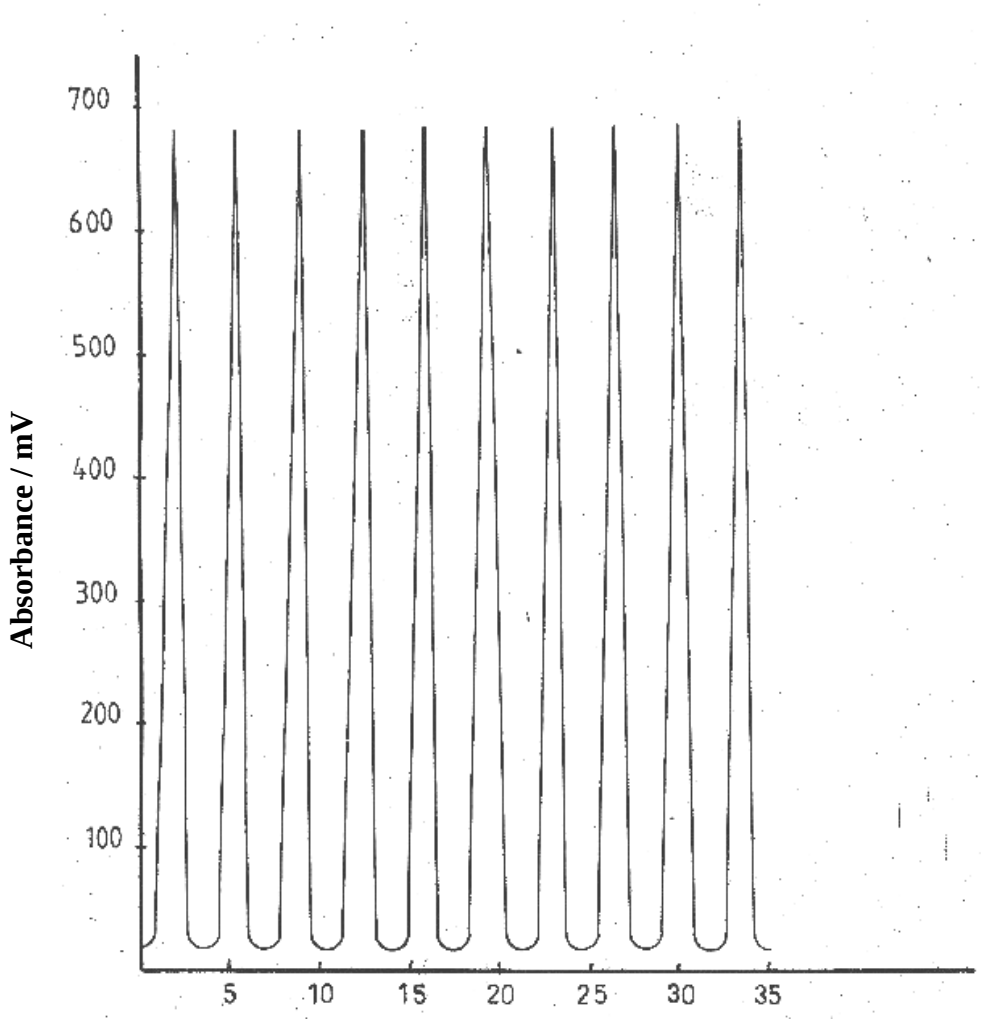

Fig. (2-8) The Reproducibility for Ten Successive Measurement of Released Iodine for 2.5×10^{-4} mol. L^{-1} of HCl

Table 2-1: Shows the Reproducibility for Ten Successive Measurements of Released Iodine

HCl concentration	Peak height Cm(n=10)	Peak mV(n=10)	$\overline{X}$ =mV	δ_n-1	R%	$\overline{X} \pm t\frac{\delta_n - 1}{\sqrt{N}}$
2.5×10^{-4} mol.l^{-}	13.1	524	524	0	0	524

2-5-4 The study of temperature effect

The reaction (I^- - IO^-_3 – $H_3{}^+O$) is done in different temperatures (28°, 30°, 35°, 40°, 45°, and 60°) using the newely developed unit by putting the reaction coil in a water bath set; at the required temperature. From the Fig. (2-9) there is no effect of temperature on the above reaction.

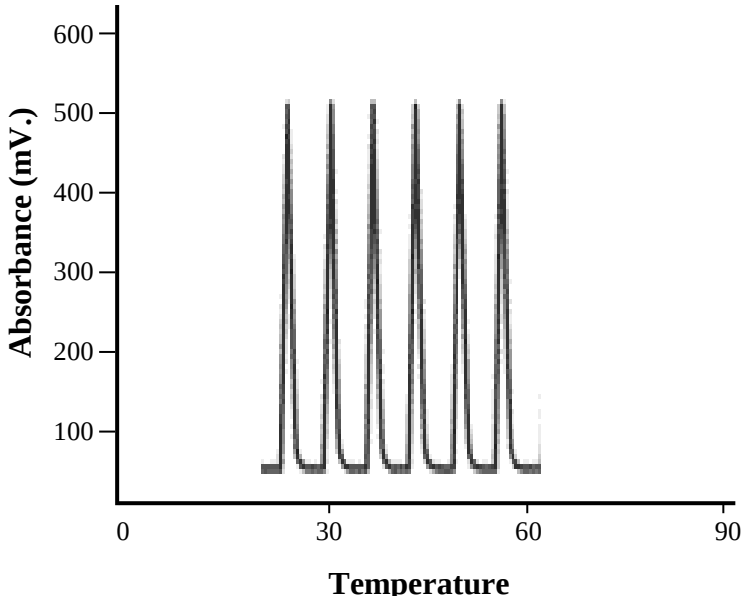

Fig. (2-9) Temperature effect

2-5-5 The Study of the Dead Volume

For the study of the dead volume, special importance in continuous flow injection technique is of value to know the accurate results obtained, when the dead volume is small, the results may be the best to measure the dead volume in the developed unit. Three experiments were done, at the first one the iodine formed from the system (I^- - IO^-_3 – $H_3{}^+O$), the carrier solution was I^- and injection IO^+_3 in loop(1), the H_2O was injected instead of $H_3{}^+O$ in loop(2). No response was got in this experiment. In the second experiment, $H_3{}^+O$ was injected in loop(1) and the H_2O was injected in loop(2) and the carrier solution was I^-. No response was obtained from this experiment as well. At the thired experiment IO^-_3 was injected in loop(2), $H_3{}^+O$ was injected in loop(1) and the carrier solution was H_2O and there was also no response. This mean that there was no dead volume and the unit was well designed.

2-6 The Style of work of the newly developed unit

The basic of the reaction is the hydronium ion ($H_3{}^+O$) which represent the acidic part from the water molecule and the hydroxide ion (OH^-) represents the conjugated base to the spontaneous analysis of the water molecule as follows

$$2\ H_2O \rightleftharpoons H_3{}^+O + OH^-$$

All acids are applied to give the hydronium ion ($H_3{}^+O$) thus the strong, medium, weak and very weak acids. This unit is applied to determine the trace concentrations from all kinds of acids by using potassium iodide and potassium iodate, the red iodine is formed and can be measured in 350 nm.

$$IO_3^- + 5I^- + 6H^+ \longrightarrow 3I_2 + 3H_2O$$

This depends on the loading of potassium iodate in L_2 and acid in L_1 as shown in Fig. (2-10, 2-11), and using potassium iodide as a carrier solution, which keeps potassium iodate and acid each in its loop until measurement, which changes the flow of the carrier solution to L_1, L_2 and then their meeting, completing their reaction which is shown above as in the following diagram for the purpose of clarity:

Valve No.	1	2	3	4	5	6
Valve ways	a-b-c	d-e-f	g-h-i	L-m-n	o-p-q	r-s-t

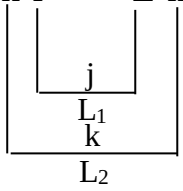

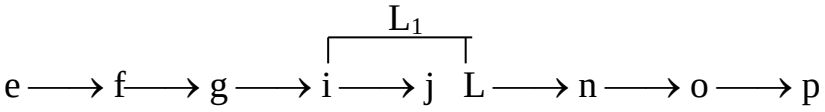

This represents the loading of iodate. The separation of carrier solution from the loading system L_1 and L_2 is across the delay reaction coil and according to the way

b ⟶ a ⟶ S ⟶ t ….

and according to the Fig. (2-11 , i, ii, iii, iv), the way of measurement is as follows as in Fig. (2-11, IV).

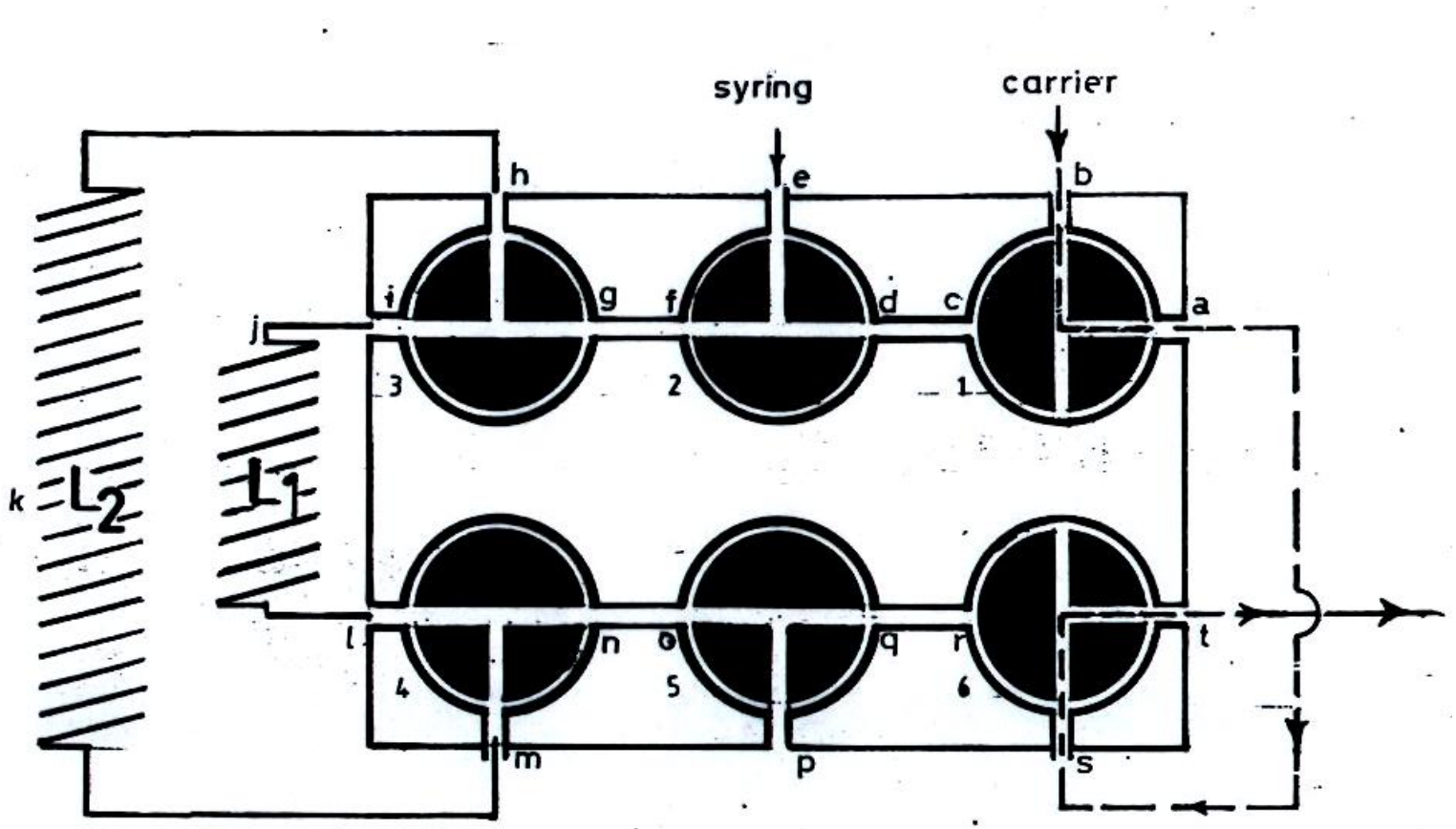

Fig. (2-10) The valves system

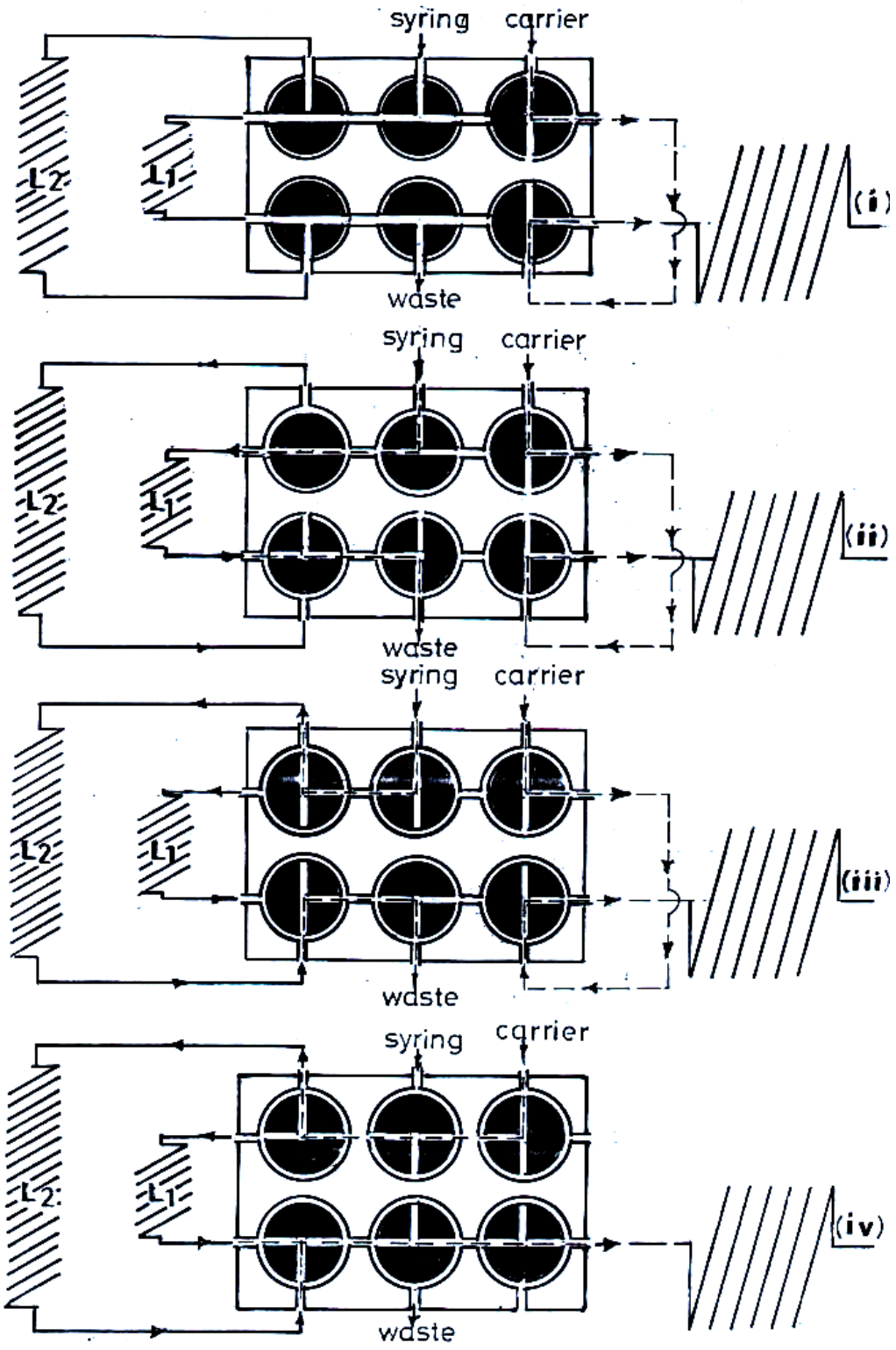

Fig. (2-11) shows the loading and injection of the sample

Chapter two

2.1 Chemicals

All chemicals were used as supplied without further purification

No.	Chemicals	Purity %	Supplied company
1	Nitric Acid	70	BDH
2	Sulphuric Acid	98	BDH
3	Hydrochloric Acid	35	BDH
4	Acetic Acid	99.5	BDH
5	Formic Acid	99	BDH
6	Citric Acid	99.5	BDH
7	Hydrogen Peroxide	30	BDH
8	Sodium Nitrate	98	BDH
9	Sodium Nitrite	96	BDH
10	Copper Sulfate	99	BDH
11	Potassium Iodate	99.5	BDH
12	Copper Nitrate	95	BDH
13	Manganese	97	BDH
14	Tin Chloride	97	BDH
15	Znic Chloride	98	BDH
16	Ferous Ammonium Alum	95	BDH
17	Silver Nitrate	99.8	BDH
18	Potassium Chromate	99.5	BDH
19	Potassium Dichromate	99.5	BDH
20	Sodium Carbonate	99.5	BDH
21	Sodium Sulphate	99.5	BDH
22	Perchloric Acid	70	Merck

23	Phosphoric Acid	85	Merck
24	Potassium Iodide	99.5	Merck
25	Cadmium Nitrate	99.5	Merck
26	Ammonium Chloride	99.5	Merch
27	Sodium Phosphate	99	Merck
28	Potassium Nitrate	99	Fluka
29	Manesium Chloride	99	Fluka
30	Cadmium	99.9	Fluka
31	Ferric Nitrate	98	Fluka
32	Lead Nitrate	95	Hopkin and Williams
33	Potassium Bromide	100	M & B
34	Chromium Nitrate	95	Riedel de heanag

2.3 Apparatus

No.	Instrument or Equipment	Company
1	Tubing Pump Model 395 A	U.S.A
2	Spectronic 21 (Uv-Vis)	Milton Roy U.S.A
3	Pm 8222 Dual-pen Recorder	Philps Holland
4	6-Ways Injection Value (Merging Zone Version)	Home made
5	Reaction Coil Made From Glass I.D=1.5mm O.D=6 Mm, Length 2m	Home made
6	Flow Injection Cell (1 Cm)	Home made
7	Cadmium Reductor Coloumn 22 Cm Length Of 0.8 Cm Bore Tubing (Glass)	Home made

8	Tubes A- Sample loop, Made from Teflon (1 Mm I.D) B- Glasses (2 Mm I.D) C- Nipples	
9	Ph M62 Standard pH Meter	Orion-U.S.A

2-2-1 Reagents Stack Solutions

Were made up in advance as follows:

- Nitric acid, 1M. Dilute 128 ml of 70% HNO_3 (sp.gr, 1.42) with distilled water in a 2L calibrated flask.
- Sulphuric acid, 1M. Dilute 108.68 ml of 98% H_2SO_4 (sp. Gr, 1.8) with distilled water in a 2L calibrated flas.
- Hydrochloric acid, 1M. Dilute 176.05 ml of 35% HCl (sp. Gr, 1.18) with distilled water in a 2L calibrated flask.
- Perchloric acid, 1M. Dilute 173 ml of 70% $HClO_4$ (sp. gr, 1.66) with distilled water in a 2L calibrated flask.
- Phosphoric acid, 1M. Dilute 136.5 ml of 85% H_3PO_4 (sp. gr, 1.69) with distilled water in a 2L calibrated flask.
- Acetic acid, 1M. Dilute 115 ml of 99.5% CH_3COOH (sp. gr, 1.05) with distilled water in a 2L calibrated flask.
- Formic acid, 1M. Dilute 76.3 ml of 99% HCOOH(sp. gr, 1.22) with distilled water in a 2L calibrated flask.
- Trifluoro acetic acid, 1M. Dilute 19.14 ml of 99 % CF_3COOH(sp. gr, 1.49) with distilled water in a 2L calibrated flask.
- Potassium iodide (0.1M) was prepared by dissolving 16.6g in distilled water and complete to 1L.

- Hydrogen peroxide, 30% used to prepare of H_2O_2 stock solution and standards after standardization with Std $KMNO_4$ Solution.
- Sodium nitrate (0.1M) was prepared by dissolving 4.25g of an oven dried sodium nitrate (for 1.5h at 100°C) in distilled water and diluting to 500ml. The solution was treated with few drops of Chloroform and kept in a refrigerator.
- Sodium nitrite (0.1M) was prepared by dissolving 3.45g (dried for 1.5h at 110°C) Sodium nitrite in distilled water and made up to 500ml. It was standardized against a 0.02M premanganate solution, treated with few drops of Chloroform and stored in a refrigerator.
- Copper sulfate, 1% W/V.
- Potassium iodate (0.1M) was prepared by dissolving 10.695g in distilled water and completed to 500ml.

2-2-2- Interferences solutions

All the solutions were prepared at the concentration of 1000ppm by dissolving an appropriate amount of each substance in distilled water and completed to 250ml volumetric flask.

2-2-2-1 The cation solution

Substance	Chemical formula	Interference ion	Weight (g)
Cadimium Nitrate	$Cd(NO_3)_2.4H_2O$	Cd^{2+}	0.68603
Copper Nitrate	$Cu(NO_3)_2.3H_2O$	Cu^{2+}	0.95058
Manganese Nitrate	$Mn(NO_3)_2.4H_2O$	Mn^{2+}	1.14224
Tin Chloride	$SnCl_2.2H_2O$	Sn^{2+}	0.31337
Chromium Nitrate	$Cr(NO_3)_2.9H_2O$	Cr^{3+}	1.92394
Lead Nitrate	$pb(NO_3)_2$	Pb^{2+}	0.39963

Znic Chloride	$ZnCl_2$	Zn^{2+}	0.52112
Magnesium Chloride	$MgCl_2.6H_2O$	Mg^{2+}	2.09080
Ferous Ammonium Alum	$(NH_4)_2SO_4.FeSO_4.6H_2O$	Fe^{2+}	1.75540
Ammonium Chloride	NH_4Cl	NH^+_4	0.74290
Potassium Nitrate	KNO_3	K^+	0.64645
Sodium Nitrate	Na_2NO_3	Na^+	0.57602
Silver Nitrate	$AgNO_3$	Ag^+	0.39370
Ferric Nitrate	$Fe(NO_3)_3.9H_2O$	Fe^{2+}	1.80851

2-2-2-2 Anion Solution

Substance	Chemical formula	Inteferebnce ion	Weight (g)
Potassium Chromate Nitrate	K_2CrO_4	CrO^{2-}_4	0.20928
Potassium Nitrate	KNO_3	NO^-_3	0.40767
Potassium Dichromate	$K_2Cr_2O_7$	$Cr_2O^{2-}_7$	0.32547
Potassium Bromide	KBr	Br^-	0.37229
Znic Chloride	$ZnCl_2$	Cl^-	0.52112
Sodium Carbonate	Na_2CO_3	CO^{2-}_3	0.44162
Sodium Sulphate	Na_2SO_4	SO^{2-}_4	0.36987
Sodium Phosphate	Na_3PO_4	PO^{3-}_4	0.43175

2-4 Design of a new manifold System

Building of a new developed unit includes three important parts which are the valve, the cell, and the coil.

2-4-1 The valve

Three designs of the value are constructed which are five –3way. Seven 3-way and six 3-ways plastic valves.

2-4-1-1 Five 3-ways valve

This design with one loop moves at 90° degree at three directions. The liquid passes in the five 3-way valves as illustrated in Fig. (2-1). The design includes two parts: the first one shows the loading of the sample loop, and the second part does the introduction of sample into reaction manifolds through injection position as shown in Fig. (2-2). This design gave results but the repeatability was not accepted and was obsolete due to irreproducible results.

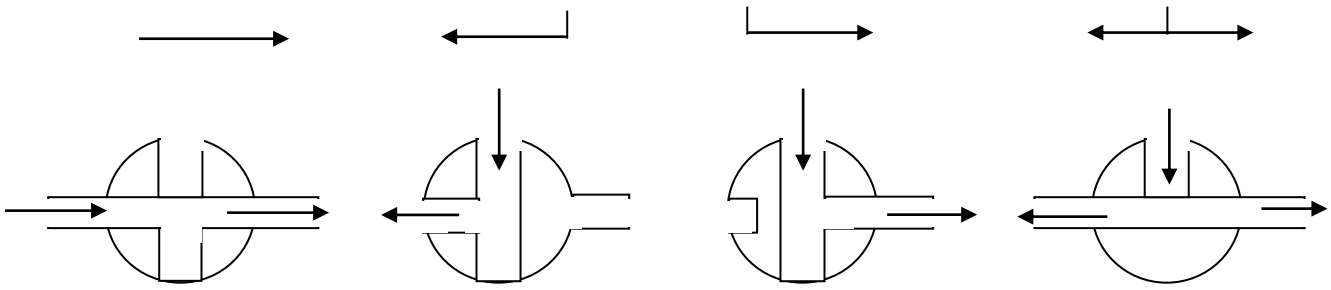

Fig. (2-1): Selection of Liquid Travel

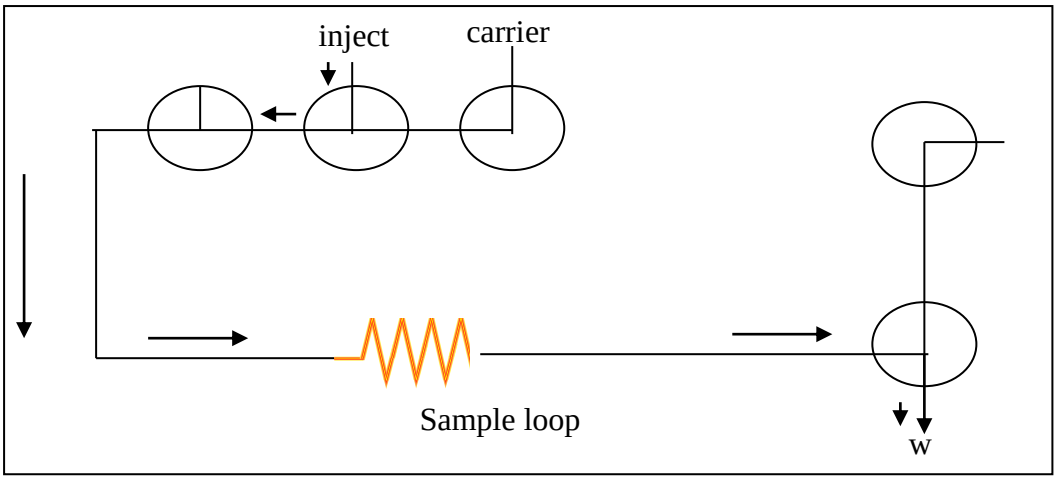

(a)

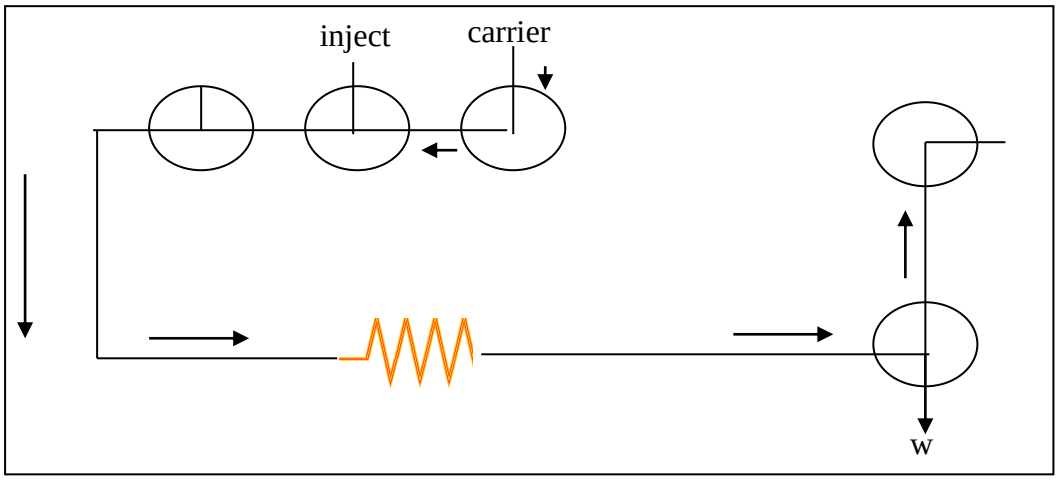

(b)

Fig. (2-2) (a) Loading of the loop sample, (b) Introduction of sample into reaction manifold.

A modified version with the added knowledge first experience was used to try a second attempt to have a new setting leading to a better sample introduction design.

2-4-1-2 The Seven 3-way Valves

This design contains seven 3-way valves, which move at 90 degree with three directions and two loops. Good results were obtained from this design but the repeatability was not accepted. Fig. (2-3) shows this design.

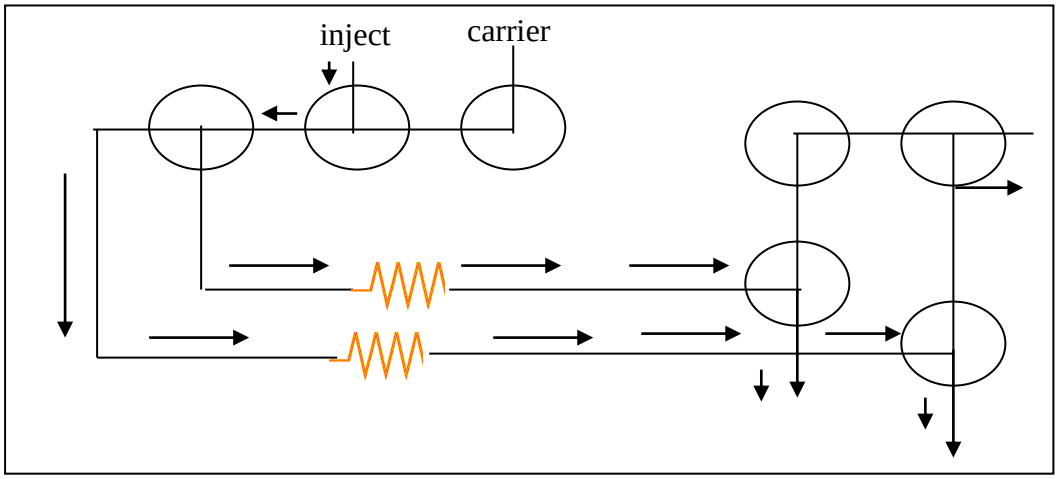

(a)

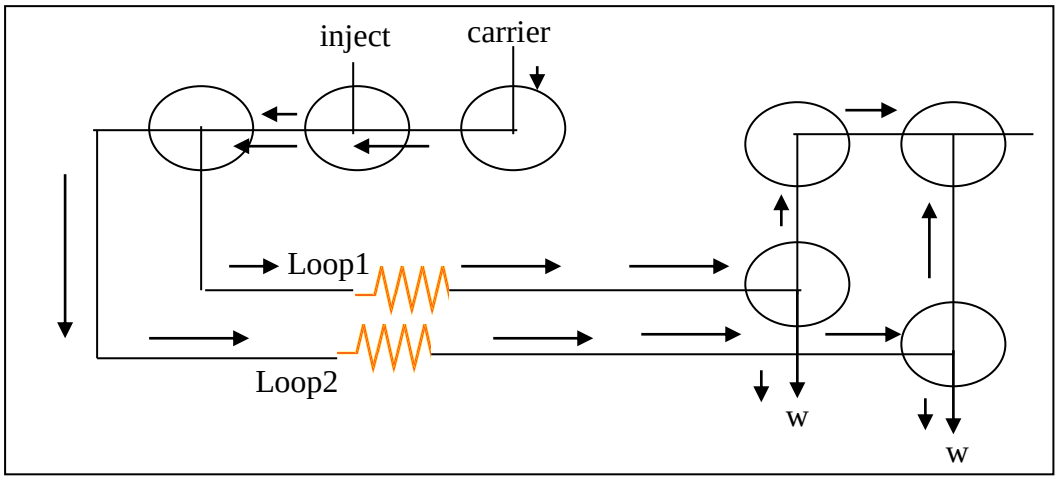

(b)

Fig. (2-3) A Show the loading of the Sample Loops b. Introduction of Sample into Reaction Manifold.

2-4-1-3 Six 3-way Plastic Valves

This design containes six 3-ways plastic valves, which move at 90 degree with three direction and two loops as shown in Fig. (2-4). This type of valves gave good repeatability and were used us a part in the newely developed unit.

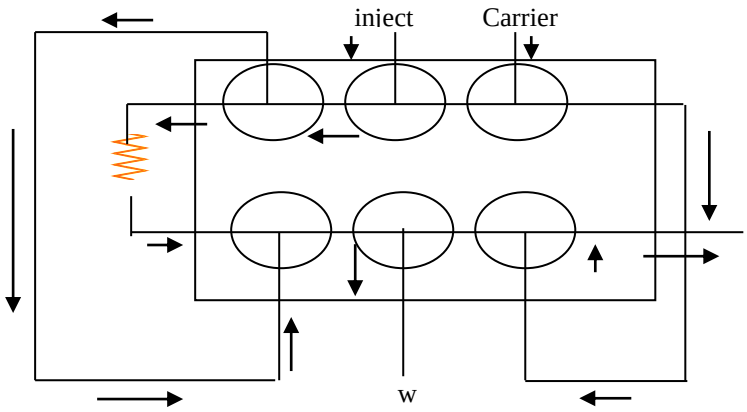

(a)

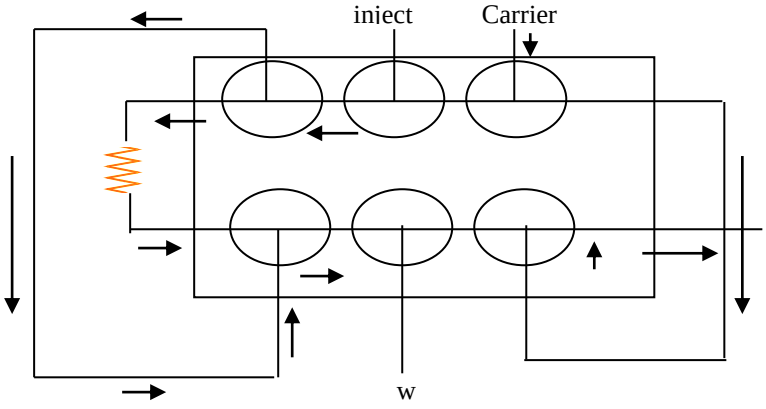

(b)

Fig. (2-4) a) Loading of Sample loops. b) Show the Introduction of Sample into Reaction Manifold.

2-4-2 Flow-through Cell

The flow-through cell was one of the important part in the newely developed unit, which the light paned and the absorbance operation happened to give response. Fig. (2-5A) shows the original cell which is not available; Therfore, a new cell was designed from the available materials. The construction of the cell underwent periodic and different stages. The first stage was shown in Fig. (2-5B) during the research, and was digged from in-side consist two tubes: one of them is for the intery of liquid and the second for letting it out. The contact with the area of the passing of light made of quartiz that was gathered from broken quartiz cells. This cell was connected in the developed unit that gave results, but the repeatability was not acceptable because of the difficulties of controlling the air inside the cell. Fig. (2-5 C,D) shows the second and the third stages which change through it the position of the tube that the liquid goes out.

The two stages gave results, but the repeatability was not acceptable. Fig. (2-5 E) represent, another form of a cell which was made, was design will the ends of the two tubes (in and out liquid) akin to the figure “eight” in Arabic to avoid the air bubbles, but it did not give acceptable results because the existence of air bubble causes pressure on the liquid and finally unstability of reading. The new stage (fifth) was designed in waking curved surface; the lower end represents the entery liquid and the upper end the going out of the liquid. Here the air bubbles were removed that enters and exit quickly, this cell gives acceptable results but less sense because the dilution, as shown in Fig. (2-5 F).

Fig. (2-5 G) shows the sixth stage which was designed and it gathered all the features required. The final and the most fit design was the one with an inclined out-left surface which ensured that any trapped air bubble with never been the path of the light source of the spectrophotometer and also ensure an enclosed volume above liquid level

that incase of relase oxygen or any gaseous by product with not affect the measurements. This cell gave acceptable repeatability through the work conducted in this project and was used as the most suitable are used can be replaced by available materials.

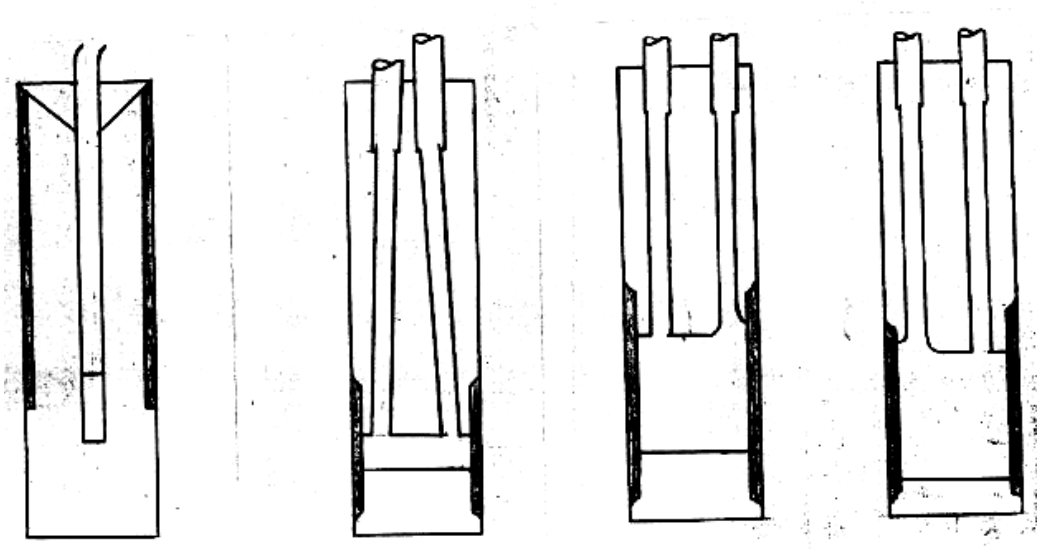

(A) **(B)** **(C)** **(D)**

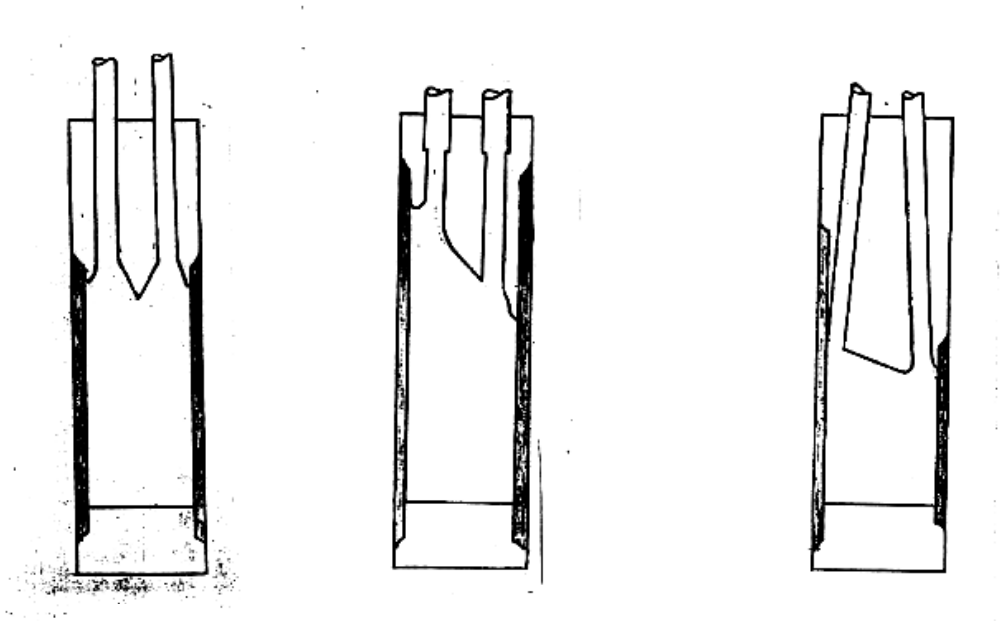

(E) **(F)** **(G)**

Fig. (2-5) cells design

2-4-3 The Reaction Coil

The reaction coil represent the mixing, at a pre selected reaction time (depending on flow rate, length of the tube, the diameter and kind of material the coil in made of). The coil receives a turbulent flow of mixed reactant component which homegenizes through travel inside the coil. Various lengths were used as seen in Fig. (2-6) which shows that 2m is most optimum value.

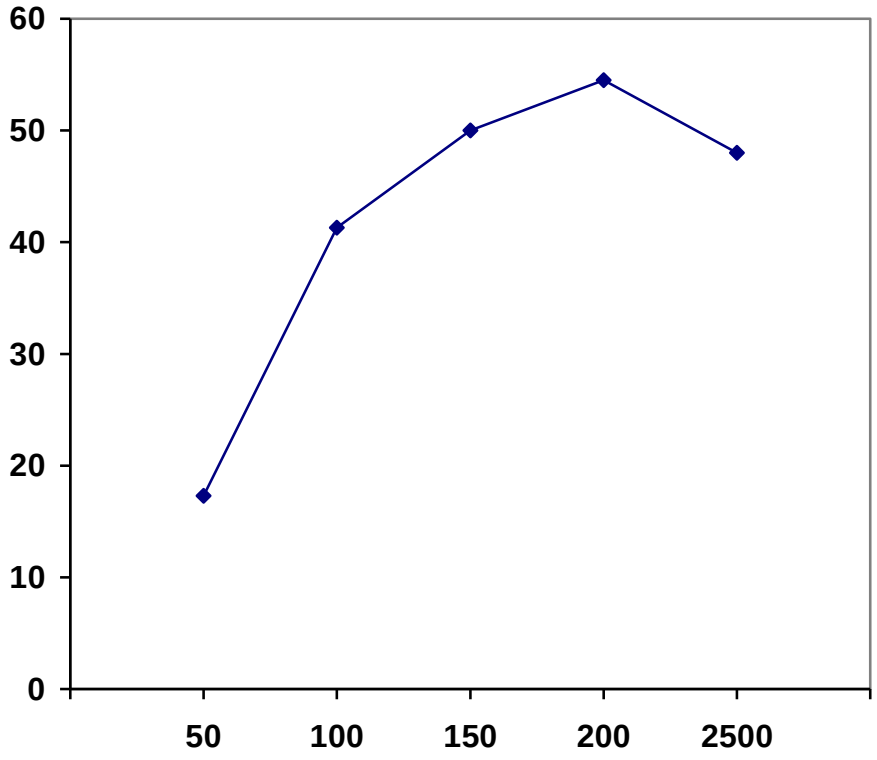

Fig. (2-6) Optimization of delay reaction coil length

2-5 General Properties

2-5-1 The Measure of λ_{max}

Insitu prepares iodine solution made by reacting 10^{-3} M of each KI, KIO_3 and H_2SO_4, and then from in. Thus form more or less measurable iodine formed. It can be seen that ≅350 nm at dilute solution in the optimum maximum wavelength while at little higher concentration (i.e. prepared solution) 363 nm is the highest λ_{max} obtained. Measurements were done at 350 nm which agree quite well with reported λ_{max} at the literature.

2-5-2 The study of dispersion

Through two experiments, the study of dispersion was done. The first experimental , the usage of the unite as in Fig. (2-7). The iodine solution which was formed from the system (I^--IO^-_3-$H_3{}^+O$) was pumped instead of the distilled water (carrier solution) and measurement of the iodine obsorbance was at wavelength of 350 nm. It was noticed that the increase in the absorbance at continuous form until reaching a constant absorbance, which represented non-exist was of the effect of dispersion by convection or diffusion. This state represent C_o=976 mv as shown in Fig. (2-7).

In the second experiment, the carrier solution was the distilled water. The iodine solution was injected at the same consternation which was used in the first experiment, then the absorbance was measured and the

results were less than that in the first experiment. This state represents C=960 mV. The reason for this difference was the convection or diffusion which cause the spread of the iodine on the surfaces of the tubes by mixing the sample with the carrier solution

$C_o - C = 976 - 960 = 16$ mV

The dispersion is expressed as a ratio between the response without dispersion to the response occurred as shown in the dark areas in Fig. (2-7)

The dispersion is measured

$$D = \frac{C_o}{C} = \frac{976}{960} = 1.016$$

From the value above we conclude that the dispersion is a limit state in this newely are developes. The dispersion depends on the length of the distance between the injection value and the flow through cell, the average flow and the injected volume of the sample or the length of its way.

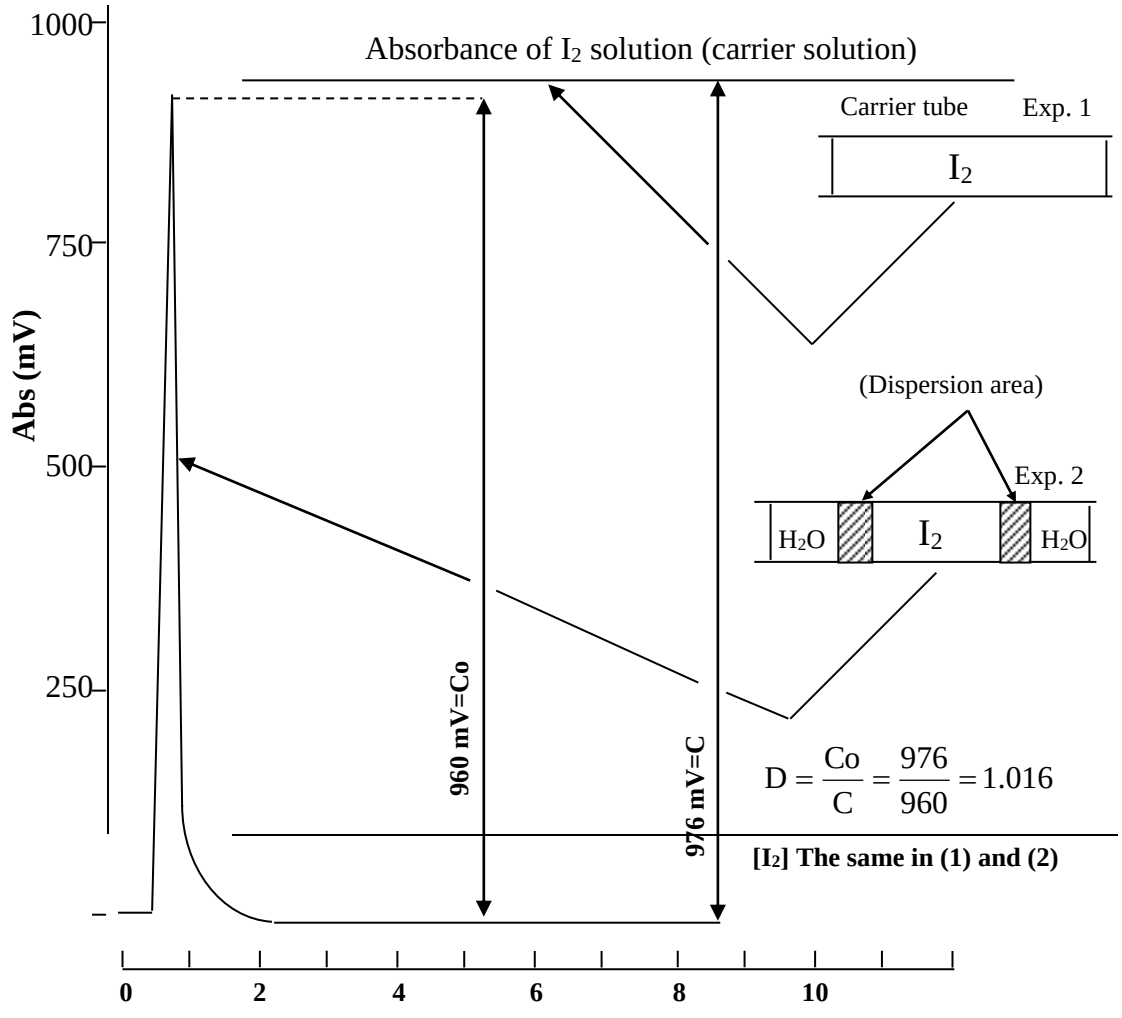

0

Fig. (2-7) The Dispersion

2-5-3 Reproducibility

For the study of the reproducibility of the newely developed unit shown in Fig. (2-8), a concentration of 2.5×10^{-4} M of HCl was taken, under the usage of all the optimum conditions (the chemical changes, KI(6×10^{-2}M), KIO3 (4×10^{-4}M), and physical changes, volume of injected sample (40µl), flow rate 2.3ml.min^{-1}. It was obtained of a high reproducibility with standard deviation equal to zero by a short analysis time as shown in Fig. (2-8) and table (2-1).

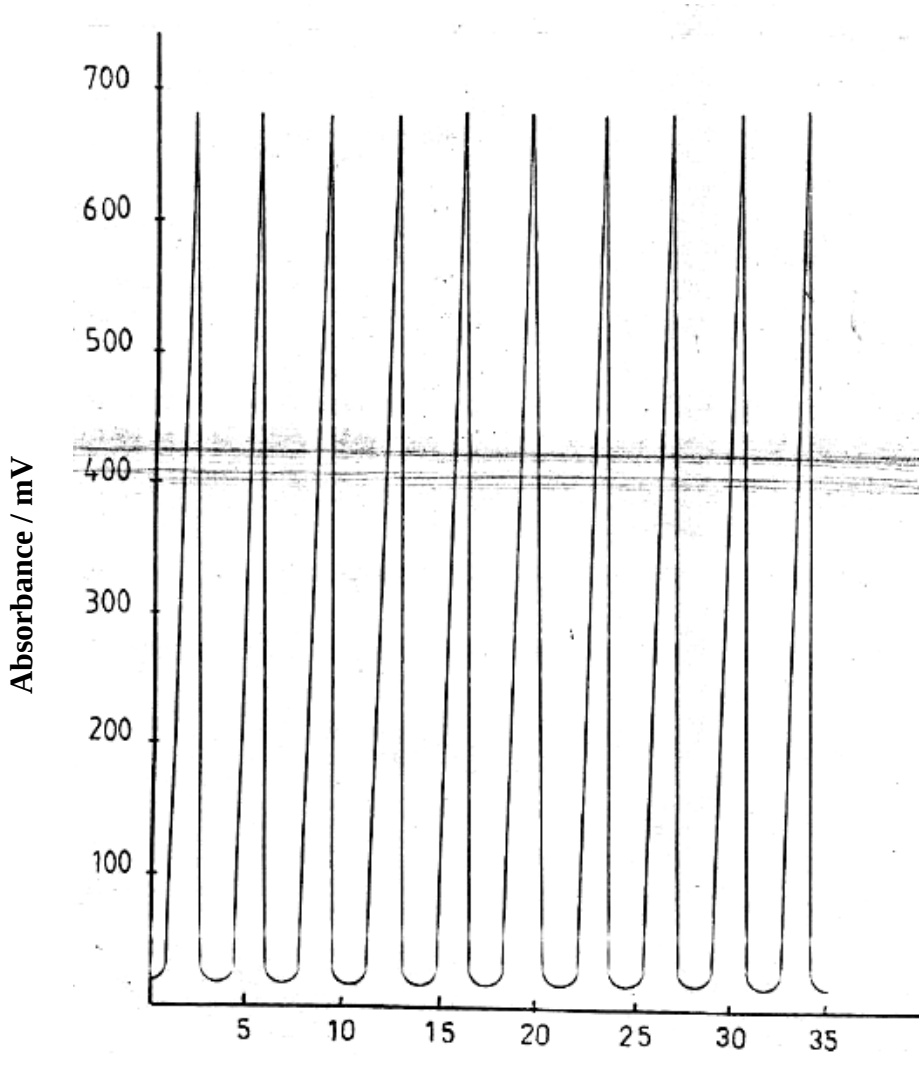

Fig. (2-8) The Reproducibility for Ten Successive Measurement of Released Iodine for 2.5×10^{-4} mol. L^{-1} of HCl

Table 2-1: Shows the Reproducibility for Ten Successive Measurements of Released Iodine

HCl concentration	Peak height Cm(n=10)	Peak mV(n=10)	$\overline{X}$ =mV	δ_n-1	R%	$\overline{X} \pm t\frac{\delta_n - 1}{\sqrt{N}}$
2.5×10^{-4} mol.l^{-}	13.1	524	524	0	0	524

2-5-4 The study of temperature effect

The reaction (I^- - IO^-_3 – $H_3{}^+O$) is done in different temperatures (28°, 30°, 35°, 40°, 45°, and 60°) using the newely developed unit fig. ( ) by putting the reaction coil in a water bath which organize the required temperature. From the Fig. (2-9) there is no effect of temperature on the above reaction.

Fig. (2-9) Temperature effect

2-5-5 The Study of the Dead Volume

For the study of the dead volume, special importance in continuous flow injection technique is of value to know the accurate results obtained, when the dead volume is small, the results may be the best to measure the dead volume in the developed unit. Three experiments were done, at the first one the iodine formed from the system (I^- - IO^-_3 – $H_3{}^+O$), the carrier solution was I^- and injection IO^+_3 in loop(1), the H_2O was injected instead of $H_3{}^+O$ in loop(2). No response was got in this experiment. In the second experiment, $H_3{}^+O$ was injected in loop(1) and the H_2O was injected in loop(2) and the carrier solution was I^-. No response was obtained from this experiment as well. At the thired experiment IO^-_3 was injected in loop(2), $H_3{}^+O$ was injected in loop(1) and the carrier solution was H_2O and there was also no response. This mean that there was no dead volume and the unit was well designed.

2-6 The Style of work of the newly developed unit

The basic of the reaction is the hydronium ion ($H_3{}^+O$) which represent the acidic part from the water molecule and the hydroxide ion (OH^-) represents the conjugated base to the spontaneous analysis of the water molecule as follows

$$2\ H_2O \rightleftharpoons H_3{}^+O + OH^-$$

All acids are applied to give the hydronium ion ($H_3{}^+O$) thus the strong, midum, weak and very weak acids. This unit is applied to determine the trace concentrations from all kinds of acids by using potassium iodide and potassium iodate, the red iodine is formed and can be measured in 350 nm.

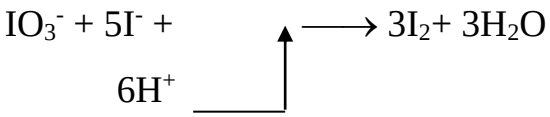

This depends on the loading of potassium iodate in L_2 and acid in L_1 as shown in Fig. (2-10, 2-11), and using potassium iodide as a carrier solution, which keeps potassium iodate and acid each in its plastic loop until measurement, which changes the flow of the carrier solution to L_1, L_2 and then their meeting, completing their reaction which is shown above as in the following diagram for the purpose of clarity:

Valve No.	1	2	3	4	5	6
Valve ways	a-b-c	d-e-f	g-h-i	L-m-n	o-p-q	r-s-t

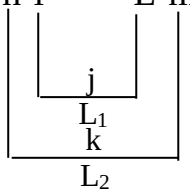

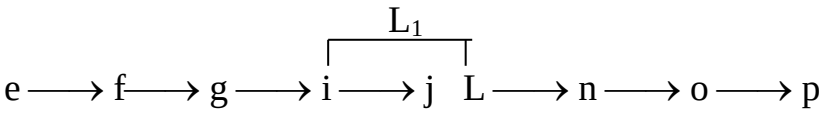

This represents the loading of iodate. The separation of carrier solution from the loading system L_1 and L_2 is across the delay reaction coil and according to the way

b ⟶ a ⟶ S ⟶t ….

and according to the Fig. (, I, ii, iii, iv), the way of measurment is as follows as in Fig. (2-11, IV).

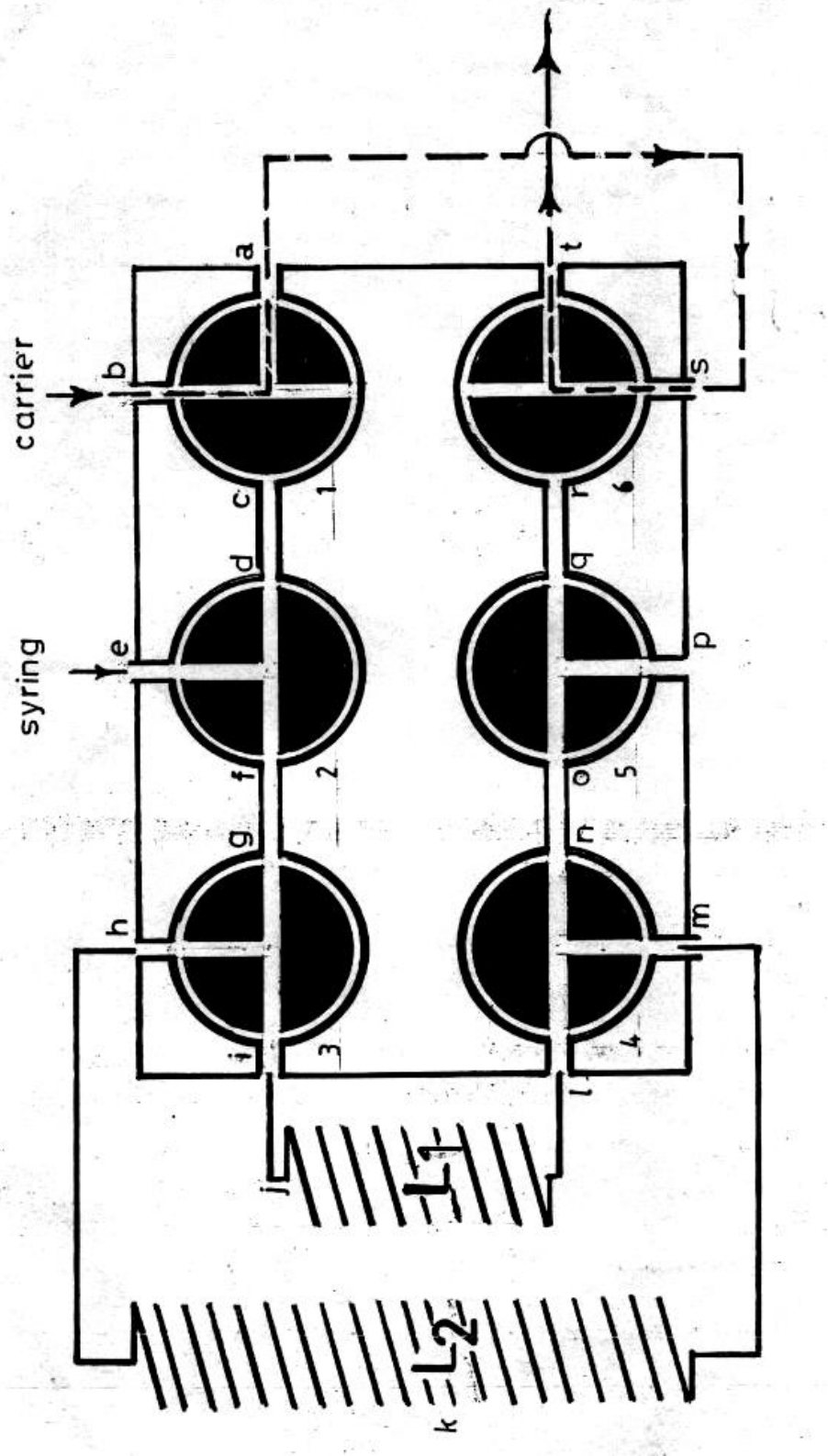

Fig. (2-10) The valves system

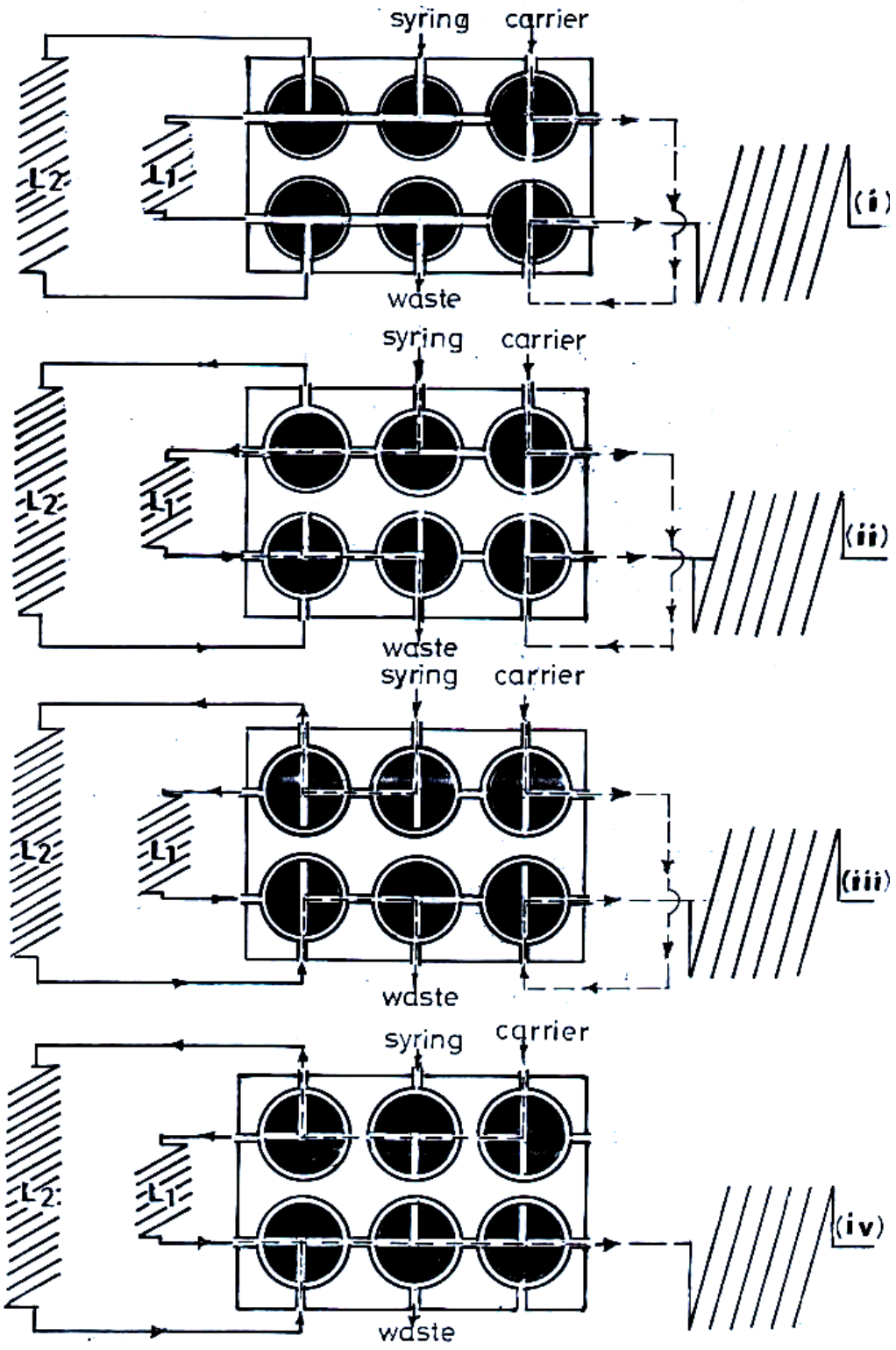

Fig. (2-11) shows the loading and injection of the sample

3-2 Determination of Nitrate and Nitrite

3-2-1 Chemical Optimisation

3-2-1-1 Effect of the Acid Concentration

Fig. (3-5) shows the variation of absorbance of released iodine expressed as average peak height in mV versus the concentration of H_3^+O at 6×10^{-2}M potassium iodide and 1.5×10^{-3}M nitrite. The optimum concentration is 2×10^{-1}M.

3-2-1-2 Effect of Potassium Iodide Concentration

Fig. (3-6) shows the variation of absorbance of released iodine expressed as average peak height in mV versus the concentration of potassium iodide at 2×10^{-1}M acid and 1.5×10^{-3}M nitrite. The optimum concentration is 7×10^{-2}M.

3-2-2 Physical Optimization

3-2-2-1 Effect of Sample Volume

Sample volumes (10, 20, 30, 40 and 45μl) were evaluated and the results were plotted in Fig. (3-7). A sample volume of 40 μwas chosen as the optimum volume.

3-2-2-2 Effect of Acid Volume

Different acid volumes of 20, 30, 40, 55 and 60μl can be achieved by inserting different length of tubes into the valve acid loop. Fig. (3-8) shows that 55 μl is the optimum volume.

3-2-2-3 Effect of Temperature

The effect of temperature on the reaction of I^--NO^-_2, H_3^+O system was studied. It was found that there was no effect of the temperature on the reaction for temperature between 20-40°C.

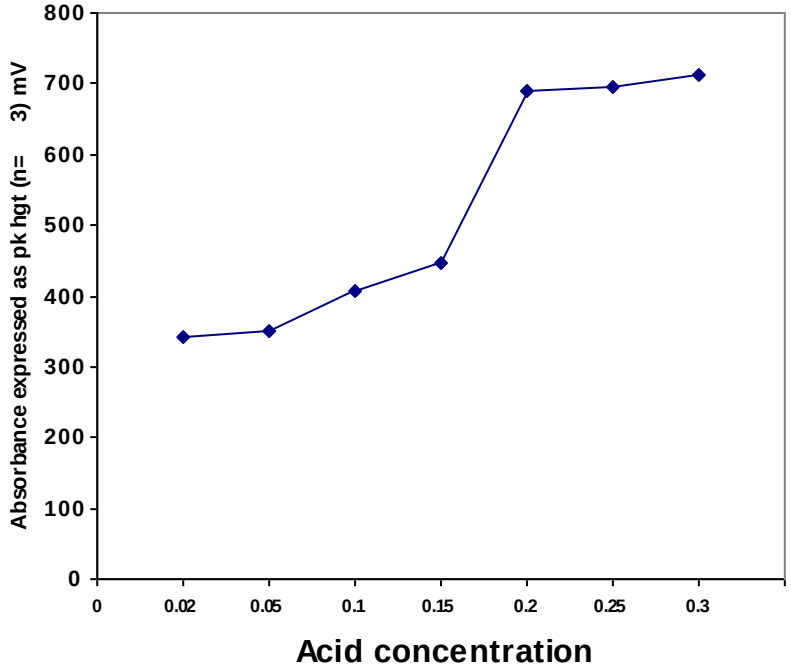

Fig. (3-5) variation of absorbance of released iodine expressed as average peak height (mV).versus the concentration of acid .

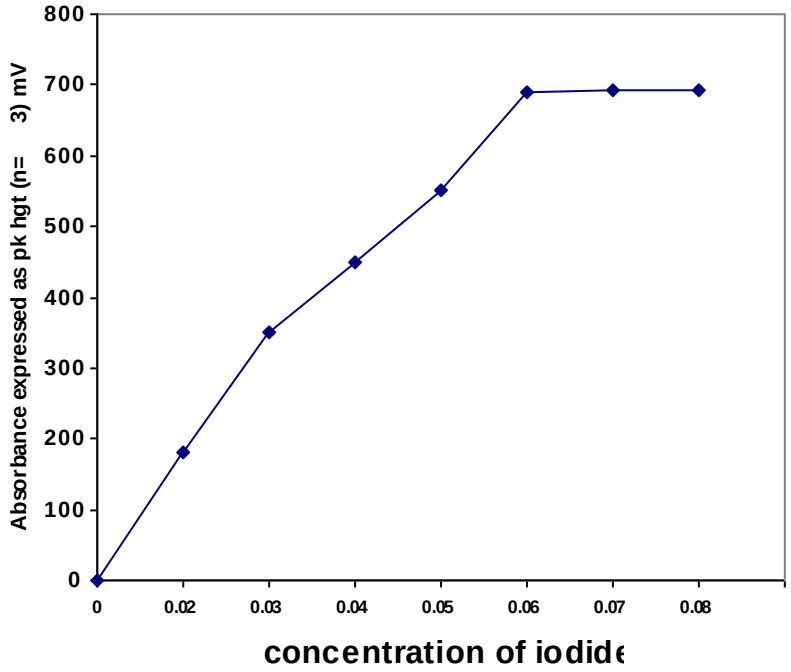

Fig. (3-6) variation of absorbance of released iodine expressed as average peak height (mV).versus the concentration of potassium iodide .

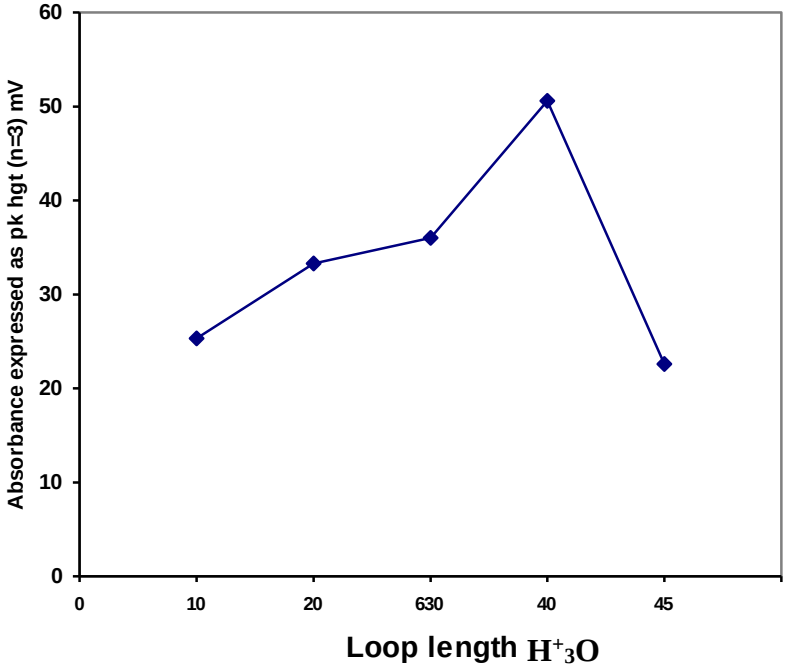

Fig. (3-7) variation of absorbance of released iodine expressed as average peak height (mV).versus the sample volume .

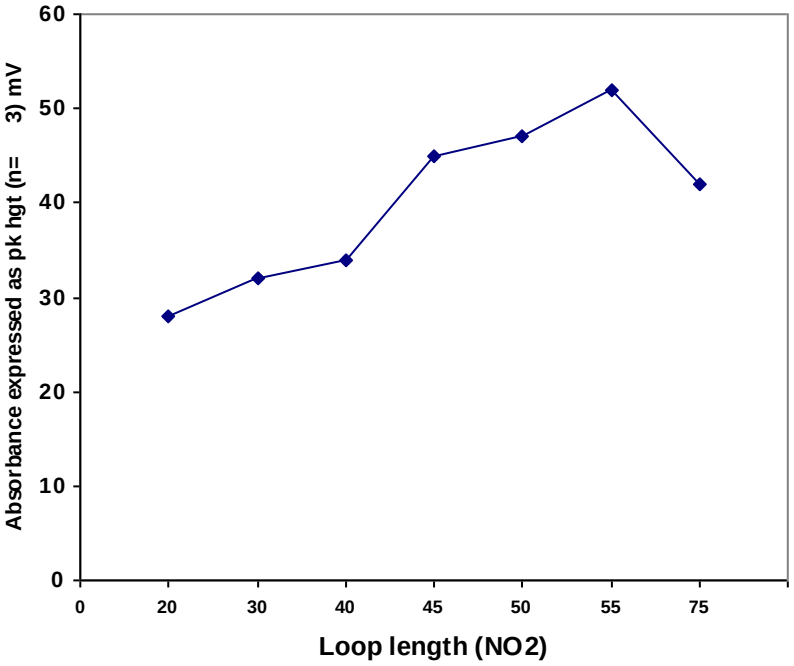

Fig. (3-8) variation of absorbance of released iodine expressed as average peak height (mV).versus the acid volume.

3-2-2-4 Effect of flow rate

Different flow rates 0.8, 1.1, 1.4, 1.7, 2, 2.3 and 2.6 ml.min^{-1} were used to measured the absorbance of iodine released at 7×10^{-2}M potassium iodide, 2×10^{-1}M acid and 1.5×10^{-3}M nitrite. The 2.3 ml.min^{-1} is the optimum value.

3-2-2-5 Effect of mixing coil nitrite

Different delay reaction coil length 50, 100, 150, 200, and 250 cm were used to measure the absorbance of relased Iodine at 7×10^{-2} potassium iodide, 2×10^{-1} M acid and 1.5×10^{-3} M nitrite. Table (3-4) shows that 200cm is the optimum value.

3-2-3 Calibration Curve of Nitrite

Series of nitrite solution 0.4, 0.6, 0.8, 1, 2, 4, 6, 8, 10 and 20 $\times10^{-5}$M were prepared from stock solutions under the optimum conditions of reagent and manifold variables as indicated in Table (3-5). The calibration graph is linear in the concentration range (0.4-8) $\times10^{-5}$M. Table (3-6) shows the linear equation results.

Table (3-4) The effect of mixing coil length

Length	mV	$\overline{X}$ mV	δ_{n-1}	R%	$\overline{X} \pm t\frac{\delta_{n-1}}{\sqrt{n}}$
50	16, 16, 16	16	0	0	16
100	41, 41, 41	41	0	0	41
150	45, 45, 45	45	0	0	45
200	56, 56, 56	56	0	0	56
250	50, 50, 50	50	0	0	50

Table (3-5) optimum working conditions for the determination of nitrite and nitrate ion

Parameters	Optimum value
Acid concentration	2×10^{-1}mol.L^{-1}
Potassium iodide concentration	7×10^{-2}mol.L^{-1}
Sample volume	40 μl
Acid volume	55 μl
Flow-rate	2.3 ml. min^{-1}
Mixing coil length	200 cm

3-2-4 Calibration curve for nitrate

A serial of nitrate solution were prepared 0.1, 0.2, 0.3, 0.4, 0.5, 0.6, 0.7, 0.8, 0.9, 1, 1.5, 2, 3 and 4×10^{-3}M. nitrate was reduced to nitrite by cadimum copperized. Table (3-7) shows the linear regression of coefficient and sensitivity.

Table (3-6) The linear equation results for the iodine released by the injection of 40μl of nitrite sample during the system ($NO^-_2+I^-+H_3O^+$)

Range of linear concentration mol.l$^{-1}\times10^{-5}$	Slope(b) at confidence limit 95% for (n-2) $b\pm S_bt$	Intercept(b) at confidence limit 95% for (n-2) $(a\pm S_at)$	t from table at confidence limit 95% for n-2	Calculate $t=\frac{\lvert r\rvert\sqrt{n-2}}{\sqrt{1-r^2}}$	Correlation coefficient r	Linearity $\%r^2$
0.4-8	10764321.97±206984.296	-15.1646±8.3697	2.3	152.70	0.9997	0.9995

Table (3-7) The linear equation results for the iodine released by the injection of 40µl of (nitrate was reduce to nitrite) during the system ($NO^-_2+I^-+H_3O^+$)

Range of linear concentration $mol.l^{-1}\times10^{-5}$	Slope(b) at confidence limit 95% for (n-2) $b\pm S_bt$	Intercept(b) at confidence limit 95% for (n-2) $(a\pm S_at)$	t from table at confidence limit 95% for n-2	Calculate $t=\frac{\lvert r\rvert\sqrt{n-2}}{\sqrt{1-r^2}}$	Correlation coefficient r	Linearity $\%r^2$
0.2-2	419234.657 ±7742.004	-33.496916 ±1.0230	2.2	232.58	0.9999	0.9998

3-2-5 Determination of Nitrate and Nitrite in a Mixture

A mixture of 10^{-3} $mol.l^{-1}$ of nitrate and 4×10^{-5} $mol.l^{-1}$ nitrite was used to measure nitrite and nitrate. Table (3-8) shows the results when nitrate was reduced to nitrite by copperized cadmium The absorbance of 856 mV was the total for nitrite and nitrate. Table (3-9) gives the absorbance of 452 mV for nitrite only because nitrate was not reduced. Table (3-10) illustrates the absorbance of 10^{-3} $mol.l^{-1}$ only reduced to nitrite.

Total concentration of mixture expressed in mV = 865 mV

The concentration of nitrite only = 452 mV

The concentration of nitrate = 865-452 = 404 mV

The coefficiency of reducing nitrate = 99%

The concentration of nitrate only = 408 mV

Table (3-8) The absorbance of relased iodine expressed as average peak height (mV) versus the mixture of NO^-_3 and NO^-_3 (NO^-_3 reduced to NO^-_2) at constant concentration of H_3O^+ (2×10^{-1}mol.l^{-1}) and (7×10^{-2}mol.l^{-1}) potassium iodide, temperature 28°C, Flow-rate 2.3 ml.min^{-1}.

Conc. Of mixture mol.l^{-1}	Peak height (cm)	Peak height mV	$\overline{X}$ mv	δn-1	R%	$\overline{X} \pm t\frac{\delta_{n-1}}{\sqrt{n}}$
10^{-3} NO^-_3 4×10^{-5} NO^-_2	10.7, 10.7, 10.7	856, 856, 856	856	0	0	856

Table (3-9) absorbance of relased iodine expressed as average peak height (mV) versus the mixture of NO^-_3 and NO^-_3 (NO^-_3 not reduced) at the same condition table (3-8)

Conc. Of mixture mol.l^{-1}	Peak height (cm)	Peak height mV	$\overline{X}$ mv	δn-1	R%	$\overline{X} \pm t\frac{\delta_{n-1}}{\sqrt{n}}$
10^{-3} NO^-_3 4×10^{-5} NO^-_2	11.3, 11.3, 11.3	452,452,452	452	0	0	452

Table (3-10) absorbance of relased iodine expressed as average peak height (mV) versus the mixture of NO^-_3 concentration (NO^-_3 reduced to NO^-_2) at the same condition table (3-9).

Conc. Of NO^-_3 mol.l^{-1}	Peak height (cm)	Peak hight mV	$\overline{X}$ mv	δn-1	R%	$\overline{X} \pm t\frac{\delta_{n-1}}{\sqrt{n}}$
	10.2,10.2,10.2	408,408,408	408	0	0	408

3-2-6 Determination of Nitrate and Nitrite in an Industrial Water by Proposed Method and Standard Method.

Table (3-11, 3-12) shows the agreement between the results in both methods and the paired t test illustrates that flow injection method results were accepted.

3-2-7 Study of Interferences

The interference study was conducted by using 1, 2, 3 fold of interfering ions NH^{+}_{4} , Mg^{2+}, Zn^{2+}, pb^{2+}, Sn^{2+}, Fe^{2+}, Fe^{3+}, K^{+}, Ag^{+}, Cl^{-}, Br, CO^{-2}_{3}, SO^{2-}_{4}, $C_2O^{2-}_{4}$, ScN^{-} on 4×10^{-5}M nitrite. Table (3-13) tabulates the results obtained, and express the percentage interference. It can seen that there is no serious interference at the studied level.

Table (3-11): Comparison of results obtained for nitrite in an industrial water utilising the proposed method and the standard method.

Sample Conc. M	Conc. NO^{-}_{2}M		d ppm	d^{-} ppm	Paired t-test	t from table at confidence limit 95% n-1
	FIA	Standard method				
Boiling water	0	0	0	0.158		2.571
Crude	2.3	2.4	0.1		2.090	
Drinking water	2.1	2.3	0.2			
Soft	1	1.15	0.15			
Dying plant	11	11.5	0.5			
Completion	0	0	0			

Table (3-12): Comparison of results obtained for nitrate in an industrial water utilising the proposed method and standard method

Sample Conc. M	Conc. NO^-_2M		d ppm	d^- ppm	Paired t-test	t from table at confidence limit 95% n-1
	FIA	Standard method				
Boiling water	0	0	0	0.358		2.571
Crude	11	11.5	0.5		1.761	
Drinking water	8.5	9.2	1.3			
Soft	5.75	5.5	0.25			
Dying plant	28	28	0			
Completion	16.5	16.4	0.1			

Table (3-13) Effect of interferring ions

Interfernce effect											**Conc. of cation flod**
Mg^{2+}	pb^{2+}	Zn^{2+}	Sn^{2+}	Cd^{2+}	Fe^{2+}	Fe^{3+}	Na^+	NH^+_4	K^+	Ag^+	
+0.19	+0.57	+0.57	-1.90	0	-1.90	-1.95	-1.42	-0.28	-1.40	-1.40	1
+0.23	+0.57	+0.57	-1.90	0	-1.90	-1.95	-1.42	-0.31	-1.40	-1.40	2
+0.29	+0.58	+0.57	-1.90	0	-1.90	-1.95	-1.42	-0.35	-1.40	-1.40	3

Interfernce effect						**Conc. Of cation flod**
Cl^-	Br^-	CO^{-2}_3	SO^{2-}_4	$C_2O^{2-}_4$	ScN	
+1.90	+1.90	+3.80	+5.71	+4.28	0	1
+1.95	+1.93	+3.60	+5.91	+6.23	0	2
+1.97	+1.97	+3.32	+6.23	+8.24	0	3

3-2-8 Discussion

A new flow-injection spectrophotometric method for the termination of nitrate and nitrite is proposed. The method is simple, rapid, sensitive, low reagent consumption, free from interference, and low limit of detection compared with other methods.

Future prospectuses

From the experience gained through this work, one can release the potential hidden behind the system made and used through out this project. Different elements in this different valency form can be determined. As an example Amplification reaction can be used. Chemistry of using Iodine whether it is released or consumed can be conducted. Actually now in progress is the determination of copper using zero merging techniques. The introduction of the two loop merging zero valve expand the scope of new approaches for various determination.

Aim of the Project

Due to the continuos demand of flow injection analysis and because of the lock of both experience and flow injection tools which requires micro tools for micro analysis, and because it is a leading techniques, and most of the paper concerning this technique is almost restricted to foreign countries. It require micro flow through cell for almost pocket size spectrophotometer, with a necessary. Sample introduction device and chemical propellant. Main target of this project is to facillitate the check of a few home made tools at a level that is capable of performing continuos on-line analyse. An easy, fast, sensitive economic, reliable method even for a well known reactions. The $IO^{-}_{3} – I^{-}$ - $H^{+}_{3}O$ reaction system was used for establishing the test of a new home made two six-port injection valve in one unit the challenge the legend forgein six port injection valve. To our knowledge no person or company or a research institute was capable of dring so, also the flow through cell that fit usual commercial spectrophotometric is the researcher target. New mode of merging zero reaction technique using all homemade unit application of the use of this units matched to commercial spectrophotemetric for acids hydrogen peroxide, nitrate , nitrite, iodide, iodate determination were tried.

List of Tables

Table (3-2) Linear regression analysis of the linear part of the calibration graph of concentration (M) versus the absorbance expressed as peak height (mV) of the relased Iodine

Acids	**H_2SO_4**	**HNO_3**	**HCl**	**CH_3COOH**	**H_3PO_4**	**HCOOH**	**CF_3COOH**	**Citric acid**
Linear range(M)	2×10^{-5}-1.5×10^{-4}	7×10^{-5}-3.5×10^{-4}	10^{-5}-3.5×10^{-4}	6×10^{-5}-3.5×10^{-4}	10^{-4}-3.5×10^{-4}	1.5×10^{-4}-4.5×10^{-4}	1.5×10^{-4}-4.5×10^{-4}	5×10^{-5}-2×10^{-4}
Correlation coefficient	0.9971	0.9992	0.9995	0.9993	0.9993	0.9995	0.9978	0.9927
Slope	581106.768 ±611569.1282	2553256.964 ±94091.725	2943825.162 ±166991.851	2169510.861 ±8347.196	2723428.572 ±121101.252	2543571.429± 85491.618	2621724.286 ±163577.577	5333147.633± 935072.907
Intercept	88.262±52.668	160.485±19.926	228.524±54.826	119.946±65.198	241.104±29.204	337.357±27.034	325.638±43.591	207.647±3.005

The Acceptable Researches

At the Second National Conference of Chemistry: (2001). The following papers had been published.

1- On-Line semiautomated method for nitrite and nitrate ion determination through homemade merging zone kit.

2- Determination of iodide and iodate ions via semiautomated on-line merging zone technique.

3- Spectrophotometer determination of hydrogen peroxide via merging zone technique.

4- Hydronium ion determination via on-line semiautomated merging zone (Home made unit).

Published researches

1- On-line semiautomated method for nitrite and nitrate ion determination through home made merging zone kit , I.M.A. Shakir, F.H. Hussein, D.N. Taha, National journal of chemistry, **4.** 684, (2001).

2- Determination of iodide and iodate ions via semiautomated on-line merging zone technique, I.M.A. Shakir, F.H. Hussein, D.N. Taha, national journal of chemistry **4.** 716, (2001).

3- Spectrophotometer determination of hydrogen peroxide via merging zone technique, I.M.A. Shakir, F.H. Hussein, D.N. Taha, National journal of chemistry **5.** 54, (2001).

4- Hydrogen ion determination via on-line semiautomated merging zone (Home made unit), I.M.A. Shakir, F.H. Hussein, D.N. Taha, National journal of chemistry **6.** 231, (2001).

5- Determination trace concentration of acids by flow-injection analysis Iraqi patent (2002).

REFERENCES

1- K.K. Stewart. Talanta, **29.** 789, (1981).

2- J. Ruzicka, E.H. Hansan, Anal. Chim. Acta. **78** .145, (1975).

3- E.H. Hansen, International laboratory, **10**. 14, (1985).

4- O.A. Skoog. "Principiles of instrumented analysis 3rd edition Sunders College publishing; New York, P.858, (1985).

5- L. Skegges, Am. j. clin. Pathol. **13**.451. (1957).

6- W.H.C. Walker, C.A. Pennc, G.K. McGowan, Anal. Chim. Acta. **27**. 1576, (1970).

7- L.R. Snyder, H.J. Adler, Anal. Chem. **48** . 1017, (1976).

8- J.Ruzicka, E.H. Hansen, Anal. Chim. Acta. **78**. 353(1976).

9- R.D. Begg. Anal. Chem. **44**. 631, (1972).

10- E.H. Hansen, j. Ruzicha, Anal. Chim Acta, **72**. 353 (1974).

11- R. Tijssen, Anal. Chim. Acta. **114.** 71, (1980).

12- M. Valcarcel, M.D. Luquede castro "Flow injection Analysis principles and Applications" 1ST Edition, Ellis Horwood limited publishers; New York p. 44, (1987).

13- D.N. Taha "Development of methods for determination of Aulminium in River water", England, p.46, (1988).

14- A. Lorber, Z. Karpas, L. Halicz, Anal. Chim. Acta. **334.** 259, (1996).

15- R,M. Cespon-Romero, M.C. Yebra. Biurrun, M.P. Bermejo-Barrera, Anal. Chim. Acta; **327**. 37, (1996).

16- T. Guo, J. Baasner, M. Gradl, A. Kistner, Anal. Chim. Acta, **320.** 171, (1996).

17- H.D. Plessis, J. Corneliues, J. F. Staden, S. Afr. J. Chem, **52**. 1, (1999).

18- M. Renli, F. Adams, Anal. Chem. Acta**, 317** , 215, (1995).

19- K. Gradpan, P. Sooksamiti, S. Laiwraungrath, Anal. Chim. Acta. **314.** 51, (1995).

20- A.R. Elware, C.W. Mcleod, K.C. Tompson, Anal. Chem. **72.** 5725, (2000).

21- J.F. Van staden, R.I. Stefan, S. Afr. Tydskr. Chem, **52.** 1, (1999).

22- J.F. Van Staden, L.V. Mulardzi, S.Afr. Tydskr. Chem. **53.** 1, (2000).

23- J. Ruziclea, E.H. Hansen, Anal. Chim. Acta. **99.** 37, (1978).

24- J. Ruziclea, E.H. Hansen, H. Mosbak, Anal. Chim. Acta, **92.** 235, (1977).

25- E.H. Hensen, J. Ruziclea, Anal. Chim. Acta **148.** 111, (1983).

26- J. Ruzika, E.H. Hansen, A. U. Ramsing, Anal. Chim. Acta, **134.** 55, (1982).

27- J. RuziCKA, J.W.B. Stweart, E.A. Zagatto, Anal. Chem. Acta **81.** 387, (1976).

28- V.V.S. Dutt, A. Eskander, H.A. Mottola, Anal. Chem. **48.** 1207(1978)

29- J.T. Vanderslice, K.K. Stewart, A.G. Rosenfeld, D.J. Higgs, Talanta, **28.** 11, (1981).

30- J. Ruzicka, E.H. Hansen “Flow injection analysis” Awiley-Inter science publishing , 13, (1981).

31- J.H.M. Van de Berg, R.S. Delder, H.G.M. Egderink, Anal. Chim. Acta. **114.** 91, (1980).

32- R. Tijssen, Anal. Chim. Acta. 114. 71 (1980).

33- J. Ruzicka, E.H. Hansen, H.Mosbaek, Anal. Chem. **49.**1858, (1977).

34- J. Ruzicka, E.H. Hansen, E.A. Zogatto, Anall. Chim. Acta, **88.** 1, (1977).

35- M.A. Gomez-Nieto, M.D. Castro, A. Martia, M. Valcarcel, Talanta, **32.** 319, (1985).

36- A. Tijssen , Anal. Chim. Acta. **114.** 71,(1980).

37- C. Silfwerbrand, L. Nord, L.G. Danielsson, F. Ingman, Anal. Chim. Acta **160 .** 11, (1984).

38- J. Ruzicka, E.H. Hansen, "Flow-injection analysis", 2nd edition, John Wiley, New York, (1988).

39- J. Ruzicka, E.H. Hansen, A.K. Gose, Anal. Chim. Acta, **100.** 151, (1978).

40- J. Ruzicka, E.H. Hansen, Anal. Chem. **99.** 37, (1978).

41- J.B. Landis, Anal. Chim. Acta, **114.** 155, (1980).

42- M.F. Gine, H. Bergamin, E.A. Zagatto, B.F. Feis, Anal. Chim. Acta. **114.** 191, (1980).

43- J. Ruzicka, E.H. Hansen Anal. Chim. Acta. **106.** 207, (1979).

44- J. Ruzicka, E.H. Hansen Anal. Chim. Acta.**114.** 19, (1980).

45- J. Mindegarad, Anal. Chim. Acta, **104.** 185, (1979).

46- E.A.G. Zagatto, F.J. Krug, H. Bergamin, S.S. jorgensen, B.F. Reis. Anal. Chim. Acta. **104.** 279, (1979).

47- W.E. Van der linden, R. Oostervink, Anal. Chim. Acta. **110.** 419, (1978).

48- P.J. Worsfold, A. Nabi, Anal. Chim. Acta. 171. 333, (1985).

49- P.J. Worsfold, A. Hughes, D.J. Mowtherpe, Analyst . 119. 303, (1985).

50- P.J. Worsfold, A.Nabi, Anal. Chim. Acta, **179.** 307, (1986).

51- S.B. Al-Badri, M.Sc. Thesis Dept. of Chem. College of Science, University of Baghdad, 2001.

52- R.d. Levie "Principles of quantitative chemical analysis" 1st edition. McGraw. Hill Company , New York, p.47, (1997).

53- M.F. EL-Taras, E. Pungor, Anal. Chim. Acta. **82.** 285, (1976).

54- A. OLIN, B. Wallen, Anal. Chim. Acta, **151.** 65, (1983).

55- O. Astron, Anal Chim. Acta **97.** 259, (1978).

56- J.O. Schenk, E. Miler, R.N. Adams. Anal. Chem. **54.** 1452, (1982).

57- F. Ingman, A. Johansson, S. Johnsson, R. Karlsson, Anal. Chim. Acta **64.** 113, (1973).

58- L. Meites, Anal. Lett **15.** 507, (1982).

59- M. Betti, P. Papoff, L. Meites, Anal. Chim. Acta, **182.** 133, (1986).

60- M. Otto, W. Wegscheider, Anal. Chem, **57.** 63, (1985).

61- W. Lindberg, J. A. Persson, S. Wold, Anal. Chem. **55.** 643, (1983).

62- W. Lindberg, J. Ohman, S. Wold, H. Martens, Anal. Chem, Acta, **174.** 41, (1985).

63- G. Sitarama, G.G. Rao, Talanta, **19.** 212, (1972).

64- E. Harvey, A. Kurmann, Analyst. **112.** 1173, (1987).

65- B. Jaselskis, J. Nelapaty, Anal. Chem. **44.** 379, (1972).

66- Y.S. Fung, S.F. Luk, Analyst, **110.** 201, (1985).

67- S.Elnenaey, R. Soliman, Talanta, **96.** 1164, (1979).

68- K.L. Bajaj, G. Kaur, Analyst. **106.** 117, (1981).

69- M.M. Aly., Talanta **19.** 380, (1978).

70- Tt. Lawrence, C.J. Argoudelis, Anal, Chem. **41.** 171, (1969).

71- V.R. White, J.M. Fitzgerald, Anal. Chem. **44.** 1267, (1972).

72- O. Astrom, Anal. Chim. Acta, **105.** 67, (1979).

73- A.G. Fogg, A.M. Summan, Analyst, **100.** 341, (1985).

74- G. Szepesi, Freseniu' sz. Anal. Chem. **265.** 334, (1973).

75- S.S. M. Hassan, M.H. Abed, M.T.M. Zaski, Freseniu'sz. Anal. Chem, **272.** 369, (1975).

76- J.H. Mendez, A.A. Mateos, M.J.A. Parra, C.G. Maria, Anal. Chim. Acta. **184.** 243, (1986).

77- Y. Kassai, T. Tanimura, Z. Tamura, Anal. Chem. **47.** 34, (1975).

78- T. Takeuchi, R.Horikawa, T.Tanimura, Anal. Lett, **130.** 603, (1980).

79- T. Takeuchi, Y. Kabasawa, Analyst. **113**. 1673, (1988).

80- I.M.A. Shakir, A.T. Faizullah, Analyst. **115.** 69, (1990).

81- IB. Agater, RA. Jewsburg, Anal. Chim. Acta. **356.** 289, (1997).

82- H.Cui, Q.Li, R. Meng. Hz. Zhao, He. Cx, Anal. Chim. Acta, **362.** 151, (1998).

83- A.A. Ensafi, B-Rezaei, Anal. Lett. **31.** 333, (1998).

84- W.Lindberg, B.R. Kowalski, Anal. Chim. Acta. **206.** 125, (1988).

85- R.J. Poppi, C.Pasquini Chemometrucs and Intelligent Laboratory, Systems, **19.** 243, (1993).

86- C.G. Zamparonio, J.R. Rohwedder, R.J. Poppi, Talanta, **51.** 1163, (2000).

87- J.L.F.C. Lima, C.D. Mates, M. Carmo, V.F. Vaz, J. Silva. Fresenius. J. Anal. Chem **364.** 266, (1999).

88- M.C. Yebra, R .M. Cespon, Fresenius, Anal. Chem. **365.** 370, (1999).

89- I.M.A. Shakir, W.S. Ulaiwi, National journal of chemistry **1.** 1, (2001).

90- I.M.A. Shakir, N.S. Turkie, W.S. Ulaiwi, National journal of chemistry, **1.** 24 ,(2001).

91- H.A. Flaschka, A.J. Baenard, P.E. Sturrock, "Quantitative Analytical Chemistry: Vol.1, Introduction to principles" Happer and Row, publishers; p. 388, (1969).

92- V. Alexeyev, "Qualitative Analysis" Mir publishers, Moscow. p.469, (1971).

93- W. Szczepaniak, M. Waoicechowska, I.Olejniczak, Chem. Anal. (Warsaw) **46.** 337, (2001).

94- A.W. Morris, J.P. Riley, Anal. Chim. Acta. **29.** 272, (1963).

95- R.J. Elliott, A,G. Porter. Analyst, **96.** 522, (1971).

96- R.S. Lambert, R.J. DuBois, Anal. Chem. **43.** 955, (1971).

97- W.Davison, C. Woof, Analyst. **103.** 403, (1978).

98- M. Nakamura, Analyst, **106.** 483, (1981).

99- A. Tanaka, N. Nose, H. Lwasaki, Analyst, **107.** 190, (1982).

100- Griess, J.P. Philos. Trans. R. Soc. (London), **154.** 667, (1964).

101- A. Henriksen, A.R. Selmer-Olsen, Analyst, **95.** 514, (1970).

102- J.Keay, P.M.A. Menage, Analyst, **95.** 379, (1970).

103- J. Ruzicka, E.H. Hanssen, E.A. Zagatto, Anal. Chim. Acta, **88.** 1, (1977).

104- M.F. Glne, H. Bergamin F,E.A.G. Zagatto, B.F. Reis, Anal. Chim. Acta, **114.** 191, (1980).

105- L. Anderson, Anal. Chim. Acta, **110.** 123, (1979).

106- F. Jacobus, V. Staden, Anal. Chim. Acta, **138.** 403, (1982).

107- T.P. Lynch, Analyst, **113.** 1597, (1988).

108- K.K. Vernia, K.K. Stewart, Anal. Chim. Acta, **214.** 207, (1988).

109- A.R. Thornton, J.Pfab, Analyst. **114.** 747, (1989).

110- R. Nakata, M. Terashita, A. Nitta, K. Ishikawa, Analyst, **115.** 425, (1990).

111- L.Ma, M. Oshima, S. Motomizu, T. Hatteri, Bansekl kagaku, **47.** 375, (1998).

112- V. Mori. M. Bertotti, Anal. Lett, **32**. 25, (1999).

113- V. Mori, M. Bertotti, Talanta, **47.** 651, (1996).

114- Y . Kiura, K. Kusakari, Anal. Sciences, **5.** 923, (1999).

115- J.F. Van Staden, M. Makhafola, S. Afr. J. Chem., **52.** 49, (1999).

116- A.A. Ensafi, G.B. Dehaghei. Fresenius. J. Anal. Chem. **363.** 331, (1999).

117- R.A.S. Lapa, J.L.F.C. Lima, I.V.O.S. Pinto, Analusis, **28.** 295, (2000).

118- R. Higuchi, R. Goto, T. Kawashima, K. Oguma, A. Kawase, H. Ogura Bunseki Kagaku, **49.** 35, (2000).

119- K. Schulz, S. Kerber, M. Kelm, Journal. Article **3.** 225, (1999).

120- Wang, Pu-Znen, Wu. Hong, G. Song, Zhongguo Huanjing Kexue **19.** 469, (1999).

121- J. Pei, X.Y. Li. Talanta, **51.** 1107, (2000).

122- Zi, Yan-gin, Chen, Li-guo, Fenxi ceshi xuebao, **19.** 70, (2000).

123- C. Hui, F. Yanyun, A. Taicheug, Z, kun, L. jinren, Int.J. Environ. Anal. Chem. **76.** 89, (2000).

124- M. Hisakazu, K. Coll, J. Health Sci, **47.** 65, (2001).

125- Z. Yanqin, D. Lanlan, L. Chunling, Fenxi, Huaxue, **29.** 186, (2001).

126- N.A. Koupparis, K.M. Walczak. H.V. Malusadt, Analyst **107.** 1309, (1982).

127- R. Belcher, S.L. Bogdanski, A.C. Calokerinos, A. Townshend, Analyst, **106.** 625, (1981).

128- J.R.C. Rocha, L. Kosminsky, T.R.L.C. Paixao, M. Bertotti, Electro analysis, **13.** 155, (2001).

129- Y. Yang, F. Liu, J. Kang, Q. OU, J. of Crom. **834.** 393, (1999).

130- Y. Miura, H. Hamada, J. of chromotography **850.** 153, (1999).

131- Y. Michigami, Y. Yamamoto, K. Ueda, Analyst. **114.** 1201, (1998).

132- S. Nicolae, R. Tata, T. Donald, J. electrochem. Soc. **148.** E112, (2001).

133- D.R. Kecney, B.H. Bgrose, J.J. Geason, Analyst. **95.** 383, (1970).

134- G.Rod, Science, **220.** 711, (1983).

135- J.E. Bradgy, J.R. Holum "Fundamentals of chemistry" 3rd edition, p.797, (1988).

136- A.L. Lozrus, G.L. Kok, S.N. Gitin, J.A. Lin, Anal. Chem. **57.** 917, (1985).

137- R.J. Kieber, G.R. Helz, Anal. Chem. **58.** 2312, (1986).

138- K. Tomaoku, Y. Murao, K. Akiura, Anal. Chim. Acta **136.** 121, (1982).

139- P.N. Moorthy, K.N. Rao, J. Indian. Soc. **1.** 85, (1982).

140- H. Hwang, P.K. Dasgupts, Anal Chem. **58.** 1421, (1986).

141- H. Lundback, G. Johansson, Anal. Chim. Acta, **155.** 47, (1983).

142- G. Scott, W.R. Seitz, Anal. Chim. Acta, Acta, **115.** 221, (1980).

143- B. Olsson Anal. Chim. Acta, **136.** 113, (1982).

144- P.V. Zoonen, D.A. Kamminga, G. Gooljer, N.L. Velthorst, R.W. Frel. Anal. Chim. Acta. **167.** 249, (1985).

145- H. Hwang, P.K. Dasgupta, Anal. Chim. Acta, **170.** 347, (1985).

146- K. Hool, T.A. Nicman, Anal. Chem. **60.** 834, (1988).

147- M. Stigbrand, E. Ponten, K. Irgum, Anal, Chem. **66.** 1766, (1994).

148- K.S. Johnson, C.S. Arnold, S.W. Willason, C.L. Beehier, Anal. Chim. Acta, **201.** 83, (1987).

149- T. Taniai, A. Saleuragawa, T. Okutani, Anal. Sciences, **15.** 1077, (1999).

150- M. Farooqi, P. Sosnitza, M. Saleemuddin, R. Ulber, T. scheper, Applied Microbiology and brotechnology, **52.** 373, (1999).

151- D. Harms, R. Than, B. Krebs, U. Karst, Fre. J. Anal. Chem. **364.** 184, (1999).

152- K. Ito, Anal. Chem. **69.** 3628, (1997).

153- G. Zhang, H. Chen, Anal. Lett. **33.** 3285, (2000).

154- L. Kosminsky, M. Bertotti, Electroanlysis **8.** 11, (1999).

155- K.A. Anderson, B. Casey, E. Diaz, P, Markowski, B. Wright, J. Assoc. off. Anal. Chem. **16.** 3, (1998).

156- S.Z/ Yao, Z.H. Mo, L.H. Nie, Anal. Chim. Acta **215.**78, (1988).

157- T.Koh, M. Ono, Analyst, **113.** 945, (1988).

158- G.T.F. Wong, P.G. Brewer, Anal. Chim. Acta, **81.**81, (1976).

159- V.G. Diaz, C.R.T. Gonzalez, F. Montelongo, Analyst, **106.** 1224, (1981).

160- G.F. Kirkright, T.S. West, C. Woodward, Anal. Chim. Acta. **36.** 298, (1960).

161- G. Colovos, M. Haro, H. Freiser, Talanta, **17.**273, (1970).

162- J.A. Lown, R. Koile, D.C. Johnson, Anal. Chim. Acta **116.** 33, (1980).

163- R.C. Schothorst, G.D. Boef, Anal. Chim. Acta, **153.** 133, (1983).

164- K.W. Pratt, D.C. Johnson, Anal. Chim. Acta, **148.** 87, (1983).

165- R.E. Moxon, Analyst. **109.** 425, (1984).

166- K. Fujiwara, K. Fuwa, Anal. Chem. **57.**1012, (1985).

167- A. AL-Wehaid, A. Townshend, Anal. Chim. Acta. **198.** 45, (1987).

168- M.C. Gutierrez, A.G. Hens, D.P. Bendito, Analyst, **114.** 89, (1989).

169- M.A. Abdalla, H.M. AL-Swaidan, Analyst, **114.** 583, (1989).

170- K. Oguwa, K. Kitada, R. Kuroda, Mikrochim. Acta, **110.** 71, (1993).